

# DESIGN AND ANALYSIS OF SMALL SCALE WIND TURBINE SUPPORT STRUCTURES

by

**Emma Nel**

*Thesis presented in fulfilment of the requirements for the degree of Master of Science in the  
Faculty of Structural Engineering at Stellenbosch University*



Supervisors:

Dr. J. A. v. B. Strasheim

Prof. P. E. Dunaiski

December 2012

## DECLARATION

By submitting this thesis electronically, I declare that the entirety of the work contained therein is my own, original work, that I am the sole author thereof (save to the extent explicitly otherwise stated), that reproduction and publication thereof by Stellenbosch University will not infringe any third party rights and that I have not previously in its entirety or in part submitted it for obtaining any qualification.

Date:.....

# .....o.....y

.....

.

.

.

.

.

.

.

.

.

.

.

.

.

.

.

.

## SYNOPSIS

A technology that has advanced immeasurably as a result of the necessity for green energy production is the harnessing of wind energy. One of the most important aspects of a wind turbine is its supporting structure. The tower of a wind turbine needs to be sufficiently reliable and structurally sound to ensure that the design life of the wind turbine machine is unaffected. The tower also needs to be of the correct height to ensure that the full potential of energy capture is realised.

The supporting structure of a wind turbine constitutes up to as much as 30% of the total costs of a wind turbine. The most common wind turbine supporting structures seen worldwide today are Steel Monopole Towers. The large cost proportion of the tower compels the industry to investigate the most feasible alternative supporting tower structures and thus prompted the research developed in this thesis. In this thesis the focus is on small scale wind turbines (<50kW), more specifically, a 3kW Wind Turbine. The proposed alternative design the support structures of small scale wind turbines to the presently used Steel Monopole tower was a Steel Lattice tower.

Both a Steel Lattice and Steel Monopole Tower was designed for a 3kW Wind Turbine using rational design methods determined from pertinent sections of the South African design codes. The Tower designs needed to incorporate the details of the element connections, so as to encompass all of the cost parameters accurately. The foundation design of each of the towers was also required from the point of view of cost analysis completeness, and ended up playing a critical role in the feasibility analysis.

To validate the design methods, the two towers were modelled in the finite element package Strand7 and a number of different analyses were performed on the two towers. The analyses included linear static, nonlinear static, natural frequency and harmonic frequency analyses. The towers were assessed for a number of different load case combinations and were examined in terms of stress states, mass participation factors and deflections, to mention a few, for the worst loading combination cases that were encountered.

Once a final design was reached for both the Steel Lattice and Steel Monopole Towers, each element from which they were made was assessed from a structural viewpoint to determine manufacturing and construction costs.

The cost analysis was conducted by means of asking a number of leading construction companies for unit prices for each of the identified elements to be assessed.

The fabrication and construction of each of the Towers was then compared to determine which one was more feasible, in terms of each design aspect considered as well as looking at the complete end product.

It was found that the Steel Lattice Tower was more feasible from the points of view of fabrication, and construction, as well as having a far more cost effective foundation. This was a positive conclusion from the perspective of the proposal for a more feasible alternative to the presently used Steel Monopole Towers.

The outcome of the research conducted here could certainly prove to be worth considering from a wind farm development perspective, with particular focus on the up and coming Wind Industry developments in South Africa.

## AFRIKAANS SYNOPSIS

As gevolg van die noodsaaklikheid vir die produksie van volhoubare energie is 'n tegnologie wat met rasse skrede vooruitgegaan het die vir die benutting van windenergie. Een van die belangrikste aspekte van 'n windturbine is die ondersteunende struktuur. Die toring van 'n windturbine moet funksioneel en struktureel betroubaar wees om te verseker dat die ontwerpleeftyd van die windturbine masjien nie nadelig beïnvloed word nie.

Die toring moet ook die regte hoogte wees om te verseker dat die volle potensiaal van die wind energie in meganiese energie omgesit word.

Die koste van die ondersteunende struktuur van 'n windturbine verteenwoordig tot 30% van die totale koste van 'n windturbine. Die mees algemene vorm van ondersteunende strukture vir windturbines wat vandag wêreldwyd teëgekomp word, is die van 'n enkel staal buisvormige toring. Die groot koste-komponent van die toring dwing die industrie om ondersoek in te stel na die mees koste effektiewe praktiese uitvoerbare alternatiewe vir die ondersteunende toring struktuur. Hierdie aspek van die struktuur konseptualisering het gelei tot die navorsing wat in hierdie tesis onderneem is. Die fokus van die navorsing is op klein skaal windturbines (<50kW), en meer spesifiek op 'n 3kW windturbine model. Die alternatiewe ontwerp wat ontwikkel is vir klein skaal wind turbines se ondersteunende structure, is 'n staal vakwerk toring as alternatiewe vir die staal buisvormige toring.

Beide 'n staal vakwerk en staal buisvormige toring vir 'n 3kW wind turbine is ontwerp deur rasionele ontwerp metodes. Die toepaslike gedeeltes van die Suid-Afrikaanse ontwerp kodes is hiervoor gebruik. Die ontwerp vir die toring moet die besonderhede van die element verbindings in ag neem en die nodige koste parameters moet akkuraat bepaal word. Die ontwerp van die fondament van elke toring is ook noodsaaklik vir die volledigheid van die koste-ontleding en dit speel ook 'n kritieke rol in die gangbaarheid analise.

Om die ontwerp metodes te bevestig, is die twee tipes torings in die eindige element pakket, Strand7, gemodelleer en 'n aantal verskillende ontledings vir die twee torings is uitgevoer. Die ontledings sluit lineêre en nie-lineêre statiese ontledings asook natuurlike frekwensie en dinamiese ontledings onder harmoniese belastings in. Die torings is vir 'n aantal verskillende lasgevalkombinasies ondersoek en in die spannings toestande, massadeelname faktore en defleksies vir die ergste laskombinasie gevalle wat ondervind is, is geassesseer.

Sodra 'n finale ontwerp vir beide die staal vakwerk en staal buisvormige toring voltooi is, is elke element beoordeel uit 'n strukturele en materiaal oogpunt om die kostes daarvan te bepaal.

Die koste-analise is baseer op data wat voorsien is deur 'n aantal vooraanstaande konstruksie maatskappye op 'n prys per eenheid basis vir elk van die geïdentifiseerde elemente wat geassesseer moes word.

Die vervaardiging en konstruksie van elke toring is dan vergelyk om te bepaal watter een die mees haalbaar is, in terme van elke toepaslike ontwerp-aspek en deur ook die volledige eindprodukt te evalueer.

Daar is bevind dat die staal vakwerk toring uit die oogpunt van vervaardiging en konstruksie, asook as gevolg van 'n meer koste-effektiewe fondament, die voorkeur alternatiewe verteenwoordig het. Dit was 'n positiewe gevolgtrekking uit die oogpunt van die soeke na 'n ander alternatiewe as die buisvormige staal torings wat tans algemeen in gebruik is.

Die uitkoms van hierdie navorsing verdien oorweging uit 'n windplaas ontwikkelingsperspektief, met 'n spesifieke fokus op die opkomende ontwikkelinge in die wind energie industrie in Suid-Afrika.

## ACKNOWLEDGEMENTS

I would first like to thank the late Professor Dunaiski for giving me the opportunity to do my Master's degree; if it weren't for his belief in me none of this would have come to be.

Thank you to Dr. Strasheim for being such a kind and supportive Study leader.

Thank you Etienne van der Klashorst for helping me with so many hours of patience.

Thank you Dad for being my sounding board and mentor every day.

Thank you Jacques Loubser for your endless support and guidance with this endeavour, I couldn't have done it without you.

## TABLE OF CONTENTS

Declaration .....	i
Synopsis .....	ii
Afrikaans Synopsis .....	iii
Acknowledgements .....	iv
List of Figures.....	xi
List of Tables .....	xiii
List of Symbols: .....	xiv
List of Abbreviations: .....	xviii
Chapter 1: Introduction to the Design and Analysis of Small Scale Wind Turbines .....	1
Chapter 2: Literature Review.....	3
Introduction.....	3
2.1 The Understanding of Wind Energy .....	3
2.1.2 Motivation for Wind Energy.....	3
2.1.2 How Wind is turned into Energy .....	4
Density of the air: .....	4
Rotor Area:.....	4
Number of Blades: .....	6
Pitch versus Stall: .....	7
2.2 Loads Induced by the Wind on a Wind Turbine Supporting Structure.....	7
2.3 Supporting Structures .....	8
2.3.1 Tower Types .....	8
Free-standing Towers: .....	9
Lattice Style Towers: .....	9
Monopole Towers.....	10
2.3.2 Tower Height Considerations.....	11
2.3.3 Pros and Cons of each Tower Type .....	11
2.4 The Design of Supporting Towers .....	12
2.5 The Analysis of Supporting Towers .....	12
2.5.1 Finite Element Analysis .....	12
2.5.2 Feasibility Analysis.....	13
Chapter 3: Towers .....	14
The design procedure:.....	14
3.1 The Geometric Layout.....	14
3.1.1 The Geometric Layout of the Steel Monopole Tower.....	14
3.1.2 The Geometric Layout of the Steel Lattice Tower.....	16

3.2 The Boundary conditions of Tower design.....	17
3.3 Loading Conditions.....	17
3.3.1 Loading Conditions from the Wind .....	17
3.3.2 Loading conditions induced by the Wind and the Wind turbine machine.....	22
3.4 Validation of Structural design .....	24
3.4.1 Design Validation of the Steel Monopole Tower Geometry .....	26
3.4.1.1 Axial Compression .....	26
3.4.1.2 Bending-Laterally supported members.....	26
3.4.1.3 Shear .....	27
3.4.1.4 Interaction Equations: Combined bending and axial compression.....	27
3.4.2 Design Validation of the Steel Lattice Tower Structure .....	28
3.4.2.1 Design of compression members: Effective cross sectional properties of compression members.....	28
3.4.2.2 Flexural buckling of axially compressed members.....	28
3.4.2.3 Bending and axial compression.....	32
3.4.2.4 Design of Tension members:.....	32
3.4.2.5 Combined bending and axial tensile/compressive forces:.....	33
3.5 Design Iteration .....	33
3.6 General Aspects of Tower design:.....	34
3.6.1 Materials .....	34
Materials for the Circular Hollow sections.....	34
Materials for Angle sections and Plates:.....	34
Materials for Bolts: .....	34
3.6.2 Corrosion Protection .....	35
3.6.3 Access.....	35
3.6.4 Production .....	36
3.6.5 Fatigue.....	36
Chapter 4: Connection Design .....	37
4.1 Monopole Ring Flange Connections.....	37
4.1.1 Bolt Force at separation: .....	39
4.1.2 Maximum bending strength of flange following plate separation:.....	40
4.1.3 Maximum bending strength of flange when separation occurs after yielding of the flange:.....	41
4.1.4 Evaluation of the Prying Force: .....	42
4.1.5 Prying force acting before separation:.....	42
4.1.6 Separation load and fracture load of the bolts: .....	43
4.1.6.1 Separation Load: .....	44
4.1.6.2 Fracture Load of the Bolts:.....	44
4.1.7 Maximum Strength of a Joint:.....	44

4.1.8 Suggested Design Methods:.....	46
General Procedure:.....	46
Simplified Design: .....	46
4.1.9 Connection Design from basic Principles: .....	47
4.1.10 Connection Designs in Finite Element Program (Strand7):.....	48
Mid-section Connections: .....	48
Base Connection: .....	49
4.1.10.1 Connection Calculations:.....	50
Validation of the Bolt size and strength:.....	51
Validation of the flange size and strength: .....	52
4.2 Steel Lattice Tower Connections:.....	54
4.2.1 Connection type .....	54
4.2.2 Connection Design: .....	55
4.2.2.1 Choosing the appropriate bolts:.....	55
4.2.2.2 Connection details:.....	55
4.2.3 Connection Calculations:.....	56
4.2.4 General Aspects pertinent to all connection types dealt with in this chapter:.....	57
4.2.4.1 Welds:.....	57
4.2.4.2 Bolts:.....	58
Chapter 5: Foundation Design .....	60
5.1 Introduction to foundations.....	60
5.2 Steel Monopole Tower Foundation Design .....	61
5.2.1 Foundation Type .....	61
5.2.2 Foundation Dimensions .....	61
5.2.3 Foundation Calculations.....	62
5.3 Steel Lattice Tower Foundation Design.....	66
5.3.1 Foundation Type .....	66
5.3.2 Designing the Steel Base Plates.....	66
5.3.3 Designing the concrete foundation:.....	67
5.4 Conclusion .....	70
Chapter 6: Finite Element Analyses .....	71
6.1 Introduction .....	71
6.2 Steel Monopole Tower: Finite Element Analyses.....	71
6.2.1 Linear Static Analysis.....	72
The nodal reactions at the Base of the Tower:.....	75
Linear Static Analysis stress states:.....	78
6.2.2 Linear Buckling Analysis .....	78



Linear Buckling Solver: .....	78
6.2.3 Nonlinear Analysis .....	79
6.2.4 Dynamic Analyses .....	81
Natural Frequency Solver Overview: .....	81
6.2.4.1 The Effects of an Out of Balance Rotor: .....	83
Harmonic Response Solver Overview: .....	83
Harmonic Response Results: .....	84
Details of the out of balance rotor analysis: .....	84
6.2.4.2 Effects of Vortex Shedding due to wind action .....	85
Harmonic displacement response vs. time analysis: .....	85
6.3 Stress States .....	87
Harmonic Response Stress Analysis: .....	87
Vortex shedding stress analysis: .....	87
6.4 Fatigue Assessment: .....	88
6.5 Mass Participation: .....	90
Resonance Effects: .....	91
6.6 Steel Lattice Tower: Finite Element Analyses .....	93
Wind Load Modelling: .....	95
6.6.1 Linear Static Analysis .....	96
Base Response: .....	98
Linear Static stress analysis: .....	99
6.6.2 Linear buckling Analysis: .....	99
6.6.3 Nonlinear Static Analysis: .....	101
6.6.4 Dynamic Analyses: .....	102
Natural Frequency Analysis: .....	102
6.6.4.1 Dynamic Effects of an out of Balance Rotor: .....	103
6.6.5 Mass Participation: .....	105
Resonance Effects: .....	106
6.7 Stress State .....	107
Harmonic response stress analysis. ....	107
6.8 Fatigue Assessment .....	108
Chapter 7: Feasibility .....	109
7.1 Introduction to feasibility .....	109
7.1.1 Tower Specifications .....	109
7.1.1.1 Steel Monopole Tower .....	109
7.1.1.2 Steel Lattice Tower .....	109
7.2 The structural requirements of the towers .....	110

7.3 The aesthetic requirements of the towers.....	110
7.4 The constructability of the towers .....	110
7.4.1 Transportation:.....	110
7.4.2 Fabrication and Construction:.....	110
7.4.2.1 Fabrication: .....	110
First Fabricator Cost Response: .....	111
Second Fabrication Cost Response: .....	111
7.4.2.2 Construction:.....	112
Steel Tower Fabrication: .....	115
Foundation Construction: .....	116
7.5 Conclusion: .....	118
Chapter 8: Conclusion and Recommendations .....	120
List of References .....	121
Relevant South African Design Codes: .....	121
Other Resources: .....	121
Appendix A: Tower Design Calculations .....	A
A1: Steel Monopole Design .....	A
A1.1 Design Reference Parameters and Tower Resistance Calculations .....	A
Tower Geometry and Axial Compression Resistance: .....	A
Flexural and Axial Compression Resistance: .....	B
Shear Resistance: .....	C
A1.2 Wind Calculations on Steel Monopole Tower .....	D
A1.3 Actions Induced on the Tower .....	F
A1.4 Interaction Equations.....	G
A2: Steel Lattice Design .....	H
A2.1 Design Reference Parameters and Tower Resistance Calculations .....	H
Tower Geometry and Axial Compression Resistance: .....	H
A2.2 Wind Calculations on Steel Lattice Tower .....	K
Applying the Wind Loads:.....	M
Wind Load cases:.....	M
A2.3 Actions Induced on the top of the Tower .....	O
Appendix B: Connections.....	A
B.1 Steel Monopole Connections .....	A
Ring Flange Connections: Method 1 .....	A
Method 2: General theory of resistance: .....	E
B.2 Steel Lattice Tower Connections.....	G
Gusset Plate connections.....	G

Appendix C: Foundation Design.....	A
C.1 Steel Monopole Tower Foundation Design.....	A
Input Values for Prokon Foundation Design .....	A
Output from Prokon Foundation Design .....	A
Bending Schedule Output from Prokon Foundation Design.....	B
Hand Calculations for Steel Monopole Tower Foundation Design .....	C
C.2 Steel Lattice Tower Foundation Design.....	E
Input Values for Prokon Foundation Design .....	E
Output from Prokon Foundation Design .....	E
Bending Schedule Output from Prokon Foundation Design.....	E
Hand Calculations Designing the Steel Base Plates for the Steel Lattice Tower’s Foundation .....	G
Appendix D: Attached CD of Design Files .....	A

## LIST OF FIGURES

Figure 1: Power coefficient curve, parametised in accordance with the blade pitch angle, image from <a href="http://www.caspus.eclipse.co.uk/ah/publications/3dmwtucfd.pdf">http://www.caspus.eclipse.co.uk/ah/publications/3dmwtucfd.pdf</a> .....	5
Figure 2: Typical Wind Turbine Power Curve .....	8
Figure 3: Different Monopole Profiles .....	15
Figure 4: Ring Flange connection for a CHS .....	16
Figure 6: Actions Induced on Wind Turbine Support Tower .....	22
Figure 7: Flexural Buckling of an Equal Leg Angle.....	29
Figure 8: Flexural Torsional Buckling of an Equal Leg Angle.....	29
Figure 9: Dimensions and Cross-Sectional Axes of Angle Sections.....	31
Figure 10: Modes of Failure for Ring Flange Connections .....	38
Figure 11: Bending Moments developed in Ring Flange Connection Failures .....	38
Figure 12: Ring Flange Connection Details .....	39
Figure 13: Ring Flange Connection Yield Lines .....	40
Figure 14: Ring Flange Connection: yield line before separation .....	41
Figure 15: Prying Action Model .....	42
Figure 16: $P_{MAX}$ versus $T_f$ relation.....	46
Figure 17: Bolt Spacing and Tributary Length.....	47
Figure 18: Dimensional Parameters of Flange.....	48
Figure 19: Mid-section Connection Design.....	49
Figure 20: Mid-Flange and Web Stiffener Details.....	49
Figure 21: Base Flange Connection.....	50
Figure 22: Base Flange and Web Stiffener Details.....	50
Figure 23: Reaction Forces at Monopole Tower Base (SLS).....	51
Figure 24: Moments in plane 11 (direction of y-axis loading) for the base ring flange connection of the Monopole .....	53
Figure 25: Moments in plane 22 (direction of x-axis) for the base ring flange connection of the Monopole.....	53
Figure 26: Von Mises Moments in the base ring flange connection of the Monopole .....	53
Figure 27: Tresca moments in the base ring flange connection of the Monopole.....	54
Figure 28: Equal Leg Angle Section Hole Dimensioning.....	54
Figure 29: Lattice Tower, pinned connections with gusset plates.....	57
Figure 30: Failed wind turbine foundation design.....	60
Figure 31: Monopole Foundation Type .....	61
Figure 32: Monopole Foundation Equilibrium.....	62
Figure 33: Monopole Foundation equilibrium equivalent.....	62
Figure 34: Monopole Foundation Bearing Pressure layout.....	63
Figure 35: Monopole Foundation Bearing Pressure Distributions .....	64
Figure 36: Prokon Input Layout of Monopole Foundation .....	64
Figure 37: Prokon Output for Monopole Foundation .....	65
Figure 38: Monopole Schematic Bending schedule.....	65
Figure 39: Effective Base Plate Area .....	67
Figure 40: Steel Lattice Tower Foundations .....	68
Figure 41: Prokon Lattice Foundation Input .....	68
Figure 42: Prokon Lattice Foundation Output .....	69
Figure 43: Prokon Bending schedule Lattice Foundation .....	69
Figure 44: Monopole Tower Wind Turbine Connection Simulation .....	72
Figure 45: Monopole: Largest Static displacement load combination. ....	74
Figure 46: Monopole, Linear displacement distribution .....	75
Figure 47: Axes system for nodal reactions.....	75

Figure 48: FX(N) Base Reaction Forces, ULS (Worst Case) Combination 3 .....	76
Figure 49: FY(N) Base Reaction Forces, ULS (Worst Case), Combination 3 .....	77
Figure 50: FZ(N) Base Reaction Forces, ULS (Worst Case), Combination 3 .....	77
Figure 51: Monopole, Linear Buckling Factors .....	79
Figure 52: Monopole nonlinear displacement Vs. Loading .....	80
Figure 53: Initial Nonlinear Analysis: Monopole ULS (Worst Case) .....	81
Figure 54: Every second mode shape of the first 20 modes of the Steel Monopole.....	82
Figure 55: Monopole, Natural Frequency Analysis.....	82
Figure 56: Worst Case displacement occurring for harmonic response.....	85
Figure 57: Vortex shedding harmonic response, worst case displacement .....	86
Figure 58: Monopole Stress response to the dynamic loading as a result of the out of balance rotor effects....	87
Figure 59: Vortex shedding stress state .....	88
Figure 60: Stress vs. Number of Cycles for Fatigue Analysis of out of balance rotor in accordance with SANS 10162-1:2005 Clause 26 .....	89
Figure 61: Fatigue Analysis, Stress Range versus Number of cycles for Vortex shedding analysis in accordance with SANS 10162-1:2005 .....	90
Figure 62: Resonance evaluation of steel monopole .....	92
Figure 63: Connection Details between top parallel portion of the tower and the tapered portion of the tower .....	93
Figure 64: Lattice Tower Turbine Connection Simulation .....	94
Figure 65: Wind Loading Cases for square plan Steel Lattice Towers .....	95
Figure 66: Stress comparison for two different wind loads on Steel Lattice Tower.....	96
Figure 67: Displacement comparison for two different wind loads on Steel Lattice Tower .....	96
Figure 68: Different wind load cases for Square plan Steel Lattice Towers .....	97
Figure 69: Steel Lattice Tower Displacement (XY) Static Analysis, Wind Load case 1, SLS2 .....	97
Figure 70: Base Response, Steel Lattice Tower, for Wind load case 1 .....	98
Figure 71: Base Response, Steel lattice tower, for Wind Load case 2 .....	98
Figure 72: Linear Buckling Factors: Steel Lattice Tower, Wind Load Case 1.....	99
Figure 73: Linear Buckling Factors, Steel Lattice Tower, Wind Load case 2 .....	100
Figure 74: Nonlinear Displacement, Initial Nonlinear Analysis, Lattice Tower.....	101
Figure 75: Nonlinear Displacement, Initial Tower analysis, Lattice Tower.....	101
Figure 76: Natural frequency versus mode for Steel Lattice, Wind Load Case 1.....	102
Figure 77: Natural frequency comparison for Monopole and Steel Lattice Towers.....	102
Figure 78: First 10 mode shapes for Steel Lattice Tower.....	103
Figure 79: Maximum Displacement effects from dynamic analysis of out of balance rotor effects.....	104
Figure 80: Resonance effects of steel lattice tower .....	106
Figure 81: Stress state from out of balance harmonic response.....	107
Figure 82: Stress Range versus Number of cycles for fatigue analysis in accordance with SANS 10162-1:2005.....	108
Figure 83: Cost Comparison for Steel Towers and Foundations combined.....	115
Figure 84: Cost Difference between companies and Towers for Tower and Foundation costs combined.....	115
Figure 85: Steel Tower Quotation Comparison .....	116
Figure 86: Difference in cost per company and tower design for the cost of the towers.....	116
Figure 87: Cost Comparison in foundation construction for different towers and companies.....	117
Figure 88: Cost difference in foundation construction for different towers and companies.....	117
Figure 89: Comparative Entity Cost Differences.....	118

## LIST OF TABLES

Table 1: Pros and Cons of Each Tower Type .....	11
Table 2: Cost Analysis Parameters .....	13
Table 3: Table 5 SANS 10160-3:2011 .....	18
Table 4: Table 1 SANS 10160-3:2011 .....	19
Table 5: Table 2 SANS 10160-3:2011 .....	20
Table 6: Table 4 SANS 10160-3:2011 .....	21
Table 9: Equal leg angle section compression capacity .....	33
Table 10: SASCH Table 6.1 .....	34
Table 11: Spread sheet extract showing flange details .....	51
Table 12: Moment Resistance of the Flanges .....	52
Table 13: Ordinary Bolt strength calculations for Steel Lattice Tower Connections .....	56
Table 14: Bolt Capacity Calculations for Fatigue for Lattice tower Connections .....	56
Table 15: Monopole Load Case Combinations .....	72
Table 16: Maximum displacement magnitudes of Monopole for Serviceability Limit State .....	74
Table 17: Monopole, Linear Buckling Factors .....	79
Table 18: Fatigue Analysis of Steel Monopole Base .....	89
Table 19: Fatigue Assessment for Steel Monopole and vortex shedding .....	90
Table 20: Load Case Combinations, Lattice Tower .....	95
Table 21: Wind loading on the Steel Lattice Tower, displacement and stress results .....	95
Table 22: Linear Buckling Factors Steel Lattice Tower, Wind Load Case 1 .....	99
Table 23: Linear Buckling Factors, Steel Lattice Tower, Wind Load Case 2 .....	100
Table 24: Fatigue Analysis of steel lattice tower .....	108
Table 25: Cost comparison of Fabrication, Fabricator 1 .....	111
Table 26: Fabrication costs, Monopole, Fabricator 2 .....	111
Table 27: Fabrication Costs, Lattice Tower, Fabricator 2 .....	112
Table 28: Table of Item descriptions for construction .....	113
Table 29: Table of Comparative costs for each item of the Monopole Tower's construction .....	113
Table 30: Table of comparative costs for items associated with the Lattice Towers' construction .....	114
Table 31: Summary Table of Monopole Costs from construction to fabrication .....	114
Table 32: Summary Table of Lattice tower Costs from construction to fabrication .....	114
Table 33: Overall difference in costs between the monopole and steel lattice tower including construction costs .....	114
Table 34: Summary Table of Cost Comparisons between all entities averaged prices .....	118

## LIST OF SYMBOLS:

- [K] global stiffness matrix
- [K<sub>g</sub>] global geometric stiffness matrix
- [M] global mass matrix
- {x} vector of the buckling modes; or vibration mode vector
- a induction factor
- A rotor disk area
- A, B, C & D the terrain categories
- A<sub>b</sub> cross-sectional area of the unthreaded shank of the bolt
- A<sub>g</sub> gross effective area of a section
- A<sub>m</sub> shear area of the effective fusion face
- A<sub>ne</sub> net effective area of a section
- A<sub>p</sub> effective area of the compressed flange plate
- A<sub>w</sub> area of the effective weld throat, plug or slot
- b diameter
- $bP_m$  maximum tensile strength of the connection
- c<sub>0</sub>(z) topography coefficient
- c<sub>f</sub> force coefficient
- C<sub>p</sub> power coefficient
- c<sub>p,0,h</sub><sup>d</sup> base pressure coefficient
- c<sub>p,0,min</sub><sup>b</sup> value of the minimum pressure coefficient
- c<sub>pe</sub> external pressure coefficient
- c<sub>pi</sub> internal pressure coefficient
- C<sub>prob</sub> probability factor
- C<sub>r</sub> factored axial compressive resistance
- c<sub>r</sub>(z) roughness/height coefficient
- C<sub>w</sub> warping constant of a section
- d diameter of the unthreaded shank of the bolt
- D diameter of the washer face of the bolt head or nut

- $D_i$  equivalent diameter of the circular tube
- $D_p$  bolt pitch circle diameter
- $d_p$  diameter of the bolt hole
- $E$  Modulus of Elasticity
- $F_{fr}$  friction force
- $f_u$  tensile strength of the parent metal
- $f_u$  ultimate tensile strength of the bolts
- $F_w$  wind force
- $F_{w,e}$  external wind force
- $F_{w,i}$  internal wind force
- $F_{xT}$  horizontal, perpendicular static design wind load
- $f_y$  yield strength
- $F_{zT}$  vertical self-weight design load from the rotor and the nacelle
- $G$  Modulus of Rigidity
- $\chi_{G,Dead}$  partial factor for the ultimate limit state of self-weight loading
- $\chi_{Q,wind}$  partial factor regarding the limit state
- $I$  moment of inertia of a section
- $J$  torsion constant for the section
- $k$  surface roughness
- $l$  tributary length
- $l_p$  grip length, equal to twice the thickness of the flange
- $m_p$  full plastic moment per unit width of the flange
- $M_r$  factored moment resistance
- $M_u$  applied moment
- $M_{xT}$  or  $M_{yT}$  design bending moment due to rotor overhang and pseudo static wind loading
- $M_{zT}$  design torsion moment due to pseudo static wind and self-weight loads
- $P'$  tensile force applied to the specimen
- $P'_p$  yield load of the flange
- $P_p$  maximum load of the flange



- $P_s$  bolt separation load
- $q_p(z)$  peak wind speed pressure
- $R$  prying force; or radius of gyration; or rotor radius
- $Re$  Reynolds number
- $T_o$  bolt pre-load
- $T_r$  tensile resistance
- $T_s$  separation force
- $T_u$  applied tension
- $T_y$  yield strength of the bolt
- $\nu$  kinematic viscosity of the air ( $\nu=15 \times 10^{-6} \text{m}^2/\text{s}$ )
- $V$  undisturbed free-stream velocity of the air far from the turbine
- $V_b$  basic wind speed
- $V_{b,0}$  fundamental basic wind speed
- $v_p(z)$  peak wind speed
- $V_r$  shear resistance
- $V_{\text{turbine}}$  velocity of the air as it passes through the turbine blades in motion
- $V_u$  applied shear force
- $V_w$  mean free-stream wind velocity
- $W(z)$  distributed load along the tower
- $w_e$  external wind pressure
- $w_i$  internal wind pressure
- $X_u$  tensile strength of the weld metal
- $Z$  height above ground level
- $Z$  height above the ground level
- $Z_e$  elastic effective section modulus
- $Z_0$  height of the reference plane, and defined in table 1 of SANS 10160-3:2011
- $Z_c$  height below which no further reduction in wind speed is allowed as defined in table 1 of SANS 10160-3:2011
- $z_e$  reference height

- $Z_g$  gradient height, as defined in table 1 of SANS 10160-1:2011
- $Z_{pl}$  plastic effective section modulus
- $\alpha$  exponent as defined in table 1 of SANS 10160-3:2011
- $\alpha_A$  position of the flow separation
- $\alpha_{min}$  position of the minimum pressure, in degrees
- $\theta$  blade pith angle; or  $\theta$  is the angle of the axis of the weld
- $\lambda$  tip-speed ratio; or the effective slenderness; or buckling load factor
- $\rho$  density of the air
- $\sigma_u$  tensile strength of the flange material
- $\sigma_y$  yield point of the flange material
- $\phi$  material factor; or  $\phi$  is the solidity ratio
- $\Phi_b$  bolt material factor
- $\psi_{\lambda\alpha}$  end-effect factor
- $\omega$  rotor speed; or  $\omega$  is the circular frequency

## LIST OF ABBREVIATIONS:

BS British Standards

CHS Circular Hollow Section

DL Dead Load

EWEA European Wind Energy Association

FEA Finite Element Analysis

GRF Gust Response Factors

HAWT Horizontal Axis Wind Turbine

LC Load Case

SANS South African National Standards

SASCH South African Steel Construction Handbook

SLS Serviceability Limit State

SW Self Weight

SWET Stellenbosch Wind Energy Technologies

ULS Ultimate Limit State

VAWT Vertical Axis Wind Turbine

ZAR South African Rands

## CHAPTER 1: INTRODUCTION TO THE DESIGN AND ANALYSIS OF SMALL SCALE WIND TURBINES

The requirement for clean energy production world over has increased significantly in the last few years. The Kyoto Protocol which was introduced for enforcement on the 16<sup>th</sup> of February 2005 was a driving force for such requirements. The Kyoto Protocol was implemented with the view of reducing greenhouse-gas emissions produced by leading economies worldwide, by at least 5 per cent below the emission levels of 1990 between the periods 2008-2012.

A technology which has advanced immeasurably as a result of the necessity for green energy production is the wind power industry. One of the most important aspects of a wind turbine is its supporting structure. The tower of a wind turbine needs to be sufficiently reliable and structurally sound to ensure that the design life of the wind turbine machine is unaffected. The tower also needs to be of the correct height to ensure that the full potential of energy capture is realised.

The supporting structure of a wind turbine constitutes up to as much as 30% of the total costs of a wind turbine. The most common wind turbine supporting structures seen worldwide today are Steel Monopole Towers. The large cost proportion of the tower compels the industry to investigate the most feasible alternative supporting tower structures and thus prompted the research developed in this thesis. The focus is on small scale wind turbines (<50kW), more specifically, a 3kW Wind Turbine. The proposed alternative design for the support structures of small scale wind turbines to the presently used Steel Monopole tower was a Steel Lattice tower.

The merit of a more cost effective supporting tower for a wind turbine could have significant effects on the number of wind turbines that could be developed on a potential wind farm, as well as extremely positive outcomes for the Wind industry in South Africa.

The objectives of this thesis are:

1. Obtaining design criteria for the design of Steel Monopole and Steel Lattice Towers
2. Developing rational design methods for Steel Monopole and Steel Lattice Wind Turbine Towers
3. Creating Finite Element Models of each of the aforementioned Towers
4. Assessing each element of design from a cost perspective
5. Developing a feasibility analysis to compare the feasibility of each of the supporting structures from the factors determined in their design.

In order to develop an understanding of Wind Turbines, existing literature that described the way in which wind was transformed into energy as well as the kinds of loadings that could be expected on the towers of wind turbines was consulted. In researching Steel Monopole and Steel Lattice Towers, phases of the life cycle of such structures which would possibly influence the decision making of which one to use were considered by investigating the Pros and Cons of each tower. The development of the literature which was consulted is dealt with in Chapter 2.

For a thorough cost evaluation of a Steel Monopole and a Steel Lattice tower, each component that is required from a design point of view needs to be reviewed. Because most of the required information regarding wind turbine towers is proprietary information, it was decided upon to design each of the towers from scratch so as to have the best possible understanding of all of the elements which would need to be evaluated in the cost analysis.

The South African National design codes (SANS 10160:2011, and SANS 10162-1:2005) were consulted in conjunction with elements from the Eurocode (EN3-1) and the BS 8100 code in order to collectively form a rational design procedure for the two Steel Towers designed in this thesis.

The design of the Steel Monopole was a unique interpretation of the everyday tapered steel towers used for wind turbines, as it was designed as an assembly of pre-manufactured circular hollow sections. The purpose of this was to design the most cost effective possible Steel Monopole to compare to the proposed Steel Lattice tower. The Steel Lattice tower was a simple and robust design, suiting as many aesthetic qualities as possible while still adhering to stability. Many elements of the design of a Steel Lattice communication tower are the same as for a Steel Lattice Wind Turbine Tower, which implies that one has communication tower publications to consult for design guidance. Chapter 3 leads one through the process of design for the Steel Lattice and Steel Monopole Towers with all of the relevant design code extracts.

The details of any steel structure culminate in their connections. For the steel Lattice Tower gusset plate connections needed to be designed, and were done so from a geometric perspective using Autodesk Inventor Professional and SANS 10162-1:2005 to verify their strength.

The Steel Monopole towers' circular hollow sections were connected by means of circular ring flange connections. Because of the lack of South African literature detailing the design of circular ring flange connections, much research was done into the most likely yield lines which would occur in different possible modes of failure in order to assess the rational design of the Steel Monopole's connections.

Chapter 4 deals with the details of the connections of the two Steel Towers.

An important aspect to consider ensuring completeness of cost analysis is the design of the foundations of each of the two towers. The nature of the different base connections of the Steel Lattice and Steel Monopole towers resulted in different foundation designs. The construction and building quantities of each of the foundations were considered in the feasibility analysis. The designs of the foundations are covered in Chapter 5.

The design calculations executed in Chapter 3 needed to be verified and perhaps even altered through the iterative design process of Finite Element modelling and code verification. Both the Steel Monopole and the Steel Lattice Towers were modelled in the finite element package Strand7. All of the different analyses which were performed on the towers are described and presented in Chapter 6.

In Chapter 7, the feasibility from fabrication to construction of each of the towers is analysed. Each of the aspects which were identified through the design process from the structural design, construction and manufacturing which was pertinent to the cost analysis was considered. The outcome of the feasibility analysis in Chapter 7 provides worthwhile prospects for the future of wind energy development in South Africa.

A final chapter which concludes the research conducted for this thesis and makes possible recommendations as to where it might lead next is Chapter 8.

## CHAPTER 2: LITERATURE REVIEW

### INTRODUCTION

A literature review is presented in order to visit the literature that presently exists on a particular topic. The analysis and design of small scale wind turbines is a topic that has been researched in many parts, the accumulation of which is developed in this thesis, however what is significant is that in its entirety, it has not been covered to the extent that it shall be covered here.

For this reason, the literature that exists for each portion of this thesis shall be presented in the order in which the topics were developed, as follows:

1. The Understanding of Wind Energy
  - i) Motivation for wind energy
  - ii) How wind is turned into energy
2. Loads Induced by the Wind on a Wind Turbine Supporting Structure
3. Supporting Structures
  - i) Tower types
  - ii) Tower height considerations
  - iii) Pros and cons of each tower type
4. The Design of Supporting Towers
5. The Analysis of Supporting Towers
  - i) Finite Element Analysis
  - ii) Feasibility analysis

### 2.1 THE UNDERSTANDING OF WIND ENERGY

In order to be able to adequately design a supporting tower for a wind turbine, it was essential to fully understand Wind Energy.

#### 2.1.2 MOTIVATION FOR WIND ENERGY

There is an urgent and compelling case for the clean production of energy. Demand for energy is growing as the world population expands and industrialisation increases. Current production methods contribute to pollution of the environment whether we consider nuclear generation or generation of power by coal fired power stations. The latter have very large carbon footprints when seen in the context of global warming. Following the Fukushima nuclear disaster in March 2011 and as a direct consequence of the disaster the German Government, as one example, has decided to phase out its nuclear power plants and to concentrate instead on cleaner methods of producing electricity with wind power taking a new lead.

Increasing global energy costs have changed cost dynamics considerably meaning that alternative methods of power generation that were previously thought to be financially not viable are now treated with greater interest, not the least of which is wind power.

It is well known that the Kyoto Protocol that became effective on February 16, 2005, placed an obligation on industrialised countries to reduce their overall green-house gases at least 5% below the emission level of 1990 from 2008 to 2012 (Yeh, T and Wang, L, 2008: 592). Today still, most electrical energy is generated by burning fossil fuels. This form of power generation is thought to bring about adverse changes in weather conditions.

Furthermore, the burning of fossil fuels has produced severe environmental contamination in the form of acid rain, urban smog, and regional haze.

Although electricity can be generated in many ways using different kinds of energy, there is one common feature – the rotating of a turbine generator. In each instance of energy production, a fuel is used to turn a turbine, which drives a generator that feeds a grid.

A turbine is a rotary mechanical device that extracts energy from a fluid flow (air, water, other fuel) and converts it into useful work. Moving fluid acts on the blades so that they move and impart rotational energy to the rotor.

Turbines are designed to suit the particular fuel characteristics used to drive them. The same principal applies to wind-generated electricity. Although wind may be an intermittent source of energy, unlike fossil fuels, it is free and clean and there is an abundance of it. While political considerations and economics have played an important role in the development of the wind energy industry, and have contributed much to its present success, engineering still remains pivotal to its success (EWEA, 2009: 31).

Wind Turbines are most commonly utilised as a collection of units forming a wind farm. The particulars of the design strategies incorporating economics and site selection are critical to the success of wind farms. Many system integration studies that have been completed in recent years show that the number of wind farms in the USA and Europe have substantially increased in recent years. Due to the increasing number and size of wind farms across the world, the cost per kilowatt-hour of wind power generation has been reduced. This has major implications for the energy producing entities such as Eskom in South Africa. It has even greater implications for energy production in countries that have several forms of power generation, since the production costs per kilowatt-hour have become increasingly attractive. (Yeh, T and Wang, L, 2008: 592).

### 2.1.2 HOW WIND IS TURNED INTO ENERGY

A wind turbine obtains its power input by converting the force of the wind into torque acting on the rotor blades. The amount of energy which the wind transfers to the rotor depends on the density of the air, the rotor area, and the wind speed (The energy in the wind, 2011).

#### DENSITY OF THE AIR:

The kinetic energy of a moving body is proportional to its mass (or weight). The kinetic energy in the wind thus depends on the density of the air, i.e. its mass per unit of volume (The energy in the wind, 2011).

In other words the heavier the air, the more energy is received by the turbine. Air is denser when it is cold as opposed to when it's warm. At high altitudes, the air is less dense.

#### ROTOR AREA:

The rotor area determines how much energy a wind turbine is able to harvest from the wind. Since the rotor area increases with the square of the rotor diameter, a wind turbine which is twice as large can harvest four times as much energy (The energy in the wind, 2011).

Of the Important elements which should be examined regarding a wind turbine extracting energy from the wind (some of which were mentioned briefly), are the basic components of the wind turbine, including the brakes, hub, low and high speed shaft, gearbox, generator, nacelle and tower. Due to the motion of the wind turbine as well as the components of which it is made up, a wind turbine may exhibit various different movements, due to rotor and generator rotation, (Balas et al., 2003: 3781) such varying positions of the rotor are extremely important to take into account for different loading conditions.

Wind turbines can be designed as either upwind or downwind machines. In a downwind machine, the wind passes the tower first, before impinging on the rotor, with just the opposite for up-wind machines (Balas et al., 2003: 3781).

There is a difference between using the lift or drag force imposed on the blades by the wind in order to generate power. Sailors discovered very early that it is more effective to use the lift force (perpendicular to the wind) for effective propulsion. However in different regions, the orientation of the blades needs to be varied in order to harness the greatest power. From this there arise two different kinds of wind turbines, ones in which the blades are connected to a vertical shaft, named vertical-axis wind turbines (VAWT), and those in which the blades are connected to a horizontal shaft, HAWT(Hansen, 2008:4).

Horizontal axis wind turbines are the ones that shall be examined for the remainder of this research; they are also the majority of what is found in practice (Hansen, 2008:4).

Wind turbines can be classified as fixed speed (the rotor and generator rotational speeds are held constant) or variable speed. One of the main objectives for wind turbine control is to maximize power. The amount of power produced by a wind turbine can be expressed as:

$$P = \frac{1}{2} \rho A C_p V_w^3$$

Where P is the power, A is the rotor disk area,  $\rho$  the air density, and  $V_w$  the mean free-stream wind velocity (Balas et al., 2003: 3781).

$C_p$  is the power coefficient. In 1919 Albert Betz discovered that no wind turbine could convert more than 59.3% of the kinetic energy in wind to mechanical energy. This became known as Betz' Law and results in a maximum power coefficient of  $C_p=0.593$ . This is a maximum, and to calculate other values of the power coefficient, which is a function of the tip-speed ratio  $\lambda = \frac{\omega R}{V_w}$  and the blade pitch angle  $\Theta$ , where  $\omega$  is the rotor speed and R is the rotor radius, one calculates  $\lambda$  and uses it to determine the value of the power coefficient from the appropriate curve, see Figure 1. For an optimum energy production strategy, the tip-speed ratio and pitch angle should be chosen to give an optimum  $C_p$ .

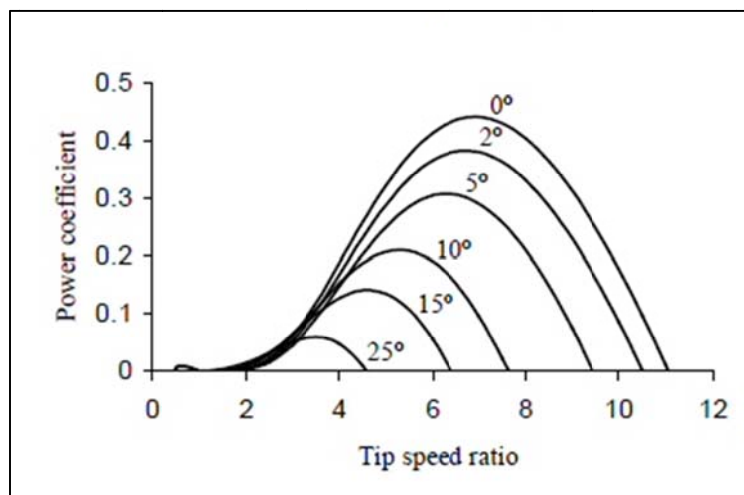


Figure 1: Power coefficient curve, parametrised in accordance with the blade pitch angle, image from

<http://www.caspus.eclipse.co.uk/ah/publications/3dmwtucfd.pdf>

The turbine should operate at this tip-speed ratio, regardless of the wind speed. Since the tip-speed ratio is a function of both rotor speed and wind speed, the rotor speed must be varied as the wind speed varies (Balas et al., 2003: 3781). For the fixed speed turbine this is not possible, although some attempt is made to optimize



energy by changing blade pitch to adjust aerodynamic torque as the wind speed varies. In the variable-speed machine, rotor speed can be changed by controlling generator torque (Balas et al., 2003: 3781).

The concept of a wind-driven rotor is ancient, and electric motors were widely disseminated, both domestically and commercially in the latter half of the 20<sup>th</sup> Century. Making a wind turbine with the historical volume of knowledge and understanding of wind energy harnessing seems simple but it is a major technical challenge to produce a wind turbine that:

1. Meets specifications (frequency, voltage, harmonic content) for standard electricity generation, with each unit operating as an unattended power station;
2. Copes with the variability of the wind (mean wind speeds on exploitable sites range from 5m/s to 11m/s, with severe turbulence in the earth's boundary layer and extreme gusts up to 70m/s), and;
3. Competes economically with other energy sources (EWEA, 2009: 63).

The function of a modern power-generating wind turbine is to generate steady quantities of network frequency electricity. Each wind turbine must function as an automatically controlled independent 'mini-power station' in order for it to fulfil its purpose effectively. The development of the microprocessor has played a crucial role in enabling cost-effective wind energy technology. A modern wind turbine is required to work unattended, with low maintenance, continuously for at least 20 years (EWEA, 2009: 63).

Following the determination of power generated by a wind turbine, a few important design elements that need to be considered are reviewed in greater detail here.

#### NUMBER OF BLADES:

The number of blades is usually two or three. Two bladed turbines are cheaper because they have one blade fewer; however as a result of just two blades they rotate faster and appear more flickering to the eyes. Three bladed turbines appear calmer and are therefore often preferred (Hansen, 2008:5).

Small-scale, multi-bladed (more than 3) turbines are still in use for water pumping. They are of relatively low aerodynamic efficiency but, with the large blade area, can provide a high starting torque. This enables the rotor to turn in very light winds and suits a water pumping duty (EWEA, 2009: 66). In general there are small benefits for rotors having an increasing number of blades. This relates to minimising losses that occur on the tips of the blades. These losses are, in aggregate, less for a large number of narrow blade tips than for a few wide ones.

In rotor design, an operating speed or operating speed range is normally selected first, taking into account issues such as acoustic noise emission as well as the flickering effect on the eye mentioned above. With the speed chosen, it follows that there is an optimum total blade area for maximum rotor efficiency (EWEA, 2009: 67). The number of blades is, in principle, open, but more blades imply more slender blades would be required for the fixed (optimum) total blade area.

It is hard to compare the two- and three-bladed designs on the basis of cost-benefit analysis. It is generally incorrect to suppose that, in a two-bladed rotor design, the cost of one of the three blades has been saved, and this is as a result of the power which is generated by two blades of a two-bladed rotor which does not equate with the power generated by two blades of a three-blade rotor.

The important factor in terms of the rotor's feasibility and how many blades to use apart from the noise and visual effects is how cost effectively the different rotors can produce a kilowatt hour. Two blade rotors generally run at a much higher tip speed than three-bladed rotors, so most historical designs would have noise problem. There is however no fundamental reason for the higher tip speed, and this should be discounted in a technical comparison of the design merits of the two versus three blades (EWEA, 2009: 68).

### PITCH VERSUS STALL:

The two principle means of limiting rotor power in high operational wind speeds are stall regulation and pitch regulation. The importance of having means by which to limit the power lies in the fact that turbines are designed structurally to withstand high winds and storms that affect the turbine statically; when the blades are not turning at the time of the high winds and storms. High winds have the potential to destroy a wind turbine if its blades are turning and the speed at which they are rotating is not controlled. Stall-regulated machines require speed regulation and a suitable torque speed characteristic intrinsic in the aerodynamic design of the rotor. As wind speed increases and the rotor speed is held constant, flow angles over the blade sections steepen. The blades become increasingly stalled and this limits power to acceptable levels, without any additional active control. In stall control, an essentially constant speed is achieved through the connection of the electric generator to the grid. Stall control is a subtle process, both aerodynamically and electrically (EWEA, 2009: 68). Stall control enables the wind turbine to essentially become less effective as the wind speed increases so as to protect the rotor from rotating too fast. As was mentioned above it is a means of control that is implemented by means of designing the blades in such a way that the speed control is intrinsic to their design.

In summary, a stall-regulated wind turbine will run at approximately constant speed in high wind without producing excessive power and yet achieve this without any change to the rotor geometry, or the rotor spinning out of control in a manner that could be detrimental to the turbine or turbine tower.

The alternative to stall-regulated operation is pitch regulation. This involves turning the wind turbine blades about their long axis (pitching the blades) to regulate the power extracted by the rotor. In contrast to stall regulation, pitch regulation requires changes of rotor geometry by pitching the blades. This involves an active control system, which senses blade position, measures output power and instructs appropriate changes of blade pitch. The introduction of the increased number of parts and the active pitch control which would need more maintenance than a stall controlled system increases the initial and on-going costs of this system. The objective of pitch regulation is similar to stall regulation, namely to regulate output power in high operational wind speeds (EWEA, 2009: 68).

## 2.2 LOADS INDUCED BY THE WIND ON A WIND TURBINE SUPPORTING STRUCTURE

The loads induced on the supporting towers as a result of the wind are divided into two different classes. First the wind acting on the tower as a pressure force is determined in accordance with SANS 10160-3:2011. Second the overturning force that the wind causes from its interaction with the rotor of the wind turbine is determined.

The Ultimate and Serviceability limit states for the aforementioned wind loads are determined by the load factors stipulated in SANS 10160-1:2011 as well as the wind speed.

In examining the wind in greater detail, the following observations were made. The conversion of the wind which passes through a wind turbine into energy as a power output is greatly dependant on Betz' Law as was discussed in section 2.1.2 .With this in mind, it is only up until a certain wind speed that the efficacy of wind energy production increases.

In Figure 2, a typical Power Curve for a Wind turbine is shown. At the cut-in wind speed of  $V_1$ , power starts being produced, in Region 2. The amount of power that can be produced by a particular wind turbine reaches its capacity at  $V_2$ .  $V_3$  indicates the wind turbines cut-out wind speed, which is the point at which the rotor turns out of the wind to protect itself from damage in higher wind speeds.

For the wind turbine designed in this thesis, the 3 kilo-watts of power desired are produced at a wind speed of 11m/s and a frequency of 300rpm. The cut-out wind speed is at 16m/s. For the wind turbine designed in this

thesis, the rotor's effective area perpendicular to the wind direction after cut out is half of the area which faces the wind before cut out. The rotor area is an important parameter in the calculation of the overturning force developed by the wind on the rotor. For these values, the forces acting on the towers calculated from the different wind speeds, result in the Serviceability Limit state loads calculated with the wind speed of 16m/s, and the Ultimate limit state loads calculated with the peak wind speed described by SANS 10160-3:2011.

Each of the aforementioned Serviceability limit state and ultimate limit state loads are then multiplied with the loading factors as described by SANS 10160-1:2011.

The other load that needs to be taken into consideration is the mass of the wind turbine nacelle and rotor, which in combination have one centre of mass. For the 3kW Wind Turbine Towers designed in this thesis, the combined mass of the nacelle and rotor is 125kg.

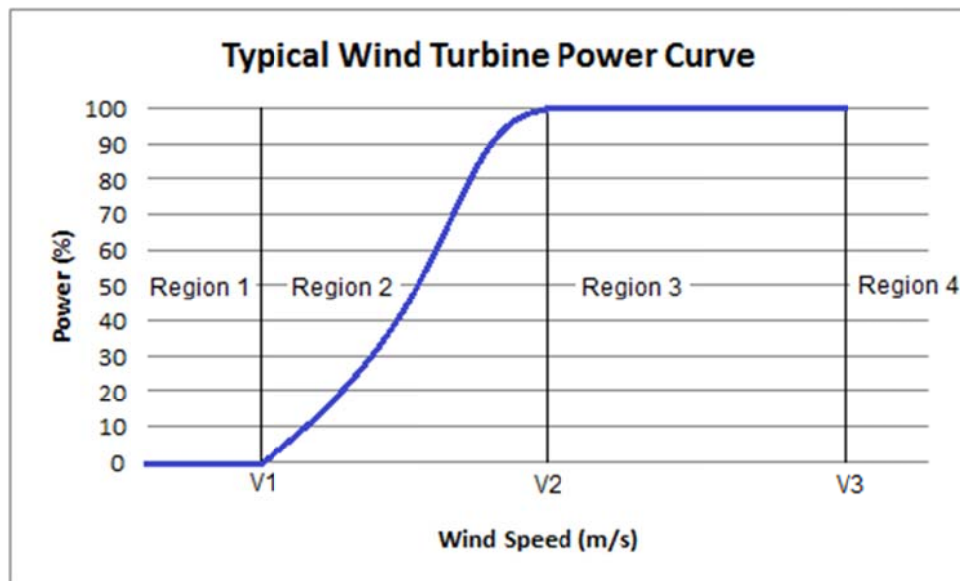


Figure 2: Typical Wind Turbine Power Curve

## 2.3 SUPPORTING STRUCTURES

The focus of this thesis is the design of two supporting towers for a 3kW wind turbine generator. The most widely used tower type for this purpose has become the Steel Monopole Tower. It was decided upon to investigate the feasibility of the equivalent design of a Steel Lattice Tower to be compared to the Steel Monopole. The existing literature pertaining to such design was difficult to obtain. Having determined in section 2.2 the forces that shall be acting on the tower, further important aspects which need to be considered in designing two such towers are examined here.

### 2.3.1 TOWER TYPES

Towers fall into categories: free standing and guyed. Freestanding towers also known as self-supporting towers and are just that, free-standing. They depend on a deep or massive foundation to prevent the tower from toppling over in high winds, and they must be strong enough internally to withstand the forces trying to bend the tower to the ground. Free-standing towers are more expensive than guyed towers but they take up less space, and in almost all instances are better suited to wind turbine supporting towers.

### FREE-STANDING TOWERS:

There are two types of freestanding towers. The most common is the truss or lattice tower, so called because it resembles the lattice work of trellis. The Eiffel tower is the best-known example of a truss tower. The monopole tower is another form of freestanding tower (Gipe, 2004: 151). Truss towers are typically more rigid than monopole towers. Towers can be designed to withstand any load, but as the size of the wind machine increases, so too, do the weight and cost of the tower supporting it. The same is true as the tower increases in height. The components become heavier, harder to move, and more costly to ship (Gipe, 2004: 151).

### LATTICE STYLE TOWERS:

Truss towers for small wind turbines can be assembled from a series of 6m sections (suitable for regular transportation). For small wind power machines, the sections may be preassembled and welded together prior to delivery. For house-hold sized turbines, the tower is shipped in parts, and must be assembled on site. Installation of truss towers usually requires a crane when they become large, and in order to lift the wind turbine onto the tower one the tower is erected. The tower is assembled on the ground, then hoisted into place and bolted to the foundation (Gipe, 2004: 152). Lattice towers that use welded steel profiles typically represent cost effective and tested solutions.

Lattice steel structures have been widely used for many large utilities including power transmission structures and telecommunication towers (Lee et al., 2006:709).

Conventional lattice steel towers used for power lines, the design of which would be comparable to the design of a turbine tower, usually comprise of angle (L-section) members. Typically there are bolted connections between secondary horizontal or bracing members; with the main members which are eccentric, and the secondary member is connected to one leg only. The towers are designed to resist design-factored loads at failure due to yielding, buckling, fracture and other limit behaviours (Lee et al., 2006:709). Although the wind turbine tower would be similar in appearance, the loadings on it would be unique as a result of the wind turbine generator attached to the top of it.

It has been noted that lattice tower structures with angle section members can be very difficult to analyse because of the complicated three-dimensional behaviour of the tower, in particular when considering large deformation and inelastic material response (Lee et al., 2006:709). This of course would also depend on the kind of software available for analysis.

Using finite element analysis, truss models have been frequently adopted for the linear analysis of lattice steel tower structures. However, it is well known that the truss model is not a good choice for obtaining the accurate nonlinear response of tower structures. The inelastic large deformation analysis using proper three-dimensional beam-column finite elements is necessary (Lee et al., 2006:709). And hence a suitable choice of finite element software to be able to perform such analyses needs to be made.

For the reliable failure analysis of lattice steel tower structures, the following are necessary:

1. Use of reliable three-dimensional L-section beam finite elements considering the combination of biaxial bending, axial stretch and shearing behaviours;
2. Modelling eccentricities of connections for members connected only on one leg;
3. Consideration of geometrical and material nonlinearities;
4. Use of proper connection models for the various typical joints (Lee et al., 2006:710).

The need to design a lattice tower for resonant dynamic response due to wind load arises when the natural vibration frequency (fundamental frequency) of the structure is low enough to be excited by the turbulence of the natural wind (Harikrishna et al., 1999:149).

The structural failure which is directly attributable to gust action emphasises the importance of these parameters in arriving at the gust wind load. The gust response factors (GRF) that will account for influence of these important parameters, is a measure of the effective dynamic load produced by gusts, and is intended to translate the dynamic response phenomenon produced by gust loading into a simpler factored static design criteria (Harikrishna et al., 1999:149). In the South African National Standards (SANS), the gust response factor has been accounted for in the above mentioned ways, in terms of having the gust loading being taken into account in the static peak wind pressure calculated in accordance with SANS 10160-3: 2011.

Currently, the wind sensitive structures are designed using a semi analytical approach with a simple model relating the upwind turbulent velocity fluctuations and fluctuating forces on the structure. In this approach, the dynamic response is treated using random vibration theory and modal analysis (Harikrishna et al., 1999:149). In most of the international design codes and standards, the gust response factor for the modal coordinate is computed using the above approach and the same value is considered for all other load effects such as bending moment, shear force etc. It is also assumed that the first mode of the structure varies linearly with height and the contribution of higher modes of vibration is neglected which in turn makes the gust response factor constant for the whole height of the structure (Harikrishna et al., 1999:149).

However, in the design of lattice towers, there is an apparent need for broadening the basis of design to include more explicitly, the load effects, such as the largest deflection, bending moment and shear force. These shall be accounted for in the accurate modelling capabilities of Strand7 Finite element package, as well as through hand calculations done in accordance with SANS 10160-1: 2011 and SANS 10162-1:2005.

## MONOPOLE TOWERS

Nearly all medium sized wind turbines are installed on monopole towers, though there are some notable exceptions. During the “great California wind rush” of the 1980s, an equal number of turbines were installed on lattice and monopole towers.

Considering the scale of today’s turbines, however, as well as aesthetic demands, these have led to the almost exclusive use of gently tapered monopole towers. Many observers consider freestanding monopole towers more aesthetically pleasing than truss towers.

This is certainly true in close up views of the towers, but it isn’t always the case. Surprisingly, monopole towers can be more visible at a distance than lattice towers, especially in silhouette. In arid regions lattice towers tend to blend into the landscape more easily (Gipe, 2004: 154). Pole or tubular towers are more expensive than lattice towers. The pole towers require a more substantial foundation than truss towers, which spread the overturning force over a wider base, and if designed correctly, shall not transmit the large overturn moments to the base, through the appropriate use of pinned connections.

The design considerations for monopole steel towers cannot be based on a particular design procedure outlined in a specific code. Rather through rational design methods and adapting the portions of the existing steel design codes to the identified elements of the monopole towers that can be designed using the codes provisions, a design procedure has to be established.

This can prove very difficult and time consuming from the point of view of special load and response phenomena which need to be considered and are particular to such types of structures. An example of such a phenomenon is Vortex Shedding, which is pertinent for slender structures with circular cross sections (Monopole towers). Design considerations such as these shall be examined in great detail in chapters to follow.

### 2.3.2 TOWER HEIGHT CONSIDERATIONS

Wind speed increases sharply with the tower height, causing a major increase in the electricity output of the system (Turbine Towers, 2011). The same small turbine can increase its power output by 30% or more if the height of its tower is 30m instead of 18m (Turbine Towers, 2011). However, the additional cost of a higher tower needs to be considered.

Usually the height of the towers and the dimensions and capacity of the turbines are intrinsically associated (Turbine Towers, 2011).

The height of a small turbine tower should take into account the height of the surrounding obstacles: to attain maximum efficiency, the height of the tower should allow the bottom of the turbine blades to be 10 meters or more above the top of any obstacle within 100 meters of the tower (Turbine Towers, 2011).

However, the tower height depends also on the turbine model and characteristics. Towers and wind turbines are often supplied together, and manufacturers demand their turbines to be mounted on their towers (Turbine Towers, 2011).

Another variable to be taken into account are the Local By-laws, they may impose height restrictions to wind towers: rules imposing maximums of 9-12 meters are common, particularly in residential areas which may have a negative impact on the electric power generated by wind turbines (Turbine Towers, 2011).

### 2.3.3 PROS AND CONS OF EACH TOWER TYPE

In examining the life cycle of a wind turbine the execution phase incorporates a number of elements to consider, such as the fabrication of the tower, how it's transported, and the ease of installation and maintenance associated with the tower type. Table 1 shows the Pros and Cons of each tower type in all the execution phase elements to be considered.

**Table 1: Pros and Cons of Each Tower Type**

Execution Phase Elements	Steel Lattice Tower	Steel Monopole Tower
<b>Fabrication</b>	The elements of a steel lattice tower, typically angle sections are easy to fabricate, and the sections of tower which are to be pre-assembled are done so through simple methods of bolting or welding.	Tapered steel monopole towers are specially fabricated from hot rolled steel. They are far more complex to fabricate than steel lattice towers, and as a result of that are most costly to fabricate.
<b>Transportation</b>	Steel lattice towers can be transported easily, and cost effectively as large numbers of elements can be stacked together and transported at one time.	Steel monopole towers need to be specially transported in large sections, or on one vehicle of abnormal sized load. Great care needs to be taken when transporting large thin walled section of tubular tower.
<b>Installation</b>	Steel lattice towers can be erected on site by means of elements that are bolted together. The level of expertise required to assemble a steel lattice wind turbine tower is no more than would be required for the everyday telecommunication steel lattice towers that are erected.	Steel monopole erection needs to be highly supervised. The tubular sections of hot rolled steel need to be crane lifted into place and the connections fixed in terms of bolted ring flanges or friction grip connections.

<b>Maintenance</b>	Steel lattice towers can be maintained on site. If an element of the tower needs replacing it can be done so on site. Steel lattice towers can be protected against corrosion by means of hot dip galvanisation during fabrication.	Steel monopole towers need to be returned to their place of fabrication if structural repairs need to be done, which is a costly exercise. Steel monopole towers can be galvanised during fabrication, however it is a rather skilled process that needs to make sure that the insides of the tubular sections are also well galvanised. Alternatively the steel monopoles can be painted and regular maintenance of the painting is done on site.
--------------------	---	--

It is clear in Table 1 that from the elements commented on, steel lattice towers have more pros than the steel monopole towers do. This is however seemingly strange when the most widely used towers are monopoles. The one aspect that was not covered in Table 1 which most commonly governs the choice of wind turbine supporting towers in developed countries is their aesthetic appraisal. It is for this reason that the pros of steel lattice towers versus the cons of the steel monopole were presented in Table 1 to exclude the subjective element of aesthetic preference.

## 2.4 THE DESIGN OF SUPPORTING TOWERS

As was mentioned in the introduction to this chapter, there is no readily available complete design method for the design of wind turbine supporting towers. Much of the information that is needed from companies that presently manufacture wind turbines is proprietary.

The design of the Steel Monopole tower for this thesis was done as an assembly of three pre-manufactured circular hollow sections which were connected to one another by means of circular ring flange connections.

The design of the Steel Lattice tower for this thesis was inspired by existing steel lattice towers, with allowance made for a straight portion at the top of the tower for the rotating blades of the wind turbine machine.

The design criteria which are prescribed by the South African design codes, in particular SANS 10162-1:2005, and SANS 10160, parts 1 and 3: 2011 were examined to design the towers. The extensive sections of the design codes which were utilised for design are presented in Chapter 3.

Other elements of design which were examined were the details of the connections required for each of the towers, as well as the foundations required for the two different towers.

## 2.5 THE ANALYSIS OF SUPPORTING TOWERS

The analysis of the two supporting towers designed for this thesis incorporated a finite element analysis which played an integral part of the design process. Apart from analysing the towers for structural stability, a cost analysis was performed on the two towers to assess which one of the two was more feasible.

### 2.5.1 FINITE ELEMENT ANALYSIS

The finite element package Strand7 was chosen to analyse the two steel towers. Strand7 has the capability of modelling a wide range of structures, which was attractive for the design of both the Steel Monopole as well as the Steel Lattice Tower.

Strand7 makes it possible to construct models, run analyses and investigate results simultaneously using a seamless interface. As well as its user-friendliness and extensive operating manual and theory manual available online, Strand7 has an extensive element library, the ability to model standard and specialist materials as well as a range of comprehensive solvers just to mention a few aspects.

The analyses which were performed on the two towers using Strand7 were the following:

1. Linear Static Analysis
2. Linear Buckling Analysis
3. Nonlinear Analysis
4. Dynamic Analyses
  - i) Natural Frequency Analysis
  - ii) Effects of an out of balance rotor
  - iii) Effects of vortex shedding due to wind action
  - iv) Harmonic Frequency Analysis
  - v) Modal Mass Participation Evaluation

## 2.5.2 FEASIBILITY ANALYSIS

The importance of having designed each of the towers from first principles and having designed the detailed connections required for each tower as well as their foundations was so that each element could be thoroughly understood when taking into account how to do a realistic and thorough cost analysis.

The elements of the execution phase which were mentioned in section 2.3.3 and were considered in the cost analysis were the following:

1. Fabrication
2. Construction

A list of elements pertaining to both of the above was given to a number of different companies who were asked for a unit price for each of the elements described in Table 2. From this it was possible to do a cost analysis for the quantities of each item that were required for each of the towers that had been designed in the preceding chapters.

The overall feasibility of the Steel Lattice tower in contrast to the Steel Monopole tower was then examined.

**Table 2: Cost Analysis Parameters**

<b>Item description</b>
<b><i>Earth Works</i></b>
1. Excavation of the foundations, including leveling and stockpiling of selected material for reuse in filling
2. Compaction of existing soil to Standard Proctor Optimum Density
3. Bituminous painting and sealing on concrete surfaces in contact with earth
<b><i>Concrete Works</i></b>
4. Reinforced Concrete
5. Steel trowel finish for slabs
6. High yield steel bar reinforcement
7. Cast in anchor bolts up to 20mm dia including templates
8. Cast in anchor bolts bigger than 20mm dia including templates
<b><i>Steel Work</i></b>
9. Preparation of shop detail drawing, fabrication, painting, delivery and erection of light steel structural steel work, complete with all the necessary cleats, shop bolts, brackets, gussets, packs and baseplates.



## CHAPTER 3: TOWERS

This chapter deals with the design procedure for the two steel towers considered for this thesis. It also examines all other aspects common to both steel towers.

The design and analysis of towers are always integrated, and obtaining the optimal design most often entails an iterative process. The design procedure begins with an initial layout of the geometry of the tower, which can be an extremely challenging task. The task of the geometric layout entails incorporating all of the special needs of the tower, as well as keeping aesthetics and economics in mind. Many of these design parameters can conflict one another, and finding a balance between the design, planning and construction is key.

### THE DESIGN PROCEDURE:

1. Geometric Layout
  - i) Monopole tower
  - ii) Lattice tower
2. Examining the boundary conditions of the Problem
3. Loading conditions
  - i) From the Wind
    - a) On the towers
    - b) As overturning forces acting on the rotor of the towers
  - ii) Wind Turbine machine effects
    - a) Mass of the nacelle and rotor
    - b) Dynamic effects
4. Validation of Geometric design
  - i) Finite Element Analysis (FEA)
  - ii) Using the FEA results in calculations specified by SANS 10162-1:2005 to validate the chosen steel elements.
5. Iterative design between steps i) and ii) in part 4 of the design procedure

Thereafter other general aspects of tower design shall be discussed.

### 3.1 THE GEOMETRIC LAYOUT

#### 3.1.1 THE GEOMETRIC LAYOUT OF THE STEEL MONOPOLE TOWER

For steel monopole towers, such as the ones shown in Figure 3 below, there are either monopoles with a constant diameter, or ones with varying diameter up the height of the tower.

For either a constant diameter monopole or a tapered monopole, the main load that needs resisting is the wind, either as a distributed wind load up the height of the tower, or as an overturning force from the wind acting on the rotor. The applied loads imposed by wind pressures on the tower need to be carefully considered for the effects of vortex shedding which may occur as a result of the circular cross-section associated with monopoles and the slenderness of wind turbine supporting towers.

The purpose of varying the diameter is because the largest moments occur about the base of the tower, where the stability is of importance. Because the motions of the tower include horizontal, vertical and even twisting motions, tensions arise at the base of a tower, where it connects with a relatively rigid earth through its foundation.

In order to take these tensions into account, the strength of the tower's lower components need to be adjusted in such a way that they can resist those moments and forces. Because the forces and moments are not as great in magnitude higher up on the tower, and in order to preserve materials and only provide what is required for resistance, the towers (most often heights > 20m) have tapered profiles.

For the case of the 16m high 3kW wind turbine tower designed for this thesis, it was decided to use standard circular hollow sections (CHS) that are regularly manufactured (as opposed to custom made sections). It was decided to use CHS of the same diameter over the height of the tower. The choices for the standard manufactured CHS were governed by the requirement of cost efficacy. Although the weight and material usage of standard CHS is higher than that of the same height tapered monopole, the cost of manufacturing a specialised tower design as opposed to using readily made sections is significantly higher.

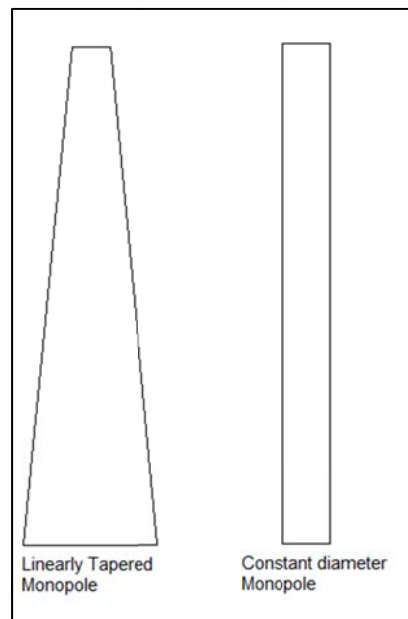


**Figure 3: Different Monopole Profiles**

The 16m high tower was divided into 3 sections of length smaller than 6m each. Each CHS then had ring flanges welded onto either end by full penetration welds. Figure 4 illustrates the ring flange connection type.



**Figure 4: Ring Flange connection for a CHS**

### 3.1.2 THE GEOMETRIC LAYOUT OF THE STEEL LATTICE TOWER

The primary load that a lattice tower of a wind turbine is subjected to is the wind; whether as a distributed load on the tower itself, or acting as an overturning force. The geometrical configuration of the tower is thus much subjected to the influence that the wind will have on it. Different geometrical layouts, such as square or triangular cross sectional layouts, will have different wind resistance. The choice of elements, such as angle sections, or circular sections creating the lattice will also affect the wind resistance of the tower.

For a tower, which stands alone without any significant masses or wind resisting objects attached to it, a triangular cross section compared to an equivalent square cross section has far less wind resistance. In terms of the internal elements, rounded elements are far less wind resistant than flat angle sections. So in order to create a free standing tower of the nature described above, with the lowest wind resistance, one would choose a triangular tower with tubular elements.

However, round sections have complicated end connections, and are also more expensive than the equivalent angle sections. Also, the optimum geometrical layout (mentioned in the paragraph preceding this one) is for the instance in which wind resistance is the focus of the layout optimisation, in an instance in which the attached objects and masses may create far greater wind resistance in comparison to that of the tower, using a square cross section, and using angle sections may fulfil other criteria. Factors to be considered in the selection process of elements include the following:

- Practical profile sizes
- The slenderness of individual members
- The price and delivery time
- Rational and cost effective production
- Uniform connection types resulting from member choice
- Facilities of hot-dip galvanising
- Transportation and erection

The manufacturing of angle sections has relatively low costs and the joints resulting from angle sections consist of bolts and plates and no welding is required on site. On the other hand the manufacturing of tubular

sections is more costly, from the point of view of price per kilo steel for tubes compared to other sections, and the connections required for tubular/round sections are more complicated and time consuming.

From the above mentioned reasons and other research, it was decided upon to have a square plan lattice tower, made from equal leg angle sections. The tower with square plan tapers inward from level ground up to the height of 13.5m, at which point it has parallel sides up to the top at 16m above ground level.

## 3.2 THE BOUNDARY CONDITIONS OF TOWER DESIGN

Both the steel monopole and the steel lattice towers were required to be 16m in height. They were both required to have adequate connections available at the top of the tower for the 3kW wind turbine machine, and the tower needed to have spatial allowance for the rotation of the 4m diameter blades of the rotor.

The Steel Monopole tower, being of constant diameter had no problem allowing space for the blade rotations of the rotor. Due to the nature of the ring flange connection on the base of the monopole tower it was designed to have a fixed base, which would transfer axial forces and moments to the foundation.

The Steel Lattice tower as was mentioned in the geometrical design had a parallel top section to allow for the rotation of the blades. The lattice design of the tower, allowed for equal leg angle sections to have pinned connections at the base of the tower which transferred no moments to the foundation, only axial forces.

## 3.3 LOADING CONDITIONS

Although there will be many elements of the design procedure for the Steel Monopole and the Steel Lattice Towers which will overlap, such as loadings, there will also be vast differences in terms of how those loads are applied to the two different structures. The design aspects most common to both designs are the applied loads associated with the 3kW wind turbine machine.

### 3.3.1 LOADING CONDITIONS FROM THE WIND

In terms of calculating the peak wind pressure acting on the tower for different heights, and also to determine the way in which the wind pressure was applied to different members, SANS 10160-3:2011 was consulted. For the sake of convenience, the sections of the SANS 10160-3:2011 that were used for calculations are repeated in this chapter. All SANS extracts are in *italics*.

First a summary of the calculation procedure followed is addressed, where after each of the steps needed in the procedure are examined.

#### ***SANS 10160-3:2011***

##### ***7.5 Wind Actions***

##### ***7.5.1 Calculation procedure***

*A summary of the calculation procedures for the determination of wind actions is given in table 5 of SANS 10160-3:2011.*

SANS 10160-3:2011		
Table 5-Calculation procedure		
1	2	3
Description	Symbol	Reference
Fundamental basic wind speed	$v_{b,0}$	Figure 1
Basic wind speed	$v_b$	Equation (1)
Terrain category	A,B,C,D	Table 2
Reference height	$z_e$	7.5.2.2
Topography coefficient	$c_0(z)$	7.3.3
Roughness/Height coefficient	$c_r(z)$	7.3.2
Peak wind speed	$v_p(z)$	equations (3) and (4)
Peak wind speed pressure	$q_p(z)$	Equation (6)
Internal pressure coefficient	$c_{pi}$	8.3.9
External pressure coefficient	$c_{pe}$	8.3.2 to 8.3.8
Internal wind pressure	$w_i$	Equation (7)
External wind pressure	$w_e$	Equation (8)
Wind Force calculated from force coefficient	$F_w$	Equations (9) and (10)
Internal Forces	$F_{w,i}$	Equation (11)
External Forces	$F_{w,e}$	Equation (12)
Friction Forces	$F_{fr}$	Equation (13)

**Table 3: Table 5 SANS 10160-3:2011**

**Section 7: wind speed and wind power**

**SANS 10160-3:2011 7.2 Basic Values:**

**7.2.1** The fundamental value of the basic wind speed,  $v_{b,0}$ , is the characteristic 10min mean wind speed, irrespective of wind direction and time of the year, measured at 10m above ground level in open country terrain with low vegetation, such as grass and isolated obstacles, with separation of at least 20 obstacle heights.

**7.2.2** The basic wind speed shall be calculated using the following equation:

$$v_b = c_{prob} v_{b,0}$$

Where  $v_b$  is the basic wind speed defined at 10m above ground terrain category B;

$v_{b,0}$  is the fundamental value of the basic wind speed corresponding to the specific geographical location, which shall be taken from figure 1 in SANS 10160-3:2011.

$c_{prob}$  is defined in section 7.2.3.

**7.2.3** The basic values are characteristic values having an annual probability of exceedance of 0.2, which is equivalent to a mean return period of 50 years. The probability factor,  $c_{prob}$ , is given in equation 2 which follows:

$$c_{prob} = \left[ \frac{1 - K \ln\{-\ln(1 - p)\}}{1 - K \ln\{-\ln 0.98\}} \right]^n$$

Where  $K$ , is the shape parameter depending on the coefficient of variation of the extreme value distribution with a value of 0.2, and  $n$  is the exponent with a value of 0.5.

Note; the return period may be taken as the design working life of the structure (see SANS 10160-1).

**7.3 Peak wind speed**

**7.3.1 Variation with height**

**7.3.1.1** the peak wind speed,  $v_p(z)$  at a height,  $z$ , above the terrain, depends on the terrain roughness and topography as well as basic speed,  $v_b$ , and shall be determined using the following equation:

$$v_p(z) = c_r(z)c_0(z)v_{b,peak}$$

Where  $v_{b,peak}=1.4v_b$ , in this equation, a conversion takes place from the 10min wind speed, in terms of which the basic wind velocities,  $v_{b,0}$  and  $v_b$ , are defined to a 3s gust wind speed.

$C_r(z)$  is the roughness factor, given in 7.3.2;

$C_0(z)$  is the topography (orography) factor, taken as 1.0 unless specified otherwise in 7.3.3.

**7.3.2 Terrain roughness**

**7.3.2.1** The terrain roughness factor,  $c_r(z)$ , accounts for the variability of the mean wind speed at the site of the structure due to

- a) the height above ground level, and
- b) the ground roughness of the terrain upwind of the structure in the wind direction under consideration.

The factor,  $c_r(z)$ , shall be determined using the following equation:

$$c_r(z) = 1.36 \left( \frac{z - z_0}{z_g - z_c} \right)^\alpha$$

Where

$Z$  is the height above the ground level;

$Z_0$  is the height of the reference plane, and defined in table 1 of SANS 10160-3:2011;

$Z_g$  is the gradient height, as defined in table 1 of SANS 10160-1:2011;

$Z_c$  is the height below which no further reduction in wind speed is allowed as defined in table 1 of SANS 10160-3:2011;

$\alpha$  is the exponent as defined in table 1 of SANS 10160-3:2011.

SANS 10160-3:2011				
Table 1-Parameters of wind profile				
1	2	3	4	5
Terrain Category	Height ( $z_g$ )	Height ( $z_0$ )	Height ( $z_c$ )	Exponent ( $\alpha$ )
A	250	0	1	0.07
B	300	0	2	0.095
C	350	3	5	0.12
D	400	5	10	0.15

**Table 4: Table 1 SANS 10160-3:2011**

**7.3.2.2** Various terrain categories are specified in table 2 of SANS 10160-3:2011.

**7.3.2.3** At low elevations above the ground level, the wind profile (i.e. magnitude of the  $c_r(z)$  factor) is strongly influenced by local surroundings, which are site specific and which may introduce acceleration of the wind flow.

This is especially relevant with in developed areas i.e. rough terrain categories. No further reductions in the wind speed below cut-off heights,  $z_c$ , which are stipulated in table 1 above, are permitted.

**7.3.2.4** The variation of the roughness factor,  $c_r(z)$ , with height, is given in table 3 of SANS 10160-1:2011.

**7.3.2.5** The terrain roughness to be used for a given wind direction depends on the distance of the terrain covered with a uniform roughness with angular  $\pm 15^\circ$  sector of this direction. Small areas, with a deviation in the roughness, which constitute less than 10% of the overall area, can be ignored.

**7.3.2.6** When there is a choice between adopting two or more terrain categories for a given area then the terrain category with the lower roughness shall be used.

**7.3.2.7** The smoother the terrain category in the upwind direction shall be adopted if a structure is situated near a change of terrain roughness at the following distances and in the following categories:

- a) Less than 2km from the smoother category A; or
- b) Less than 1km from smoother categories B and C.

In other cases the procedure described in A.2 of SANS 10160-3:2011 may be used.

SANS 10160-3:2011		
Table 2-Terrain Categories		
1	2	3
Category	Description	Illustration
A		can be seen in codes
B	Area with low vegetation such as grass and isolated obstacles (for example trees and buildings) with separations of at least 20 obstacle heights.	
C		
D		

**Table 5: Table 2 SANS 10160-3:2011**

**7.3.3 Terrain topography**

**7.3.3.1** Where the terrain topography (for example hills or cliffs) increases wind speeds by more than 5%, these effects shall be taken into account by using the topography factor,  $c_o(z)$ .

Note the recommended procedure is given in A.3 of SANS 10160-3:2011.

**7.3.3.2** The effects of topography may be neglected when the average slope of the upwind terrain is less than  $3^\circ$ . The effects of the up-wind topography have to be considered to a distance of ten times the height of the isolated topographical feature.

Sections 7.3.4 and 7.3.5 of SANS 10160-3:2011 do not need to be considered here.

**7.4 Peak wind speed pressure**

The peak wind speed pressure,  $q_p(z)$  at height,  $z$ , which includes the mean and short duration wind speed fluctuations, shall be determined using the following equation:

$$q_p(z) = 0.5\rho v_p^2(z)$$

Where  $\rho$ , is the air density, expressed in kilograms per cubic metre ( $\text{kg/m}^3$ ).

The recommended values of the air density as a function of altitude above sea level are given in table 4 of SANS 10160-3:2011.

SANS 10160-3:2011 Table 4-Air density as a function of site altitude	
1	2
Site altitude above sea level (m)	Air density $\rho$ ( $\text{kg/m}^3$ )
0	1.20
500	1.12
1000	1.06
1500	1.00
2000	0.94

**Table 6: Table 4 SANS 10160-3:2011**

*Note 1. A temperature of 20° has been selected as appropriate for South Africa and the variation of mean atmospheric pressure with altitude is allowed for in the above table.*

*Note 2. Intermediate values of  $\rho$  may be obtained from linear interpolation.*

Having determined the peak wind pressure, the details of how the wind loads are applied to the Steel Monopole are examined further by determining the pressure coefficients for circular hollow sections.

The force coefficient from section 8.10.2.1 as described by figure 30 in SANS 10160-3:2011 shall be used in the determination of the distributed wind load. This is discussed in further detail in section 3.3.2 of this thesis.

The way in which the peak wind pressure calculated in SANS 10160-1:2011 section 7.4 is applied to a steel lattice tower is up to the designer. The wind could be modelled as a pressure force on the elements facing the wind direction or as a series of point or line loads. As will be seen in Chapter 6, the manner in which the wind is modelled for a steel lattice tower has an insignificant effect on the overall response.



### 3.3.2 LOADING CONDITIONS INDUCED BY THE WIND AND THE WIND TURBINE MACHINE

The calculation procedure for determining the wind induced loading as a pressure force has now been examined. Next the other actions induced on the towers are examined. Figure 4 shows a schematic representation of the loads imposed on a wind turbine supporting tower. The loads shown in Figure 5 are pertinent to the Steel Monopole Tower as well as the Steel Lattice Tower.

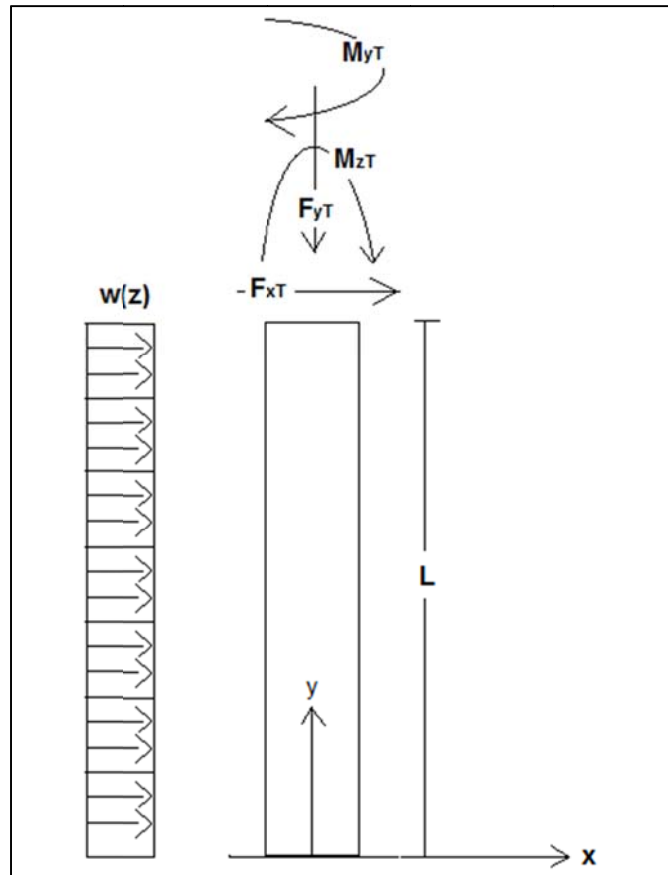


**Figure 5: Actions Induced on Wind Turbine Support Tower**

$F_{xT}$ , is the horizontal, perpendicular static design wind load on rotor and nacelle at hub height, and is calculated as follows (Peterson 2010, Report, page 40).

$$F_{xT} = \gamma_{Q,wind} q_p(z) A (4a(1 - a))$$

Where  $\gamma_{Q,wind}$  is the partial factor regarding the limit state,  $q_p(z)$  is the wind pressure at hub height,  $A$  is the swept rotor area of the blades of the wind turbine, and  $a$  is the induction factor of the turbine. The value of 'a' approaches 0.33 for a well-designed wind turbine, this is the value which is known as the Lanchester-Betz limit, and is the value at which the energy absorbed from the wind turbine is maximised. Since the objective is to create a well-designed wind turbine, the value of 'a' shall be used as 0.33 here. (Peterson, 2010, page 40). Although 'a' is regularly calculated as follows:

$$a = \frac{V - V_{turbine}}{V}$$

Where,  $V$  is the undisturbed free-stream velocity of the air far from the turbine, and  $V_{turbine}$ , is the velocity of the air as it passes through the turbine blades in motion, (rotor swept area). (Peterson, 2010, page 40).

The partial factor for the ultimate limit state is taken as  $\gamma_{Q,wind}=1.5$ , in accordance with **SANS 10160-1: 2011, Table 3-Partial factors for actions for the ultimate limit state**. The value of 1.5 is in accordance with the ultimate limit state partial factor for wind action on slender non-redundant structures that exhibit significant cross-wind response. The partial factor used for the serviceability limit state that is to be used in accordance with the  $F_{xT}$  force, is  $\gamma_{Q,wind}=0.6$ , in accordance with **SANS 10160-1: 2011 Section 8.3.1.1 The combination of actions for irreversible serviceability limit states**.

$F_{zT}$ , is the vertical self-weight design load from the rotor and the nacelle. For this self-weight component, the weight of the rotor and nacelle are added together and multiplied with the appropriate partial factor. As far as the live loading in the vertical direction is concerned, there isn't one. The partial factor for the ultimate limit state of self-weight loading is a factor of  $\gamma_{G,Dead}=1.2$ , this is in accordance with SANS 10160-1:2011, Table 3. The partial factor for the serviceability limit state of self-weight loading is  $\gamma_{G,Dead}=1.1$ . This partial factor for the serviceability limit state is in accordance with **SANS 10160-1: 2011 Section 8.3.1.1 The combination of actions for irreversible serviceability limit states**.

$M_{xT}$ , or  $M_{yT}$  is the design bending moment due to rotor overhang and pseudo static wind loading on the rotor and nacelle. This moment is simply the vertical self-weight design load multiplied with the distance by which it is eccentric, to determine the overturn moment that would cause. The moments are calculated for both instances of ultimate limit state and serviceability limit state, with the partial factors used in calculating the self-weight loads.

$M_{zT}$ , is the design torsion moment due to pseudo static wind and self-weight loads from the rotor and the nacelle. This moment holds no value for a parked wind turbine. Also for the purpose of this design procedure, the smooth bearings on which the wind turbine machine shall be mounted which naturally (not by means of mechanical instruction) turn the nacelle in and out of the direction of the wind provide little or no resistance to the turning motion. Thus for a running turbine too the torsional moment shall not be considered in this design process, as it is believed to have very little or no effect. This was in accordance with the manufacturing specifications of the wind turbine machine, however as a precaution, not shown in this thesis, a torsional moment was applied to the tower, of magnitude equal to ten per cent of the weight of the nacelle and rotor with a lever arm equal to the eccentricity caused by the centre of mass and the effects were indeed negligible.

$W(z)$  is the distributed load along the tower, which is as a result of the peak wind pressure and the external pressure coefficient  $c_{pe}$ . The load is appropriately multiplied with the partial loading factors for ultimate limit state and serviceability limit state, and the factors are the same as those used for the horizontal static design load  $F_{xT}$ . The distributed load is calculated as follows in accordance with **SANS 10160-3:2011 section 7.5.2.4** the wind pressure acting on the external surfaces,  $w_e$ , shall be obtained using the following equation;

$$w(z) = \gamma_{Q,wind} q_p(z) c_{pe}$$

Where,  $q_p(z)$  is the peak wind speed pressure;

$Z$ , is the reference height relevant to the external pressure;

$c_{pe}$ , is the pressure coefficient for the external pressure.

As it was discussed in the previous section, the distributed load from the wind shall be calculated with the force coefficient as opposed to the range of different external pressure coefficients.

In order to make the above distributed pressure force a uniformly distributed line load one would multiply it with the reference area upon which it is acting, in accordance with **SANS 10160-3:2011 section 7.5.3 Wind Forces**. One would multiply the peak wind pressure by the diameter of the tower, or width or angular steel element to obtain the distributed wind load in N/m.

Thus the equation used to calculate the distributed wind load will look as follows:

$$w(z) = \gamma_{Q,wind} q_p(z) c_f D$$

Where, the  $\gamma_{Q,wind}$  partial factor is taken as is was described earlier, and the value of  $q_p(z)$  is also as it was before, only the fore coefficient  $c_f$ , is inserted here, and is calculated as described above.  $D$  is the outside diameter of the tower for the steel monopole and the width of a steel equal leg angle section for the steel lattice tower.

### 3.4 VALIDATION OF STRUCTURAL DESIGN

The parts of the steel design code SANS 10162-1:2005 that are used to validate the structural design of the two steel towers are examined now. The first few sections are utilised for calculations that concern both the steel monopole and the steel lattice towers. For both towers, the validation of the geometric design begins with examining the effective cross sectional areas of members in terms of their slenderness ratios in tension and compression as well as the class classification of the elements in each tower.

The validation of design then examines the following:

1. Design Validation of Monopole Tower
  - i) Axial Compression
  - ii) Bending
  - iii) Shear
  - iv) Combined bending and axial compression
2. Design Validation of Steel Lattice Tower:
  - i) Effective cross sectional properties of compression members
  - ii) Flexural buckling of axially compressed members
  - iii) Design of tension members
  - iv) Combined bending and axial tensile or compressive forces

#### **SANS 10162-1:2005**

##### **Section 10.4: Slenderness Ratios**

###### **10.4.1 General**

*The slenderness ratio of a member in compression shall be taken as the ratio of effective length,  $K.L$ , to the corresponding radius of gyration,  $r$ . The slenderness ratio of a member in tension shall be taken as the ratio of the unbraced length,  $L$ , to the corresponding radius of gyration.*

###### **10.4.2 Maximum slenderness ratio**

**10.4.2.1** *The slenderness ratio of a member in compression shall not exceed 200*

**10.4.2.2** *The slenderness ratio of a member in tension shall not exceed 300. This limit may be waived if other means of flexibility, sag, vibration and slack in a manner commensurate with the service conditions of the structure, or if it can be shown that such factors are not detrimental to the performance of the structure or of the assembly of which the member is part.*

##### **Section 11: Width –to –thickness ratios: elements in compression**

###### **Classification of Sections**

**11.1.1** For the purposes of this standard, structural sections shall be designed as class 1, 2, 3 or 4 depending on the maximum width-to-thickness ratios of their elements subjected to compression, and as specified in 11.1.2 and 11.1.3. The classes are defined as follows:

a) class 1 sections will permit attainment of the plastic moment and subsequent redistribution of the bending moment;

b) class 2 sections will permit attainment of the plastic moment but need not allow for subsequent moment redistribution;

c) class 3 sections will permit attainment of the yield moment; and

d) class 4 sections will generally have local buckling of elements in compression as the limit state of structural resistance.

**11.1.2** Class 1 sections, when subject to flexure, shall have an axis of symmetry in the plane of loading and, when subject to axial compression, shall be doubly symmetric.

**11.1.3** Class 2 sections, when subject to flexure, shall have an axis of symmetry in the plane of loading unless the effects of asymmetry of the section are included in the analysis.

In order to classify the section as a specific class, one sees which category its parameters satisfy with regard to section **11.2 Maximum width-to-thickness ratios of elements subject to compression**.

**Table 3 in SANS 10162-1:2005** gives the maximum width-to-thickness ratios,  $W$ , of elements subject to axial compression. **Table 4 in SANS 101621:2005** gives the maximum width-to-thickness ratios,  $W$ , of elements subject to flexural compression. Sections with width-to-thickness ratios that exceed the maximum values in table 3 or the class limits in table 4 shall be designed as class 4 sections.

**Table 3 SANS 10162-1:2005** Maximum width-to-thickness ratios: elements in axial compression states that for circular hollow sections:

$$\frac{d}{t} < \frac{23000}{f_y}$$

Where  $f_y$  is the yield strength of the steel used to construct the tower,  $d$  is taken as the outer diameter, and  $t$  is the thickness of the section.

For Legs of angles, this would be used in the lattice tower classification:

$$\frac{b}{t} < \frac{200}{\sqrt{f_y}}$$

Where  $f_y$  is the yield strength of the steel used to construct the tower,  $b$  is taken as the width of the leg of an angle section, and  $t$  is the thickness of the section.

**Table 4 SANS 10162-1:2005** Maximum width-to-thickness ratios: elements in flexural compression states that for circular hollow sections:

$$\frac{d}{t} < \frac{13000}{f_y} \text{ class 1 sections}$$

$$\frac{d}{t} < \frac{18000}{f_y} \text{ class 2 sections}$$

$$\frac{d}{t} < \frac{66000}{f_y} \text{ class 3 sections}$$

### 3.4.1 DESIGN VALIDATION OF THE STEEL MONOPOLE TOWER GEOMETRY

#### 3.4.1.1 AXIAL COMPRESSION

**SANS 10162-1:2005 Section 13.3 Axial Compression:**

##### 13.3.1 Flexural Buckling

The factored axial compressive resistance,  $C_r$ , of doubly symmetric sections conforming to the requirements of clause 11 for class 1, 2 or 3 sections shall be taken as:

$$C_r = \varphi A f_y (1 + \lambda^{2n})^{-\frac{1}{n}}$$

Where  $n=1.34$ , for hot-rolled, fabricated structural sections, and hollow structural sections manufactured according to SANS 657-1.

$$\lambda = \frac{KL}{r} \sqrt{\frac{f_y}{\Pi^2 E}}$$

This compressive resistance only caters for loads caused by pseudo static or quasi static actions on the support tower structure due to wind loads and/or self-weight.

Torsional or torsional-flexural buckling is not examined, due to the geometric parameters which satisfy section 13.3.1 of SANS 10162-1:2005, and not 13.3.2.

Next, the bending resistance of the tower needs to be determined. When initially looking at the tower as a free-standing cantilevered column, one might be quick to assume that the bending resistance would be calculated in accordance with section 13.6 of SANS 10162-1:2005, which describes the procedure for laterally unsupported members, however, although the tower is laterally unsupported, in part c, of SANS 10162-1:2005 it is stated that for closed square and circular sections,  $M_r$  shall be determined in accordance with section 13.5.

#### 3.4.1.2 BENDING-LATERALLY SUPPORTED MEMBERS

**SANS 10162-1:2005**

##### 13.5 Bending-Laterally supported members

The factored moment resistance,  $M_r$ , developed by a member subjected to uni-axial bending moments about a principal axis and where continuous lateral support is provided to the compressive flange shall be taken as

a) For class 1 and class 2 sections

$$M_r = \varphi Z_{pl} f_y = \varphi M_p$$

b) For class 3 sections

$$M_r = \varphi Z_e f_y = \varphi M_y$$

c) For class 4 sections, further details are provided which shall be closely examined in the slightly more unlikely event that a class 4 section arises here. This is said in light of the fact that class 4 sections shall be avoided as far as is possible in terms of diameter and thickness considerations.

Where,  $Z_{pl}$  and  $Z_e$ , are the effective section moduli, taken as the plastic effective section modulus for class 1 and class 2 sections, and the elastic effective section modulus for class 3 sections. The equations for the moduli respectively are the following:

$$Z_{pl} = \frac{1}{6}(d_0^3 - d_i^3)$$

$$Z_e = \frac{\Pi(d_0^4 - d_i^4)}{32d_0}$$

### 3.4.1.3 SHEAR

The capability of the section to resist shear is slightly more intuitive, as can be seen by the following extract from the SANS.

#### **SANS 10162-1:2005**

##### **13.4 Shear**

##### **13.4.2 Webs of flexural members not having two flanges**

*The factored shear resistance for cross-sections not having flanges (e.g. solid rectangles, rounds or tees) shall be determined by rational analysis. The shear stress at ultimate load at any location in the cross-section shall not exceed  $0.66\phi f_y$ , and shall be reduced where shear buckling is a consideration.*

And so, by rational analysis it is fair to assume that the maximum shear stress resulting on the tower needs to be less than the following resisting shear stress calculated as:

$$\tau_r = 0.66\phi f_y$$

In terms of calculating the maximum shear stress occurring in the tower to check against the above equation, for circular hollow sections, the maximum shear stress which occurs on the neutral axis of the cross section is twice the average shear stress which occurs on the cross section, calculated as:

$$\tau = 2\frac{V}{A}$$

### 3.4.1.4 INTERACTION EQUATIONS: COMBINED BENDING AND AXIAL COMPRESSION

Now that the capability of the section to resist axial compression as well as bending has been determined the combination of axial compression and bending needs to be examined.

#### **Section 13.8.3 Member strength and stability-All classes of sections except class 1 and class 2 I-shaped sections**

*Members required to resist both bending moments and an axial compressive force shall be proportional so that*

$$\frac{C_u}{C_r} + \frac{U_{1x}M_{ux}}{M_{rx}} + \frac{U_{1y}M_{uy}}{M_{ry}} < 1.0$$

The following interaction equation has been adapted from the interaction equation obtained in SANS 10162-1:2005 section 13.8.3.

$$\frac{C_u}{C_r} + U_{1x}\frac{M_{ux}}{M_{rx}} < 1.0$$

The interaction equation has been adapted because in this instance of design,  $M_{ux}$  and  $M_{uy}$  is the same thing.

This relationship shall be assessed for both the ultimate limit state and the serviceability limit state. The value of  $U_{1x}$  is taken as 1 in accordance with SANS 10162-1:2005 section 13.8.2.

Shear capacity check at the base of the tower:

From rational analysis the check performed on the shear at the base of the tower is in accordance with the following:

$$\frac{V_u}{V_r} < 1.0$$

### 3.4.2 DESIGN VALIDATION OF THE STEEL LATTICE TOWER STRUCTURE

#### 3.4.2.1 DESIGN OF COMPRESSION MEMBERS: EFFECTIVE CROSS SECTIONAL PROPERTIES OF COMPRESSION MEMBERS

To verify the strength of the compression members, each element's effective cross section is examined.

In accordance with SANS 10162-1:2005 clause 10.4 Slenderness ratios, the parameters of the effective cross section and length of each member are examined to ensure that the slenderness ratio of the member does not exceed 200.

The moment of inertia of the cross section for each element, which shall be calculated about both axes is more critical for the axis about which the moment of inertia is smaller, since that is the axis about which buckling will occur, and the radius of gyration is determined according to the buckling direction.

#### 3.4.2.2 FLEXURAL BUCKLING OF AXIALLY COMPRESSED MEMBERS

Members of lattice towers may be considered as straight and axially compressed, and need to be checked for their factored axial compressive resistance.

The axial compressive resistance of each member can be calculated in accordance with SANS 10162-1:2005 clause 13.3 Axial Compression.

In the case of a member being subject to a compression load, which would fail due to instability, the resisting capacity of that member is dependent on not only the material values, but also the geometric dimensions of the member (Kiesling et al, 2003: 400). It shall be made clear in the design procedure that follows how the geometric dimensions (such as effective length,  $KL$ ) as well as the material values (such as yield strength,  $f_y$ ) are integrated into the resistance calculations.

Depending on the shape of the cross section, being singly, double or a-symmetric, the stability behaviour of the section is influenced. Also important is the position of the gravitational centre and the shearing centre, as well as the point of load action. Depending on the above mentioned criteria, flexural buckling, flexural torsional buckling or torsional buckling can occur (Kiesling et al, 2003: 406). Flexural torsional buckling or torsional buckling will be the more likely to be prevailing in members in which the slenderness ratio is lower.

Equal-leg angles are singly symmetric cross sections, the gravitational cross section of which does not coincide with the shearing centre (Kiesling et al, 2003: 406). The sections are assumed as centrally compressed such that the gravitational centre is the point at which the load is applied. A member can fail in the direction of the axis of symmetry in flexural buckling, or otherwise by flexural torsional buckling, see Figure 6.

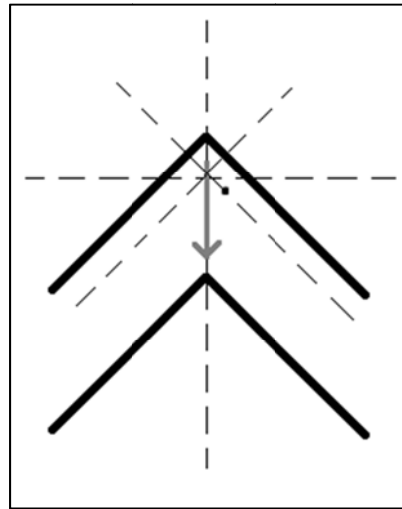


Figure 6: Flexural Buckling of an Equal Leg Angle

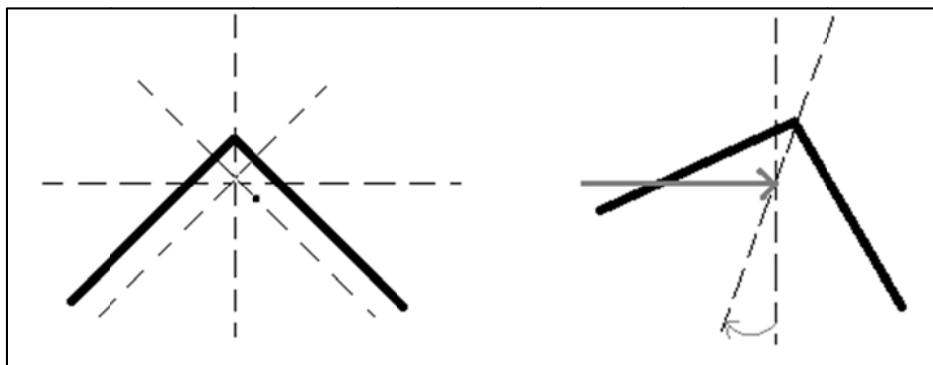


Figure 7: Flexural Torsional Buckling of an Equal Leg Angle

In the instance of flexural buckling, the cross section moves rectangularly to the axis of minimum radius of gyration, Figure 6. In the instance of flexural torsional buckling the equal leg angle moves rectangularly to the axis of symmetry, whilst translating along the other (longitudinal) axis, see Figure 7. Of the two, failing due to torsional flexural buckling will be dominant in the instance of angles with low slenderness ratios (Kiesling et al, 2003: 406).

### 13.3.1 Flexural Buckling

The factored axial compressive resistance,  $C_r$  is calculated as follows for sections conforming to the requirements of clause 11 for class 1, 2 or 3 sections:

$$C_r = \varphi A f_y (1 + \lambda^{2n})^{-\frac{1}{n}}$$

Where,  $n=1.34$  for hot-rolled, fabricated structural sections, and hollow structural sections manufactured according to SANS 657-1 (cold-formed non-stress-relieved).



$$\lambda = \frac{KL}{r} \sqrt{\frac{f_y}{\Pi^2 E}} = \sqrt{\frac{f_y}{f_e}}$$

### 13.3.2 Torsional or Torsional-flexural buckling

The factored compressive resistance,  $C_r$ , of asymmetric, singly symmetric, and cruciform or other bisymmetric sections not covered under 13.3.1 shall be computed using the expressions given in 13.3.1 with a value of  $n=1.34$  and the value of  $f_e$  taken as

b) for singly symmetric sections, with the y-axis taken as the axis of symmetry, the lesser of  $f_{ex}$  and  $f_{eyz}$ , where:

$$f_{eyz} = \frac{f_{ey} + f_{ez}}{2\Omega} \left( 1 - \sqrt{1 - \frac{4f_{ey}f_{ez}\Omega}{(f_{ey} + f_{ez})^2}} \right)$$

$$f_{ey} = \frac{\Pi^2 E}{\left( \frac{K_y L_y}{r_y} \right)^2}$$

$$f_{ez} = \left( \frac{\Pi^2 E C_w}{K_z^2 L_z^2} + GJ \right) \frac{1}{A \hat{r}_0^2}$$

$$\Omega = 1 - \left( \frac{x_0^2 + y_0^2}{\hat{r}_0^2} \right)$$

Where  $x_0$  and  $y_0$  are the principal coordinates of the shear centre with respect to the centroid of the cross section.

$$\hat{r}_0^2 = x_0^2 + y_0^2 + r_x^2 + r_y^2$$

For equal angle sections, 13.3.2 b) is the governing clause to follow, and the angle section's axes shall be defined where the U-U axis is taken as the Y-Y axis of symmetry for use in these calculations, and so by implication the V-V axis becomes the X-X axis. See Figure 8.

The values for the radius of gyration as well as the moment of inertia about a specific axis can be calculated as described above, or looked up in the South African Steel Construction handbook for a particular section.

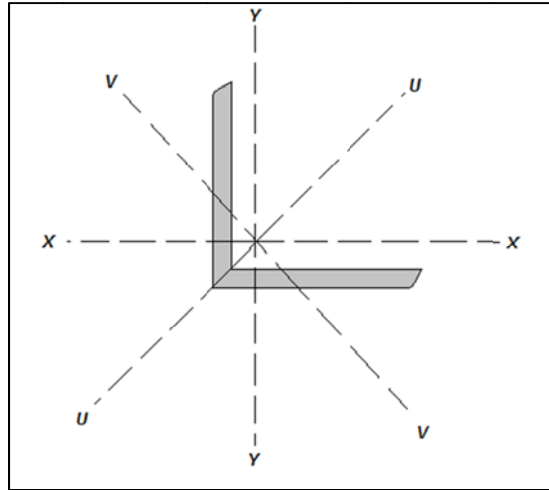


**Figure 8: Dimensions and Cross-Sectional Axes of Angle Sections**

In the possible instance in which one has an unequal angle section, the following would apply.

c) For asymmetric sections,  $f_e$  is the smallest root of

$$(f_e - f_{ex})(f_e - f_{ez}) - f_e^2(f_e - f_{ey})\left(\frac{x_0}{\hat{r}_0}\right)^2 - f_e^2(f_e - f_{ex})\left(\frac{y_0}{\hat{r}_0}\right)^2 = 0$$

Where

$$f_{ex} = \frac{\Pi^2 E}{\left(\frac{K_x L_x}{r_x}\right)^2}$$

In the instance of an unequal angle section, since there are no axes of symmetry, the x and y axis as defined horizontally and vertically in Figure 8 would remain as is for calculation purposes.

The following code extract is applicable for class 4 sections.

### 13.3.3 Class 4 members in compression

The factored compressive resistance,  $C_r$ , for sections that are designated as class 4 section according to clause 11 shall be determined by calculating the slenderness ratios of members using their gross section properties and an effective area which is calculated as follows:

a) When  $W \leq W_{lim}$

$$A_{ef} = A$$

Where

$A_{ef}$  is the effective area (see 13.3.3b));

$$W = \frac{b}{t}$$

$$W_{lim} = 0.644 \sqrt{\frac{kE}{f}}$$

' $f$ ' is the calculated compressive stress in the element ( $\leq f_y$ ), using ultimate limit loads and gross section properties;

' $k$ ' =4.0 for elements supported along both longitudinal edges; or

0.43 for elements supported along one longitudinal edge only.

When  $W > W_{lim}$ ,

$A_{ef}$  shall be determined using an effective area calculated with reduced element widths meeting either the maximum width-to-thickness ratios of class 3 sections or, where applicable, an element width equal to  $b$  to be taken as:

$$b_{ef} = 0.95t \sqrt{\frac{kE}{f}} \left( 1 - \frac{0.208}{W} \sqrt{\frac{kE}{f}} \right)$$

Which results in  $A_{ef} = A_g - 2(b - b_{ef})t$ .

### 3.4.2.3 BENDING AND AXIAL COMPRESSION

Bending about both principal axes combined with axial compression forces represents the most general loading of a member in a lattice tower (Kiessling et al, 2003: 408). In order to verify the design of members for these conditions, one would verify that the interaction equations were satisfied as was done in accordance with clause 13.8 of SANS 10162-1:2005.

### 3.4.2.4 DESIGN OF TENSION MEMBERS:

In order to verify the choice of the section of a member in terms of its capability to resist tensile forces, one will need to determine the tensile resistance of each member to a tensile force which should be relatively large in comparison to any compressive forces that member is required to resist. The tensile resisting capacity of a member is dependent on the nature of the end connections of the member.

In accordance to the SANS 10162-1:2005 clause 12 and 13.2 Axial tension member and connection resistance, the tensile resistance is calculated as follows.

#### 12 Gross and net areas

##### 12.1 Application

*Members in tension shall be proportioned on the basis of the areas associated with the potential failure modes. Members in compression shall be proportioned on the basis of the gross area.*

##### 12.2 Gross area

*Gross areas shall be calculated by summing the products of the thickness and the gross width of each element (flange, web, leg or plate), as measured normal to the axis of the member.*

##### 12.3 Net area and effective net area

12.3.1 The effective net area,  $A_{ne}$  shall be determined by summing the critical net areas,  $A_n$ , of each segment along a potential path of minimum resistance calculated as follows:

a) for a segment normal to the force (i.e., in direct tension)

$$A_{ne} = w_n t$$

b) for a segment inclined to the force

$$A_{ne} = w_n t + \frac{s^2 t}{4g}$$

12.3.2 In calculating  $w_n$ , the width of the bolt holes shall be taken as 2mm larger than the specified hole diameter. Where it is known that drilled or punched-and-drilled holes will be used, this allowance may be waived.

### 13.2 Axial tension member and connection resistance

The factored tensile resistance,  $T_r$ , developed by a member subjected to an axial tensile force shall be taken as

a) The least of

- i)  $T_r = \phi A_g f_y$
- ii)  $T_r = 0.85 \phi A_{ne} f_u$
- iii)  $T_r = 0.85 \phi A'_{ne} f_u$

And for pinned connections,

$$T_r = 0.75 \phi A_n f_u$$

### 3.4.2.5 COMBINED BENDING AND AXIAL TENSILE/COMPRESSIVE FORCES:

This was done in accordance with SANS 10162-1:2005 section 13.8.3, detailed in section 3.4.1.4 above. The equation is repeated here for convenience.

$$\frac{C_u}{C_r} + \frac{U_{1x} + M_{ux}}{M_{rx}} + \frac{U_{1y} + M_{uy}}{M_{ry}} \leq 1.0$$

## 3.5 DESIGN ITERATION

For the instances in which unsuitability of structural members were determined through the geometrical validation process, those members were improved and the process was run through again until the optimal members had been selected.

For the design of the Steel Monopole Tower, the smallest, thinnest CHS's were chosen in accordance with the boundary conditions of slenderness, and the 508x12.7mm CHS's were found suitable for all design parameters once modelled in Strand7.

The Steel Lattice Tower, constructed of equal leg angle sections of varying sizes, had all members examined for the design parameters stipulated in section 3.4 above. It was found through iterative design that the initial 50x50x3mm Angles (the smallest used in the tower design) were inadequate and were upgraded to 50x50x5mm Angles. The calculation results for this are shown in Table 7.

**Table 7: Equal leg angle section compression capacity**

Testing of Section Capacity			
Section	$C_u$	$C_r$	check
<b>50x50x3</b>	61865.54	59542.47	NOT OK
<b>50x50x5</b>	61865.54	101739.8	OK

### 3.6 GENERAL ASPECTS OF TOWER DESIGN:

For the Steel Monopole and the Steel Lattice Towers designed for this thesis design considerations which are relevant to both towers in general are the following:

1. The Materials
2. Material Protection
3. Tower Access
4. Tower Production
5. Fatigue

#### 3.6.1 MATERIALS

##### MATERIALS FOR THE CIRCULAR HOLLOW SECTIONS

The monopole design for this thesis incorporated the use of Circular Hollow Sections (CHS). In South Africa the Steel Institute recommends that Grade S355JR steel be utilised for steel design.

##### MATERIALS FOR ANGLE SECTIONS AND PLATES:

The angles used in lattice towers need to be sufficiently strong to withstand a number of different weather elements, as well as dynamic and vibrational loadings and also static loads. A superior capacity to deformation reduces the local stress peaks in the elements which aids in avoiding the development of cracks (Kiessling et al, 2003: 379).

The angle sections shall be made out of Structural steel. The term “structural steel” may be used to define steel for elements whose primary purpose is to support loads or resist forces which act on a structure (SASCH, 2008: 2.3). Both SANS 10162: Part 1 and SANS 2001-CS 1 require that steel for structural applications must comply with the requirements of SANS 1431.

The present situation in South Africa is that steel sections are produced to EN 10025-Hot rolled products of structural steels- Part 2: Technical delivery conditions for non-alloy structural steels, and specifically to Grade S355JR of the standard (SASCH, 2008: 2.3). The exception to the rule is the case of equal angle sections up to 50x50mm that are commonly made from commercial quality steel, and equal leg angle sections that are bigger than 50x50mm up to the size of 80x80mm that are made in either commercial quality or 355JR steel (SASCH, 2008: 2.3).

The mechanical properties of the different types of steel are given in Table 2.1 of the South African Steel Construction Hand Book.

##### MATERIALS FOR BOLTS:

Bolts of two property classes are commonly used for structural purposes in South Africa: Class 4.8 and Class 8.8 bolts. Both classes of bolts are commonly used with Class 8 nuts, although Class 5 nuts are permissible for class 4.8 bolts. The mechanical properties of bolts are given in Table 6.1 of The South African Steel Construction Handbook (SASCH). Table 6.1 also contains information on property Class 10.9, which is, from an economic standpoint not recommended for standard use, but rather for friction grip bolting. See Table 8 below.

**Table 8: SASCH Table 6.1**

SASCH Table 6.1
--------------------

Mechanical Properties of Bolts					
Property		Property Class			
		4.8	8.8		10.9
			d≤16mm	d>16mm	
Tensile Strength (MPa)	Nominal	400	800	800	1000
	Minimum	420	800	830	1040
Yield Stress (MPa)	Nominal	320	-	-	-
	Minimum	340	-	-	-
0.2% Proof Stress (MPa)	Nominal	-	640	640	900
	Minimum	-	640	640	940
Elongation at fracture (%)	Minimum	14	12	12	9

Table 6.2 in the South African Steel construction handbook shows the dimensions of the different sized bolts.

### 3.6.2 CORROSION PROTECTION

Structural steel is subjected to corrosion in the presence of moisture and oxygen. In a corrosive environment, the steel can be protected by painting, hot dip galvanising or metal spraying (SASCH, 2008: 2.8). The corrosion of a metal may be encouraged through contact with another metal in moist conditions; this is known as bimetallic, galvanic or electrolytic corrosion. It is thus advised that one insulate steel from other materials to prevent such accelerated corrosion in the areas of contact (SASCH, 2008: 2.8).

Virtually all of the steel lattice towers today are comprised of elements that have been hot dip galvanised. Hot dip galvanising incorporates creating a protective layer of iron-zinc alloy which is formed on the steel during the hot dip galvanising and above that layer one made of pure zinc is constituted.

After approximately ten to fifteen years the zinc layer will be weathered to such an extent that an alternative corrosion protection will be necessary. In areas of particularly corrosive atmospheres, the number of years in which the protection needs renewing may be vastly reduced (Kiessling et al, 2003: 378). There is however another method, in which together with the hot-dip galvanisation, a paint coating is applied directly to the elements. The galvanising together with the paint layer acts in a synergetic manner resulting in a more than doubled life cycle as that achieved by only one corrosion method alone (Kiessling et al, 2003: 379).

Obtaining an aesthetically pleasing hot dip galvanising finish is a function of the appropriate steel design, good fabrication and correct steel chemical composition. The chemical composition encompasses the amount of silicon (Si) and Phosphorus (P). For mining applications the Si should be between 0.15 to 0.3% with P less than or equal to 0.02%. For architectural purposes the Si should be 0.03% with P less than or equal to 0.01% (SASCH, 2008 2.12).

### 3.6.3 ACCESS

Steel lattice towers need to be ascended by experienced staff during construction and maintenance. In order to accommodate this, accordingly designed access needs to be provided. Ladders within the faces of the body of the structure can be installed (Kiessling et al: 2003, 377). Access should be installed on self-supporting steel structures, starting at a height of 3m above the ground to discourage unauthorised access of the structure by

strangers as well as vandalism. The access ladders can be a permanent fixture on the towers, or temporary attachments at times of maintenance (Kiessling et al: 2003, 377).

### 3.6.4 PRODUCTION

In the manufacturing process, the manufacturing of holes for bolts is a vital step in the production of steel lattice towers. There are a number of ways in which the holes can be made, they can be drilled or punched or subpunched and reamed. Punching full-size is a fast, economical way to get precise hole size, but the material thickness that can be punched is limited (Kiessling et al, 2003: 378).

In the manufacturing of steel monopoles, it is crucial to ensure that the fabricator is capable of high quality welding seems suitable to the hot rolled steel sections.

### 3.6.5 FATIGUE

The effect of cyclic loading is important to examine in design so as to avoid failure by fatigue. The following extract from the South African design codes is for fatigue considerations.

#### **SANS 10162-1:2005**

#### **26 Fatigue**

##### **26.1 General**

*In addition to complying with the requirements of clause 26 for fatigue, any member or connection shall also comply with the requirements for the static load conditions using the factored loads. Specified loads shall be used for all fatigue calculations. A specified load less than the maximum specified, but acting with a greater number of cycles, may govern and shall be considered. Members and connections subjected to fatigue loading shall be designed, detailed and fabricated so as to minimize the stress concentrations and abrupt changes in cross-section. The life of the structure shall be taken as 50 years, unless otherwise stated.*

##### **26.2 Proportioning**

*In the absence of more specific information, which is subject to the approval of the owner, the requirements of clause 26 in its entirety provide guidance in proportioning members and parts. Fatigue resistance shall be provided only for those loads considered to be repetitive.*

In Chapter 6, the details of the dynamic analyses which were conducted with respect to any possible repetitive loads are dealt with. The possibility of fatigue from repetitive cycles is minimised to the largest possible extent by using holding down bolts in accordance with the strength requirements in section 13.12.1.3.

The stress ranges to which the elements are exposed are also virtually negligible in terms of fatigue and the number of repetitive loads that may be applied in the tower's design life.

All of the detailed calculations done with respect to the design procedure covered in this chapter are shown in Appendix A.

Furthermore the Foundations of the two steel towers as well as the connection details for the two towers need to be designed, and are done so in the following two chapters.

## CHAPTER 4: CONNECTION DESIGN

This chapter serves to explain the process used to design the connections required in both the Steel Monopole and Steel Lattice towers.

The Steel Monopole tower required ring flange connection design for the points at which the three different sections of tower were joined, as well as a connection at the base of the tower which experienced the greatest moments and axial forces throughout the tower.

The Steel Lattice tower required the design of pinned connections for the ends of each member in the tower. As shall be discussed in this chapter under the pinned connections topic, the requirement of gusset plate design as a result of space limitations and redundancy design for bolts was also introduced.

### 4.1 MONOPOLE RING FLANGE CONNECTIONS

Researching a number of different publications to find a suitable design method for the detailed design of ring flanges connected by a number of tension bolts revealed that there was an immense amount of literature covering a number of detailed finite element analyses of the many complex aspects that arise in ring flange connections. Furthermore no immediate clear and concise design method was available.

In an article published by the department of Structural Engineering at the University of Tokyo, entitled “Bolted Tension Flanges Joining Circular Hollow Section Members” written by B. Kato and R. Hirose in 1985, a theoretical analysis of ring flange connections was developed.

The following design procedure was adopted from the theoretical analysis developed in the above mentioned article.

The first important element that was mentioned in the article was that for all ring flanged joints, high strength bolts were tightened to produce a pre-load of 60% of the proof load.

As shall be the case with the design of the ring flanges for the turbine tower, the wall thickness of the tubes is thinner than the corresponding flange thickness.

Theoretical analysis suggests that failure could occur because of one of three modes of failure:

1. Flexural failure of the flange plate
2. Fracture of the high-strength bolts, or
3. Fracture of the tube in tension.

The above 3 mentioned modes of failure are illustrated in Figure 9. The bending moments that develop as a result of such failures are illustrated in Figure 10.



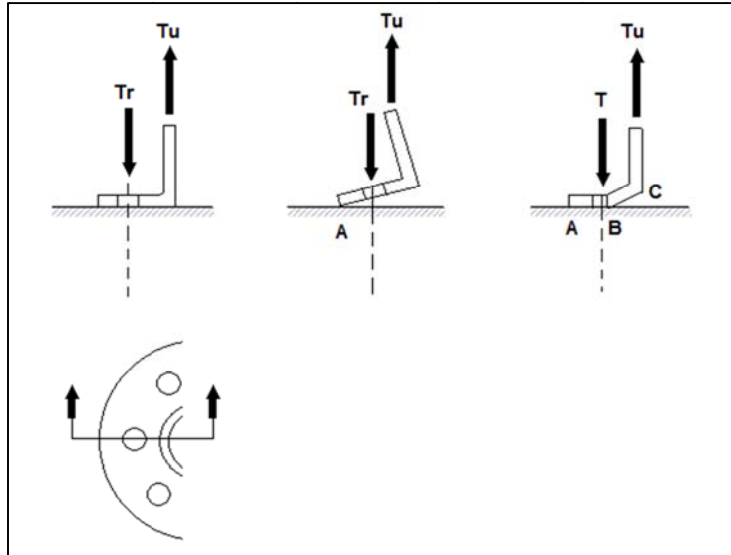


**Figure 9: Modes of Failure for Ring Flange Connections**

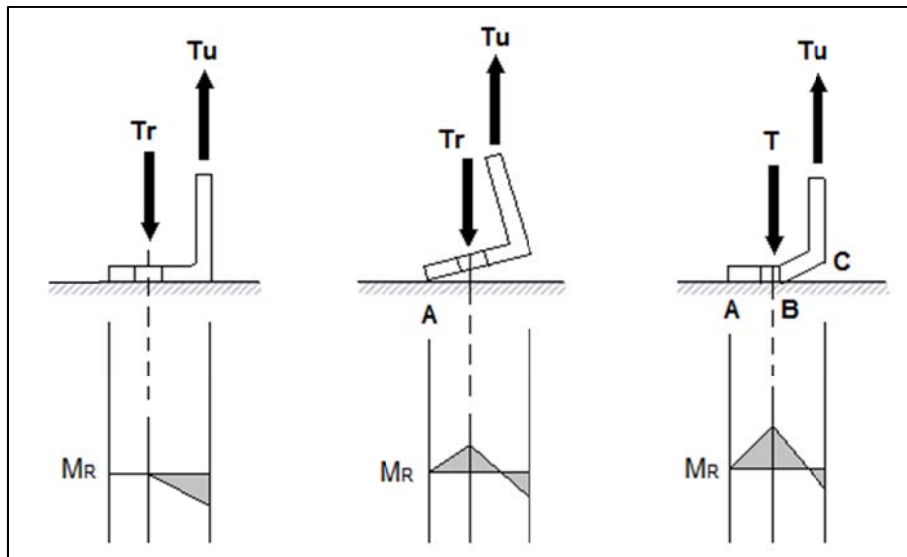


**Figure 10: Bending Moments developed in Ring Flange Connection Failures**

Theoretical analysis examines the bending strength of the flange plates by using the yield line theory, and the tensile force acting on the high-strength bolts is evaluated considering the prying force acting from the opposite side of the flange through the contact area.

The flange strength and the bolt force will reach different values depending on whether or not the ultimate state is reached before or after the occurrence of separation (perfect release of bolt pre-load).

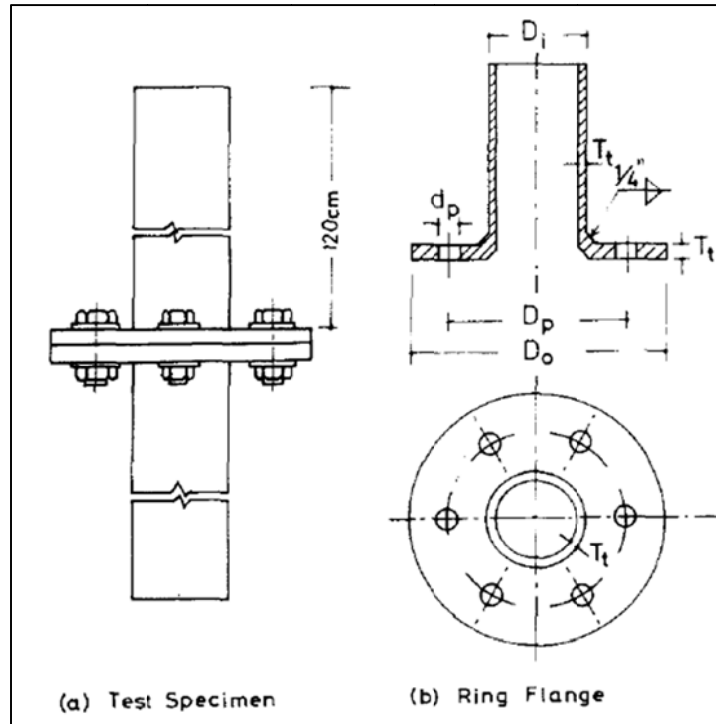


Figure 11: Ring Flange Connection Details

#### 4.1.1 BOLT FORCE AT SEPARATION:

First to be evaluated is the relationship between the force acting on the bolts at the instant of separation, a so called separation force,  $T_s$ , and the bolt pre-load  $T_o$ . The relationship is given as:

$$T_s = \alpha T_o$$

$$\alpha = 1 + \frac{A_b}{A_p}$$

In the above equations,

$A_b$  = the cross sectional area of the unthreaded shank of the bolt

$A_p$  = the effective area of the compressed flange plate

From the research conducted by the University of Cardiff as well as the University of Tokyo, the equation adopted for the determination of  $A_p$  is the following:

$$A_p = \frac{\pi}{4} \left[ \left( D + \frac{l_p}{6} \right)^2 - d_p^2 \right]$$

$D$  = the diameter of the washer face of the bolt head or nut, and

$l_p$  = the grip length, equal to twice the thickness of the flange

$d_p$  = the diameter of the bolt hole.

Using the above formulae, the different Separation force versus Bolt pre-load ( $T_s$  vs.  $T_o$ ) relationships are defined:

$$T_s = T_o \quad \text{for } 0 < T_o < \frac{T_y}{\alpha}$$

$$T_s = T_y \quad \text{for } \frac{T_y}{\alpha} \leq T_o$$

$$\alpha = 1 + \frac{d^2}{(D + \frac{d_p}{6})^2 - d_p^2}$$

$T_y$  = the yield strength of the bolt

$d$  = the diameter of the unthreaded shank of the bolt.

#### 4.1.2 MAXIMUM BENDING STRENGTH OF FLANGE FOLLOWING PLATE SEPARATION:

Due to the fact that the formation of a collapse mechanism in the flange occurs after the release of the bolt pre load, the constraint around the bolts need not be considered. A collapse mechanism is considered by looking at the possible patterns of yield lines along which the flange might collapse, and within this examination the existence of bolt holes is ignored. The suggested yield lines, taken from the theoretical analysis are the following:

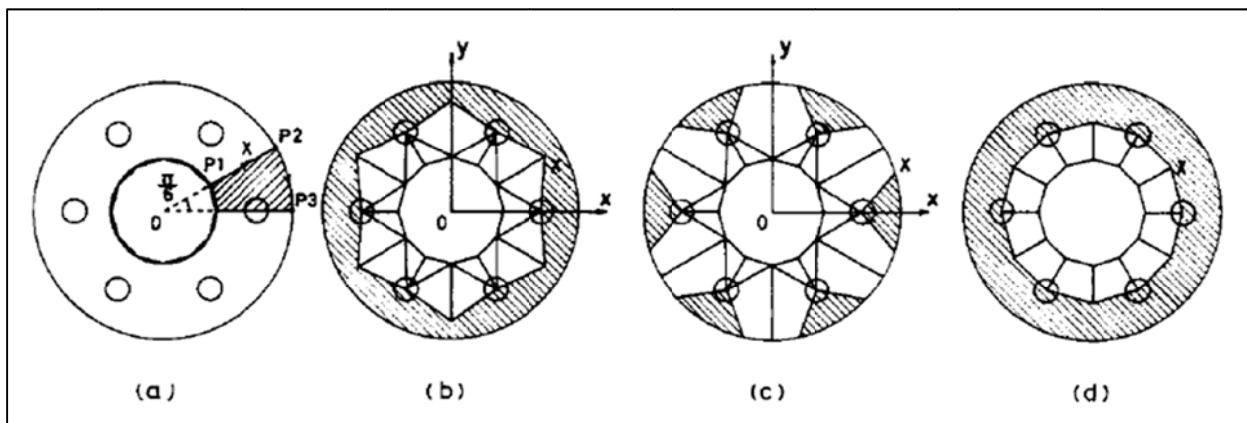


**Figure 12: Ring Flange Connection Yield Lines**

The equations that follow will need slight adaption, since they are developed for the above shown figures, where 6 bolts are considered. The analysis proceeds with the following steps:

1. First, as shown in Figure 12, the circular tube (flange) is approximated by taking a portion of the section; a twelfth of the flange is analysed taking symmetry into account. Of course the twelfth here is specific to the connection having 6 bolts, so in general one would take:

$$\text{portion of flange examined} = \frac{1}{2(\text{number of bolts})}$$

2. Next, different points on the section are examined, and different yield lines are determined for different positions of that point, and the result is that of different yield line patterns, which can be seen in part b and c of Figure 12.
3. Next the virtual plastic work done by the different points chosen in step two are examined for the different patterns shown above, and the location of the point at which the least virtual work is done is

the one which occurs at the intersection of lines P1 and P2 in part a) of Figure 12, which result in the bolt pitch circles displayed in part d) of Figure 12.

4. Finally, by applying the yield line theory to the yield pattern in part d) of Figure 12, the yield load of the flange,  $P_p$ , and the maximum load of the flange,  $P_u$  is obtained. The way in which they are calculated is shown in the equations below (Kato & Hirose, 1985):

$$P_p = U m_p$$

$$m_p = \frac{1}{4} T_f^2 \sigma_y$$

$$U = 48 \tan\left(\frac{\Pi}{12}\right) \left(\frac{D_p}{D_p - D_i}\right)$$

$$P_u = \frac{\sigma_u}{\sigma_y} P_p$$

$m_p$  = the full plastic moment per unit width of the flange

$D_p$  = the bolt pitch circle diameter

$D_i$  = the equivalent diameter of the circular tube

$\sigma_y$  = the yield point of the flange material

$\sigma_u$  = the tensile strength of the flange material.

The equivalent diameter ( $D_i$ ) for ring flanges defines the location of the plastic hinge line around the tube, which for the case of a ring flange which is joined by a fillet weld, happens to arbitrarily lie half way through the width of the fillet weld, leaving the equivalent diameter equal to the outer diameter of the tube, plus effectively, one weld width (Kato & Hirose, 1985).

Note here that the development of the equation for U in step 4 above is also particular to the example shown in Figure 11 for 6 bolts. The equation for U would need to be adapted to the number of bolts used as well as the portion of the flange examined for virtual plastic work. A proposed general equation for U is the following:

$$U = 8(\text{number of bolts}) \tan\left(\frac{\Pi}{2(\text{number of bolts})}\right) \left(\frac{D_p}{D_p - D_i}\right)$$

#### 4.1.3 MAXIMUM BENDING STRENGTH OF FLANGE WHEN SEPARATION OCCURS AFTER YIELDING OF THE FLANGE:

Where washers are used at the bolt heads and nut faces, a rigid zone can develop before separation takes place. A simple yield pattern which takes this zone into account is depicted below:

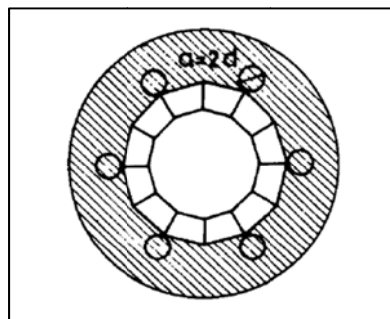


Figure 13: Ring Flange Connection: yield line before separation

Since the limit of the yield line is taken to the outer edge of the washer face, the outer diameter of the washer needs to be taken into account in calculating the yield load of the flange,  $P'_p$ , and the maximum load of the flange,  $P'_u$ , which is reached before separation occurs. The updated equations are:

$$P'_p = U'm_p$$

$$P'_u = \left(\frac{\sigma_u}{\sigma_y}\right)P'_p$$

$$U' = \left(48 \tan \frac{\pi}{12}\right) \left(\frac{D_p - a}{D_p - a - D_i}\right)$$

It is noted that strictly speaking the yield line theory is only applicable to the evaluation of the full plastic strength (yield strength) of the plate. However, it is assumed that the load-carrying capacity will increase almost linearly up until it reaches a maximum value of  $m_u$ , and (Kato & Hirose, 1985);

$$m_u = \frac{1}{4} T_f^2 \sigma_u$$

#### 4.1.4 EVALUATION OF THE PRYING FORCE:

If a flange is flexible, when the connection is subjected to a tensile force, it will bend, and the flange will be subject to a reaction force from the opposite flange through the contact face they share. The prying forces are examined separately for before and after separation.

#### 4.1.5 PRYING FORCE ACTING BEFORE SEPARATION:

When a flange yields before separation takes place, the prying force is distributed over the shaded area shown in the Figure 12 or Figure 13. In order to determine an estimate of the prying force, because the example in the article has 6 bolts, a twelfth of the circular flange is modelled as a rigid body on an elastic foundation, as shown below:

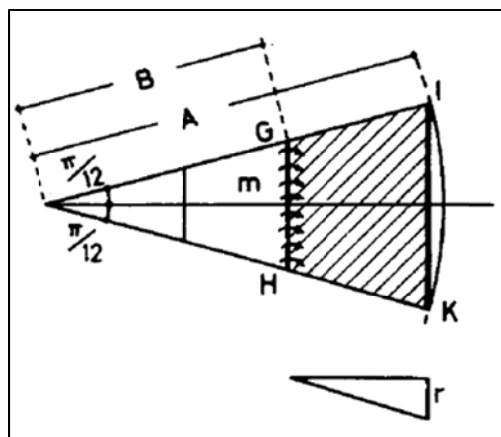


Figure 14: Prying Action Model

In the above twelfth of the circular flange, the arc of the section is approximated by a linear segment. A bending moment, of magnitude between  $m_p$  and  $m_u$ , is applied per unit length of the yield line GH. A reaction force per unit length along line IK is calculated such that there is equilibrium of the bending moment about line GH. It is assumed that the prying force is linearly distributed towards the edge of the flange as depicted by the shaded area in Figure 14.

The aforementioned bending moment equilibrium about the yield line GH is written as:

$$m \cdot 2 \cdot B \cdot \sin \frac{\Pi}{12} = \frac{1}{6} \left\{ \left( r \cdot \sin \frac{\Pi}{12} \right) \left[ (A - B) \cos \frac{\Pi}{12} \right]^2 (3A + B) \right\}$$

The above equation can be solved for r:

$$r = \frac{12 \cdot B \cdot m}{\left[ (A - B) \cos \frac{\Pi}{12} \right]^2 (3A + B)}$$

Then the total reaction acting throughout the circular flange, R, is:

$$R = \left( \frac{48 \cdot B(2A + B)m}{(A - B)(3A + B)} \right) \tan \frac{\Pi}{12}$$

Taking note that this is the pre-separation state,  $A = D_o/2$  and  $B = D_p/2 - a/2$ . Introducing A and B into the above equation for the reaction R, a ratio of *prying force* to *external load* at this level of hinge moment m is calculated. The external load  $P'(m) = U'm$  is obtained by replacing the  $m_p$  with m.

$$\beta_1 = \frac{R}{P'(m)} = \frac{(D_p - a - D_i)(2D_o + D_p - a)}{(D_o - D_p + a)(3D_o + D_p - a)}$$

It is assumed that the above ratio is also applicable to the state when the flange is elastic.

When the flange has yielded and separation takes place, the reaction force will be distributed along the edge line of the flange, line IK in Figure 14. In order to calculate the reaction per unit length of line IK, call it  $r_s$ , the equilibrium of the bending moment about line GH is calculated as:

$$m \cdot 2 \cdot B \cdot \sin \frac{\Pi}{12} = r_s (A - B) \left( \cos \frac{\Pi}{12} \right) \left( 2 \cdot A \cdot \sin \frac{\Pi}{12} \right)$$

And then  $r_s$  can be solved for:

$$r_s = \frac{B \cdot m}{A(A - B) \cos \frac{\Pi}{12}}$$

And the corresponding total reaction acting throughout the circular flange,  $R_s$ , is:

$$R_s = 24 \left( \frac{B \cdot m}{A - B} \right) \tan \frac{\Pi}{12}$$

Taking note that this is the post separation state,  $A = D_o/2$  and  $B = D_p/2$ . If A and B are introduced into the above equation for  $R_s$ , then once again the ratio of the prying force to the external load at this level of hinge moment, m, can be determined:

$$\beta_2 = \frac{R_s}{P(m)} = \frac{D_p - D_i}{2(D_o - D_p)}$$

No prying action will act when the flange remains elastic at the time of separation, but a reaction will occur as soon as yielding of the flange begins due to further increases of the load (Kato & Hirose, 1985).

#### 4.1.6 SEPARATION LOAD AND FRACTURE LOAD OF THE BOLTS:

#### 4.1.6.1 SEPARATION LOAD:

Separation of the bolts in the connection takes place when the sum of the tensile force applied to the specimen,  $P'$ , and the prying force,  $R$  reach the separation force of the bolts,  $\Sigma T_s$ , defined in the above section on bolt forces at separation (4.1.1). This equation form is the following:

$$P' + R = (1 + \beta_1)P = \Sigma T_s$$

Or

$$P' = P_s = \frac{\Sigma T_s}{1 + \beta_1}$$

Where  $P_s$  is the bolt separation load.

#### 4.1.6.2 FRACTURE LOAD OF THE BOLTS:

*Fracture of the bolts occurring after yielding of the flange:*

Here, the maximum tensile strength of the connection,  ${}_bP_m$ , is derived as follows:

$$P + R_s = (1 + \beta_2)P = \Sigma T_u$$

Or

$$P = {}_bP_m = \frac{\Sigma T_u}{1 + \beta_2}$$

In which  $T_u$  is the tensile strength of a bolt, and it is noted here, that this process is necessarily accompanied by bolt separation.

*Fracture occurring before yielding of the flange:*

Here, the maximum tensile strength of the connection,  ${}_bP_m^o$ , is given as follows, since no prying action will be imposed on the bolts:

$${}_bP_m^o = \Sigma T_u$$

#### 4.1.7 MAXIMUM STRENGTH OF A JOINT:

Having viewed all of the important factors which influence the maximum strength of a joint, a summary is presented here:

1. Critical loads corresponding to flange failure
  - i. When the flange yields and reaches its maximum strength before separation takes place, yield load of the connection:

$$P'_p = U'm_p$$

$$\text{Maximum load of the connection: } P'_u = \left(\frac{\sigma_u}{\sigma_y}\right)P'_p$$

- ii. When the flange yields after separation takes place, the yield load of the connection:

$$P_p = Um_p$$

$$\text{Maximum load of the connection: } P_u = \left(\frac{\sigma_u}{\sigma_y}\right)P_p$$

2. The critical loads corresponding to bolt failure

i. Bolt separation load (yield load)

$$P_s = \frac{\Sigma T_s}{1 + \beta_1}$$

ii. Maximum load of the joint when yielding of flange occurs first

$$bP_m = \frac{\Sigma T_u}{1 + \beta_2}$$

iii. Maximum load of joint when the bolts yield and fracture before yielding of the flange occurs,

$$bP_m^o = \Sigma T_u$$

Depending on the relative magnitudes of the above values, the maximum strength of the connection is determined as follows:

1. Connection material fracture occurring before separation

1i. Failure of the flange takes place when  $P'_u < P_s$ . Thus the maximum connection strength is:

$$P_{max} = P'_u$$

1ii. Failure of the bolts does not occur because bolt failure must precede bolt separation.

2. Connection failure occurring at the instant of separation

2i. Failure of the flange takes place when  $P_u < P_s < bP_m$  or when  $P_u < bP_m < P_s$ . The maximum connection strength is:

$$P_{max} = P_s$$

2ii. Failure of the bolts occurs when  $bP_m < P_p < P_s < P_u$  or  $P_p < bP_m < P_s < P_u$  or  $bP_m < P_u < P_s$ . The maximum connection strength is:

$$P_{max} = P_s$$

3. Connection failure where the flange yields before bolt separation occurs

3i. Failure of the flange is reached before fracture of the bolts occurs, when  $P_s < P_u < bP_m$ . The maximum connection strength is:

$$P_{max} = P_u$$

3ii. Bolt failure occurs immediately after yielding of the flange, when  $bP_m < P_s < P_p < bP_m^o$  or  $P_s < bP_m < P_p < bP_m^o$ . The maximum connection strength is:

$$P_{max} = P_p$$

3iii. Failure of the bolts occurs between the yielding of the flange and flange failure, when  $P_p < P_s < bP_m < P_u$  or  $P_s < P_p < bP_m < P_u$ . The maximum joint strength is:

$$P_{max} = bP_m$$

4. Connection strength occurs due to rupture of the bolts occurring before the flange yields, when  $bP_m^o < P_p$ . The maximum connection strength is:

$$P_{max} = bP_m^o$$

5. When the tensile strength of the tube is lower than any of the above mentioned connection strengths, failure in the tube will occur first.

Because all of the above equations and strength conditions are functions of the bolt's diameter, tube diameter, bolt pitch circle diameter, flange diameter, and flange thickness, the failure mode of a connection is determined by the relative sizes of the above mentioned geometrical parameters (Kato & Hirose, 1985).



### 4.1.8 SUGGESTED DESIGN METHODS:

#### GENERAL PROCEDURE:

The strengths,  $P_p$ ,  $P_u$  and  $P'_u$  increase with decrease of bolt pitch circle diameter,  $D_p$ , as can be observed in the above equations. The distance of bolthole from the tube wall, however, is limited by the practicalities of bolt-tightening. The minimum  $D_p$  is set to  $D_p=D_i+3d$ , assuming that the minimum feasible bolt distance is 1.5d. Other observations such as how the ratios  $\beta_1$  and  $\beta_2$  decrease with an increased flange diameter also may influence the choice of flange diameter, however for practical purposes, it also looks ugly having too large a flange. The flange diameter is set to  $D_o=D_p+4d$  as an optimum size, assuming the distance from the centre of the bolt hole to the edge of the flange is to be 2d.

#### SIMPLIFIED DESIGN:

The relationship between the maximum strength of a connection and the flange thickness is shown in the following figure:

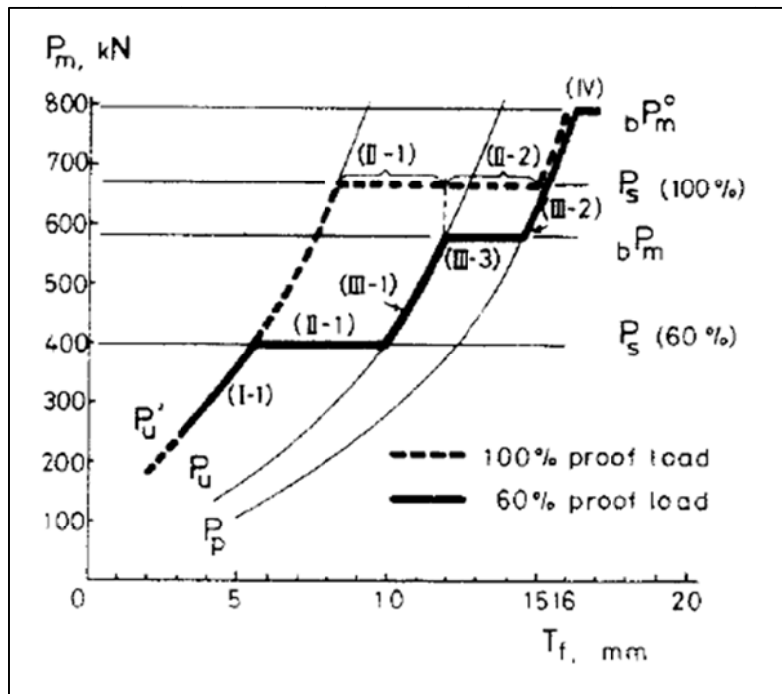


Figure 15:  $P_{MAX}$  versus  $T_f$  relation

The above values are obtained using the limited connection geometry stipulated above under general procedure (4.1.8). It can be seen that the connection strength can be increased considerably by using the larger pre-load for the bolts for a certain region of flange thickness. When the flange thickness exceeds a critical value, bolt failure occurs before yield of the flange. In this case the connection strength can be attributed to the strength of the bolts since the prying force will not influence the behaviour. Such a design can be considered to be most effective if the increase of weight of the joint is not substantial. If this design is adopted, the maximum strength of the joint should be proportioned to be larger than the yield strength of the tube, since sufficient deformation capacity cannot be expected in the joint itself (Kato & Hirose, 1985).

#### 4.1.9 CONNECTION DESIGN FROM BASIC PRINCIPLES:

From the knowledge gained through extensive research done into the design of circular ring flanges, the following design method is developed from the basic principles of equilibrium, and a similar approach to the design method for prying action presented in the South African Steel Construction Handbook (SASCH).

For the design of the ring flange connections, from the finite element analysis done in Strand7, the tensile and compressive forces at the connection points were known, as well as the applied moment that needed resisting due to the imposed loads.

However, the dimensions of the flanges and the number of bolts and the intervals at which they were to be spaced were initially estimated. Iterative cycles of design and calculation were then done until an appropriate design capable of resisting the applied loads was defined.

The first step was deciding upon the number of bolts, and the spacing between them.

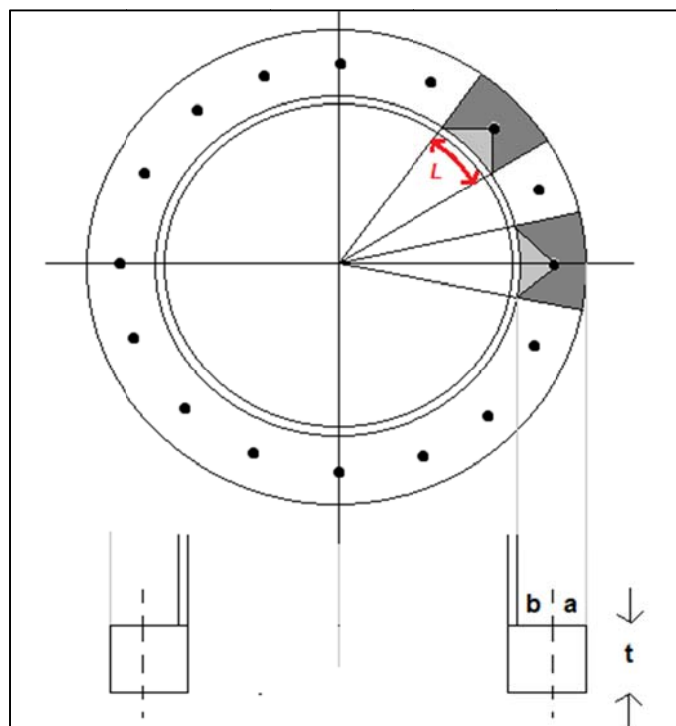


**Figure 16: Bolt Spacing and Tributary Length**

Figure 16 illustrates the layout of bolts chosen to begin the design procedure. The bolts were chosen as M20, Class 10.9S bolts in accordance with recommendations from the SANS design codes, as stipulated in SANS 10162-1:2002 section 22. The bolts were spaced radially at 22.5 degrees, which allowed for 4 bolts per quarter of the flange.

The next step in the design was to check the resisting capability of the bolts collectively as well as the resisting capacity of the flange, which still needed dimensional values.

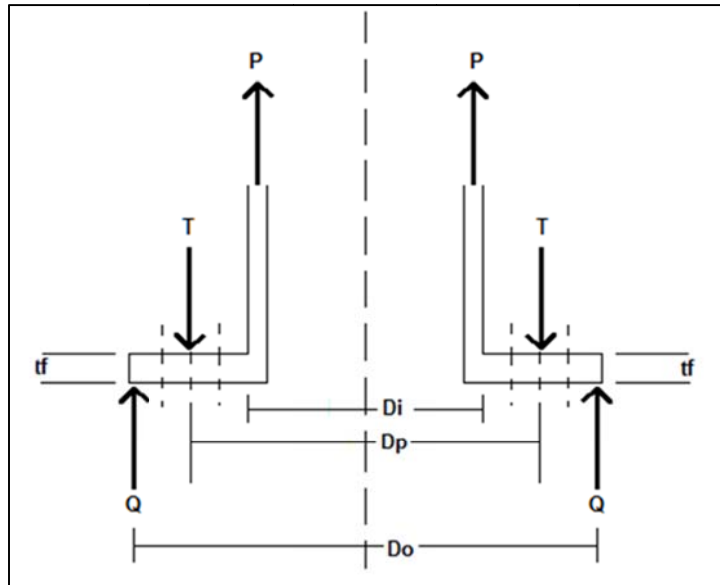


**Figure 17: Dimensional Parameters of Flange**

Here, there are a number of different sequences in which the various dimensions can be determined, or the resisting capacities calculated. Either way, one will need the assistance of a finite element analysis, either for the required forces occurring at the specified connection points in order to determine a flange thickness and width, or otherwise to determine an appropriately sized flange from iterative modelling in the finite element program, in which case the resisting capacity of the designed flange could be checked against the applied loads and moments.

It was opted here to model a flange connection in Strand7 with an initially arbitrary flange thickness and then run an analysis. The Strand7 model could then be altered in the terms of the flange thickness until the stresses developed in the flange connections were acceptable. The distances between the centre of the bolts and the wall of the tower as well as the distances between the centre of the bolts and the outer edge of the flange were chosen in accordance with the distances outlined in the South African Steel Construction handbook for the minimum allowable distances with regard to machining and bolt installation tools.

The following section handles the connection designs that were developed using Strand7, followed by the calculations done in order to ensure the resistance capacity of the connections.

#### 4.1.10 CONNECTION DESIGNS IN FINITE ELEMENT PROGRAM (STRAND7):

##### MID-SECTION CONNECTIONS:

The connections at the mid points within the tower, at the vertical heights of 6m and 11m respectively were designed to be 20mm thick, with web stiffeners at 22.5 degree radial spacing's, which lie exactly in between each bolt. The web stiffeners were chosen at 10mm thick and 100mm high along the height of the tower, and triangularly stretched to the edge of the 100mm wide flanges. All steel used in this design was S355JR.

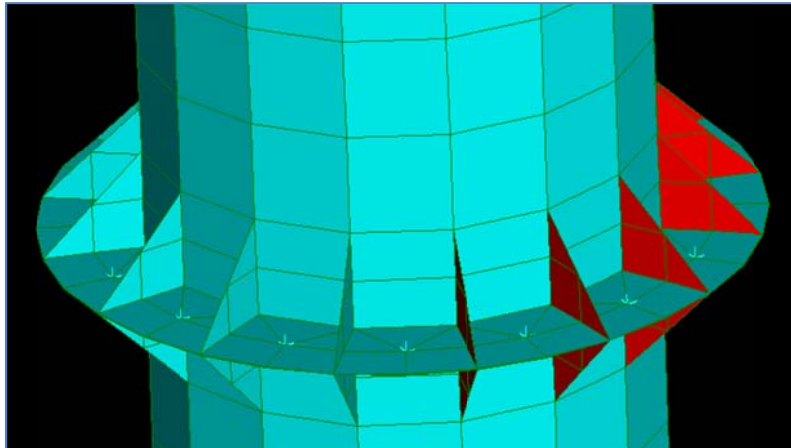


Figure 18: Mid-section Connection Design

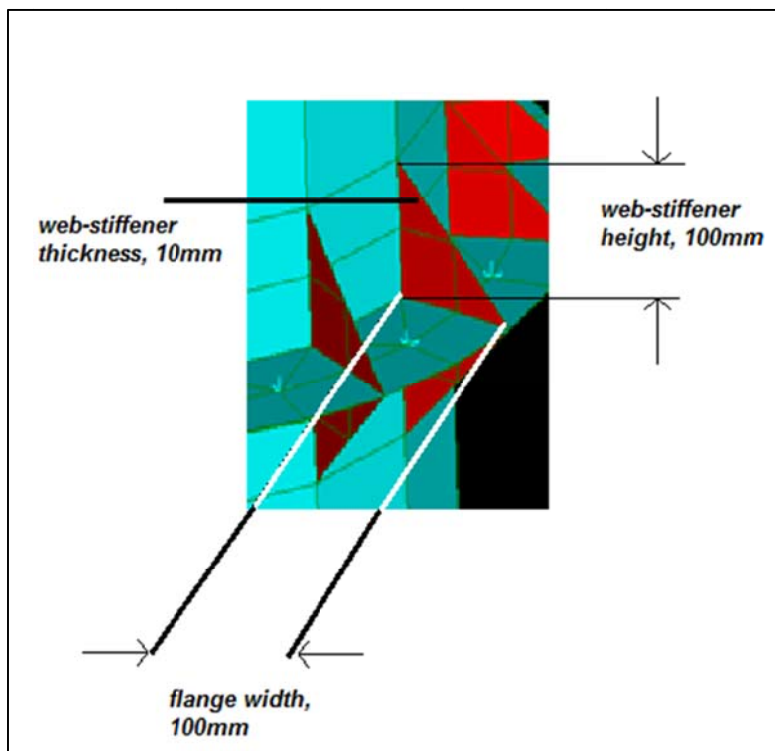


Figure 19: Mid-Flange and Web Stiffener Details

The connections were modelled such that there was a 1mm gap between the two connecting flanges, and at the placement of the bolts, rigid links were used to connect the two flanges, so as best to simulate the bolted connection for analysis .

#### BASE CONNECTION:

The flange connection design at the base had a 40mm thick flange, and web-stiffeners that was 200mm high, 20mm thick and stretched triangularly to the edges of the flanges through a distance of 130mm. Once again the web-stiffeners were spaced at 22.5 degrees radially, and were so placed exactly in between the bolts around the flange, which are M20 Class 10.9S bolts.

From the modelling accuracy of the base connection, the points at which the bolts were modelled were fixed for all degrees of translational and rotational displacement.

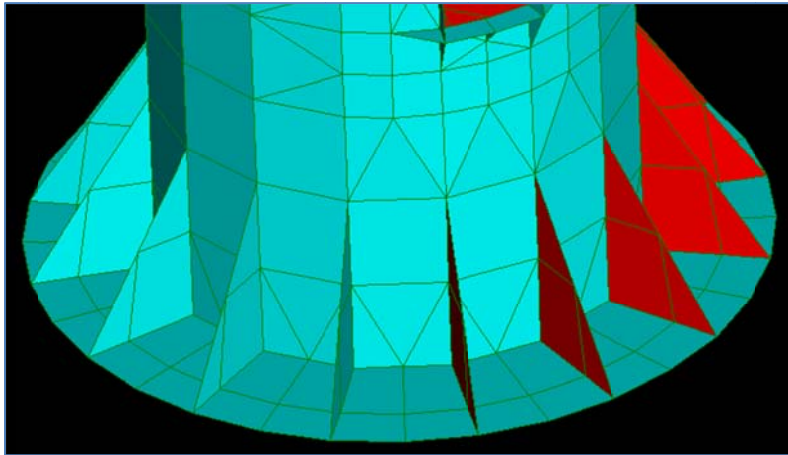


Figure 20: Base Flange Connection

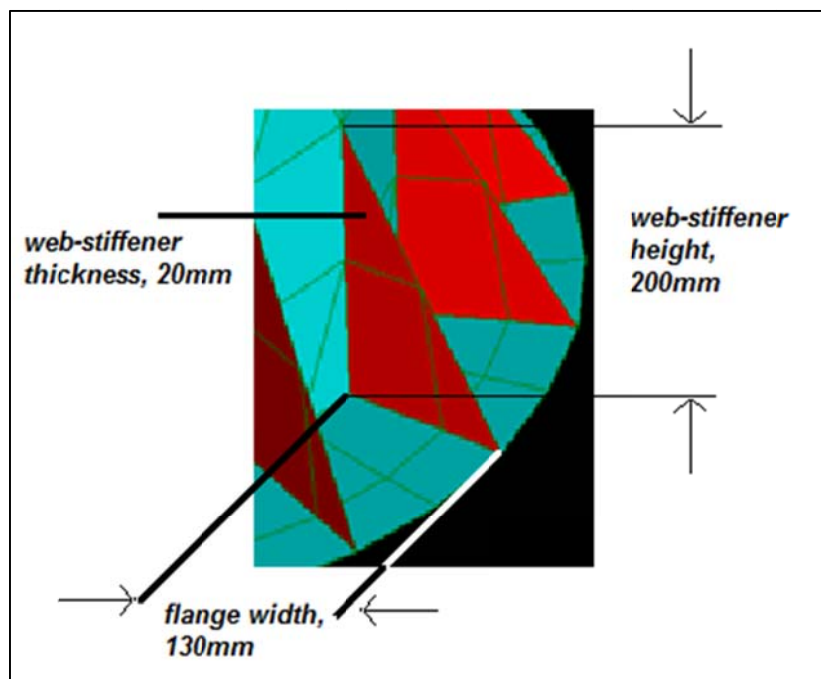


Figure 21: Base Flange and Web Stiffener Details

#### 4.1.10.1 CONNECTION CALCULATIONS:

The values given in the spread sheet extract in Table 9 can be correlated visually with Figure 16. The tributary length of each bolt which is noted as  $L$  in Figure 16 was taken as one 16<sup>th</sup> of the external diameter of the tower. Figure 16 also illustrates the distance between the bolt centre and the tower as well as the distance between bolt centre and edge of flange noted as “b” and “a” respectively.

**Table 9: Spread sheet extract showing flange details**

<b>Tributary length l</b>	
l	0.10 m
$\phi$	0.90
<b>flange strength</b>	
$f_y$	3.35E+08 Pa
<b>Maximum design strength of bolt to avoid fatigue</b>	
$f_u$	2.62E+08 Pa
	see SANS 10162-1:2005 clause 26
<b>bolt strength calculated with 262 MPa in accordance with SANS 10162-1:2005 clause 13.12.1.3</b>	
$A_b$	314.16 mm <sup>2</sup> M20
$\phi_b$	0.80
$T_r$	49385.84 N
<b>At Base Connection:</b>	
<i>From Diagram</i>	
a	0.05 m
b	0.08 m
t	0.04 m
<b>At mid and top connections</b>	
<i>From Diagram</i>	
a	0.05 m
b	0.05 m
t	0.02 m

The bolt strength in the above spread sheet was calculated in accordance with the aforementioned equation from SANS 10162-1:2005.

**VALIDATION OF THE BOLT SIZE AND STRENGTH:**

Because with a prying action the tensile force of the bolts in a connection subject to a tensile loading may be significantly increased, it is necessary to check if the capacity of the bolt is capable of handling the potential increase in load due to the prying.

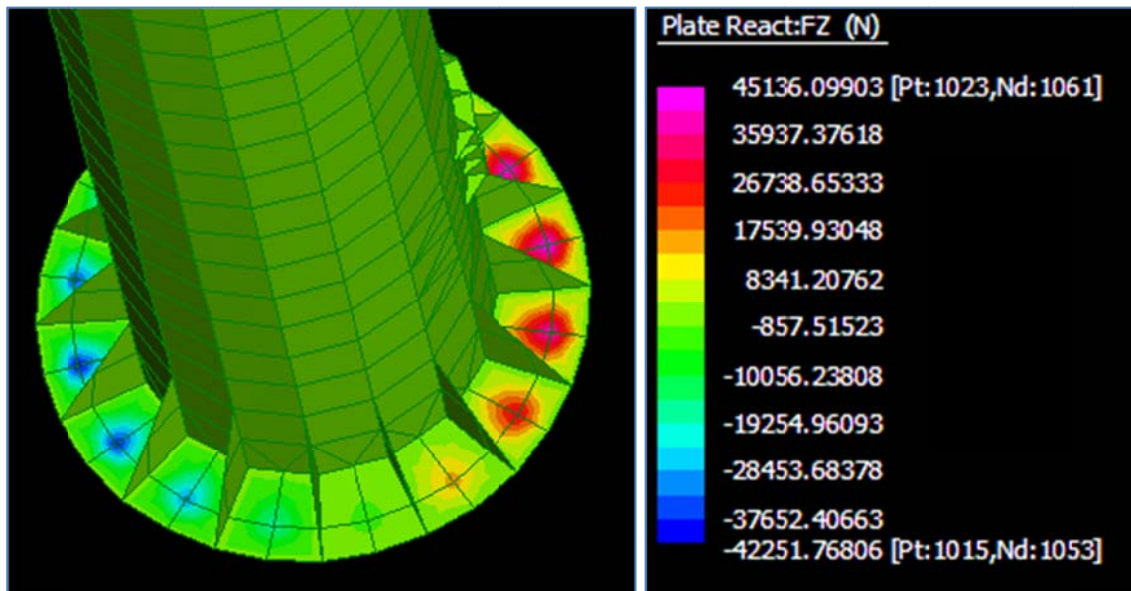


**Figure 22: Reaction Forces at Monopole Tower Base (SLS)**

Figure 22 from the finite element analysis in Strand7, shows the reaction forces at the points of bolt placement along the base flange connection for the SLS load case. In comparing the magnitude of the forces that need to

be resisted, the tensile force that the M20 bolts can resist as calculated in Table 9 ( $T_r=49\text{kN}$ ) is most certainly adequate.

The reason that the SLS was the load case chosen to examine the reaction forces required to be resisted was for the design instance of fatigue. The clause outlined in 13.12.1.3 of SANS 10162-1:2005 is discussed at the end of this chapter and explains this in further detail.

**VALIDATION OF THE FLANGE SIZE AND STRENGTH:**

The theoretical design magnitude which the flanges can resist through calculations incorporates the steel's yield strength and the flange thickness as well as the tributary length of each bolt. The design strength of the flanges once theoretically calculated were compared to the forces and stresses that they are required to resist in accordance with the output from Strand7.

The moments which the flanges were able to resist, for plasticity and elasticity respectively, are calculated in accordance with the following equations:

$$M_{pl} = \varphi f_y \left( \frac{lt^2}{4} \right)$$

$$M_e = \varphi f_y \left( \frac{lt^2}{6} \right)$$

In Table 10 the moments were calculated in accordance with the elastic moment of resistance, for a more conservative approach.

**Table 10: Moment Resistance of the Flanges**

<b><i>Moment resistance of the flanges respectively are:</i></b>					
<b>At Base Connection</b>			<b>At mid and top connections</b>		
$M_r$	8.02E+6	Nmm/mm	$M_r$	2.00E+6	Nmm/mm

These may be compared to the moments that are required to be resisted that are obtained from Strand7.

For a range of different moments that arise in the base flange in different planes, shown in Figure 23 through to Figure 26, the moments that the flanges are able to resist far out-weigh the magnitude of the imposed loads, and thus validating that the geometric dimensions, and related strengths are more than adequate for the connection design.

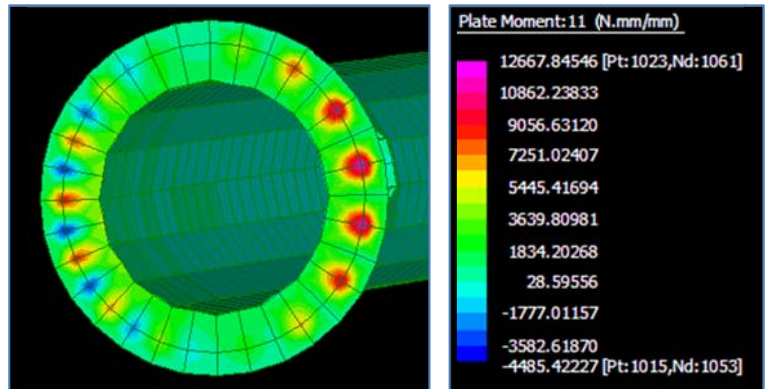


Figure 23: Moments in plane 11 (direction of y-axis loading) for the base ring flange connection of the Monopole

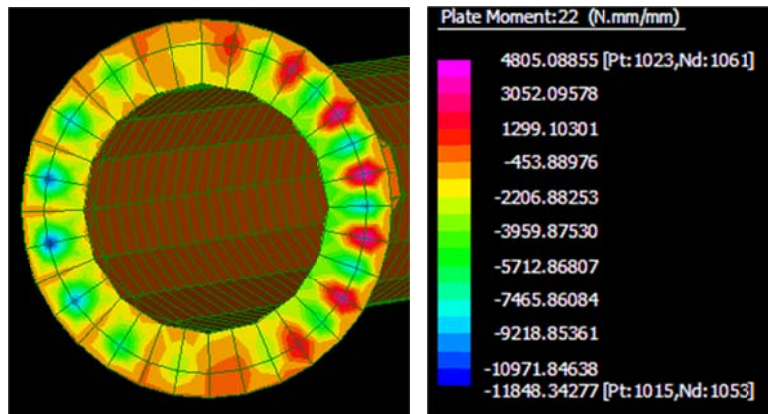


Figure 24: Moments in plane 22 (direction of x-axis) for the base ring flange connection of the Monopole

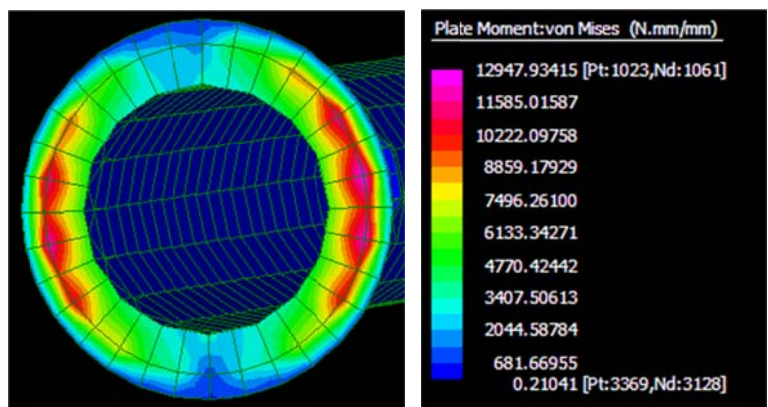


Figure 25: Von Mises Moments in the base ring flange connection of the Monopole



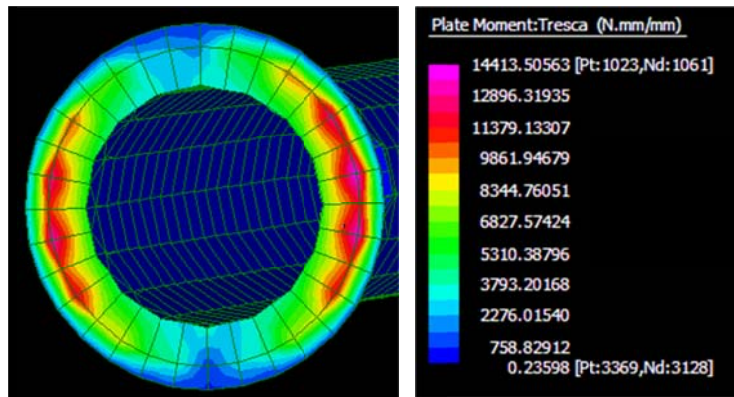


Figure 26: Tresca moments in the base ring flange connection of the Monopole

## 4.2 STEEL LATTICE TOWER CONNECTIONS:

### 4.2.1 CONNECTION TYPE

Bolted connections are the most widely used in element connections for steel lattice towers. This element connection type is suitable for hot-dip galvanised members and bolts that are galvanised and then connected afterwards. A tolerance of between 1 and 2mm is provided between the diameter of the bolt and the diameter of the hole. Members are often connected with one bolt only, in particular all redundant members in lattice frameworks and bracings of less heavily loaded towers (Kießling et al, 2003: 376).

No more than 6 bolts should be used in a line for a connection, so that the individual strength of each bolt is utilised. Where the fore mentioned connection type is inadequate, one may design a connection with two parallel lines of fasteners.

The width of the angle sections chosen will by implication also determine the largest possible bolt diameter allowed. The arrangement of the chosen/ required bolts should be done in such a way that the arrangement of the bolt holes should prevent corrosion and local buckling and facilitate the installation of bolts.

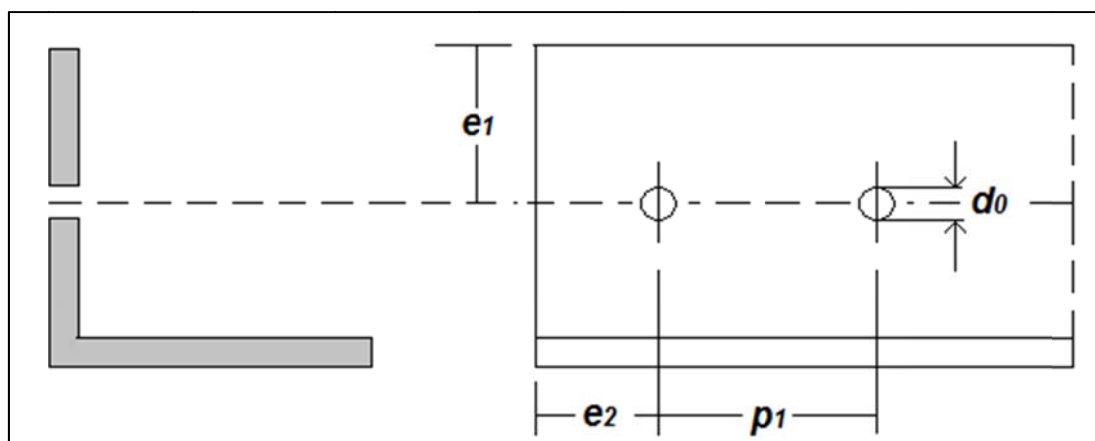


Figure 27: Equal Leg Angle Section Hole Dimensioning

The parameter measurements that are recommended for the above connection are as follows:

$$e_1 \geq 1.2d_0$$

$$e_2 \geq 1.5d_0$$

$$\min(1.4t; 200\text{mm}) < p_1 \leq 2.5d_0$$

In accordance with the recommendations for corrosion prevention:

$$e_{1max} \& e_{2max} \leq 40\text{mm} + 4t$$

Where  $t$ , is the thickness of the thinner of the connected parts (Kiessling et al, 2003: 376).

## 4.2.2 CONNECTION DESIGN:

### 4.2.2.1 CHOOSING THE APPROPRIATE BOLTS:

The connection design for Steel Lattice towers is determined by the necessity of bolts and or welds. The connections between bracing members and outer leg members in the Steel lattice tower were designed to be pinned connections. In order to create an actual pinned connection the bracing members were to be bolted to the outer leg members, and where appropriate to one another.

The initial calculations to determine what size bolts to use for the connections, tested the shear bearing capacity of different sized bolts and compared their bearing capacity to the maximum axial forces developed in the members. It was determined that in fact a single bolt has sufficient strength to resist the largest applied axial force, however it was decided upon for the following reasons to use two M16 bolts at each connection instead of just one.

If one were to only use one bolt at the end of each member as a connection, the connection would most likely behave well in tension; however it would cause a significant loss in flexural stiffness at the connection location in the instance of compression. Flexural stiffness is important when the member carries compression because Euler buckling is dependent on such stiffness. Because of the K-bracing configuration in a number of the bracing members, it is a certainty that some of the members will be in compression, and so the need for more than one bolt would already be justified.

Another reason to use more than one bolt is to introduce redundancy. Redundancy significantly increases system reliability, and so implicitly decreasing risk associated with failure by introducing more than one bolt at each connection.

Lastly another advantage found in using multiple bolts at each end is for practical construction purposes; when there are two bolt holes, the one hole can be used to align the other with a spud wrench.

### 4.2.2.2 CONNECTION DETAILS:

In order for a connection to be truly pinned, the lines along which the centroids of each member lie need to all meet at a point. If this is the case the pinned connection shall have no moments created by means of any eccentricities at the point of fixity.

In order for the three and in some instances five members of each nodal point in the lattice tower to be pinned connections, welded plate girder connections had to be designed because of space constrictions.

The plates of determined strength and thickness were then to be welded onto the outer leg members at the appropriate points by means of fillet welds, and the bracing members then bolted onto those plates by means of two M16 bolts with the appropriate spacing.

### 4.2.3 CONNECTION CALCULATIONS:

In Table 11 and Table 12 the calculations that determined the number of bolts of specific size for difference capacity requirements were determined.

The dimensions of the gusset plates were determined through three dimensional modelling of the pinned connections on Autodesk inventor Professional 2011. Figure 19 shows the placement of such a connection.

Attached in the Connections Appendix are isometric detailed drawings of the gusset plate connections.

**Table 11: Ordinary Bolt strength calculations for Steel Lattice Tower Connections**

Shear Bolt Resistance

SANS 10162-1:2005

Clause 13.12.1.2

**Ordinary Grade 8.8 bolt yield strength**

70x70x6			100x100x8		
$g_1$	40	mm	$g_1$	50	mm
$d_{max}$	16	mm	$d_{max}$	24	mm
$\phi_b$	0.8		$\phi_b$	0.8	
$A_b$	201.0619	mm <sup>2</sup>	$A_b$	452.3893	mm <sup>2</sup>
$f_u$	830	Mpa	$f_u$	830	Mpa
$n$	2				
$V_r$	56072.15	N	$V_r$	126162.3	N
$V_{r,n}$	112144.3				
$V_u$	62016	N	$V_u$	62016	N
$V_u/V_r$	0.553002		$V_u/V_r$	0.491557	
check	OK		check	OK	

**Table 12: Bolt Capacity Calculations for Fatigue for Lattice tower Connections**

70x70x6			100x100x8		
$g_1$	40	mm	$g_1$	50	mm
$d_{max}$	20	mm	$d_{max}$	24	mm
$\phi_b$	0.8		$\phi_b$	0.8	
$A_b$	314.1593	mm <sup>2</sup>	$A_b$	452.3893	mm <sup>2</sup>
$f_u$	262	Mpa	$f_u$	262	Mpa
$n$	3		$n$	2	
$V_r$	27656.07	N	$V_r$	39824.74	N
$V_{r,n}$	82968.21		$V_{r,n}$	79649.48	
$V_u$	62016	N	$V_u$	62016	N
$V_u/V_r$	0.747467		$V_u/V_r$	0.778612	
check	OK		check	OK	

Table 12 shows the effects of reduced bolt strength having been taken into account for fatigue, and hence increasing the required number of bolts.

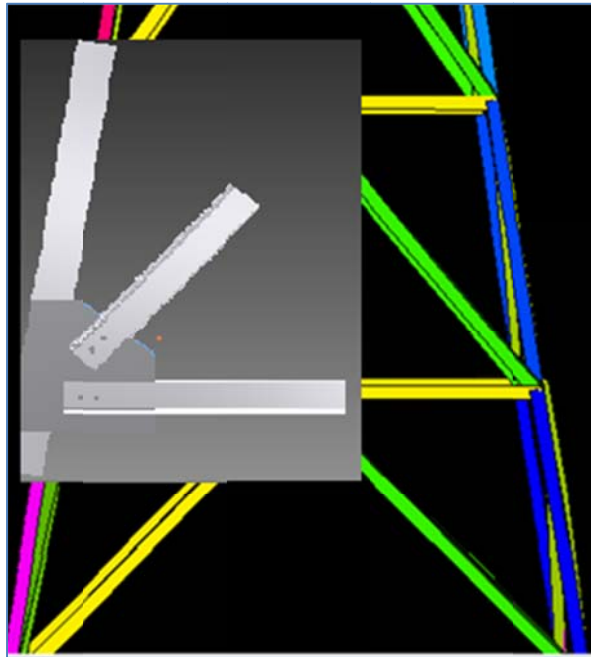


Figure 28: Lattice Tower, pinned connections with gusset plates

#### 4.2.4 GENERAL ASPECTS PERTINENT TO ALL CONNECTION TYPES DEALT WITH IN THIS CHAPTER:

##### 4.2.4.1 WELDS:

For the Monopole Tower, the welding required in fabrication, was that of the ring flanges welded onto each CHS of the tower. The welds were stipulated as full penetration welds. The weld metal was detailed as E70XX, which has a tensile strength of 480MPa, and because the base material of the tower is S355JR, with a tensile strength of 470MPa, the weld effects can be ignored and the tower can be analysed as if there were no welds.

For the steel lattice tower, the gusset plates which were illustrated in Figure 28 needed to be welded onto the outer legs of the steel tower in the fabrication process. The welds were stipulated as fillet welds in accordance with SANS 10162-1:2005. The top 2.5m of the tower where the elements were 50x50x5 equal leg angle sections, were also pre-welded together in the fabrication phase by fillet welds designed in accordance with SANS 10162-1:2005.

#### **SANS 10162-1:2005**

##### **13.13.2.2 Fillet Welds**

*The factored resistance for shear and tension-shear or compression-induced shear shall be taken as the lesser of*

a) *For the base metal*

$$V_r = 0.67\phi_w A_m f_u ; \text{ or}$$

b) *For the weld metal*

$$V_r = 0.67\phi_w A_w X_u (1.00 + 0.50 \sin^{1.5} \theta)$$

Where  $\vartheta$  is the angle of the axis of the weld with the line of action of the force (zero degrees for a longitudinal weld and 90 degrees for a transverse weld), and the other terms are defined in 13.12.2.1. Conservatively,  $(1+0.5\sin^{1.5}\vartheta)$  can be taken as 1.

Extracts from **13.12.2.1:**

$A_m$  is the shear area of the effective fusion face ( $\text{mm}^2$ ),  $f_u$  is the tensile strength of the parent metal (MPa),  $A_w$  is the area of the effective weld throat, plug or slot ( $\text{mm}^2$ ) and  $X_u$  is the tensile strength of the weld metal (MPa).

#### 4.2.4.2 BOLTS:

For a structure like the wind turbine supporting towers in this thesis, it is recommended that pretensioned bolts are used in the design of the connections. In accordance with the South African Steel Construction handbook (SASCH), the following is detailed with regard to High Strength friction grip (HSFG) bolting.

“Friction grip bolted connections are connections in which shear force is transmitted by the friction developed between the fraying surfaces of the connected parts, which are clamped together by high pretensioned forces in the bolts.” They continue by stating, “The bolts are of high-strength material and are pretensioned during installation to a force of at least 70% of their tensile resistance.” Furthermore, as can be seen in SANS 10162-1:2005 clause 22.2.2 part d which is described below, for any structures which include the possibility of cyclic loading HSFG bolts must be used.

In a friction grip bolted connection, it is necessary to ensure that after the bolts have been tightened they are all tensioned to a minimum value given in the table below which out of SANS 10094:

SANS 10094		
Table 1-Minimum Bolt Tension		
Nominal size of Bolt	Minimum bolt tension T (kN)	
	Class 8.8S	Class 10.9S
M16	91	114
M20	142	178
M24	205	257
M30	326	408
M36	475	595

#### 6.2.2.2 Washers used with class 10.9S bolts

When class 10.9S bolts and class 10S nuts are used to join components of any grade of steel of an ultimate tensile strength of less than 585 MPa, hardened washers shall be fitted under both bolt head and nut or, in the case of components of higher strength, fit a washer under only the member that is rotated. Ensure that bearing surfaces are normal to the axis of the bolt to within  $1^\circ$ , and where a tapered washer is used to achieve this, provide a flat, hardened washer between the tapered washer and the bolt head or nut.

Note, only Class 10.9 nuts may be used with class 10.9S bolts.

#### SANS 10162-1:2005

#### 13.12 Bolts

**13.12.1.3 Bolts in tension**

The factored tensile resistance developed by a bolt in a joint subjected to tensile force, shall be taken as:

$$T_r = 0.75\phi_b A_b f_u$$

Where  $\phi_b=0.8$ , and the calculated tensile force,  $T_w$ , is independent of the pretension and shall be taken as the sum of the external load plus any tension caused by prying action.

A high-strength bolt subjected to tensile cyclic loading shall be pretensioned as for friction grip connections (see clause 22). Connected parts shall be arranged so that prying forces are minimised, and so in no case shall the prying force exceed 30% of the externally applied load. The permissible range of stress under specified loads, based on the shank area of the bolt, shall not exceed 214MPa for class 8.8S bolts or 262MPa for class 10.9S bolts.

In Lieu of calculating the actual fatigue stress range, which requires the effect of bolt pretension to be taken into account, the stress range may be simply taken as the calculated stress based on the shank area of the bolt under specified loads, including the prying force, and independent of the pretension force.

**SANS 10162-1:2005****Clause 22. Design and Detailing of bolted connections.****22.1 General**

This clause deals primarily with class 4.8, 8.8, 8.8S, 10.9 and 10.9S bolt assemblies complying with the relevant parts of SANS 1700, of equivalent fasteners. The bolts might or might not be required to be installed to a specific minimum tension depending on the type of connection.

**22.2 Design of bolted connections****22.2.2 Use of high-strength friction-grip bolts**

Pre-tensioned high-strength friction-grip bolts (class 8.8S or 10.9S) shall be used in

a) friction-grip connections where slippage cannot be tolerated (such connections include those subject to fatigue or to frequent load reversal, or those in structures sensitive to deflection),

d) connections subject to impact or cyclic loading

e) connections where the bolts are subject to cyclic tensile loading (see 13.12.2.3).

The design procedure developed for the ring flange and gusset plate connections have been handled in this chapter and the detailed connection calculations are shown in Appendix B.

## CHAPTER 5: FOUNDATION DESIGN

This chapter examines the details of the two foundations designed for the Steel Monopole, and the Steel lattice tower respectively.

First the design of the Steel Monopole Tower's Foundation shall be reviewed, followed by the design of the Steel lattice tower's foundation.

### 5.1 INTRODUCTION TO FOUNDATIONS

The purpose of a foundation is to transfer the loads from the structure to the ground, without causing the ground to fail in shear or to allow excessive settlement of the structure to occur (Marshall and Robberts). These requirements are met by ensuring the bearing pressure below the foundation does not exceed a specified **permissible bearing pressure**. This is done in accordance with SABS 0161 (1980).

Accounting for the design of the foundation in terms of the Strand7 model is also important from the point of view of the stiffness of the ground, foundation and the way in which the tower interacts with the foundation and stiffness of the supporting ground. The importance in the stiffness arises due to the possible effect the stiffness of the base of the tower will have on the results obtained from dynamic analyses done on the tower.

The foundation design is also extremely specific to the site of installation. The stiffness of the ground, mentioned above, is related to the elastic modulus of the ground at the site. Thus one needs to know the type of ground, the density of the ground as well as the other soil properties such as Poisson's ratio and elastic modulus. In order to obtain the above parameters, suitable soil tests must be done (Marshall and Robberts).

For the purposes of completeness of design and also a more complete cost analysis it was decided upon to do a provisional foundation design for a selected ground type.



**Figure 29: Failed wind turbine foundation design**

## 5.2 STEEL MONOPOLE TOWER FOUNDATION DESIGN

### 5.2.1 FOUNDATION TYPE

In accordance with the Cement and Concrete Institute's "Analysis and Design of Concrete Structures", a **simple footing** was designed for the Monopole Tower foundation.

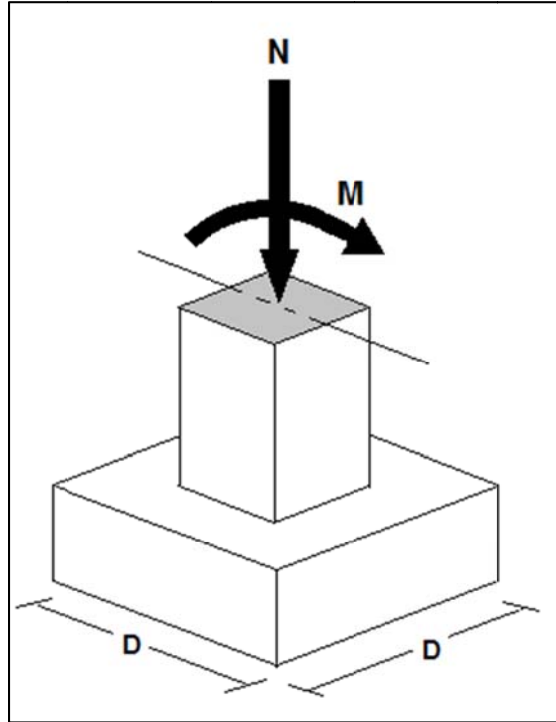


**Figure 30: Monopole Foundation Type**

Figure 30 shows the layout of the simple footing with a column protruding out of it with an applied axial force and bending moment. It was decided upon to have a foundation that looked geometrically exactly the same as Figure 30, where the tower would lie on top of the column. This decision was based on the calculated moment applied to the foundation, which induced such a large propensity for overturn that the foundation design would comply with the need to be buried a certain depth below the ground to help resist the overturn forces.

### 5.2.2 FOUNDATION DIMENSIONS

The dimensions of the concrete foundation were decided upon by means of a static equilibrium equation which took the applied moment of overturn ( $M$ ) equated to the concrete foundation and top soil's capability to resist that overturn ( $M_R$ ) about the most likely point ( $O$ ), see Figure 31. This resulted in the appropriate dimensional volumes of concrete, as well as the depth to which the soil would need to be excavated to bury the foundation. In accordance with the South African National Standards (SANS), the safety factor for overturn of 1.5 was applied,  $M_R/M=1.5$ .



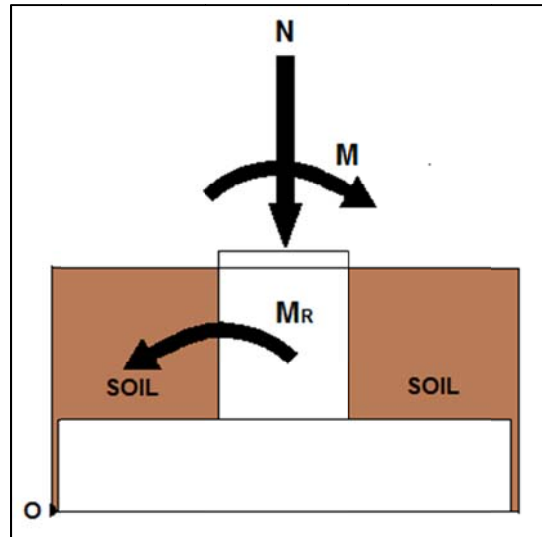


Figure 31: Monopole Foundation Equilibrium

### 5.2.3 FOUNDATION CALCULATIONS

Once the appropriate foundation dimensions had been obtained, the next step was to determine which category of design the foundation fitted into to determine whether the induced bearing pressure was acceptable. The design category was based on the ratio between the applied moment divided by the axial load, which was then compared to a theoretical ratio of  $D/6$ , where  $D$  is the base width of the foundation. The ratio is then used to transform the combined moment and axial force into a single force to consider, an axial load, with eccentricity  $e$ . This ratio ( $D/6$ ) and the use of it which follows were prescribed by the Analysis and Design of Concrete Structures by John M. Robberts and Vernon Marshall.

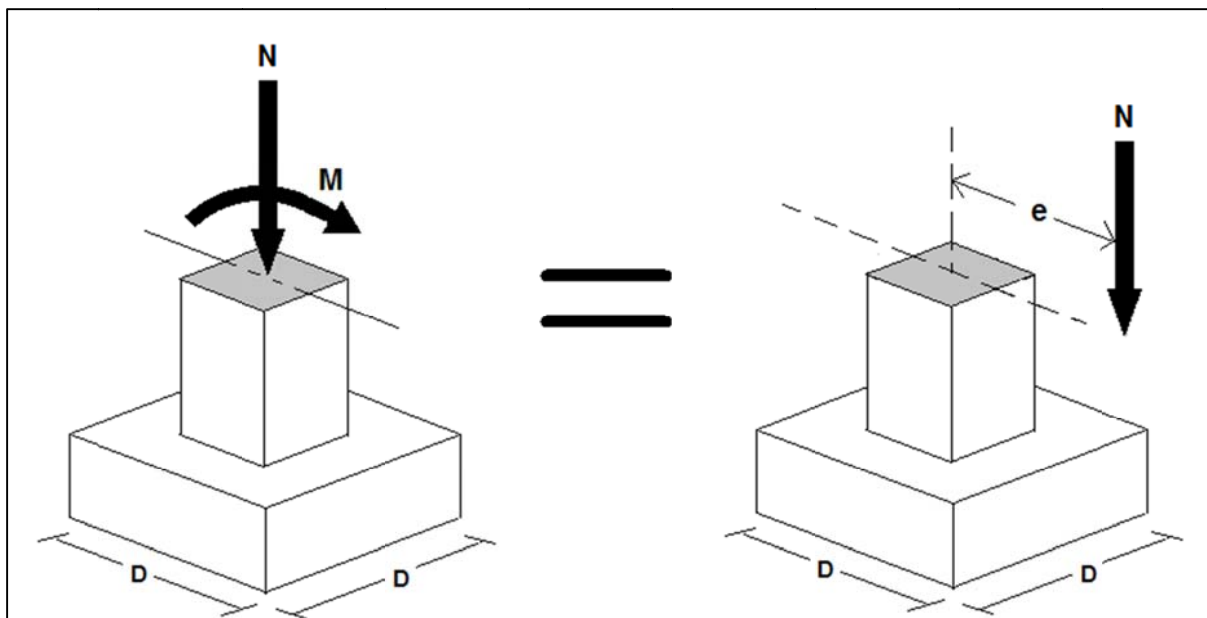
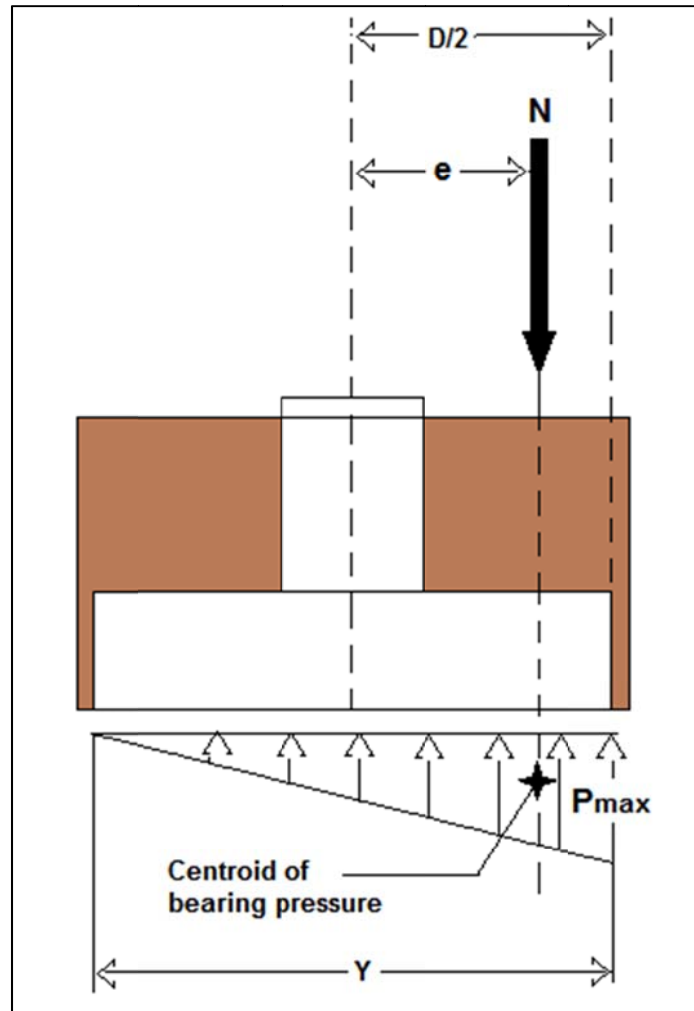


Figure 32: Monopole Foundation equilibrium equivalent

In the process of transforming the co-acting applied moment and axial force to act as a single axial force with an eccentricity (which was determined from the ratio between moment and axial force), one needs to make sure to take into account the increased magnitude in axial force as a result of the self-weight of the concrete foundation footing as well as the soil that is to be placed on top of it. This tends to vastly reduce the ratio, and

from a situation where with an extremely large moment the eccentricity distance “ $e$ ” in Figure 32 would be extended beyond the distance of the base dimension, it is brought to a reasonable distance within that dimension which then allows one to calculate the applied bearing pressure.

The applied bearing pressure is calculated next which in the instance of the above design category is approximated as a linear distribution beneath the concrete footing. This can be seen in Figure 33.



**Figure 33: Monopole Foundation Bearing Pressure layout**

The design equations used to calculate the maximum and minimum bearing pressures below the foundation depend on the design category of  $D/6$  and whether “ $e$ ” is bigger or smaller than this ratio. For the foundation designed for the Monopole in this thesis, it was designed for both the ratio of  $e > D/6$  and  $e < D/6$ . The difference in bearing pressure distribution below the foundation for the two different ratios are shown in Figure 34, these were brought about by changing the base dimension of the foundation from 3m, ( $e > D/6$ ) to 4m ( $e < D/6$ ).

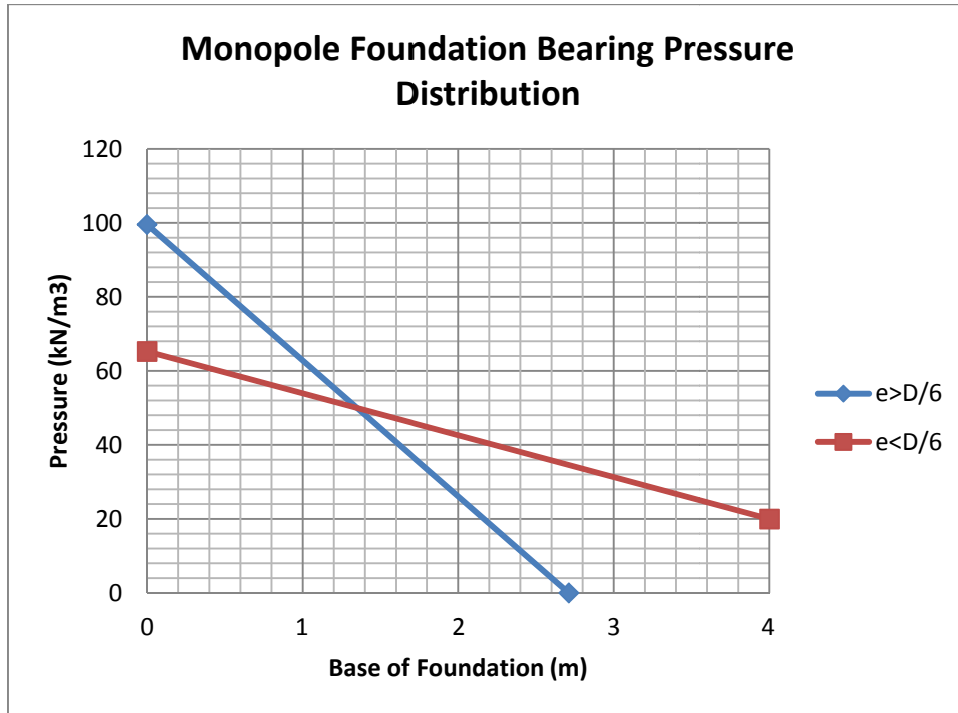


Figure 34: Monopole Foundation Bearing Pressure Distributions

Due to the overall maximum bearing pressure of the wider footing ( $D=4\text{m}$ ) being significantly smaller and having a more even pressure distribution it was decided upon to use the foundation with a base dimension of  $D=4\text{m}$ .

The design moment for such a foundation was calculated as can be seen in the Monopole foundation calculations Appendix C. The theoretical design moment was closely comparable to the design moment calculated in the finite element package Prokon, and it was decided upon to do the rebar quantity calculations and layout using Prokon, see Figure 35 and Figure 36.

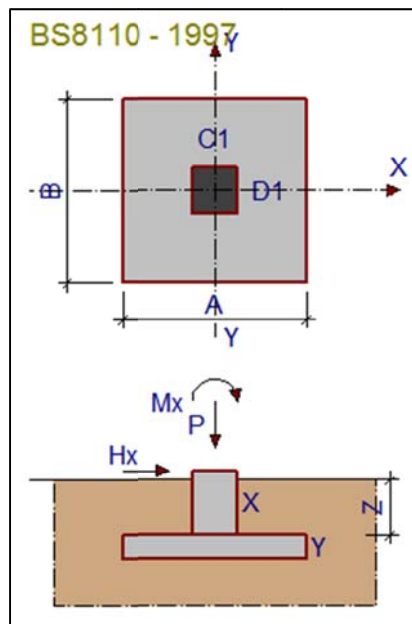


Figure 35: Prokon Input Layout of Monopole Foundation

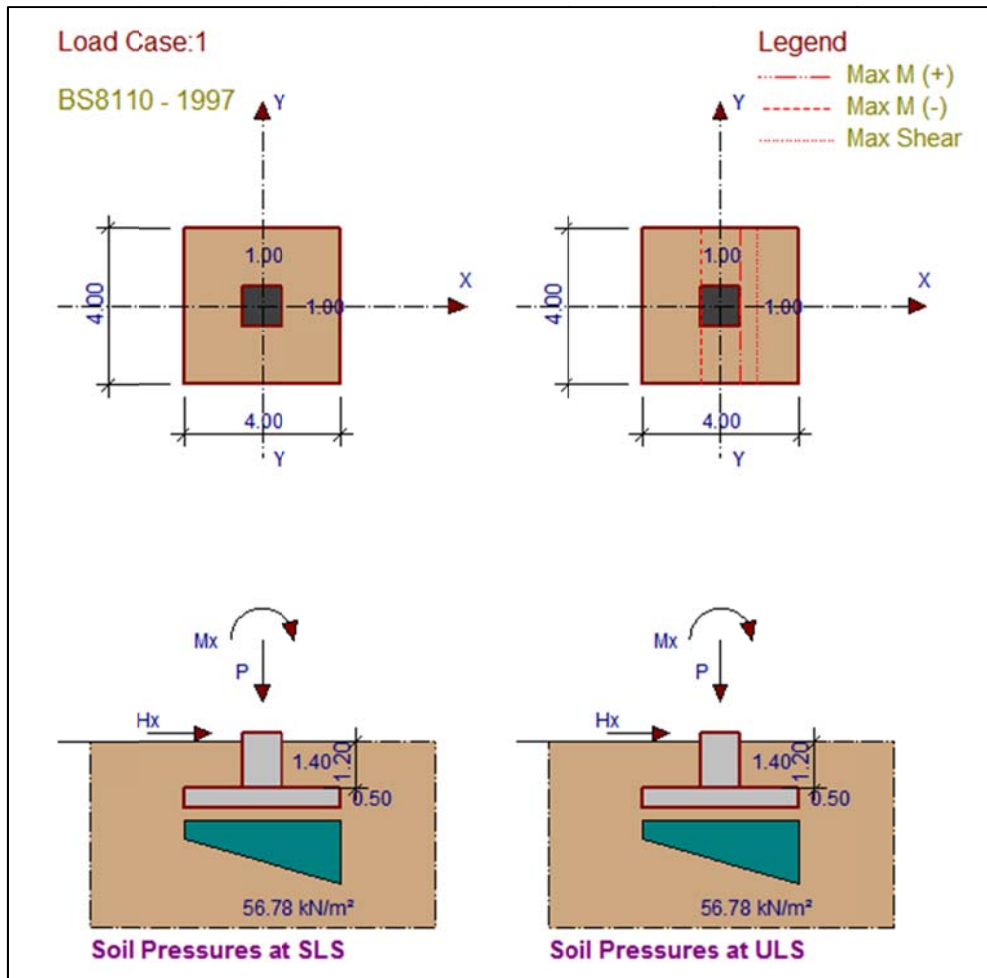


Figure 36: Prokon Output for Monopole Foundation

From the Prokon output, Figure 37 shows the bending schedule which was generated, which for cost analysis purposes enables one to calculate the amount of reinforcing steel required in a foundation of this nature.

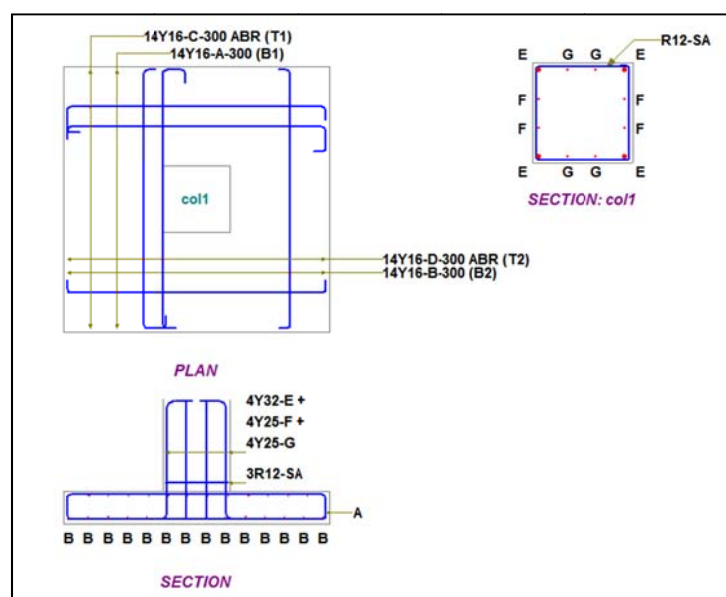


Figure 37: Monopole Schematic Bending schedule

## 5.3 STEEL LATTICE TOWER FOUNDATION DESIGN

### 5.3.1 FOUNDATION TYPE

The foundation design for the Steel lattice tower was much simpler than the design process negated by the large overturn moments of the Monopole Tower. The steel lattice tower by nature reduces the magnitude of the forces at the foundation because of its structure and ability to spread loads throughout its members with pinned end connections.

The Steel lattice tower's outer supporting legs, being equal angle sections, needed to be welded onto appropriately sized steel base plates which would then be bolted onto the concrete foundation by means of two bolts to mimic a pinned connection which would transfer no moments to the foundation.

### 5.3.2 DESIGNING THE STEEL BASE PLATES

Due to the nature of a pinned connection, which was the connection for which the base points of each leg was designed and modelled, axial loads are the only forces that need to be taken into account from a design point of view. The loading on a wind turbine supporting tower needs to be examined for the instances of the largest loads being moved from one leg to the other along with the motions of the wind turbine.

For this reason the largest axial forces developed in a single leg for the ultimate limit state were utilised in designing the requirements of the base plate for each of the legs, which were all to be identical.

The Ultimate Limit state loads from Load Case two, where the wind loading was applied to the tower diagonally were utilised since they developed the largest axial forces in the legs.

The steel base plates were designed in accordance with the South African Steel Construction Handbook, section **4.2.2 Centrally-loaded bases**, derived from BS 5950: 2000.

- a) Firstly the required steel area of the base plate required in terms of the applied axial force is calculated, which can then be used as a lower bound parameter as a minimum area for the base plate.

$$A_{baseplate} = \frac{C_u}{\phi_b f_{cu}}$$

*where,  $\phi_b = 0.6$*

- b) Secondly the required effective area around the column base needs to be determined, an area which is projected at least a distance "c" away from the column base all the way around the column, see Figure 38. In order to determine the value of parameter "c" the following quadratic equation is solved:

$$A_{baseplate} = 5c^2 + (\text{column perimeter}) \cdot c + \text{column area}$$

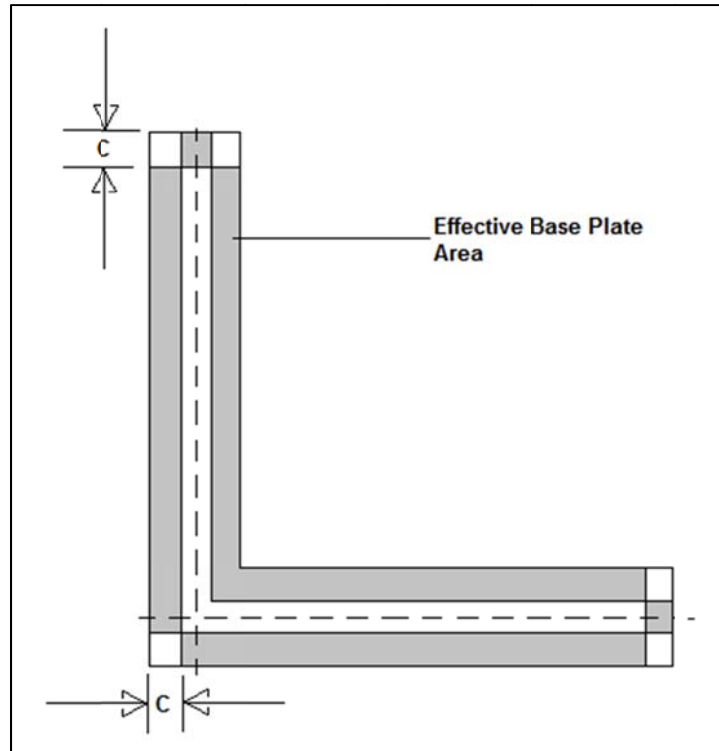


**Figure 38: Effective Base Plate Area**

- c) Lastly, the thickness of the plate needs to be determined from the following equation:

$$t = \sqrt{\frac{3w}{0.9f_y} \cdot c}$$

Where  $w$ =pressure under the plate ( $\leq 0.6f_{cu}$ ), and  $f_y$  is the yield stress of the plate.

One must just check that the base plate's thickness is not less than the thickness of the flange of the column.

Once the above three steps have been done, a rational calculation can be made taking into account the above proposed minimum dimensional parameters as well as the minimum spacing allowances for bolted connections suggested in the South African Steel Construction Handbook to determine the most appropriate plate size for the base plates.

### 5.3.3 DESIGNING THE CONCRETE FOUNDATION:

In order to obtain a concrete reinforced foundation comparable to the kind of footings designed for the Monopole Tower, Prokon was utilised. However, the design was far more simple, since it consisted of four smaller square foundation blocks that were placed on top of the ground, which also contained comparably little steel reinforcing. The only load applied to each of the concrete foundations was an axial load, which was applied on top of the steel base plate.

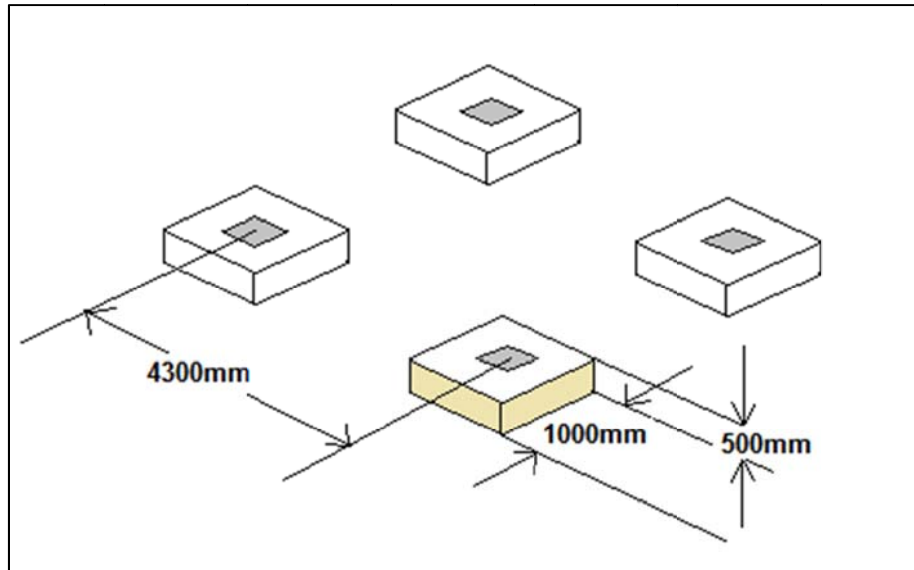


**Figure 39: Steel Lattice Tower Foundations**

In Prokon the foundation footings shown in Figure 39 were modelled, however, in order to model the steel base plates so that the analysis incorporated the loads applied to them, they were modelled as infinitely flat “column stubs”. Because Prokon has been programmed to suggest steel reinforcing in the “column” section of the base, it is shown in the output for the elements of the model which were used to model the base plates. However, since they are infinitely thin and make no physical allowance for reinforcing that can of course be ignored as no such thing exists, the “column stubs” are purely there to better simulate the applied loads in the foundation.

Figure 40 shows the input diagram for design in the finite element package Prokon. Figure 41 shows the output design from Prokon, and the bending schedule for the steel reinforcement required in each of the concrete foundation footings is shown in Figure 42.

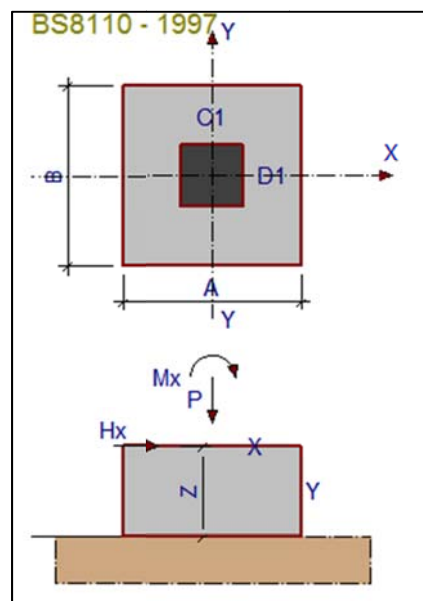


**Figure 40: Prokon Lattice Foundation Input**

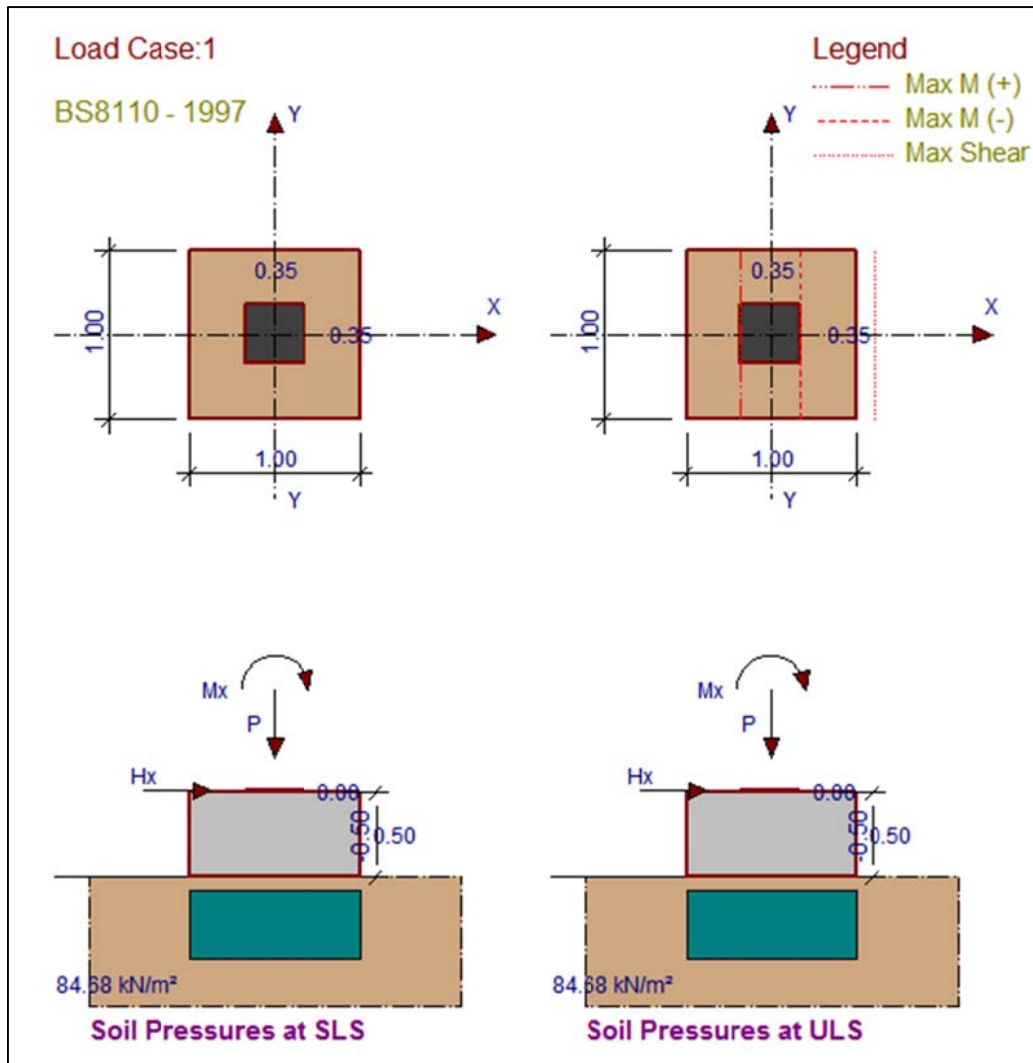


Figure 41: Prokon Lattice Foundation Output

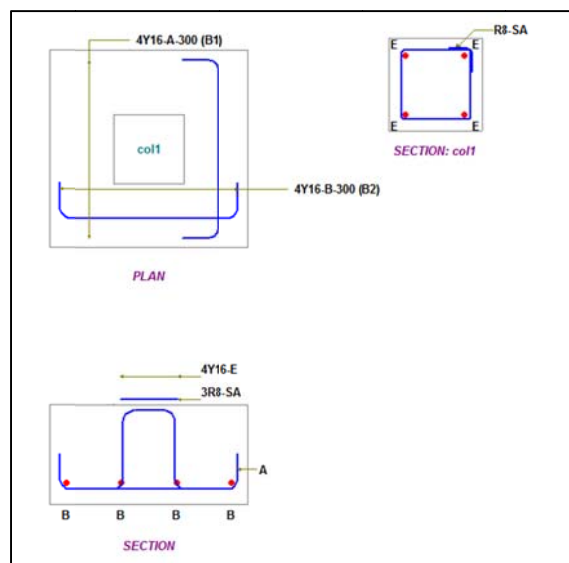


Figure 42: Prokon Bending schedule Lattice Foundation



## 5.4 CONCLUSION

All of the quantitative information gathered from the foundation designs for the Steel Monopole and the Steel Lattice towers is used in the feasibility chapter to provide greater insight into the effects the different foundation designs have on the overall feasibility of the different tower types.

The design procedure utilised in designing the foundations was handled in this chapter, and the detailed calculations are shown in Appendix C.

## CHAPTER 6: FINITE ELEMENT ANALYSES

### 6.1 INTRODUCTION

This chapter examines the finite element modelling of the two Steel Towers designed for this thesis. First the way in which the steel Monopole Tower was modelled will be described, followed by the results obtained from the analyses performed on the tower. Thereafter, the modelling procedure for the steel lattice tower is discussed and the results of the analyses performed for that tower.

The analyses that were performed on each of the towers were the following:

1. Linear Static Analysis
2. Linear Buckling Analysis
3. Nonlinear Analysis
4. Dynamic Analyses
  - i) Natural Frequency Analysis
  - ii) Effects of an out of balance rotor
  - iii) Effects of vortex shedding due to wind action
  - iv) Harmonic Frequency Analysis
  - v) Stress states and Fatigue assessment
  - vi) Modal Mass Participation Evaluation

### 6.2 STEEL MONOPOLE TOWER: FINITE ELEMENT ANALYSES

The Steel Monopole Tower designed for this thesis was modelled in the finite element analysis package Strand7. The monopole was modelled with plate elements of varying thickness; it was modelled as being fixed at the base and with the loading effects of a simulated wind turbine machine acting on the top of the tower. The effects of the wind turbine machine were simulated by means of creating a conical formation of rigid links at the tower top to which a further rigid link was attached in order to make allowance for the simulated eccentric centre of mass of the combined nacelle and rotor of the wind turbine machine, modelled as a lumped mass at the end of the extended rigid link (see Figure 43 below). The force that shall be described as the overturn force in the following sections accounted for the action of the wind on the blades of the Wind Turbine Machine. The calculation details of the overturn force were described in Chapter 3 in section 3.3.2. The overturn force simulated the action of the wind on the blades of the rotor as a function of hub height and wind speed and was applied at the peak of the conical formation of rigid links in Strand7, seen in Figure 43.

In Strand7 different aspects of the tower were modelled as separate load cases and then combined by means of linear load case combinations which accounted for the actions defined for a number of different Serviceability and Ultimate Limit states in accordance with SANS 10160-1:2011.

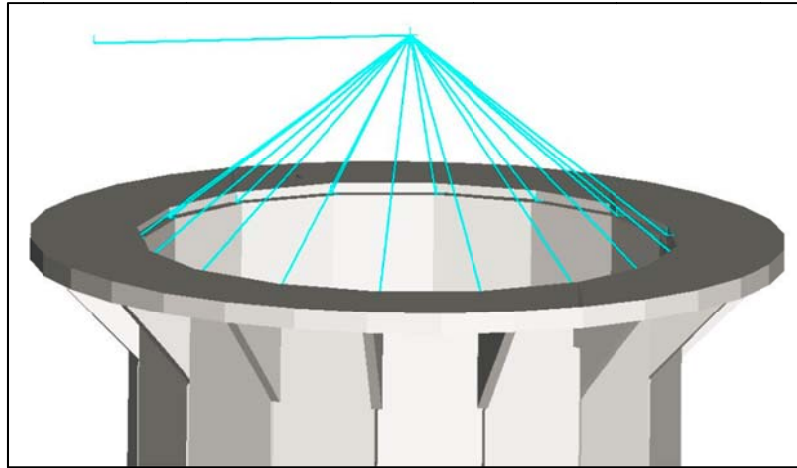


**Figure 43: Monopole Tower Wind Turbine Connection Simulation**

The following aspects were modelled as separate load cases; the self-weight (SW) of the tower, the dead load (DL) weight of the simulated equipment (wind turbine machine), the wind action on the tower, and the Ultimate Limit State (ULS) and Serviceability State (SLS) overturning actions. The overturning action is defined by a horizontal force applied at hub height and is dependent on the swept rotor area and the approaching wind speed, wanting to push the tower over. The naming of the overturning forces as the ULS and SLS overturning forces respectively was done so in accordance with the explanation given in section 2.2 for how the serviceability limit state overturn force from the wind is defined up until 16m/s and the ultimate limit state is defined from 16m/s wind upwards. They are load cases to be used in the load combinations stipulated in Table 13. Included in the SLS overturn and ULS overturn load cases are the effects of the wind acting along the tower.

The overturning actions were calculated differently for the ULS and SLS because the operating wind speeds of the 3kW wind turbine is up to 16m/s. At speeds beyond 16m/s the turbine rotor turns out of the wind so as to avoid damage to the unit at higher wind speeds. For this reason the wind speed of 16m/s was used to calculate the SLS forces acting on the tower induced by wind, and the peak wind speed as specified by SANS 10160-3:2011 was used for the ULS forces acting on the tower induced by wind. Table 13 illustrates the linear load combinations that are in accordance with the load factors for ULS and SLS in SANS 10160-1:2011. Incorporated in the Overturn (ULS & SLS) Load cases respectively are the wind actions acting on the tower for the different wind speeds as was described above.

**Table 13: Monopole Load Case Combinations**

Load Cases	ULS1 (SW)	ULS 2 (No Wind)	ULS 3 (Worst Case)	SLS 1 (SW)	SLS 2 (No Wind)	SLS 3 (Worst Case)
SW	1.2	1.2	1.2	1	1	1
Equipment DL	0	1.2	1.2	0	1	1
Overturn (ULS), wind speed>16m/s	0	0	1.5	0	0	0
Overturn (SLS), wind speed<16m/s	0	0	0	0	0	0.6

The following analyses were done on the Monopole tower so that it could be assessed in terms of stability and deflections, as well as how it would respond to dynamic loading effects.

### 6.2.1 LINEAR STATIC ANALYSIS

The linear static analysis is utilised to examine the deflections caused by the linear load combinations shown in Table 13.

A linear static solution by Strand7 is obtained assuming that the behaviour of the structure is linear and that the loading on the structure is static (static loads do not change in magnitude or direction with time). For the response of a structure to be linear, the mechanical behaviour of all materials in the model must follow Hooke's law; that is, element forces are linearly proportional to element deformation and when the loading is removed, the material returns to its original shape. In addition, the structure's deformation must be so small after loading that the deformed geometry is undistinguishable from the original, unloaded geometry. Because of these two assumptions, solutions can be arbitrarily combined to consider more complex loading conditions, such as the load combinations shown in Table 13 for the monopole modelled here (Strand7 theory manual).

All the deflections that were obtained for the different load cases were examined. The direction in which the tower was loaded in the model was in the Y-direction with regard to how the wind and overturn forces were imposed on the tower.

Figure 44 illustrates the load combination for which the displacement of the top of the tower for the linear static analysis (in the Y-direction) is assessed, which is the Serviceability Limit state load case for which all loads are incorporated.

The output from Strand7 comes in the form of the visual displays in Figure 44, which shows the deformed tower's deflections exaggerated by a factor of 10% for visual effect. Strand7 also displays a log file, which was used for the maximum displacements of the serviceability limit state tabulated in Table 14.

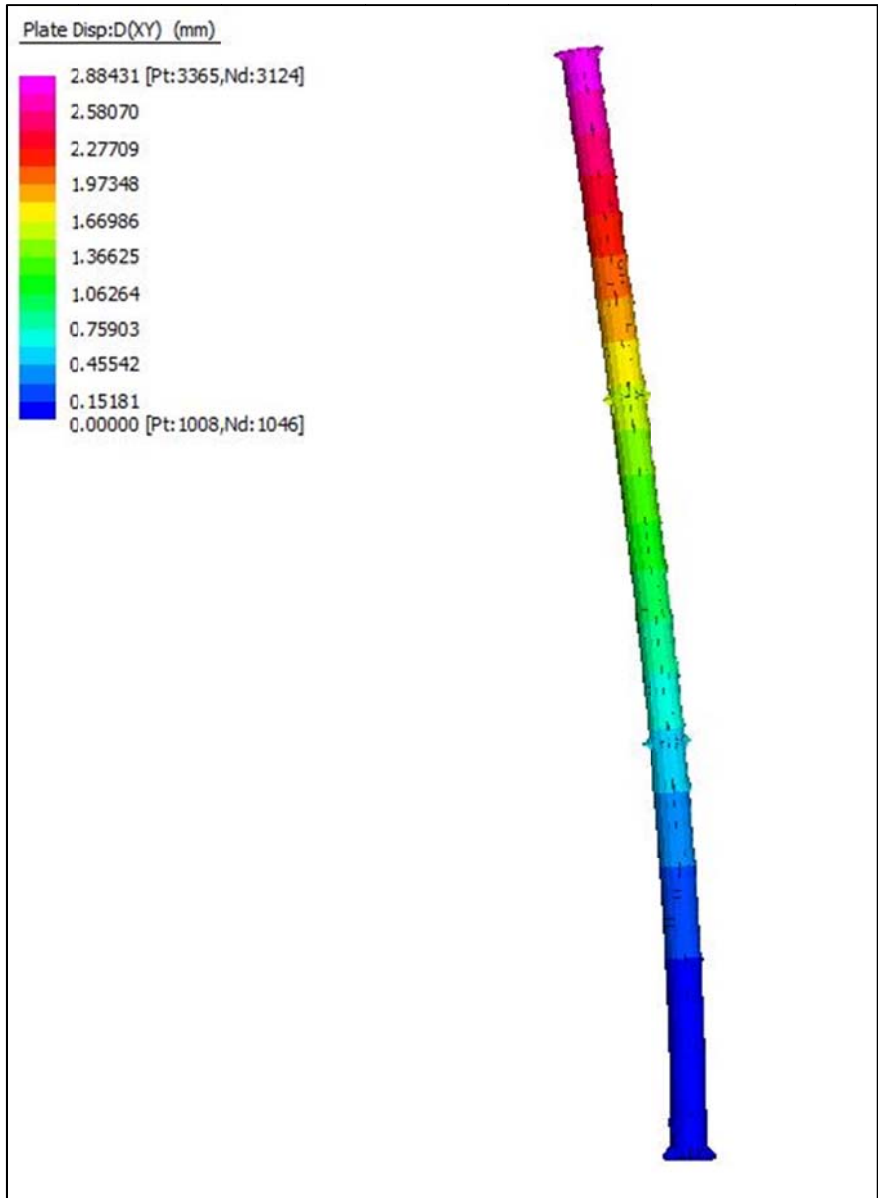


Figure 44: Monopole: Largest Static displacement load combination.

Table 14: Maximum displacement magnitudes of Monopole for Serviceability Limit State

Case	DX (mm)	DY (mm)	DZ (mm)
SW	0.00	0.01	0.06
Equipment DL	0.00	0.39	0.02
Overturn (ULS)	0.02	33.23	0.98
Overturn (SLS)	0.00	4.23	0.13

The deflections throughout the height of the tower are shown graphically in Figure 45 for the analysis of the Ultimate limit state (Worst case scenario) in which all loads are applied with maximum loading factors as was shown in Table 13.

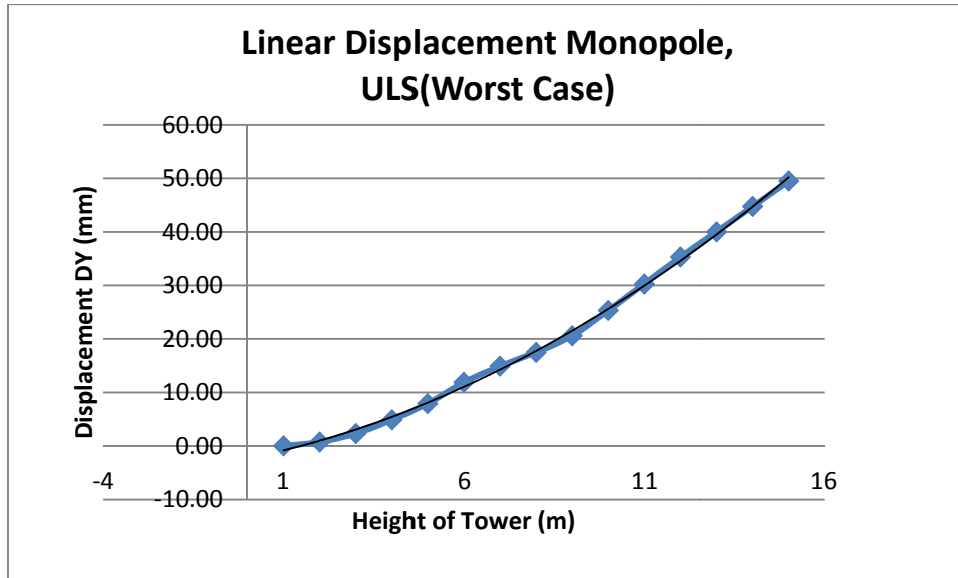


Figure 45: Monopole, Linear displacement distribution

THE NODAL REACTIONS AT THE BASE OF THE TOWER:

The linear static analysis results were also utilised to determine the nodal reactions at the base of the tower in order to verify the choice of holding down bolts as well as obtaining the base forces and reactions needed to design the foundation.

Figure 47, Figure 48 and Figure 49 illustrate the plate force distributions as resultant forces in the X, Y and Z directions respectively, under the Base of the tower. Figure 47, Figure 48 and Figure 49 would be applicable for any points about the vertical z-axis for the instances in which the wind turbine rotates with the wind and so the design of the base flange needed to be done in such a way as to resist the largest possible tension and compression forces that were developed here.

The reactions are shown relative to the axes system shown in Figure 46.

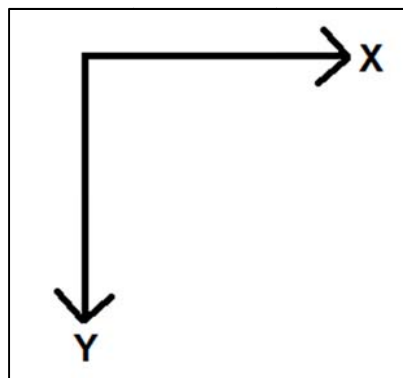


Figure 46: Axes system for nodal reactions

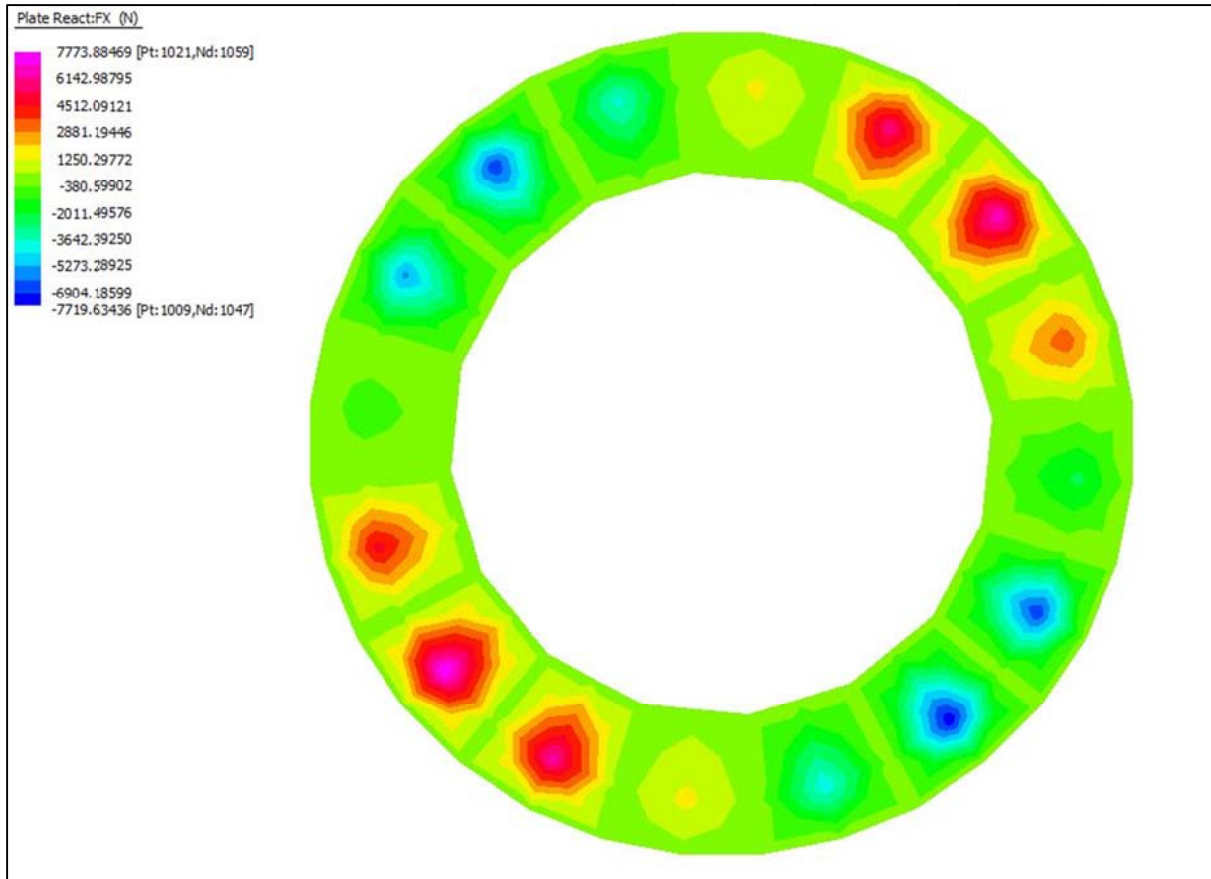


Figure 47: FX(N) Base Reaction Forces, ULS (Worst Case) Combination 3.

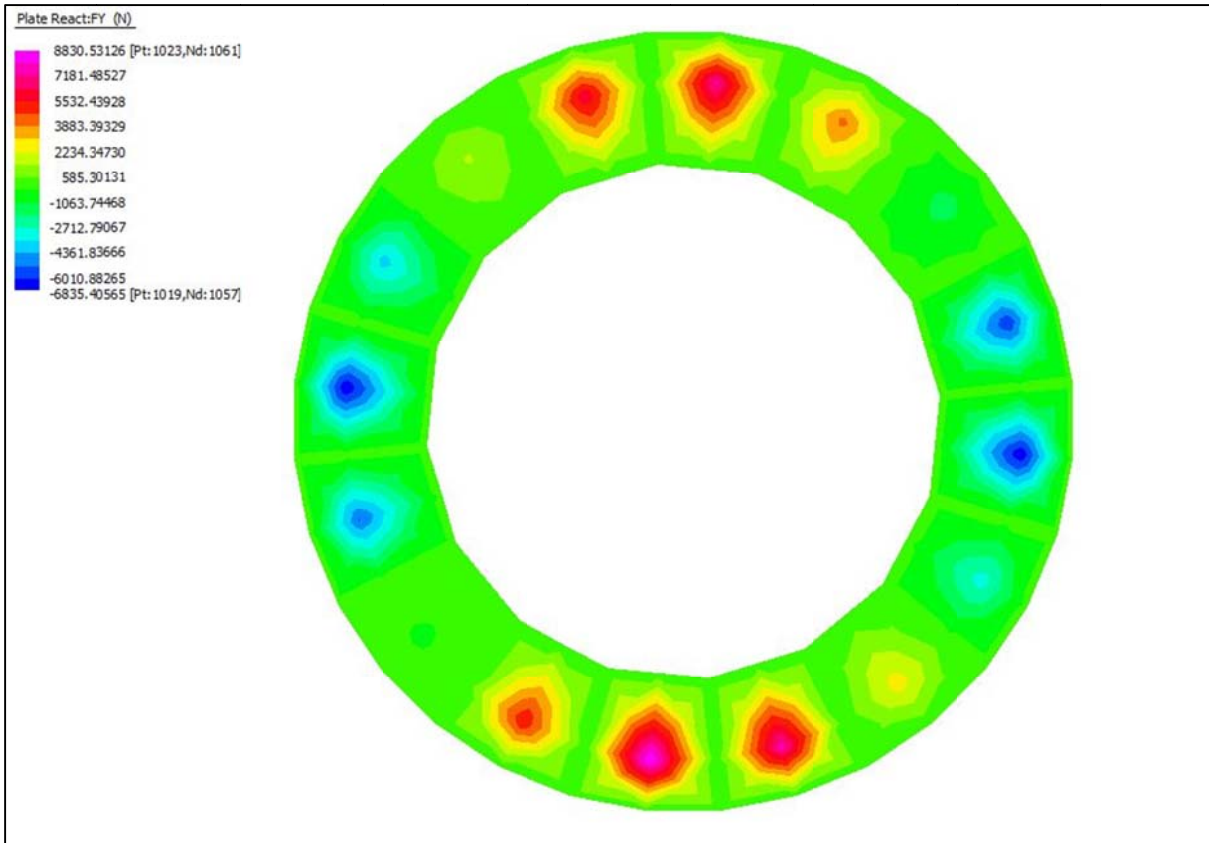


Figure 48: FY(N) Base Reaction Forces, ULS (Worst Case), Combination 3

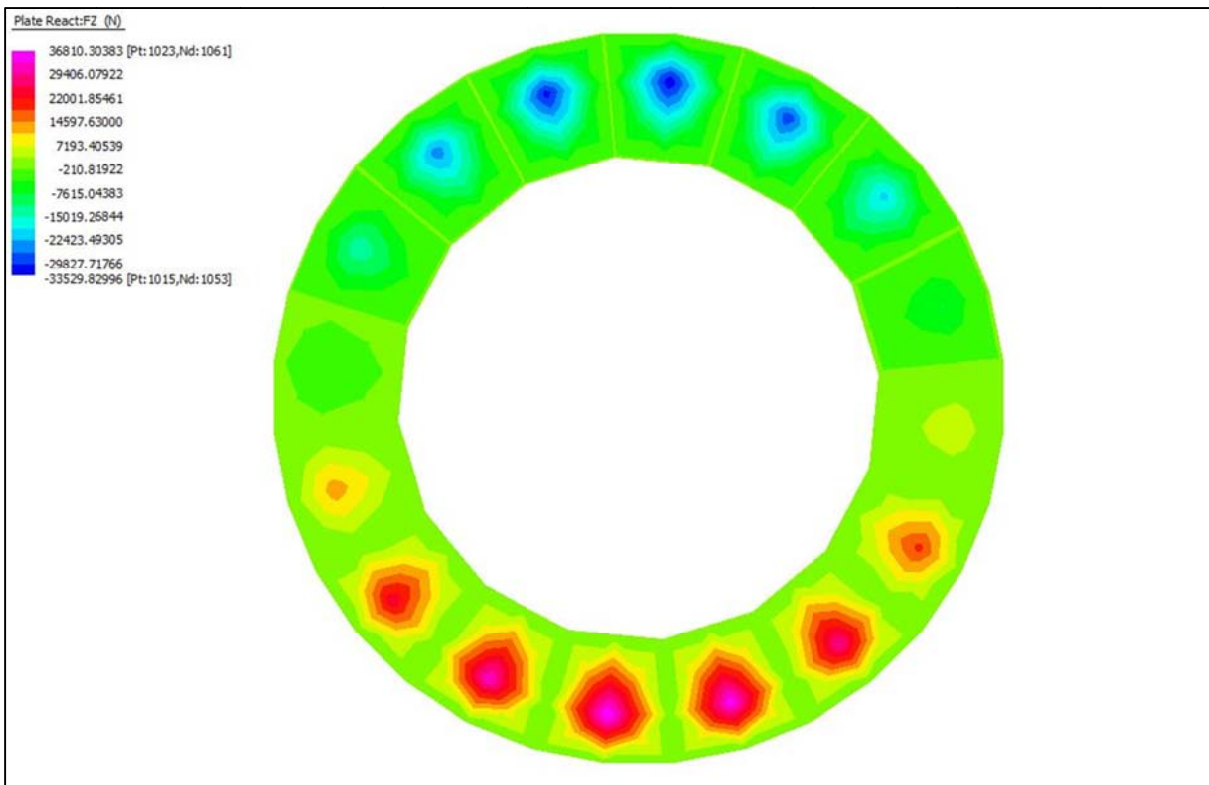


Figure 49: FZ(N) Base Reaction Forces, ULS (Worst Case), Combination 3



**LINEAR STATIC ANALYSIS STRESS STATES:**

In order to assess the stress state of the Steel Monopole for the linear static analysis, the stress distributions for the load combination ULS 3 as described in Table 13 were examined. In terms of the von Mises Stress state of the plate elements, as well as the Tresca Stress state of the plate elements none of the stress states exceed the elastic material limit (355MPa) of the S355JR grade steel that the Steel Monopole Tower was designed to.

**6.2.2 LINEAR BUCKLING ANALYSIS**

Before presenting the Linear Buckling analysis results, an overview of the linear buckling solver is addressed. It is noted here that the linear buckling analysis is an upper bound solution.

**LINEAR BUCKLING SOLVER:**

The Linear Buckling Solver in Strand7 calculates the buckling load factors and corresponding mode shapes for a structure under given loading conditions. It is based on the assumptions that there exists a bifurcation point where the primary and secondary loading paths intersect, and before this point is reached, all element stresses change proportionally with the load factor.

A linear buckling solution is obtained from solving an eigenvalue problem:

$$[K]\{x\} = \lambda[K_g]\{x\}$$

Where;

$[K]$  is the global stiffness matrix;  $\{x\}$  is a vector of the buckling modes,  $\lambda$  is the buckling load factor and  $[K_g]$  is the global geometric stiffness matrix.

The geometric stiffness matrix, also known as the initial stress stiffness matrix, is a symmetric matrix dependent on the element stress level. It reflects the effect of the geometric change on elements from a known stress value. For beam and plate bending structures, the geometric stiffness matrix represents the stiffening effect due to the tensile axial/membrane stresses.

The buckling solution is only possible when an existing solution is available for determining the current stress state of the structure, which is required for the calculation of the element geometric stiffness matrix. In Strand7, both the Linear Static Solver and the Nonlinear Static Solver solutions can be used to start the Linear Buckling Solver solution (Strand7 Software).

The Linear Buckling analysis determines a bifurcation point, where the primary and secondary loading paths intersect. At the bifurcation point more than one equilibrium position is possible. The primary path is not usually followed after loading exceeds this point and the structure is in the post-buckling state. The slope of the secondary path at the bifurcation point determines the nature of the post-buckling behaviour. A positive slope indicates that the structure will have post buckling strength whilst a negative slope means that the structure will snap through or simply collapse.

Real structures have geometric and loading imperfections, often causing the primary curve and the bifurcation point to disappear.

For real structures, linear buckling analyses are best for preliminary design, and studying the effects of various parameters.

There are many factors present in real structures that have a large influence on the stability and critical buckling load. The Linear bifurcation analysis neglects all of these and assumes that the structure is perfect.

Consequently, the predicted buckling load will always be an over estimate of that for a real structure (Strand7 Software).

Strand7 calculates the buckling factors for each load combination separately. Figure 50 illustrates how the load buckling factors differ in magnitude for the different load combinations.

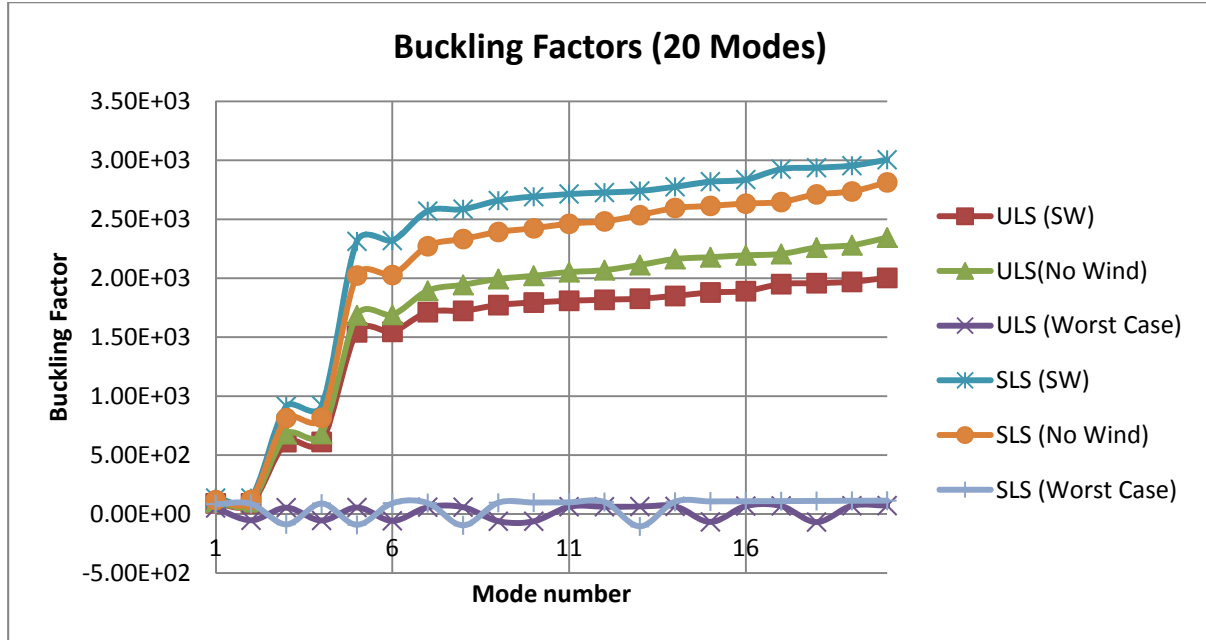


Figure 50: Monopole, Linear Buckling Factors

Table 15: Monopole, Linear Buckling Factors

Mode	SW	ULS (SW)	ULS (No Wind)	ULS (Worst Case)	SLS (SW)	SLS (No Wind)	SLS (Worst Case)
1	135.5	90.3	99.6	51.2	135.5	119.5	83.2
2	136.0	90.6	100.0	-53.0	136.0	119.9	86.4
3	914.8	609.8	678.0	53.6	914.8	813.6	-87.9
4	918.1	612.1	680.4	-55.0	918.1	816.4	89.1
5	2313.4	1542.3	1686.3	55.5	2313.4	2023.5	-90.9
6	2319.1	1546.0	1689.5	-57.3	2319.1	2027.4	92.1

In Figure 50, the ULS and SLS worst case scenario load cases both stopped converging after two modes, whereas the rest stopped converging after 6 modes. This can most likely be explained by the complexity of the algorithms used in solving the buckling load factors in Strand7. Table 15 shows the buckling factors for the first 6 modes of each load combination that was defined in Table 13. Any buckling factor larger than 1 implies that buckling is not expected but ultimate limit state load factors apply. Where negative buckling factors are shown, they indicate a load reversal, for example rather than the load buckling factor applying for tension, it occurs with the magnitude shown but for compression.

### 6.2.3 NONLINEAR ANALYSIS

In the nonlinear analysis, due to the incremental nature of the solution, a number of load steps need to be defined, for which a number of equilibrium iterations is done. It is no longer possible to have linear load combinations in a nonlinear analysis, because the manner in which the different loading components are to be applied to the structure follows the real world loading sequence.

In the nonlinear analysis, the self-weight of the structure along with the dead load of the applied equipment is imposed and analysed initially. The results of this initial analysis are then utilised as the initial conditions for a

second nonlinear analysis in which the wind loads are applied. The load factors are taken into account at the beginning of each of these analyses by means of multiplying the overall applied loads by the appropriate factors.

Although the majority of engineering structures operate within the linear regime and the assumptions made for the linear solution are valid, there is a wide class of problems that do exhibit nonlinear behaviour. The nonlinear static solver predicts the behaviour of structures with nonlinear behaviour being taken into account. In Strand7, three different types of nonlinearities can be included: geometric, material and boundary nonlinearity.

For the nonlinear analysis performed on the Monopole tower, the loading was applied in 20 increments of equal size, starting from a zero load and ending up at the appropriately factored load.

For the same design case as was illustrated above in the static linear analysis, the static nonlinear analysis of the monopole was done as follows. First a static nonlinear analysis was done where the self-weight and dead load of the equipment were the only applied loads with ultimate limit state loading factors of 1.2. A second non-linear analysis was done, where the results from the initial analysis were used as the initial conditions. In the second nonlinear analysis, only the wind and over turning forces were applied with a load factor of 1.5, for the ultimate limit state. Figure 51 illustrates the progression of the maximum displacement, which occurred at the top of the tower, relative to the load increments applied. The Strand7 Nonlinear Static Solver uses an algorithm based on Newton-Raphson method.

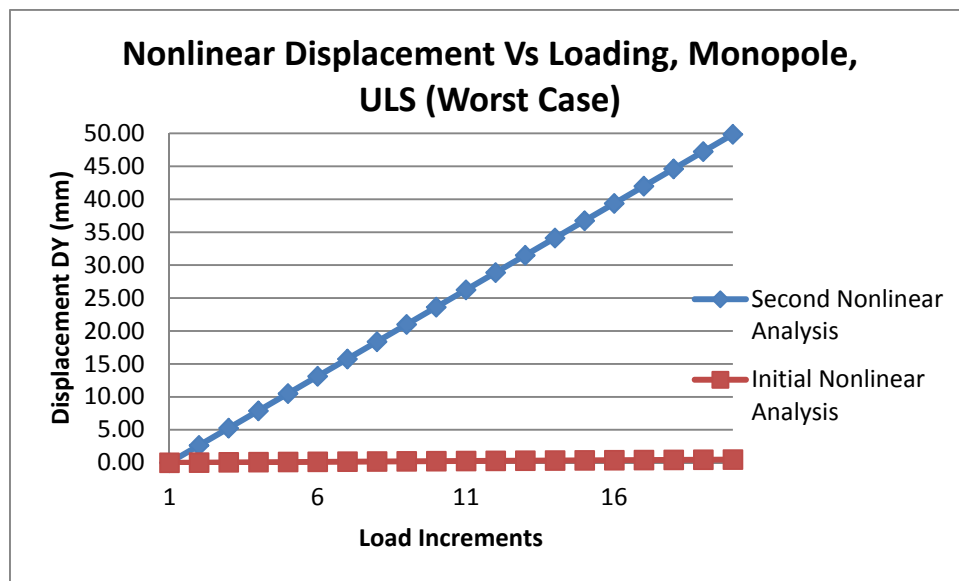
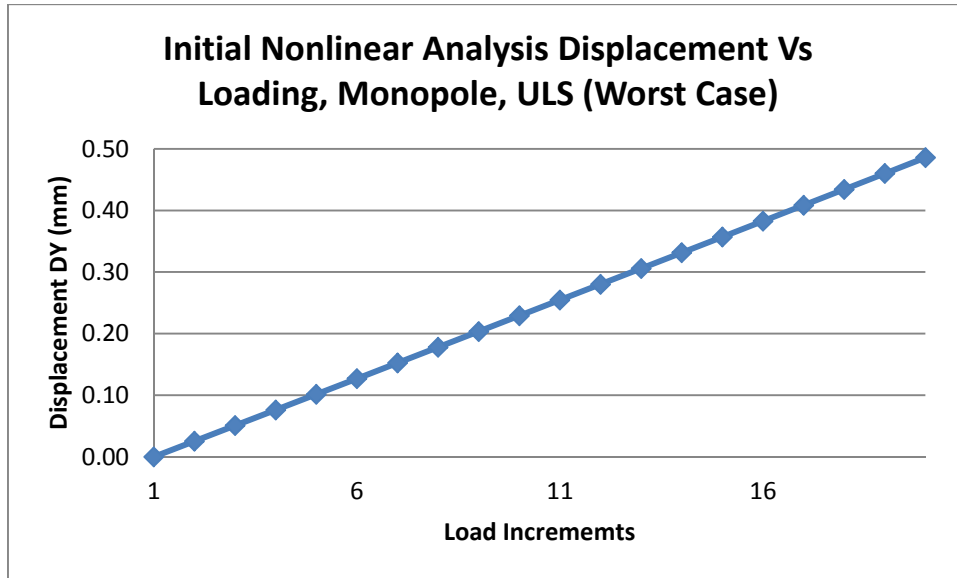


Figure 51: Monopole nonlinear displacement Vs. Loading

Because the scale of displacements for the initial and second nonlinear analyses is so different, the initial analysis displacement where only the self-weight of the tower and the dead load of the equipment were applied is plotted separately in Figure 52:



**Figure 52: Initial Nonlinear Analysis: Monopole ULS (Worst Case)**

The displacements illustrated in Figure 52 essentially act as initial geometric imperfections in the second static nonlinear analysis that is done, and so the results obtained from the final nonlinear analysis are less conservative in terms of the buckling potential and the degree of deflection to be concerned with in comparison with a linear buckling analysis.

#### 6.2.4 DYNAMIC ANALYSES

The dynamic forces investigated here were not necessarily the governing load cases in the overall design; they were however assessed as accidental load cases.

The dynamic analyses performed on the towers in this thesis were preceded by a Natural Frequency analysis, performed by the Natural frequency solver in Strand7. Following the natural frequency analysis, the following aspects were examined:

1. The effects of an Out of Balance Rotor
2. The effects of Vortex Shedding

#### NATURAL FREQUENCY SOLVER OVERVIEW:

The natural frequency solver is used to calculate the natural frequencies (or free vibration frequencies) and corresponding vibration modes of an undamped structure. The natural frequency analysis problem is formulated as the following eigenvalue problem:

$$[K]\{x\} = \omega^2[M]\{x\}$$

Where  $[K]$  is the Global stiffness matrix,  $[M]$  is the global mass matrix,  $\{x\}$  is the vibration mode vector, and  $\omega$  is the circular frequency (radians/sec), natural frequency =  $\omega/2\pi$  [Hz].

The results obtained from a natural frequency analysis include a set of eigenvalues, and their corresponding eigenvectors.

The eigenvalues obtained from the eigenvalue problem represent the natural frequencies for each vibration mode. The eigenvectors represent a vector of nodal displacements that define the free vibration mode shapes of the structure. For each of the calculated natural frequencies, there is one corresponding eigenvector. Note here that the mode shapes (eigenvectors) are sets of relative displacements for the structure vibrating in that

particular mode under no external excitation. These eigenvectors can be shown in the same way as node displacements, but the absolute scale is normalised to a maximum displacement of 1.0.

The mode shapes of every second mode for the first 20 modes of the Steel Monopole are shown in Figure 53, only every second mode is shown because of the axisymmetric geometry of the structure; every other mode shape is the same.

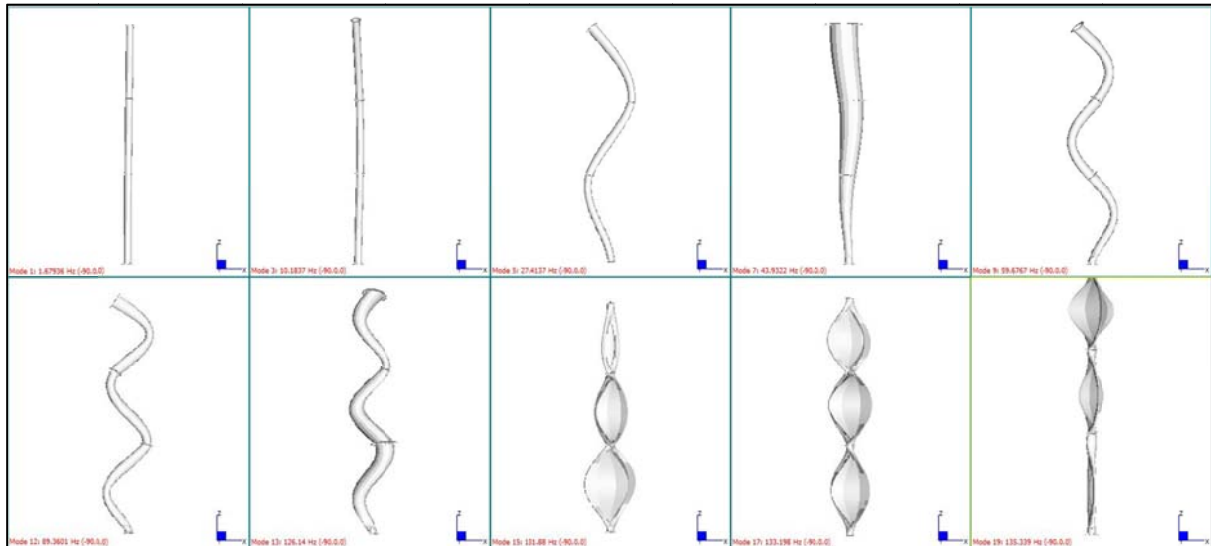


**Figure 53: Every second mode shape of the first 20 modes of the Steel Monopole**

The natural frequency for the first 20 modes was plotted for different damping ratios ranging between 5 and 10%, which didn't alter the response and is shown in Figure 54. The damping ratios were chosen as they are typical rule of thumb ratios for steel structures.

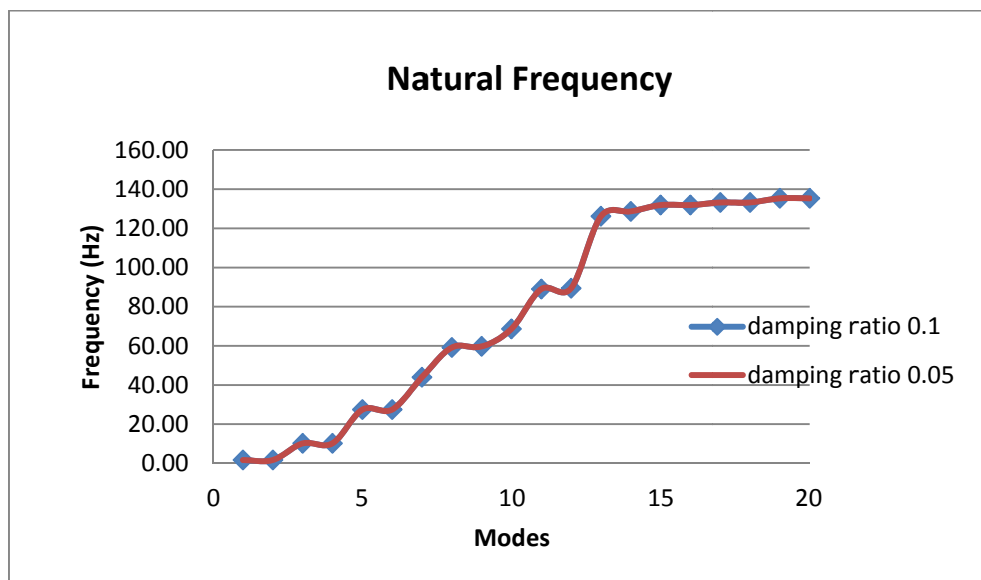


**Figure 54: Monopole, Natural Frequency Analysis**

### 6.2.4.1 THE EFFECTS OF AN OUT OF BALANCE ROTOR:

The 3kW wind turbine machine, for which the supporting structures in this thesis were designed, was stipulated to not induce any out of balance rotor disturbances, such that the effects of a possible out of balance rotor could essentially be ignored for the purposes of tower design.

However, it was decided to investigate the effect of accidental out of balance rotating forces on the tower, from the perspective of a potential accidental load case, and the understanding of what the effects might be.

Therefore the investigation done on the effects of the out of balance rotor was for the purposes of conservative design accounting for accidental load cases, and to examine what possible stresses could arise as a result of such repetitive out of balance forces that could result in fatigue in the base connection, from the stresses occurring in the weld and flange plate.

In order to determine the possible effects of an out of balance rotor on the tower, a harmonic response analysis was done. Harmonic response is examined for the purpose of assessing the human response criteria as well as the fatigue and displacement states of the structure if exposed to repetitive loading.

For wind turbine towers, the human response to dynamic loading does not need to be considered, as the machine would not be operational when any human ascends the tower.

The importance of examining the fatigue of the tower for this accidental load case is because such an out of balance force could occur without being visible to the naked eye, and so be subjecting the tower to dynamic loading without the effects being noted. If this was the case fatigue causing structural failure could occur and this must be avoided as far as is possible.

#### HARMONIC RESPONSE SOLVER OVERVIEW:

Harmonic analysis is used to predict the steady state dynamic response of a structure subjected to sinusoidally varying loads. A structure will initially vibrate in an irregular manner after a sinusoidal load is applied. This is referred to as the transient stage. After the transient stage, all points within the structure will vibrate in the same sinusoidal fashion with a frequency identical to the forcing frequency,  $\omega$ , but generally with different amplitudes and different phase angles. This part of the response is known as the steady state stage. The harmonic response solver calculates the maximum values of the steady state response and the associated phase angles (Strand7 Software).

Strand7 allows two types of harmonic loading of which only one type may be included in a given solution.

The harmonic response solution relies on natural frequencies, and must therefore be given the correct natural frequency file in order to complete the solution correctly.

The same natural frequency result file can be used to run the Harmonic Solver as many times as needed with different harmonic solution settings such as frequency range and damping values.

The response of the full structure is calculated by superposition of the modal response considering the magnitudes and phase angles of the modal responses. This is based on the closed form solution.

For the Response vs. Frequency solution type, an envelope of the maximum values of the response is given in the result file at each forcing frequency step. When damping is included, these maximum values may not occur simultaneously and for this reason, the results for the phase angles are given. Output data includes the maximum values of nodal reaction, displacement, velocity, acceleration and phase angle as well as node and element forces, moments and stress.

For the Response vs. Frequency solution type, the solution is calculated at equally spaced steps over the user specified frequency range. Additional steps are automatically introduced at the natural frequencies within the specified range to capture peak responses.

It is however very important to assess the Response vs. Time solution as well to understand the transient phase affects that could cause an unwanted response on the tower in the phase through which the turbine starts rotating until it is at its fully operational speed.

#### HARMONIC RESPONSE RESULTS:

The results of the analysis are absolute maximum envelope values of the steady state dynamic response. The maximum values do not occur at the same time. Consequently the results don't present an equilibrium state of the structure and they do not correspond to the maximum stress results. The stress at one particular point is just the maximum value that occurred at that particular point during the steady state stage of the dynamic response.

#### DETAILS OF THE OUT OF BALANCE ROTOR ANALYSIS:

For a conservative simulation, 10% of the total weight of the rotor and nacelle combined was calculated and applied to the tower to account for the out of balance forces that could possibly arise because of the rotor not being perfectly in balance. The 10% of the total weight of the rotor and nacelle combined which was calculated and applied was done so as two vectors of equal magnitude, one in the vertical direction, and one in the horizontal direction at the appropriate point of application. The point at which the vectors were applied was the same point at which the overturning forces were applied, the hub height of the wind turbine machine. The two vectors were then given a loading participation factor of one, such that they were both imposed, and then were applied with a phase angle of 90 degrees between them so as to simulate the rotating motion of the rotor. The vectors were applied with a frequency which was equal to the equivalent operating frequency of the wind turbine rotor in revolutions per minute, which equates to a 5Hz frequency. A modal damping ratio of 5% was specified.

The observed response of the tower to the out of balance rotor was negligible, in terms of the degree to which it displaced the tower, seen in Figure 55.

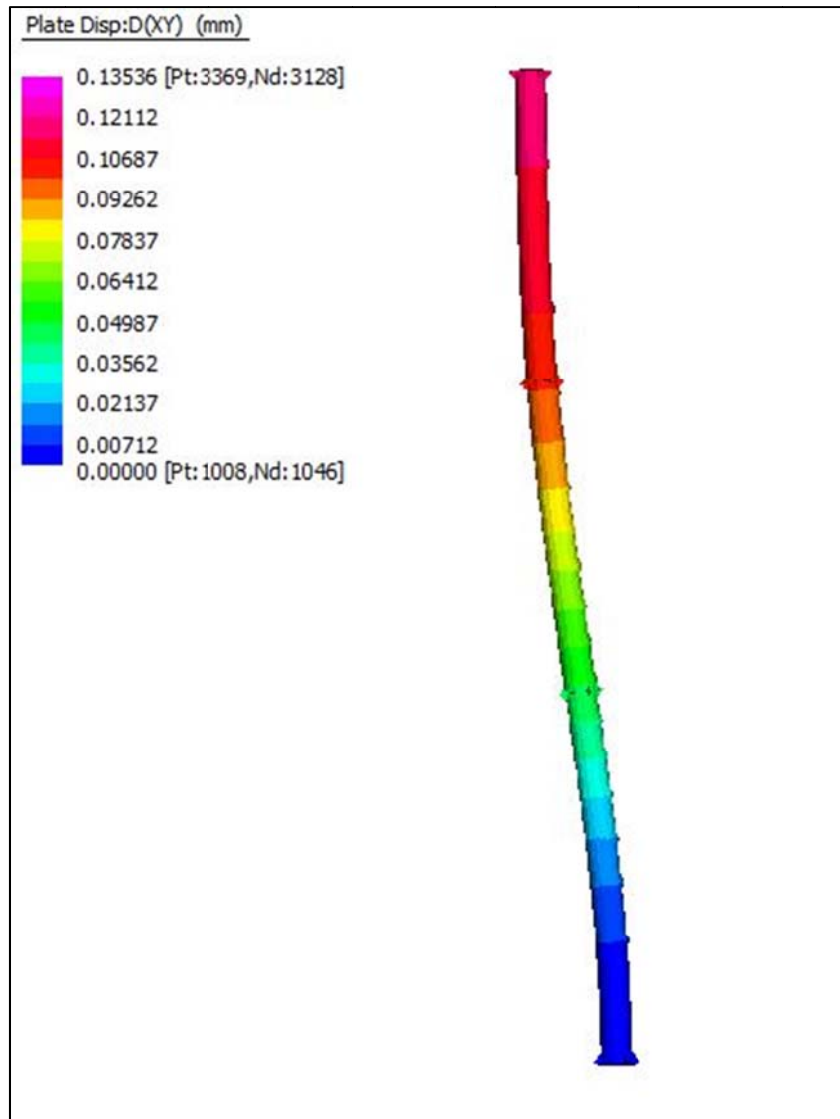


**Figure 55: Worst Case displacement occurring for harmonic response**

Because of the repetitive nature of a dynamic load, the tower base still needs to be assessed for fatigue, even with such low displacements, this is done in section 6.3.

#### 6.2.4.2 EFFECTS OF VORTEX SHEDDING DUE TO WIND ACTION

To examine the effects of vortex shedding, the harmonic response solver in Strand7 was used, where the chosen analysis type of the harmonic response vs. time analysis was used to examine the effects that shall be discussed here.

##### HARMONIC DISPLACEMENT RESPONSE VS. TIME ANALYSIS:

In order to analyse the different possible effects that the wind could have on the tower if it coincided with the vortex shedding frequency of the tower, the wind was applied as a series of nodal loads of calculated magnitude at the appropriate nodes, on two opposing sides of the tower. The wind load was then given the same frequency as the vortex shedding frequency, 11.2Hz, and each of the opposing wind loads were given loading factors of 1, and a phase angle difference between them set at 180 degrees.



The effects as a displacement response versus time were examined to see the kinds of possible excitations the tower might experience having the wind load applied at the same harmonic frequency as the calculated vortex shedding frequency with the following results.

Figure 56 shows the maximum displacements which occurs during the possible resonance effect of the vortex shedding frequency coinciding with the natural frequency of the supporting structure, the effects of which are negligible. However, as a result of the repetitive loading condition the vortex shedding could induce, it is important to still examine the stress range that the tower is subjected to under this loading condition for fatigue; this is examined in sections 6.3 and 6.4.

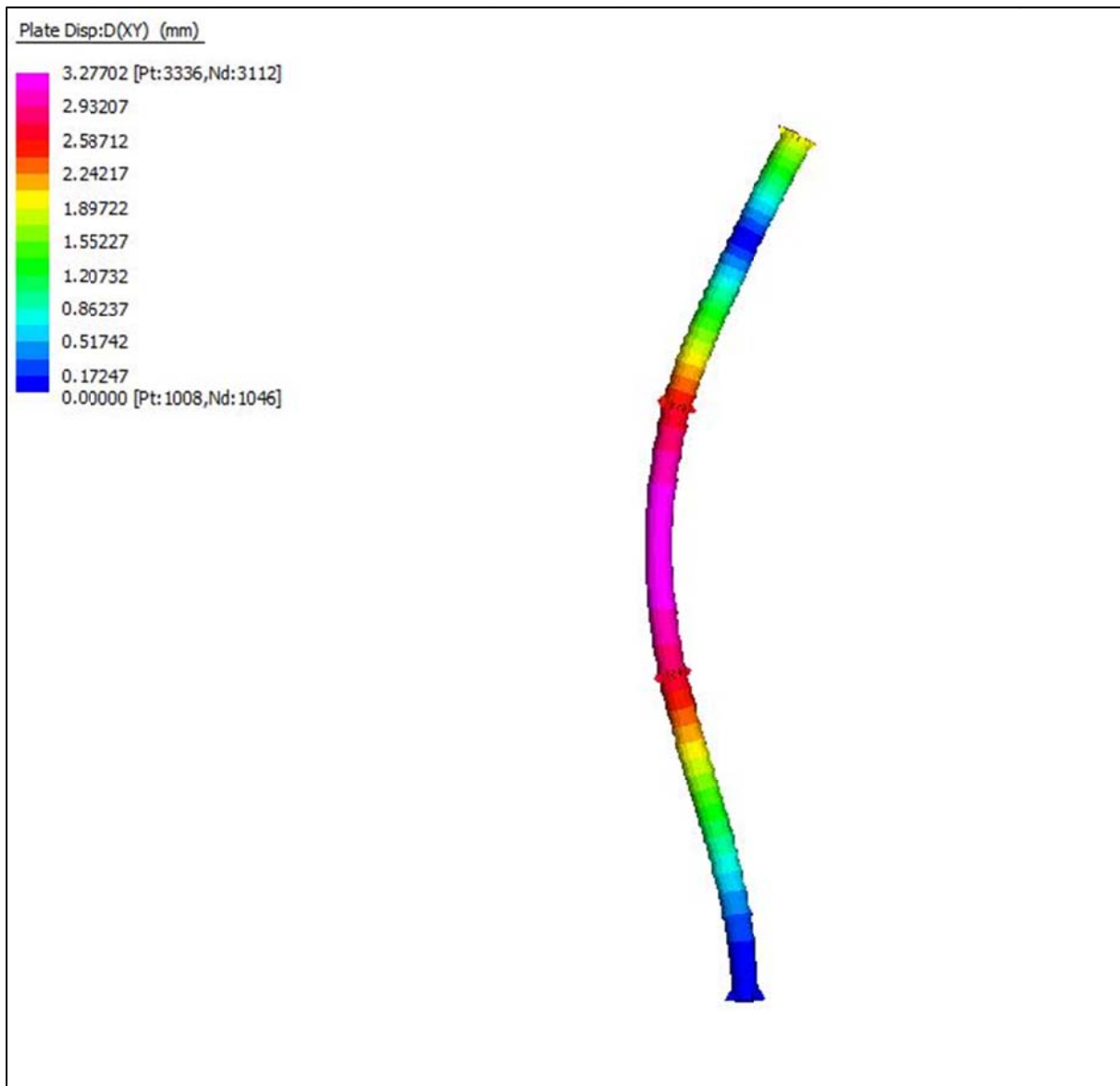


**Figure 56: Vortex shedding harmonic response, worst case displacement**

### 6.3 STRESS STATES

#### HARMONIC RESPONSE STRESS ANALYSIS:

The stress range which a structure is subjected to in the harmonic response analysis is essential to examine to determine the effects the repetitive loading may have had on the fatigue state of the structure. Figure 57 shows the base of the steel monopole tower, and the range of stresses it is subjected to under harmonic loading. The stress range is extremely low.

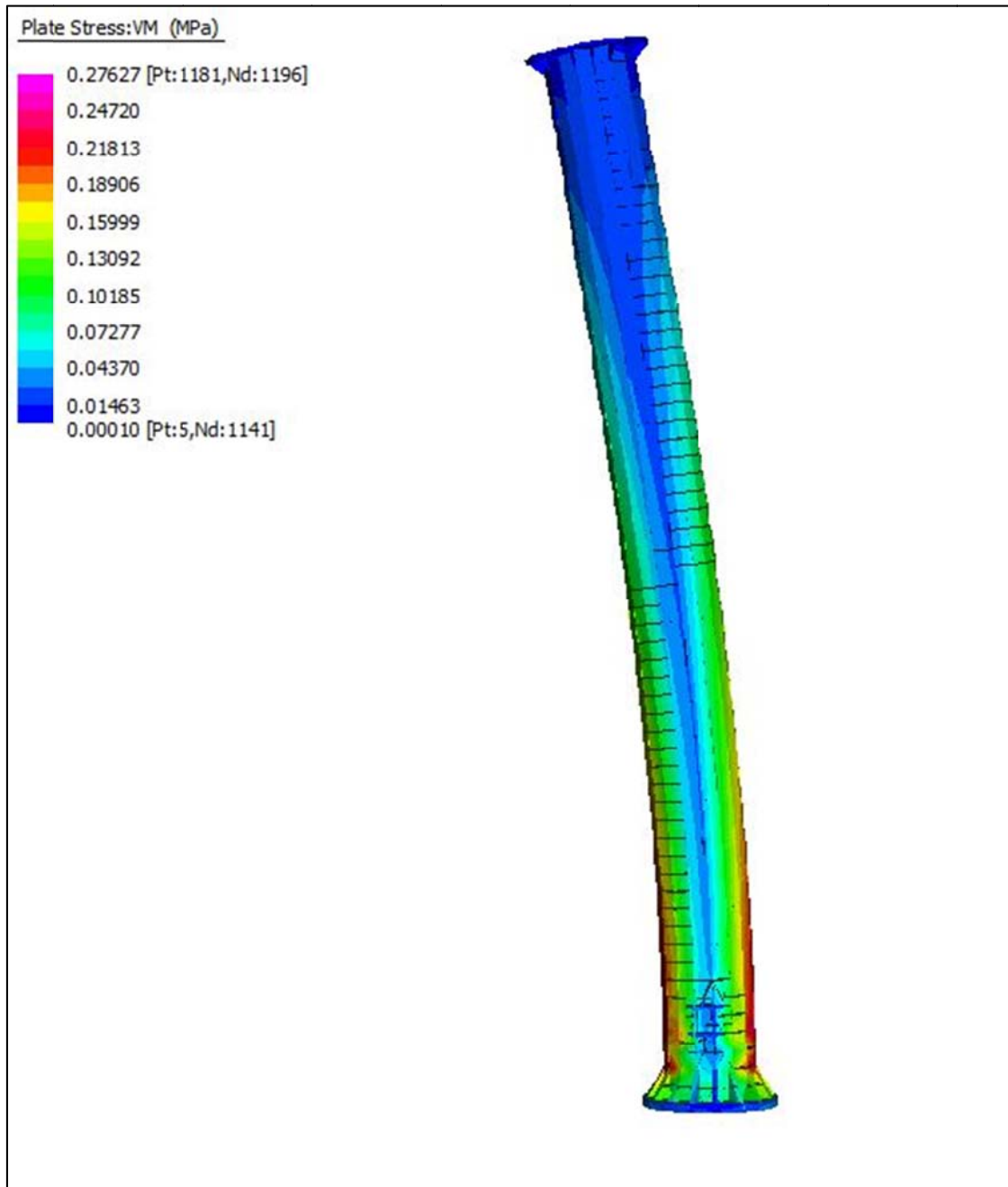


**Figure 57: Monopole Stress response to the dynamic loading as a result of the out of balance rotor effects**

#### VORTEX SHEDDING STRESS ANALYSIS:

As a result of the way in which the vortex shedding was analysed as a dynamic load, the stress range which the structure was subjected to under the repetitive loading of the wind as the vortex shedding frequency was examined as a precaution to avoid fatigue. Figure 58 shows the stress range which this dynamic loading

subjects the supporting structure to and it is of extremely low stress, to such an extent that fatigue can be ignored.

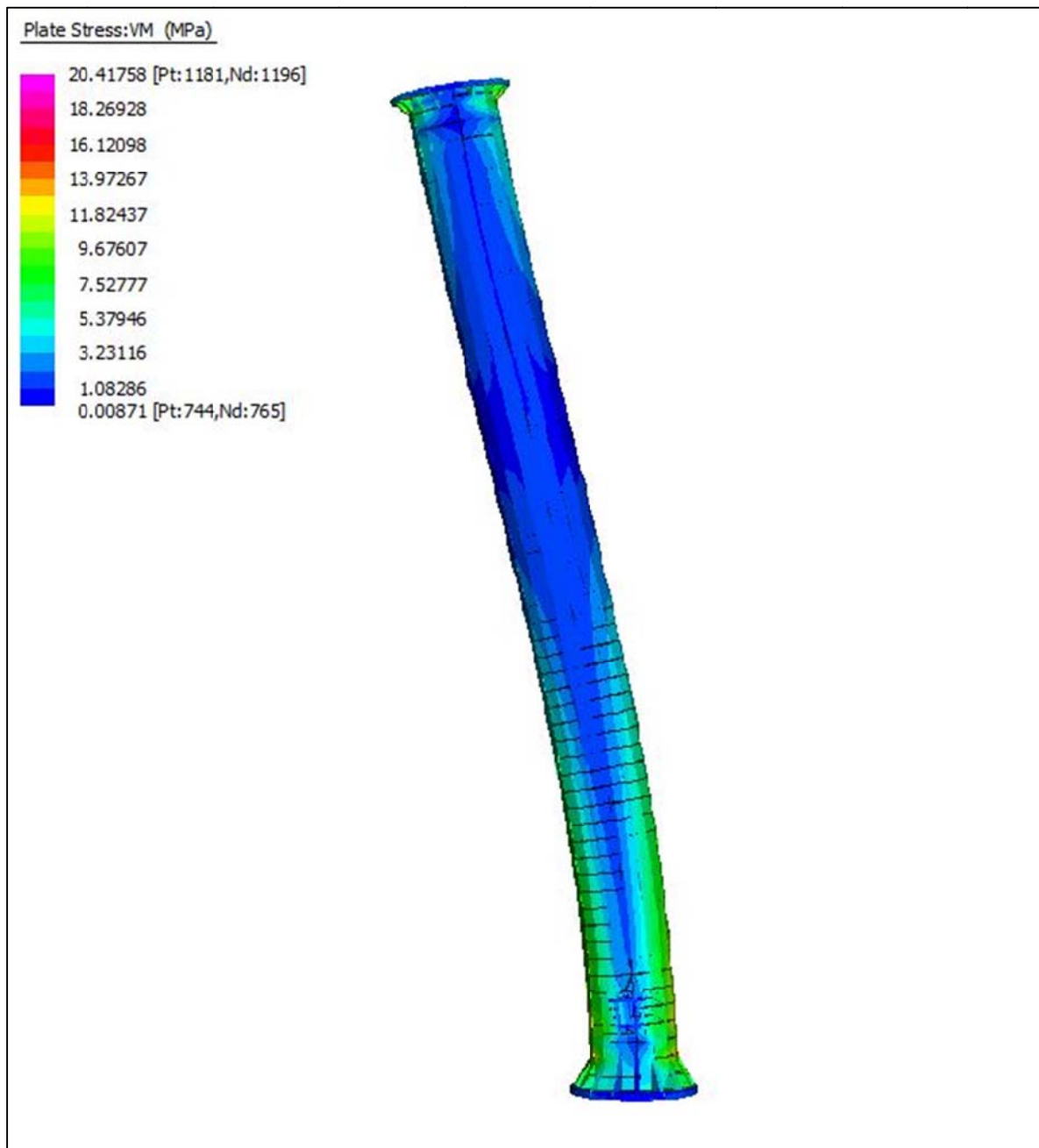


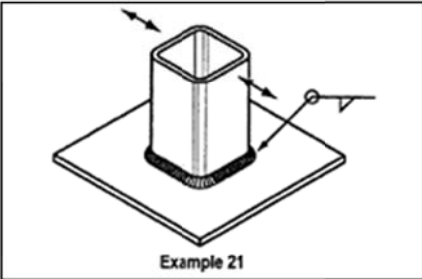
Figure 58: Vortex shedding stress state

#### 6.4 FATIGUE ASSESSMENT:

Following the assessment of the stress range which the out of balance rotor would subject the supporting tower to as this would be a possible continuous loading, the fatigue effects that such loading would have on the base of the steel monopole tower are examined. In accordance with SANS 10162-1:2005 Clause 26.3.2, the data shown in Table 16 was analysed. The tower was analysed for the instance in which an out of balance rotor was running 24 hours of the day 365 days a year. It was determined that the fatigue effects of such an accidental load case are negligible and so will not be the cause of structural failure.

**Table 16: Fatigue Analysis of Steel Monopole Base**

Fatigue Analysis [SANS 10162-1:2005 Clause 26.3.2]			
Structure Life Time	20	yrs	
Yearly Use	365	days	
Daily Use	24	hours	
Exciting Frequency (fe)	5	Hz	
			Cycles 3.15E+09 duty cycles
Detail Type	E1		
Fatigue Life Constant ( $\gamma$ )	1.29E+11		
Const Amp Stress Lim ( $f_{srt}$ )	18	MPa	
Fatigue Life Constant ( $\gamma'$ )	4.15E+13		
Cycles	2.20E+07		
Stress Range ( $f_{sr}$ )	0.3	MPa	
Fatigue Resistance ( $f_{fr}$ )	NA	MPa	Adjusted Cycles 1.71E+16 duty cycles



Example 21

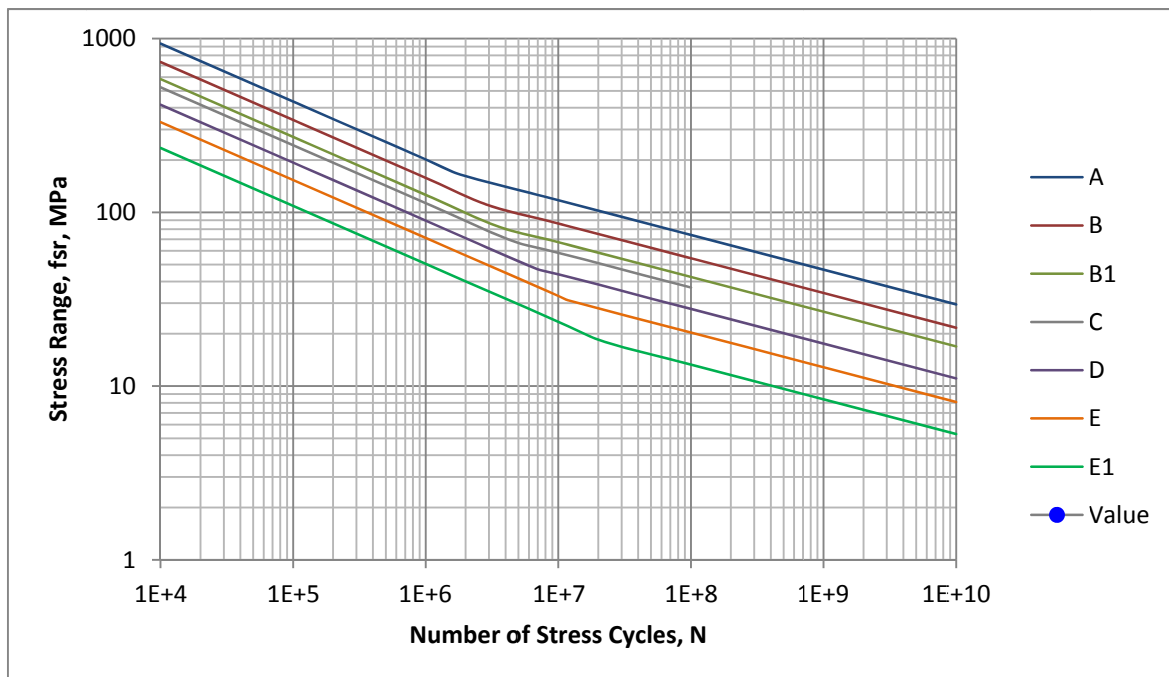
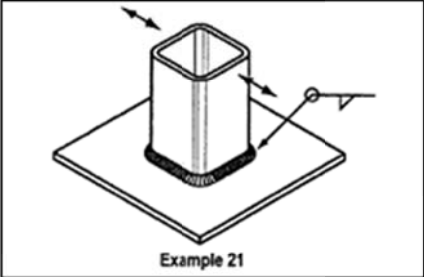


**Figure 59: Stress vs. Number of Cycles for Fatigue Analysis of out of balance rotor in accordance with SANS 10162-1:2005 Clause 26**

The reason that no blue dot indicating a value on Figure 61 appears is as a result of it not occurring in any visible margin of the graph on the scale which is shown, as it represents such small stress and such a large number of cycles.

**Table 17: Fatigue Assessment for Steel Monopole and vortex shedding**

Fatigue Analysis [SANS 10162-1:2005 Clause 26.3.2]			
Structure Life Time	20	yrs	
Yearly Use	365	days	
Daily Use	24	hours	
Exciting Frequency ( $f_e$ )	5	Hz	
			Cycles <span style="border: 1px solid black; padding: 2px;">3.15E+09</span> duty cycles
Detail Type	<b>E1</b>		
Fatigue Life Constant ( $\gamma$ )	1.29E+11		
Const Amp Stress Lim ( $f_{srt}$ )	18	MPa	
Fatigue Life Constant ( $\gamma'$ )	4.15E+13		
Cycles	2.20E+07		
Stress Range ( $f_{sr}$ )	30	MPa	
Fatigue Resistance ( $f_{fr}$ )	3.45	MPa	Adjusted Cycles <span style="border: 1px solid black; padding: 2px; color: red;">4.78E+06</span> duty cycles



Example 21

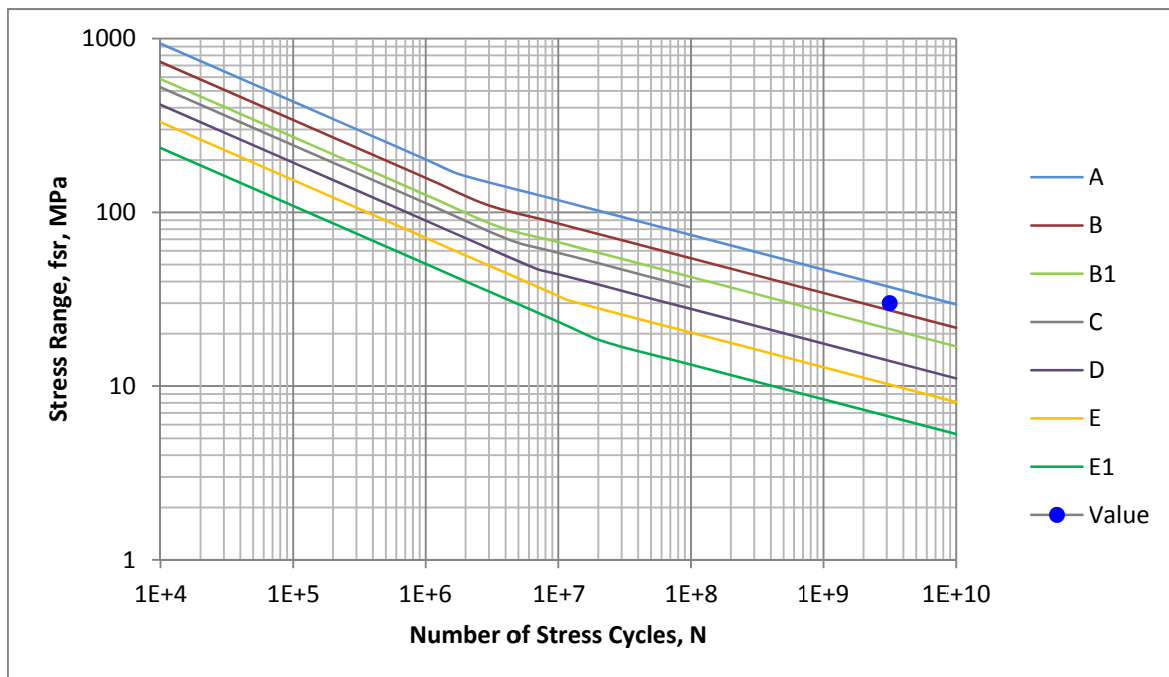


**Figure 60: Fatigue Analysis, Stress Range versus Number of cycles for Vortex shedding analysis in accordance with SANS 10162-1:2005**

### 6.5 MASS PARTICIPATION:

In order to assess if the mass participation of the steel monopole tower was sufficient, in terms of representing the mass distribution through modelling the tower as closely to how it would be having been constructed, the mass participation for translational and rotational excitations were examined. From the output of the Natural frequency solver, it was observe that after just 20 modes the mass participation was at over 90%, indicative of an excellent representation of mass distribution through modelling.

MODE PARTICIPATION FOR TRANSLATIONAL EXCITATION						
Mode	Frequency (Hz)	Modal Mass (Eng)	Modal Stiff (Eng)	PF-X (%)	PF-Y (%)	PF-Z (%)
1	1.6794E+00	7.8453E-01	8.7349E+01	0.554	59.116	0.000
2	1.6830E+00	7.8348E-01	8.7607E+01	59.069	0.553	0.000
3	1.0184E+01	1.0255E+00	4.1986E+03	0.148	18.628	0.005
4	1.0202E+01	1.0133E+00	4.1637E+03	18.633	0.148	0.000
5	2.7414E+01	1.2355E+00	3.6656E+04	5.816	0.018	0.000
6	2.7451E+01	1.2853E+00	3.8237E+04	0.018	5.824	0.019
7	4.3932E+01	5.0112E-01	3.8183E+04	0.112	0.000	0.000
8	5.9145E+01	1.0872E+00	1.5014E+05	0.000	3.228	0.395
9	5.9677E+01	9.6044E-01	1.3503E+05	3.252	0.000	0.000
10	6.8618E+01	1.4149E+00	2.6301E+05	0.000	0.028	77.324
11	8.8989E+01	1.1548E+00	3.6102E+05	0.000	1.995	0.202
12	8.9360E+01	1.0495E+00	3.3085E+05	1.983	0.000	0.000
13	1.2614E+02	6.9072E-01	4.3388E+05	0.774	0.000	0.000
14	1.2861E+02	1.0833E+00	7.0734E+05	0.000	1.013	0.043
15	1.3188E+02	7.6377E-01	5.2442E+05	0.002	0.012	0.000
16	1.3188E+02	4.5242E-01	3.1065E+05	0.000	0.001	0.000
17	1.3320E+02	9.8624E-01	6.9078E+05	0.002	0.009	0.000
18	1.3320E+02	6.1918E-01	4.3370E+05	0.000	0.001	0.000
19	1.3534E+02	3.4988E-01	2.5300E+05	0.000	0.000	0.000
20	1.3534E+02	3.5463E-01	2.5645E+05	0.000	0.001	0.000
----- TOTAL MASS PARTICIPATION FACTORS				90.362	90.577	77.988

MODE PARTICIPATION FOR ROTATIONAL EXCITATION						
Mode	Frequency (Hz)	Modal Mass (Eng)	Modal Stiff (Eng)	PF-RX (%)	PF-RY (%)	PF-RZ (%)
1	1.6794E+00	7.8453E-01	8.7349E+01	78.274	0.733	0.000
2	1.6830E+00	7.8348E-01	8.7607E+01	0.733	78.243	0.000
3	1.0184E+01	1.0255E+00	4.1986E+03	10.035	0.080	0.000
4	1.0202E+01	1.0133E+00	4.1637E+03	0.080	10.102	0.002
5	2.7414E+01	1.2355E+00	3.6656E+04	0.001	0.412	0.275
6	2.7451E+01	1.2853E+00	3.8237E+04	0.354	0.001	0.001
7	4.3932E+01	5.0112E-01	3.8183E+04	0.000	0.715	67.860
8	5.9145E+01	1.0872E+00	1.5014E+05	1.797	0.000	0.000
9	5.9677E+01	9.6044E-01	1.3503E+05	0.000	1.496	2.429
10	6.8618E+01	1.4149E+00	2.6301E+05	0.004	0.000	0.000
11	8.8989E+01	1.1548E+00	3.6102E+05	0.766	0.000	0.000
12	8.9360E+01	1.0495E+00	3.3085E+05	0.000	0.750	1.433
13	1.2614E+02	6.9072E-01	4.3388E+05	0.000	1.256	5.151
14	1.2861E+02	1.0833E+00	7.0734E+05	1.068	0.000	0.000
15	1.3188E+02	7.6377E-01	5.2442E+05	0.015	0.003	0.000
16	1.3188E+02	4.5242E-01	3.1065E+05	0.002	0.000	0.000
17	1.3320E+02	9.8624E-01	6.9078E+05	0.012	0.002	0.000
18	1.3320E+02	6.1918E-01	4.3370E+05	0.002	0.000	0.000
19	1.3534E+02	3.4988E-01	2.5300E+05	0.000	0.000	0.000
20	1.3534E+02	3.5463E-01	2.5645E+05	0.001	0.000	0.000
----- TOTAL MASS PARTICIPATION FACTORS				93.145	93.792	77.153

**RESONANCE EFFECTS:**

In having determined the natural frequencies of the tower, as well as what proportion of mass that participates with each mode, the possible effects of resonance can be assessed.

Because the machine’s operating frequency is 5Hz, modes 1 with natural frequency (1.67Hz) and 2 with natural frequency (1.68Hz) are the most crucial to examine, as they shall be experienced in the transient phase from the rotor being stationary at 0Hz until it is running at a fully operational speed of 5Hz. Examining a range of frequencies that encompass the operating frequency, such as the following: 0.6(operating frequency) to 1.6(operating frequency), the natural frequencies can be evaluated for resonant peaks in accordance with the proportion of modal mass participating within that range. Figure 62 is illustrative of this for the steel monopole tower, however there is not a significant resonant peak within the pertinent operating frequency range, and so the tuning of the steel monopole is adequate.

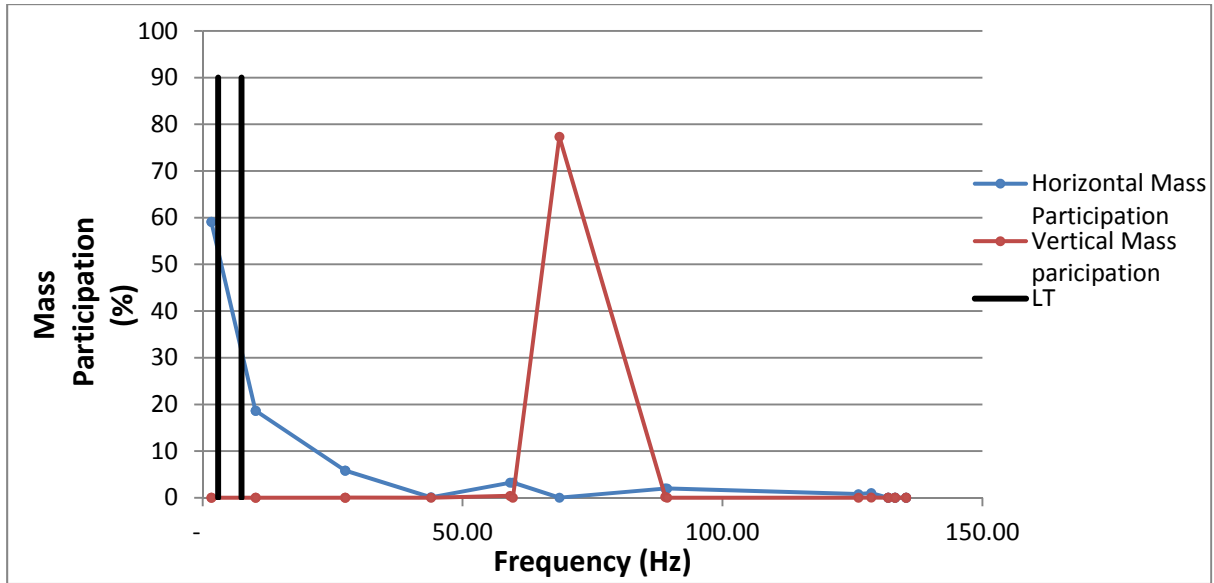


Figure 61: Resonance evaluation of steel monopole

## 6.6 STEEL LATTICE TOWER: FINITE ELEMENT ANALYSES

The Steel lattice supporting tower for the 3kW wind turbine was designed and then analysed using the finite element package Strand7.

The analyses that were performed on the Steel Lattice Tower were outlined and described in the introduction to this chapter and are repeated here:

1. Linear Static Analysis
2. Linear Buckling Analysis
3. Nonlinear Analysis
4. Dynamic Analyses
  - i) Natural Frequency Analysis
  - ii) Effects of an out of balance rotor
  - iii) Effects of vortex shedding due to wind action
  - iv) Harmonic Frequency Analysis
  - v) Stress states and Fatigue assessment
  - vi) Modal Mass Participation Evaluation

The tower was designed with a top portion which had parallel sides which fitted into a bottom section that tapered gradually down to level ground; see Figure 62 for connection details between the two tower sections. The structural members chosen for the design varied in size from 50x50x5mm equal angle leg sections to 70x70x6mm sections to the largest sections which were 100x100x8mm sections at the bottom. The structural members' connections were modelled as pinned.

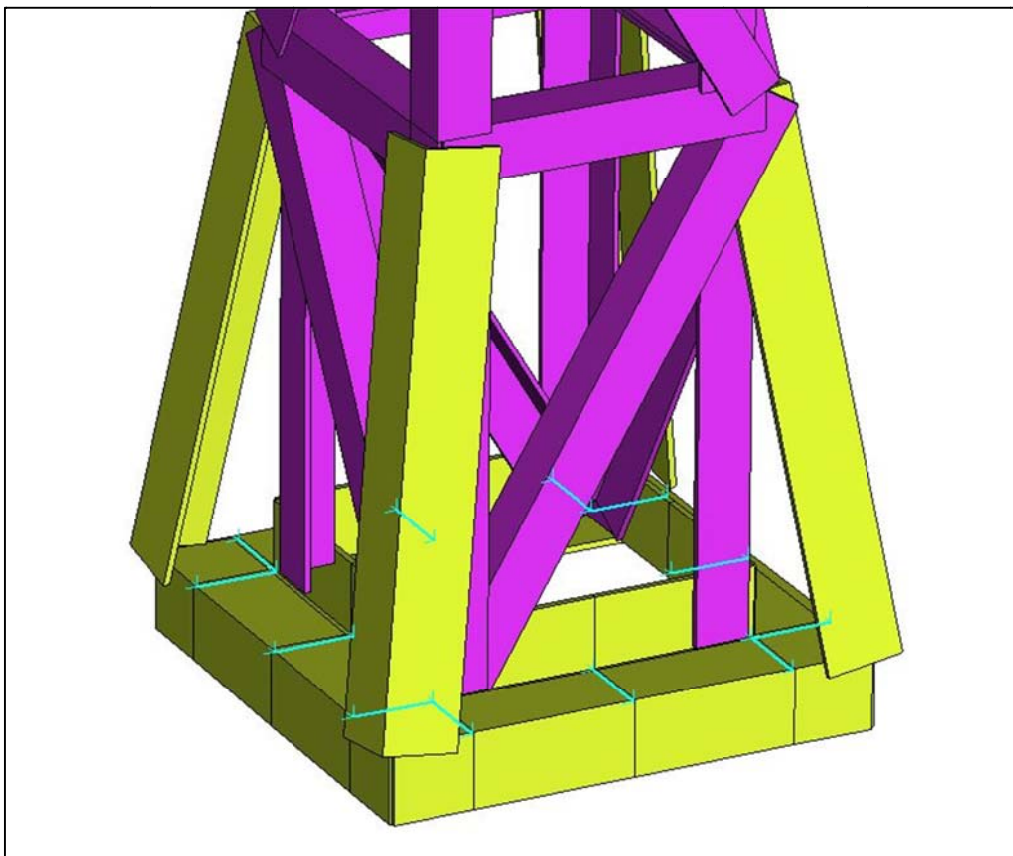


**Figure 62: Connection Details between top parallel portion of the tower and the tapered portion of the tower**



The effects of the wind turbine machine acting on the top of the tower were simulated by means of a prismatic assembly of rigid links that met at a central position and then had an extending rigid link that could create the appropriate point at which the eccentric centre of mass of the rotor and nacelle could be applied as a lumped mass. The model of the top of the tower is shown in Figure 63. The force that shall be described as the overturn force in the following sections accounted for the action of the wind on the blades of the Wind Turbine Machine. The calculation details of the overturn force were described in Chapter 3 in section 3.3.2. The overturn force simulated the action of the wind on the blades of the rotor as a function of hub height and wind speed and was applied at the peak of the conical formation of rigid links in Strand7, seen in Figure 63.

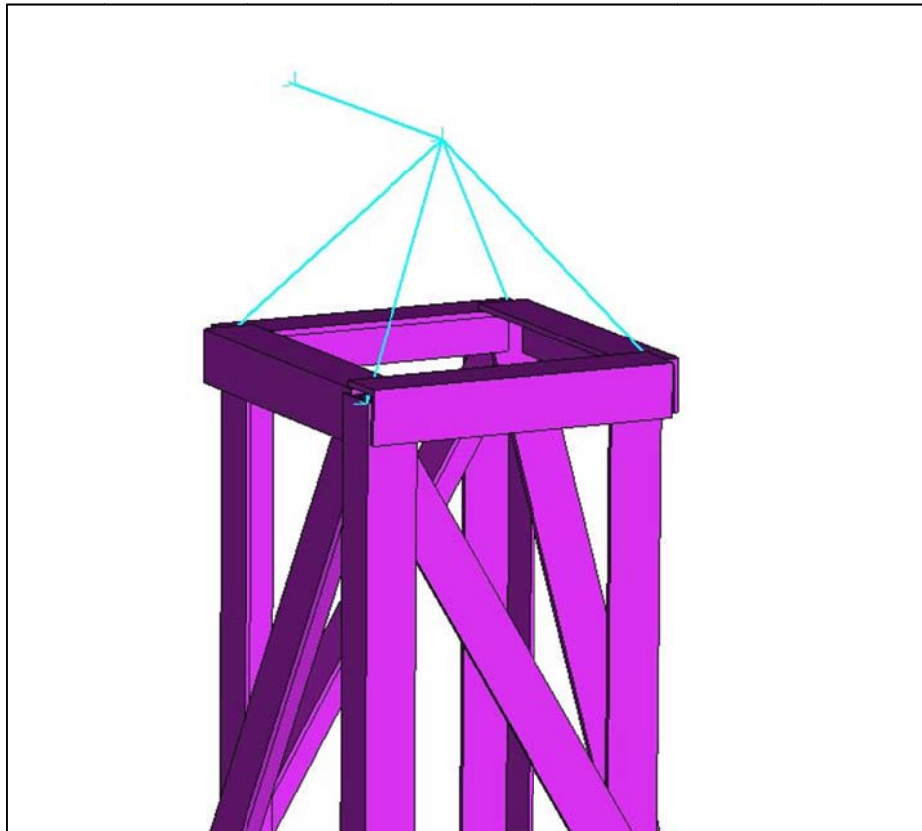


**Figure 63: Lattice Tower Turbine Connection Simulation**

For a steel lattice tower that has a square plan section, two wind loading directions were considered. For the two different wind load cases, two separate models were created and each of the load combinations specified in accordance with SANS 10160-1:2011 were applied to the models. Figure 64 shows the two wind loading cases in plan view.

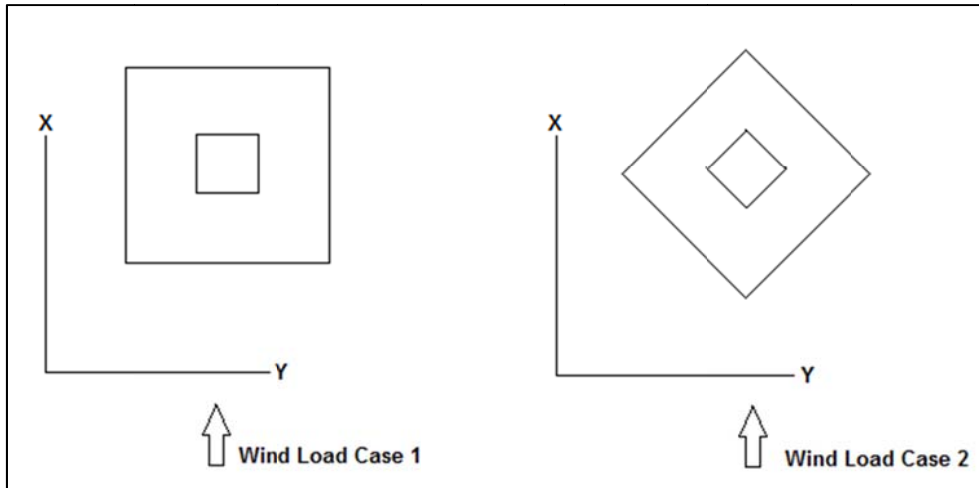


**Figure 64: Wind Loading Cases for square plan Steel Lattice Towers**

Table 18 shows, for each of the above wind loading cases, the load combinations that were applied to the steel lattice tower.

**Table 18: Load Case Combinations, Lattice Tower**

Load Cases	ULS 1	ULS 2	ULS 3	SLS 1	SLS 2
<b>SW</b>	1.2	1.2	0.9	1	1
<b>Equipment DL</b>	1.2	1.2	0.9	1	1
<b>Overturn (ULS)</b>	0	1.5	1.5	0	0
<b>Overturn (SLS)</b>	0	0	0	0	0.6
<b>Wind Normal</b>	0	1.5	1.5	0	0.6

**WIND LOAD MODELLING:**

The design implications of the way in which the steel lattice tower was loaded for the wind actions on the tower was investigated to determine the extent of effect that different loadings may have on the results of deflection and stress.

Two extreme loading options were examined, 1. The front and back members were loaded with a distributed wind load and 2. Only the front members were loaded with a distributed wind load.

The first of the two options equates to twice the total applied load of the second option. The results are tabulated in Table 19, and graphed in Figure 65 and Figure 66.

**Table 19: Wind loading on the Steel Lattice Tower, displacement and stress results**

Option	Displacement (DX) SLS2 (mm)	Max Axial Stress ULS3 (MPa)	Total Applied Load (X), (N)
1 (Back and front)	9.99	89.68	30247.9
2 (Front only)	8.73	84.49	15215.9
difference	1.26	5.19	15032

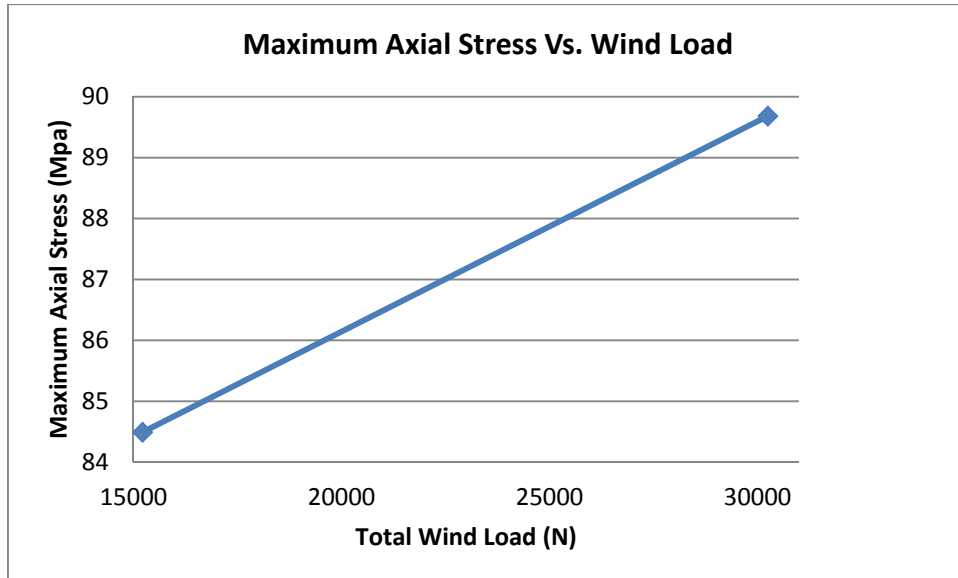


Figure 65: Stress comparison for two different wind loads on Steel Lattice Tower

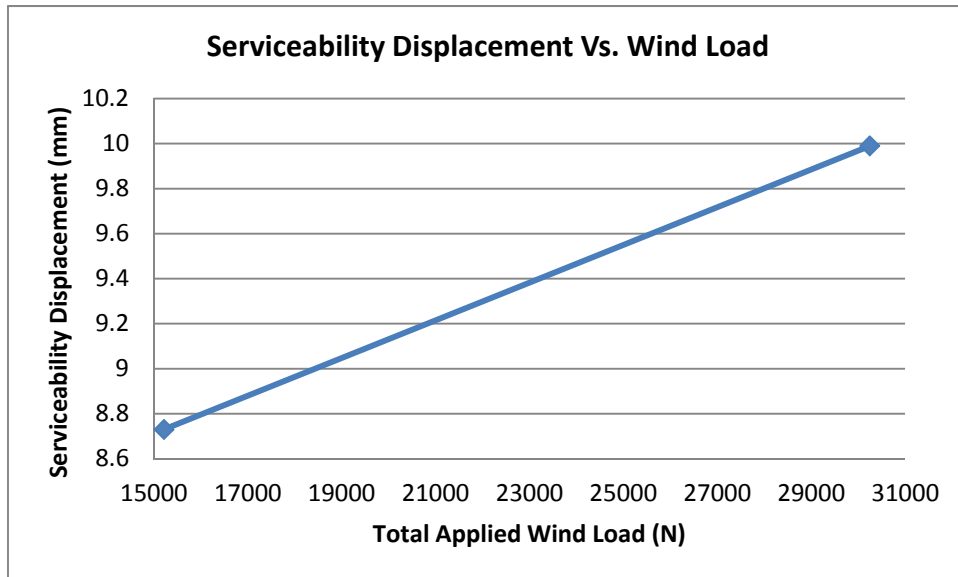


Figure 66: Displacement comparison for two different wind loads on Steel Lattice Tower

From the results in Table 19 it can be deduced that the wind load modelling particulars on the members of the Steel Lattice Tower would not influence the end results significantly. For conservative design, option 1 of the two options was chosen in the final model.

### 6.6.1 LINEAR STATIC ANALYSIS

The first analysis of the steel lattice tower was the linear static analysis.

In Figure 68, the displacement result for the load combination SLS2 as defined in Table 18 is shown for wind load case 1. The magnitude of displacement difference for the two load cases 1 and 2 when examined is within 0.01mm from one another. Figure 67 below shows the directions in which the two different wind load cases were modelled.

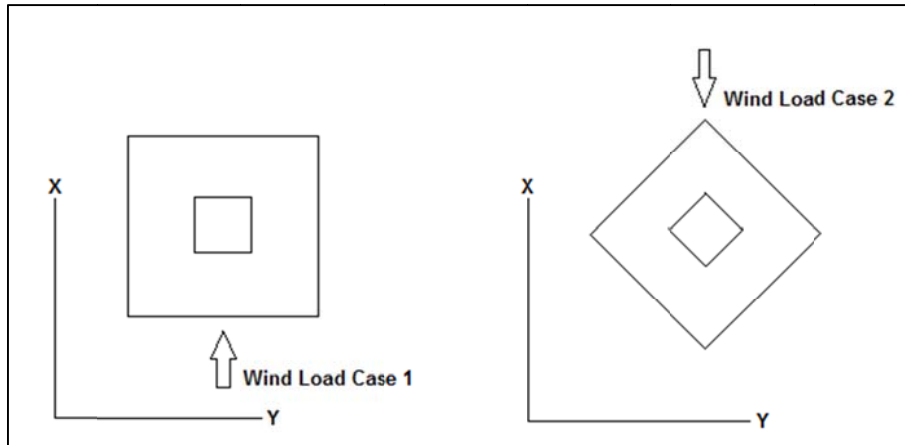


Figure 67: Different wind load cases for Square plan Steel Lattice Towers

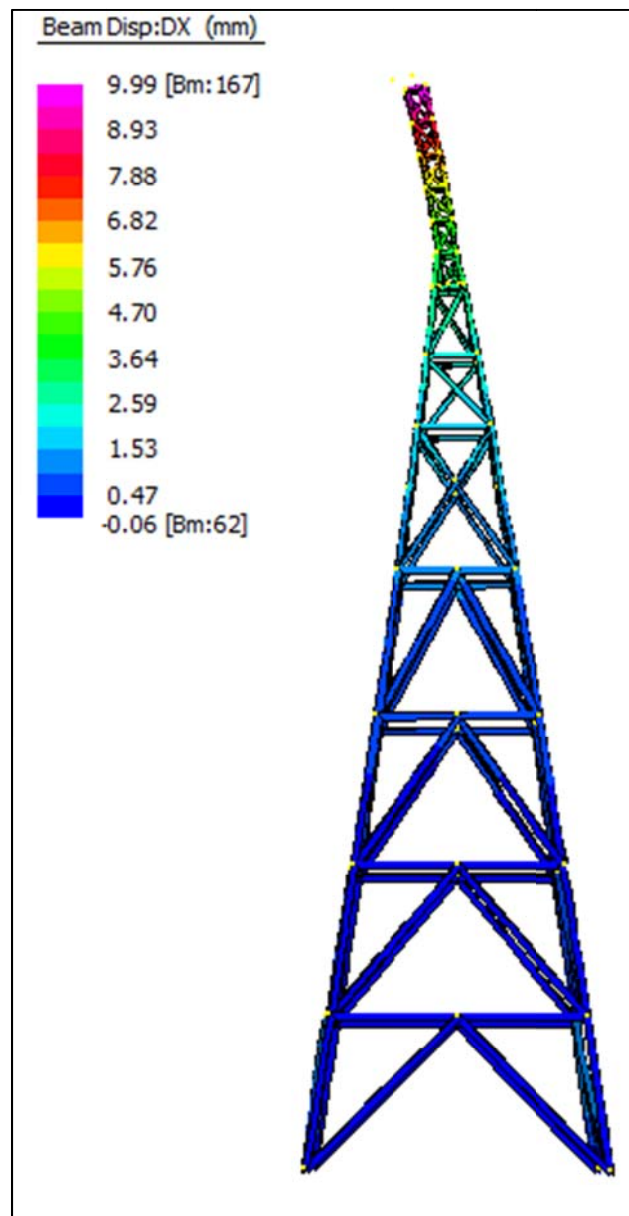
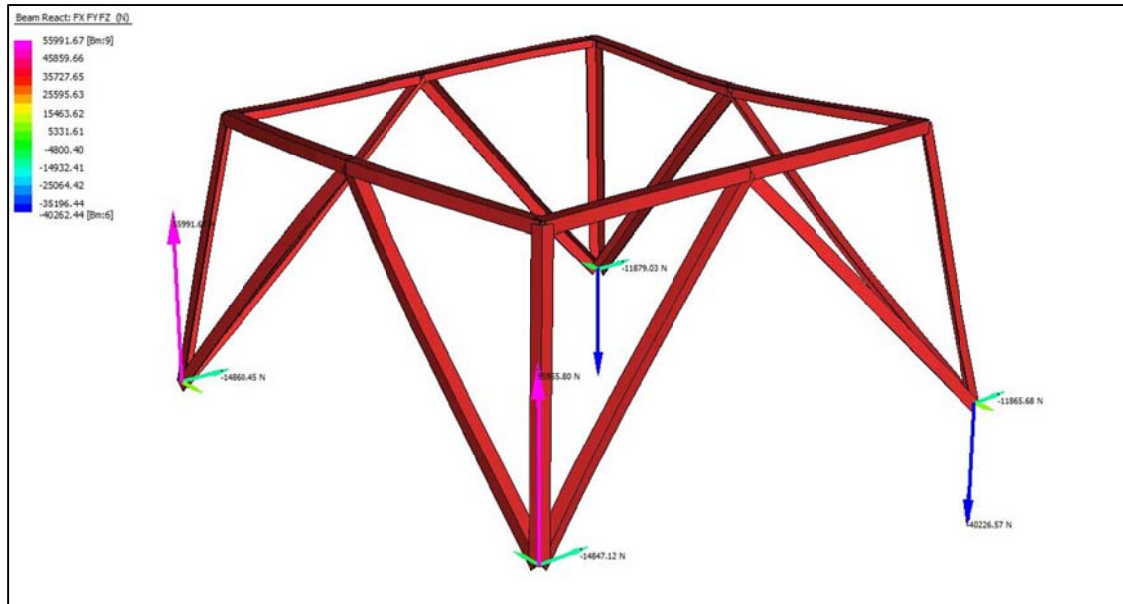


Figure 68: Steel Lattice Tower Displacement (XY) Static Analysis, Wind Load case 1, SLS2

**BASE RESPONSE:**

The base nodal reaction forces and moments were also obtained from the linear static analysis, and utilised for the design of the steel base plates and foundations required for this tower.

For the Steel lattice tower the base reaction forces are shown in Figure 69 and Figure 70 for the two different wind load cases. The forces are depicted for the ULS2, see Table 18, (Worst Case) scenarios for each wind load case respectively, so that the highest loads can be illustrated. The loads are shown in vector form acting on the four base points of the lattice tower in Figure 69 and Figure 70.



**Figure 69: Base Response, Steel Lattice Tower, for Wind load case 1**

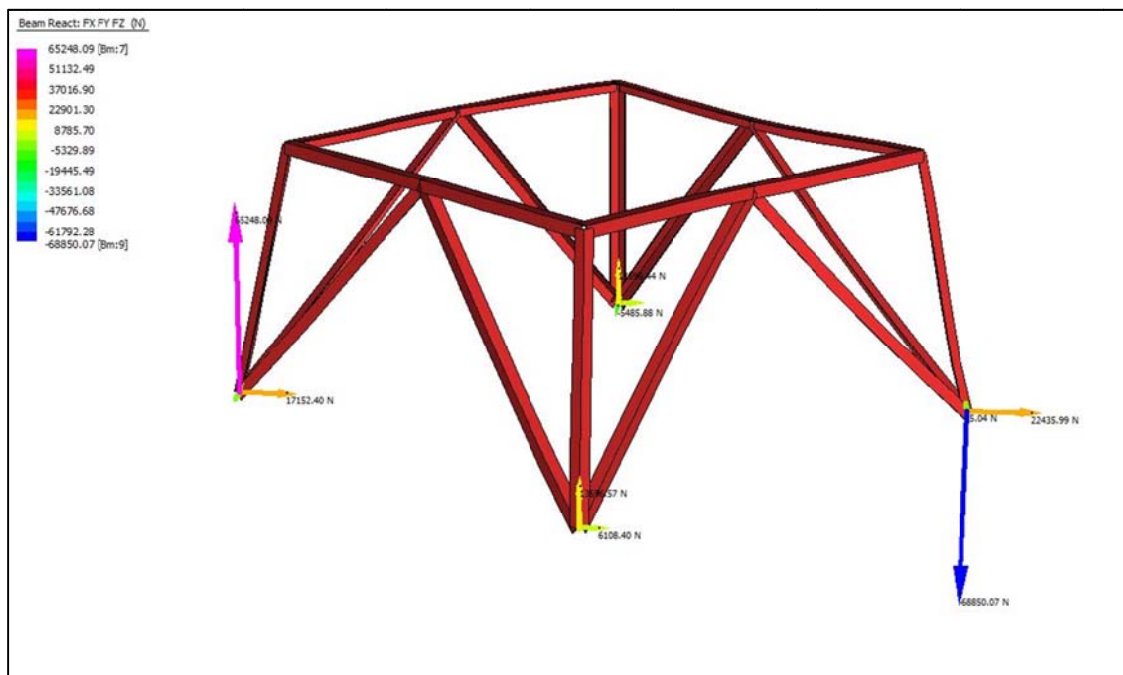


**Figure 70: Base Response, Steel lattice tower, for Wind Load case 2**

**LINEAR STATIC STRESS ANALYSIS:**

In order to assess the stress state of the Steel Lattice Tower for the linear static loading, the stress distributions for the load combination ULS 2 as described in Table 18 were examined. In terms of the Axial Stress state of the beam elements, as well as the Total Fibre Stress state of the beam elements and the Torsional Stress state none of the stress states exceed the elastic material limit (355MPa) of the S355JR grade steel that the Steel Lattice Tower was designed to.

**6.6.2 LINEAR BUCKLING ANALYSIS:**

The linear buckling factors are plotted in Figure 71 for wind load case 1 of the Steel lattice tower and Figure 72 for wind load case 2. The buckling factors are shown for all of the different linear load combinations which were defined in Table 18. In Table 20 and Table 21 the first 6 buckling factors for each of the wind load cases are shown, the negative values in Table 20 and Table 21 are the buckling factors which didn't converge.

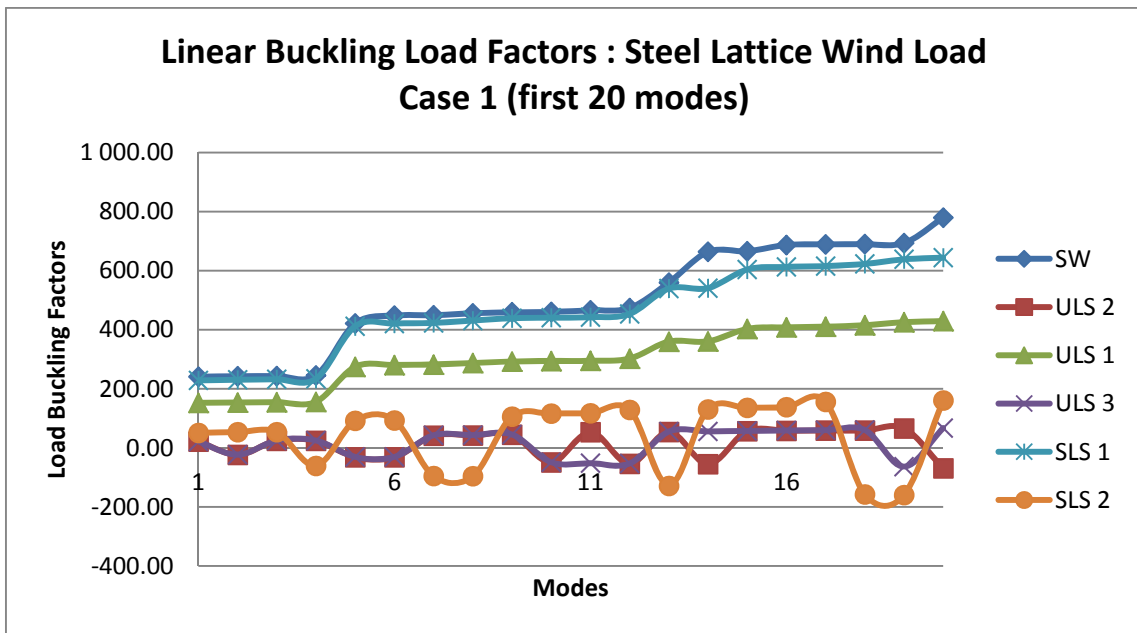


**Figure 71: Linear Buckling Factors: Steel Lattice Tower, Wind Load Case 1**

**Table 20: Linear Buckling Factors Steel Lattice Tower, Wind Load Case 1**

Mode	SW	ULS 1	ULS 2	ULS 3	SLS 1	SLS 2
1	241.1	152.4	21.4	21.6	228.7	50.9
2	242.5	153.6	-23.3	-23.1	230.4	53.2
3	243.3	154.7	24.1	24.9	232.0	53.3
4	245.1	156.0	24.1	24.9	234.0	-61.0
5	421.1	274.5	-31.7	-30.5	411.8	92.0
6	447.8	280.6	-31.8	-30.6	420.8	93.2

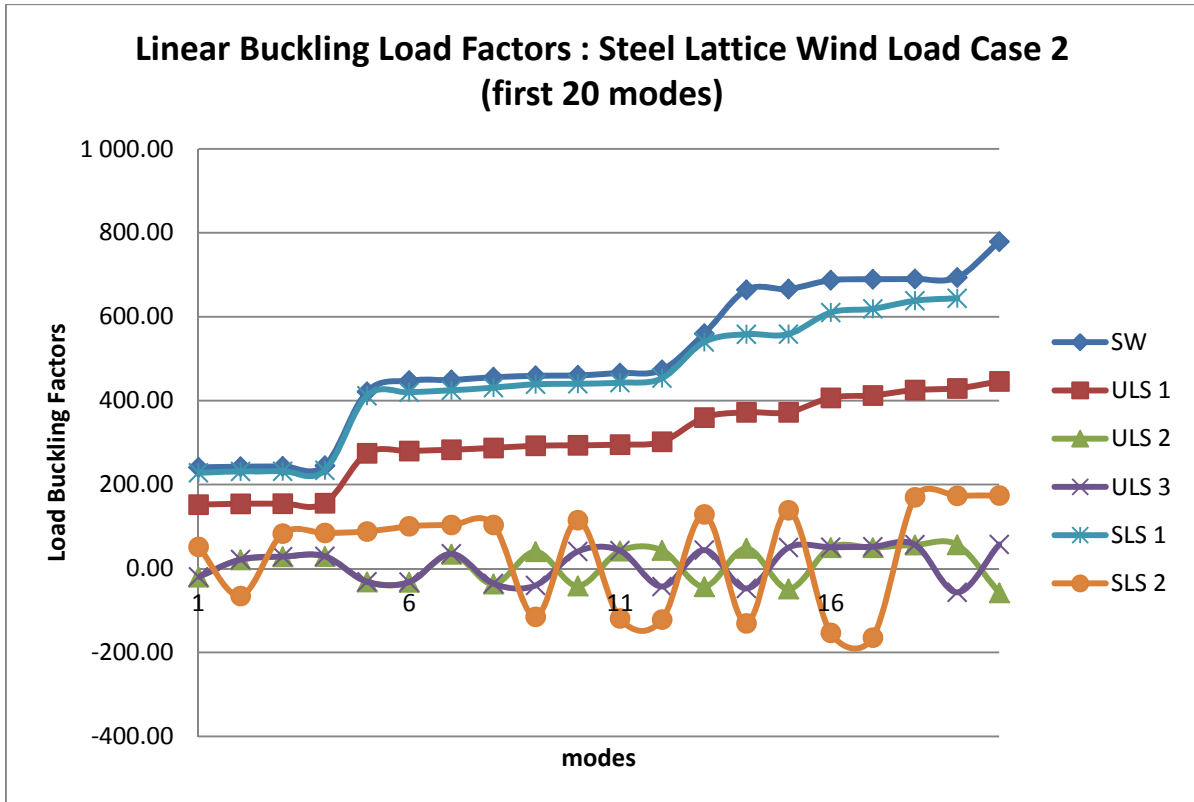


Figure 72: Linear Buckling Factors, Steel Lattice Tower, Wind Load case 2

Table 21: Linear Buckling Factors, Steel Lattice Tower, Wind Load Case 2

Mode	SW	ULS1	ULS 2	ULS 3	SLS 1	SLS 2
1	241.1	152.2	-20.4	-19.9	228.3	51.8
2	242.6	154.3	20.8	21.4	231.4	-65.3
3	243.4	154.5	28.0	28.4	231.7	83.2
4	245.1	155.9	28.8	29.2	233.8	84.9
5	421.2	274.5	-31.8	-31.4	411.8	88.1
6	447.9	279.9	-32.7	-32.2	419.9	100.8

### 6.6.3 NONLINEAR STATIC ANALYSIS:

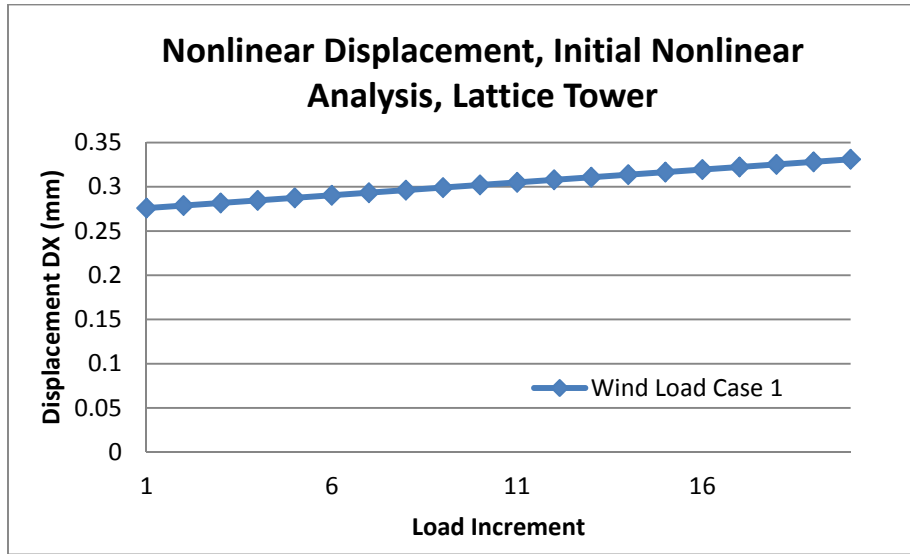


Figure 73: Nonlinear Displacement, Initial Nonlinear Analysis, Lattice Tower

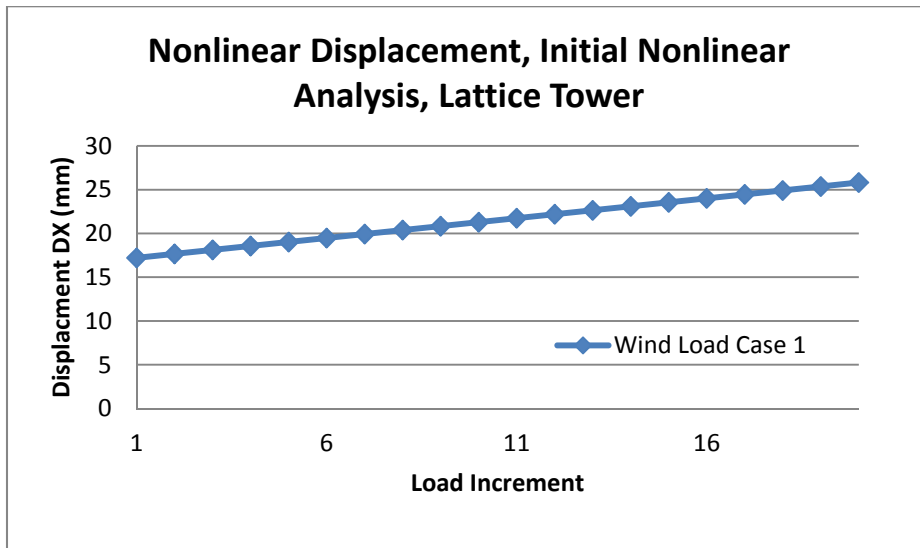


Figure 74: Nonlinear Displacement, Initial Tower analysis, Lattice Tower

The intention here was to place the displacement vs. loading increment for the two wind loading cases on the same graphs; however, the steel lattice tower for wind load case two was unable to be analysed as a result of Software limitations.



### 6.6.4 DYNAMIC ANALYSES:

The first analysis which was done to precede and enable the other analyses in this section was a natural frequency analysis.

#### NATURAL FREQUENCY ANALYSIS:

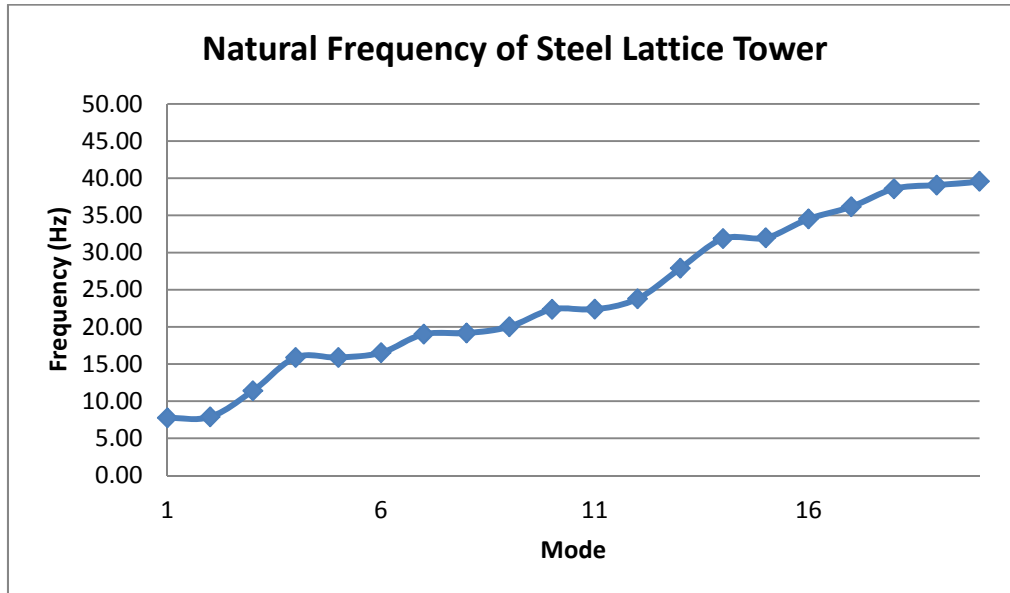


Figure 75: Natural frequency versus mode for Steel Lattice, Wind Load Case 1

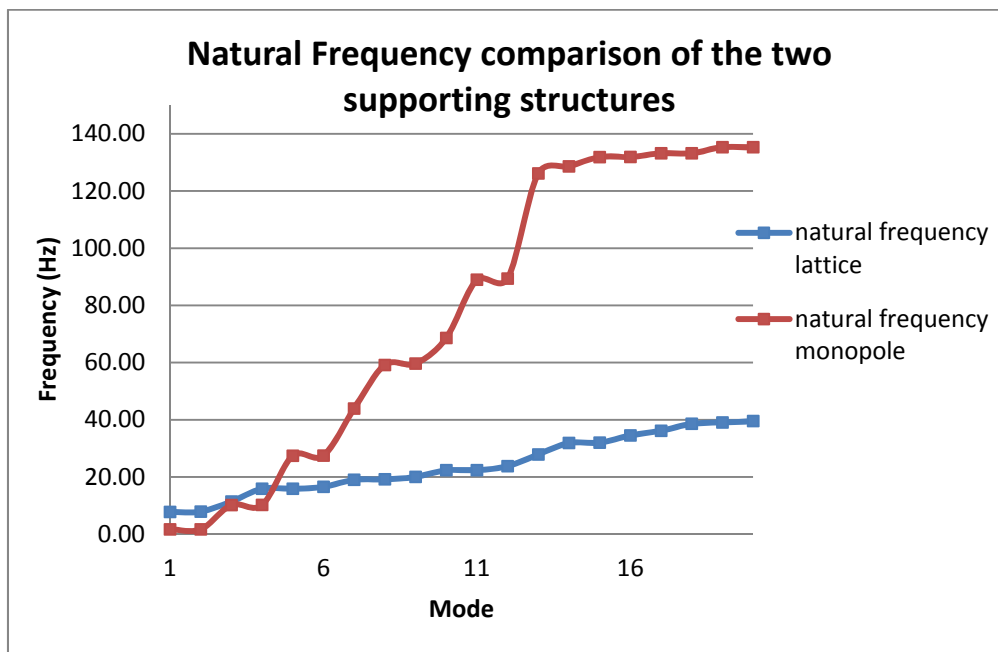
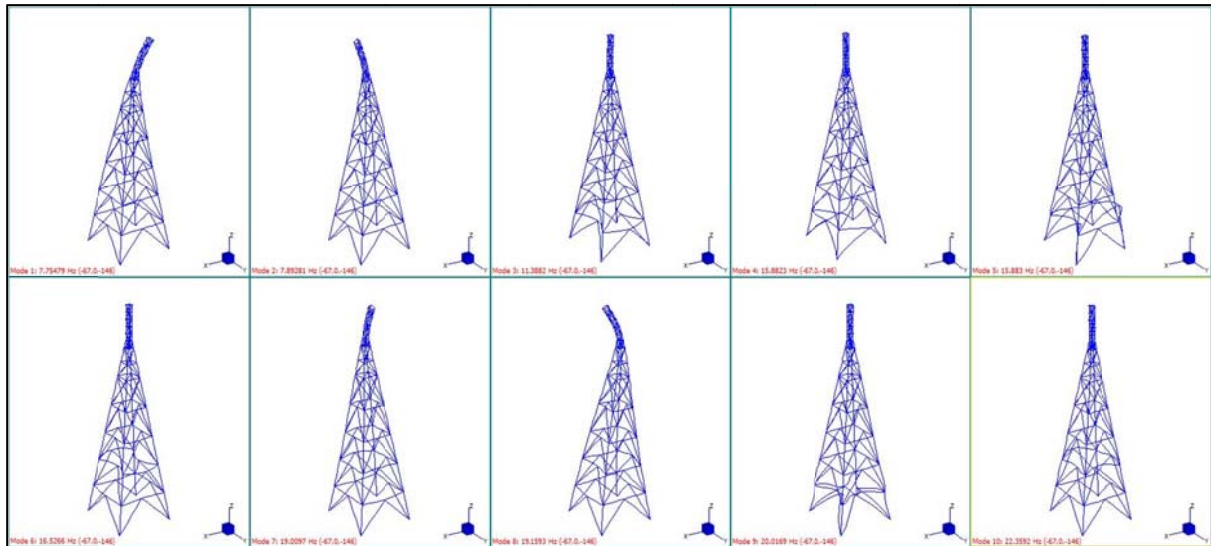


Figure 76: Natural frequency comparison for Monopole and Steel Lattice Towers

Figure 77 shows the first 10 modes shapes for the natural frequency analysis for the Steel Lattice Tower.



**Figure 77: First 10 mode shapes for Steel Lattice Tower**

#### 6.6.4.1 DYNAMIC EFFECTS OF AN OUT OF BALANCE ROTOR:

The 3kW wind turbine machine, for which the supporting structures in this thesis were designed, was stipulated to not induce any out of balance rotor disturbances, that the effects of a possible out of balance rotor could essentially be ignored for the purposes of Tower design.

However, it was decided to investigate the effects of accidental out of balance rotating forces on the tower top, from the perspective of a potential accidental load case, and the understanding of what the effects might be. Therefore the investigation done on the effects of the out of balance rotor was for the purposes of conservative design accounting for accidental load cases, not loadings that were expected to occur.

For a conservative simulation the out of balance forces that could possibly arise because of the rotor not being perfectly in balance, 10% of the total weight of the rotor and nacelle combined was calculated and applied as two vectors of equal magnitude, one in the vertical direction, and one in the horizontal direction at the appropriate point of application. The point at which the vectors were applied was the same point at which the overturning forces were applied, the hub height of the wind turbine machine. The two vectors were then given a loading participation factor of one, such that they were both imposed, and then were applied with a phase angle of 90 degrees between them so as to simulate the rotating motion of the rotor. The vectors were applied with a frequency which was equal to the equivalent operating frequency of the wind turbine rotor in revolutions per minute, which equates to a 5Hz frequency. A modal damping ratio of 5% was specified.

Figure 78 shows the maximum displacements which occur during the harmonic response versus time analysis as a result of the out of balance rotor effects, and as can be see, the displacements are negligible.

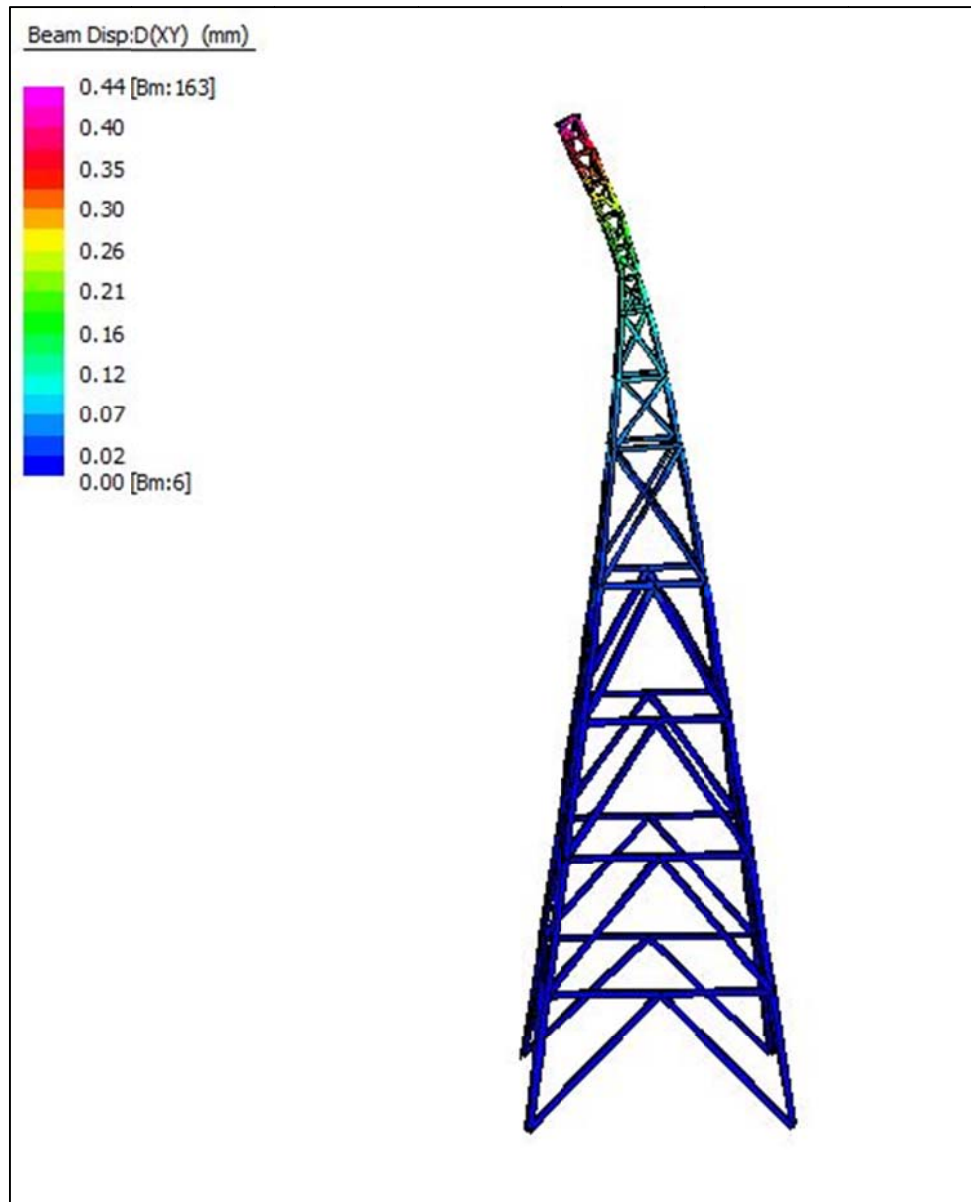


Figure 78: Maximum Displacement effects from dynamic analysis of out of balance rotor effects

### 6.6.5 MASS PARTICIPATION:

In order to assess if the mass participation of the Steel Lattice Tower was sufficient, in terms of representing the mass distribution through modelling the tower as closely to how it would be having been constructed, the mass participation for translational and rotational excitations were examined. From the output of the Natural frequency solver, it was observe that after just 20 modes the mass participation was between 70% and 90%, indicative of an excellent representation of mass distribution through modelling.

MODE PARTICIPATION FOR TRANSLATIONAL EXCITATION						
Mode	Frequency (Hz)	Modal Mass (Eng)	Modal Stiff (Eng)	PF-X (%)	PF-Y (%)	PF-Z (%)
1	7.7548E+00	2.0912E-01	4.9646E+02	3.304	15.304	0.005
2	7.8928E+00	2.1544E-01	5.2985E+02	15.709	3.355	0.024
3	1.1388E+01	2.5417E-01	1.3014E+03	0.000	0.000	0.000
4	1.5882E+01	1.2459E-01	1.2408E+03	0.044	8.541	0.000
5	1.5883E+01	1.2453E-01	1.2402E+03	8.428	0.043	0.000
6	1.6527E+01	2.3053E-01	2.4857E+03	0.000	0.000	0.000
7	1.9010E+01	6.0814E-01	8.6759E+03	1.060	34.465	0.003
8	1.9159E+01	6.5590E-01	9.5051E+03	34.816	1.198	0.082
9	2.0017E+01	2.4401E-01	3.8598E+03	0.000	0.000	0.140
10	2.2359E+01	1.3305E-01	2.6260E+03	0.083	0.639	0.001
11	2.2380E+01	1.3408E-01	2.6514E+03	0.468	0.061	0.010
12	2.3772E+01	1.9633E-01	4.3799E+03	0.000	0.000	0.000
13	2.7884E+01	2.1761E-01	6.6795E+03	0.000	0.000	0.137
14	3.1875E+01	1.4212E-01	5.7005E+03	0.833	3.614	0.013
15	3.1990E+01	1.3954E-01	5.6378E+03	3.180	0.735	0.062
16	3.4517E+01	1.3979E+00	6.5754E+04	0.000	0.000	0.000
17	3.6158E+01	1.0903E-01	5.6275E+03	0.000	0.000	0.000
18	3.8583E+01	7.4552E-02	4.3813E+03	0.496	2.040	0.088
19	3.9078E+01	6.0927E-02	3.6732E+03	1.637	0.563	0.508
20	3.9579E+01	5.9716E-02	3.6931E+03	0.003	0.001	0.361
-----						
TOTAL MASS PARTICIPATION FACTORS				70.061	70.560	1.434

MODE PARTICIPATION FOR ROTATIONAL EXCITATION						
Mode	Frequency (Hz)	Modal Mass (Eng)	Modal Stiff (Eng)	PF-RX (%)	PF-RY (%)	PF-RZ (%)
1	7.7548E+00	2.0912E-01	4.9646E+02	41.837	8.801	0.671
2	7.8928E+00	2.1544E-01	5.2985E+02	9.400	41.542	0.001
3	1.1388E+01	2.5417E-01	1.3014E+03	0.000	0.000	0.000
4	1.5882E+01	1.2459E-01	1.2408E+03	1.217	0.006	0.073
5	1.5883E+01	1.2453E-01	1.2402E+03	0.006	1.184	0.061
6	1.6527E+01	2.3053E-01	2.4857E+03	0.000	0.000	0.000
7	1.9010E+01	6.0814E-01	8.6759E+03	35.962	1.122	0.059
8	1.9159E+01	6.5590E-01	9.5051E+03	1.281	36.459	0.363
9	2.0017E+01	2.4401E-01	3.8598E+03	0.000	0.000	0.000
10	2.2359E+01	1.3305E-01	2.6260E+03	0.106	0.015	0.011
11	2.2380E+01	1.3408E-01	2.6514E+03	0.026	0.196	0.012
12	2.3772E+01	1.9633E-01	4.3799E+03	0.000	0.000	0.000
13	2.7884E+01	2.1761E-01	6.6795E+03	0.000	0.000	0.000
14	3.1875E+01	1.4212E-01	5.7005E+03	0.803	0.182	0.057
15	3.1990E+01	1.3954E-01	5.6378E+03	0.141	0.628	0.101
16	3.4517E+01	1.3979E+00	6.5754E+04	0.000	0.000	0.000
17	3.6158E+01	1.0903E-01	5.6275E+03	0.000	0.000	0.000
18	3.8583E+01	7.4552E-02	4.3813E+03	0.800	0.190	0.340
19	3.9078E+01	6.0927E-02	3.6732E+03	0.204	0.599	0.274
20	3.9579E+01	5.9716E-02	3.6931E+03	0.002	0.000	0.000
-----						
TOTAL MASS PARTICIPATION FACTORS				91.783	90.926	2.026

**RESONANCE EFFECTS:**

In having determined the natural frequencies of the tower, as well as what proportion of mass that participates with each mode, the possible effects of resonance can be assessed.

Because the machine’s operating frequency is 5Hz, and the first natural frequency is 7.75, there will be no problems in the transient or any other phase of the machine’s operation with respect to resonance. The steel lattice tower is perfectly tuned in this respect.

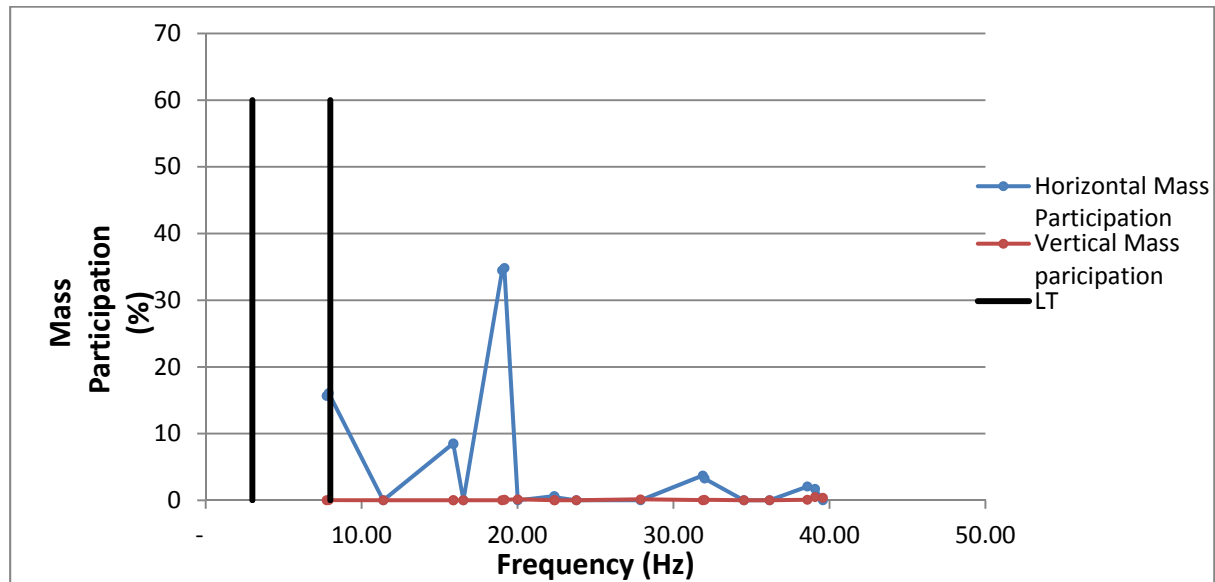


**Figure 79: Resonance effects of steel lattice tower**

## 6.7 STRESS STATE

### HARMONIC RESPONSE STRESS ANALYSIS.

The stresses which were the most significant as a result of the harmonic response to the out of balance rotor effects occurred in the connection of the top parallel portion of the steel lattice tower to the bottom tapered section. The Stress range to which this section of the tower was subjected is shown in Figure 80. The stress range is extremely low.

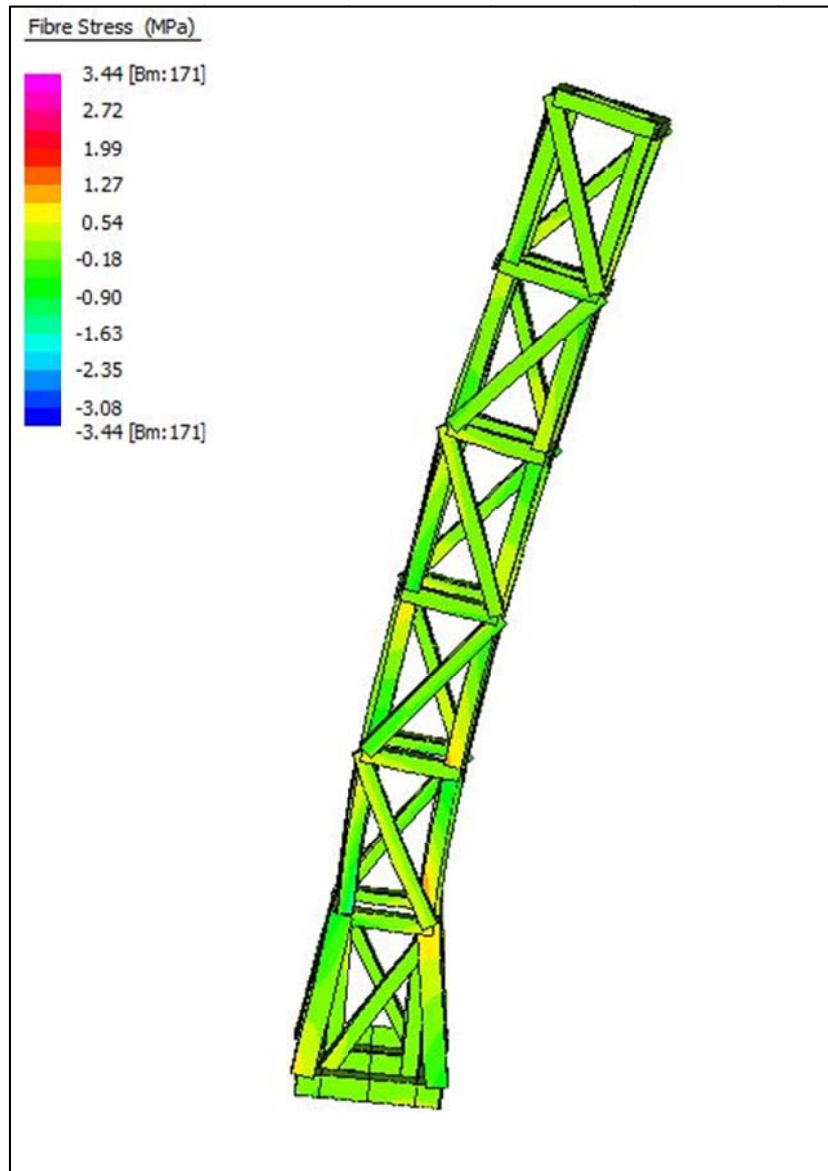


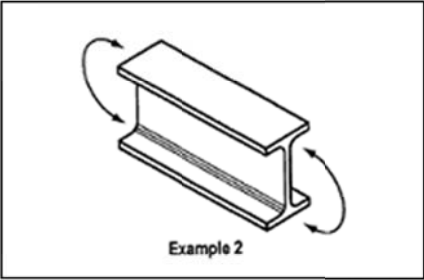
**Figure 80: Stress state from out of balance harmonic response**

### 6.8 FATIGUE ASSESSMENT

Following the stress state analysis in section 6.7, the fatigue state of the elements in the steel lattice tower was assessed in terms of the effect a repetitive loading of an out of balance rotor would have on the structure. As can be seen in Table 22 the tower was analysed for the instance in which the turbine machine was running 24 hours a day 365 days a year with an out of balance rotor, and the effects of fatigue in the members are negligible.

**Table 22: Fatigue Analysis of steel lattice tower**

Fatigue Analysis [SANS 10162-1:2005 Clause 26.3.2]			
Structure Life Time	20	yrs	
Yearly Use	365	days	
Daily Use	24	hours	
Exciting Frequency (fe)	5	Hz	
			Cycles 3.15E+09 duty cycles
Detail Type	A		
Fatigue Life Constant ( $\gamma$ )	8.19E+12		
Const Amp Stress Lim ( $f_{srt}$ )	165	MPa	
Fatigue Life Constant ( $\gamma'$ )	2.23E+17		
Cycles'	1.82E+06		
Stress Range ( $f_{sr}$ )	7	MPa	
Fatigue Resistance ( $f_{fr}$ )	NA	MPa	Adjusted Cycles 1.33E+13 duty cycles



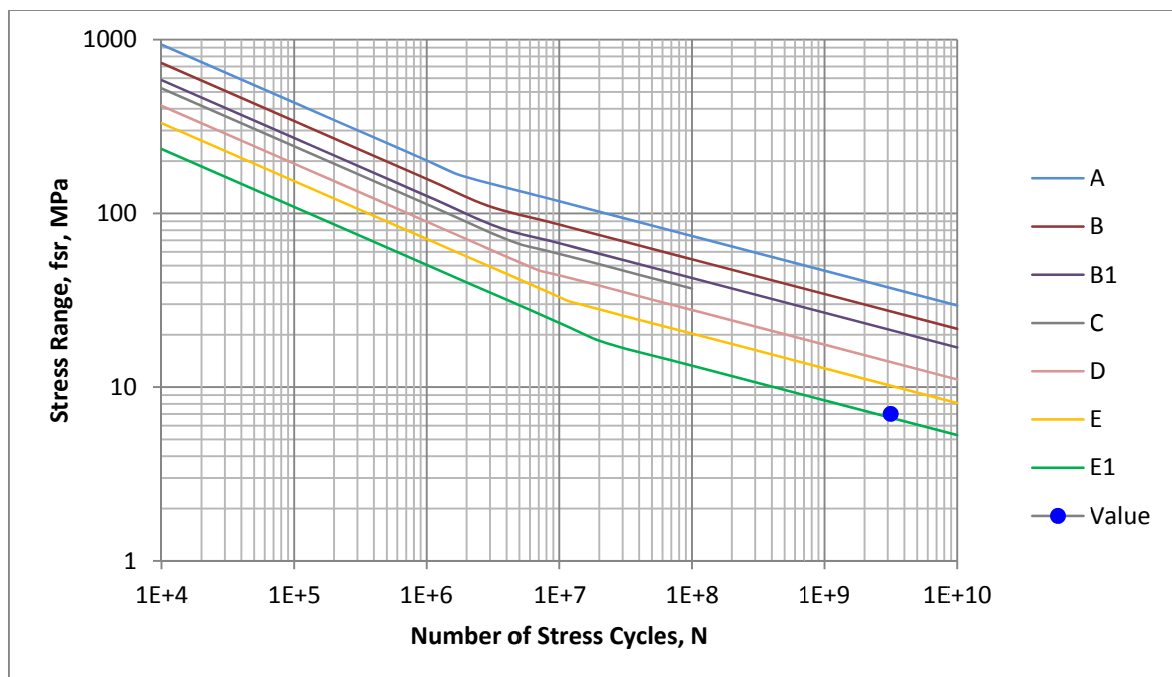


**Figure 81: Stress Range versus Number of cycles for fatigue analysis in accordance with SANS 10162-1:2005**

## CHAPTER 7: FEASIBILITY

### 7.1 INTRODUCTION TO FEASIBILITY

Prompted by enquiries from industry, it was decided to investigate the feasibility of designing a steel lattice alternative to the most commonly used steel monopole tower as a supporting tower for a small scale wind turbine.

The purpose of this chapter is to develop an understanding and an insight into the design aspects that were taken into account for the cost analysis of the two different steel supporting towers.

The items dealt with in evaluating the costs of the two steel towers designed in this thesis were the following:

1. The tower specifications
  - i) Steel Monopole Tower
  - ii) Steel Lattice Tower
2. The structural requirements of the towers
3. The aesthetic requirements of the towers
4. The constructability of the towers:
  - i) Transportation Considerations
  - ii) Fabrication Considerations
  - iii) Construction Considerations
5. Overall cost comparison

#### 7.1.1 TOWER SPECIFICATIONS

##### 7.1.1.1 STEEL MONOPOLE TOWER

The tower specifications for the steel monopole tower designed for this thesis were prescribed by the Stellenbosch Wind Energy Technologies Pty Ltd (SWET) Company. SWET is a spin-off company started by the Electrical Engineering department at Stellenbosch University. The University has a 50% share of the company. SWET has produced a new small wind turbine technology which it wants to thoroughly test and eventually commercialise. A 3kW prototype machine was built in November of 2011. SWET needed a turbine tower design which it could use with the wind turbine prototype. To help SWET with this design the Civil Engineering Department was approached.

The design parameters set by SWET were that the tower needed to be 16m high, with sections no longer than 6m, and it was to be as cost effective as possible. From the requirement of cost efficacy, it was decided to examine the possibility of designing a monopole that was constructed from existing circular hollow sections (CHS) to reduce fabrication costs.

To establish the most realistic cost benchmark for comparative purposes it was decided to design the lightest possible option within the bounds of regularly manufactured and fabricated circular hollow sections. The circular hollow sections needed ring flange connections welded onto each end of the tubular sections, which also had web stiffeners welded on at specified points, of specified size. It must be emphasised that the only objective here was the cheapest solution for an effective monopole tower.

##### 7.1.1.2 STEEL LATTICE TOWER



To design a cost effective alternative to the Monopole Tower, with comparable strength and reliability, the Steel Lattice Tower designed in this thesis had still to be more cost effective than the monopole designed out of existing CHS.

In terms of design boundaries given by SWET, the only boundaries specified for the design of the steel lattice tower were the height of 16m, and that tower sections be no longer than 6m.

## 7.2 THE STRUCTURAL REQUIREMENTS OF THE TOWERS

Both the steel lattice tower and the steel monopole tower were required to have adequate strength in order to withstand the loadings unique to the 3kW wind turbine to be mounted on top of either one. The structural requirements and design were described in detail in Chapter 3.

## 7.3 THE AESTHETIC REQUIREMENTS OF THE TOWERS

The most dominating aspect in present day choice of supporting tower for wind turbines is the aesthetics of the tower. An overwhelming opinion is that the steel monopole is more aesthetically pleasing than a steel lattice tower.

The Steel Lattice Tower design, while having to be structurally sound, suffered the complicating requirement of having to be aesthetically pleasing when compared to Steel Monopole tower design. The manner in which that was approached included considering the balance of the number of members used to the available open space between them, as well as symmetry and proportion, and an overall shape that was sufficiently familiar and pleasing.

## 7.4 THE CONSTRUCTABILITY OF THE TOWERS

While the aesthetics and practicalities were considered, it was important to bear in mind fabrication methods that would avoid complex details. Special consideration was given to the sizes of the fabricated elements since this would have a critical bearing on the ease of their transportation to site.

### 7.4.1 TRANSPORTATION:

The Steel Monopole tower and the Steel Lattice tower were both designed so that they didn't have any components longer than 6m. Dissembled parts could then be transported on regular freight vehicles, thereby eliminating the need for costly abnormal freight vehicles.

### 7.4.2 FABRICATION AND CONSTRUCTION:

Obtaining sufficient information to make valid comparisons of costs presented severe challenges. Manufacturers and contractors were reluctant to disclose proprietary information for research purposes and those who did provided information on condition of strict anonymity. This meant that considerable care had to be taken to compare like with like and in order to reach the best outcome the comparisons were done in stages.

The first sets of costs obtained were based on fabrication alone. The second sets of costs obtained were for construction of the towers and included fabrication costs. This was done as an additional test of the validity of the fabrication information given in the first set of costs. Of great significance in the second sets of comparison were the considerably higher foundation costs of the monopole design.

The cost aspects of fabrication of the two towers shall be discussed first and there after the construction.

#### 7.4.2.1 FABRICATION:

To assess the fabrication costs of the two different towers, the design information for the required assembly of the two different towers was sent to three different steel fabricators in South Africa for quotations. Of these two responded.

The responses differed significantly.

#### FIRST FABRICATOR COST RESPONSE:

The first fabricator used the masses of the towers as its most significant variable. The reason was that they have a flat fee of ZAR30/kg for the fabrication of the Steel Lattice Towers, including the steel supply. Limited consideration is given to exact design since lattice design variations have small effect on the final price and are simply accounted for in the price. Their manufacturing price was ZAR48/kg for the Steel Monopole Tower fabrication.

Table 23 illustrates the comparative difference.

**Table 23: Cost comparison of Fabrication, Fabricator 1**

Tower Style	Cost (ZAR/kg)	Mass (kg)	Total Cost (ZAR)
Steel Monopole	48	2800	134400
Steel Lattice	30	2500	75000

The difference in cost between the two towers is R59 000 which is considerable especially when expressed as a percentage. The Monopole was 79.20% more expensive.

#### SECOND FABRICATION COST RESPONSE:

The second fabricator dealt with the elements of fabrication in greater detail as shown in Table 24.

**Table 24: Fabrication costs, Monopole, Fabricator 2**

DESCRIPTION	QTY	UNIT	SUPPLY AND FABRICATE Amount
<b>Steel Work</b>			
Circular Section - 5m (2 Off)	1.6	t	R 77 096.13
Circular Section - 6m	1.0	t	R 46 257.68
Bolts - M20	32.0	No	R 55.20
Mid type flange	3.0	No	R 12 661.50
Base type flange	1.0	No	R 3 627.10
Corner Stiffeners (8 Off)	0.013	t	R 543.79
Side stiffeners (6 Off)	0.003	t	R 125.66
Rectangular Section	0.03	t	R 1 598.88
<b>TOTAL EXCL. VAT</b>			<b>R 141 965.92</b>

The Steel lattice Tower's quotation is shown in Table 25.

Table 25: Fabrication Costs, Lattice Tower, Fabricator 2

DESCRIPTION	QTY	UNIT	SUPPLY AND FABRICATE
			Amount
<b>Steel Work - Parallel tower Bracing</b>			
Angle 50x50x5 (33.2m)	0.13	t	R 5 060.27
Angle 100x100x8 (157.50m)	1.92	t	R 74 740.91
Angle 70x70x6 (39.94m)	0.30	t	R 11 678.30
Gusset plates (60 plates)	0.34	t	R 18 968.83
Base Plate	0.02	t	R 1 335.60
<b>TOTAL</b>			<b>R 111 783.91</b>

The difference in cost between the two towers from the second fabricator's quotation was R30 182. While this difference is less than that for the first quotation it is still significant, especially when expressed as a percentage. In this case the Monopole was 27.00% more expensive.

#### 7.4.2.2 CONSTRUCTION:

Three leading companies provided construction costs. They were asked to show the cost of steel fabrication separately to enable validation of the information contained in the other quotations. As mentioned above these companies all wished to remain anonymous to protect their proprietary information, and are for the purposes of the next section shown as Company A, Company B and Company C respectively.

In addition to the steel fabrication costs it was requested that the quotations for the construction costs should include the **construction of the foundations**, from **excavation** to **quantities of concrete** required to build the foundations.

Table 26 indicates which costs were considered in the detailed pricing of the two different towers that were designed for this thesis.

**Table 26: Table of Item descriptions for construction**

Item description
<b>Earth Works</b>
1.Excavation of the foundations, including leveling and stockpiling of selected material for reuse in filling
2.Compaction of existing soil to Standard Proctor Optimum Density
3. Bituminous painting and sealing on concrete surfaces in contact with earth
<b>Concrete Works</b>
4. Reinforced Concrete
5. Steel trowel finish for slabs
6. High yield steel bar reinforcement
7. Cast in anchor bolts up tp 20mm dia including templates
8. Cast in anchor bolts bigger than 20mm dia including templates
<b>Steel Work</b>
9. Preparation of shop detail drawing, fabrication, painting, delivery and erection of light steel structural steel work complete with all the necessary cleats, shop bolts, brackets, gussets, packs baseplates etc.

Table 27 shows the total price for each item considered in the Monopole design within the categories of **Earth Works**, **Concrete Works** and **Steel Work**.

**Table 27: Table of Comparative costs for each item of the Monopole Tower's construction**

Monopole			Company A		Company B		Company C	
Item description	Unit	Quantity	Unit Price (ZAR)	Total (ZAR)	Unit Price (ZAR)	Total (ZAR)	Unit Price (ZAR)	Total (ZAR)
<b>Earth Works</b>								
1	m <sup>3</sup>	27.2	71	1939	111	3030	78	2132
2	m <sup>3</sup>	18	6	108	12	207	13	242
3	m <sup>2</sup>	43.8	60	2621	183	8004	80	3503
<b>Concrete Works</b>								
4	m <sup>3</sup>	9.4	4980	46811	2417	22720	1764	16580
5	m <sup>2</sup>	1	27	27	21	21	21	21
6	t	0	14253		13070		11721	
7	nr	0	200		215		97	
8	nr	16	200	3200	248	3969	112	1791
<b>Steel Work</b>								
9	t	2.8	45254	126711	33594	94064	42777	119776

Table 28 shows the total price for each item considered in the design for the Steel Lattice tower within the categories of **Earth Works**, **Concrete Works** and **Steel Work**.

**Table 28: Table of comparative costs for items associated with the Lattice Towers' construction**

Lattice Tower			Company A		Company B		Company C	
Item description	Unit	Quantity	Unit Price (ZAR)	Total (ZAR)	Unit Price (ZAR)	Total (ZAR)	Unit Price (ZAR)	Total (ZAR)
<b>Earth Works</b>								
1	m <sup>3</sup>	0	71	0	111	0	78	0
2	m <sup>3</sup>	0	6	0	12	0	13	0
3	m <sup>2</sup>	4	60	239	183	731	80	320
<b>Concrete Works</b>								
4	m <sup>3</sup>	2	4980	9960	2417	4834	1764	3528
5	m <sup>2</sup>	4	27		21		21	
6	t	0	14253		13070		11721	
7	nr	0	5981		215		97	
8	nr	0	5981		248		112	
<b>Steel Work</b>								
9	t	2.5	45254	113135	33594	83986	42777	106943

In order to correctly compare the values, the totals for each category, Earth Works, Concrete Works and Steel Work are shown in Table 29 for the steel monopole tower, and Table 30 for the Steel Lattice tower.

**Table 29: Summary Table of Monopole Costs from construction to fabrication**

Company	A	B	C
<b>Earth Works (ZAR)</b>	4669	11242	5877
<b>Concrete Works (ZAR)</b>	101519	26710	18392
<b>Steel Work (ZAR)</b>	126711	94064	119776
<b>Grand Total (ZAR)</b>	232898	132016	144045

**Table 30: Summary Table of Lattice tower Costs from construction to fabrication**

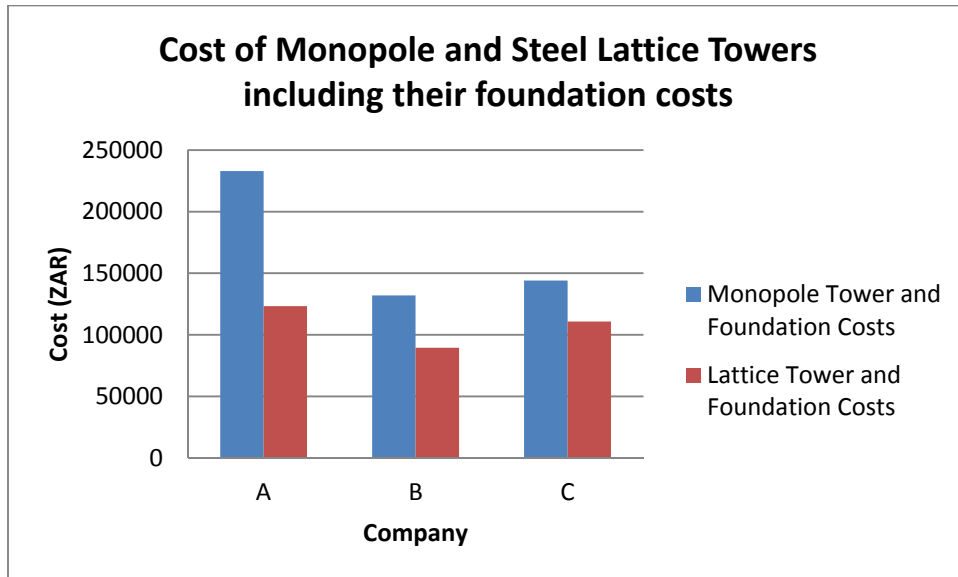
Company	A	B	C
<b>Earth Works (ZAR)</b>	239	731	320
<b>Concrete Works (ZAR)</b>	9960	4834	3528
<b>Steel Work (ZAR)</b>	113135	83986	106943
<b>Grand Total (ZAR)</b>	123334	89551	110790

Table 31 shows the total cost difference between the Steel Monopole tower and the Steel Lattice tower. The costs that were assessed to arrive at such a monetary discrepancy were the total costs of companies A, B and C for all categories which included foundation construction as well as steel fabrication and erection.

**Table 31: Overall difference in costs between the monopole and steel lattice tower including construction costs**

Company	A	B	C
<b>Overall difference (ZAR)</b>	109564	42465	33255

The cost comparisons made in Table 29 and Table 30 are shown graphically in Figure 82.



**Figure 82: Cost Comparison for Steel Towers and Foundations combined**

It can be concluded that consistently higher prices are found for Steel Monopole towers as compared to Steel Lattice towers. The differences in cost between the Steel Monopole tower and the Steel Lattice tower have been plotted in Figure 83. Figure 83 by implication shows not only the cost difference between each kind of tower but also the difference as quoted by the different companies, resulting in companies A, B and C in ascending order as being the most cost effective.

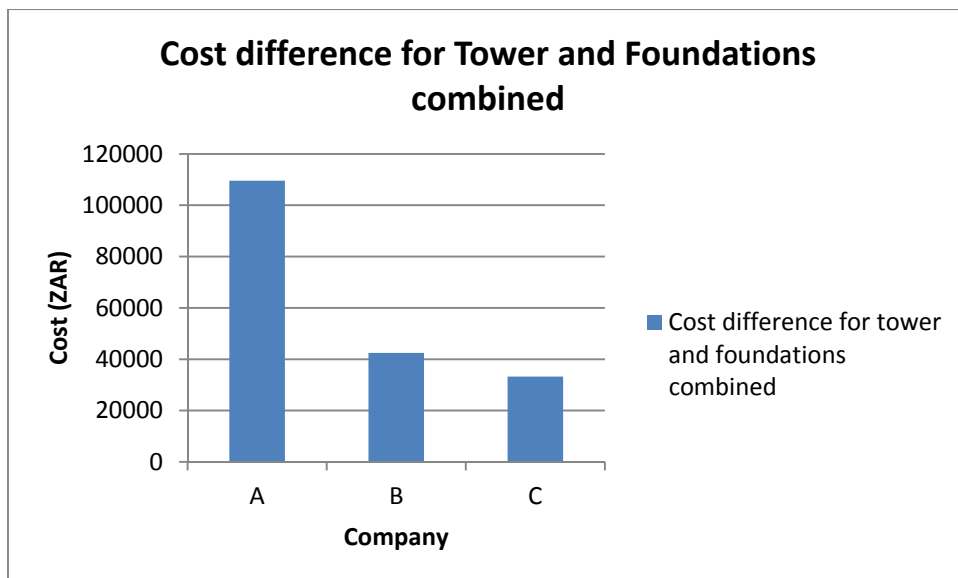


**Figure 83: Cost Difference between companies and Towers for Tower and Foundation costs combined**

**STEEL TOWER FABRICATION:**

Figure 84 shows the cost of fabricating and erecting the steel towers, exclusive of foundation construction. It is abundantly clear that the cost of the Steel Lattice towers, regardless of the Company from which the quotation came, was the least costly in each of the 5 instances.

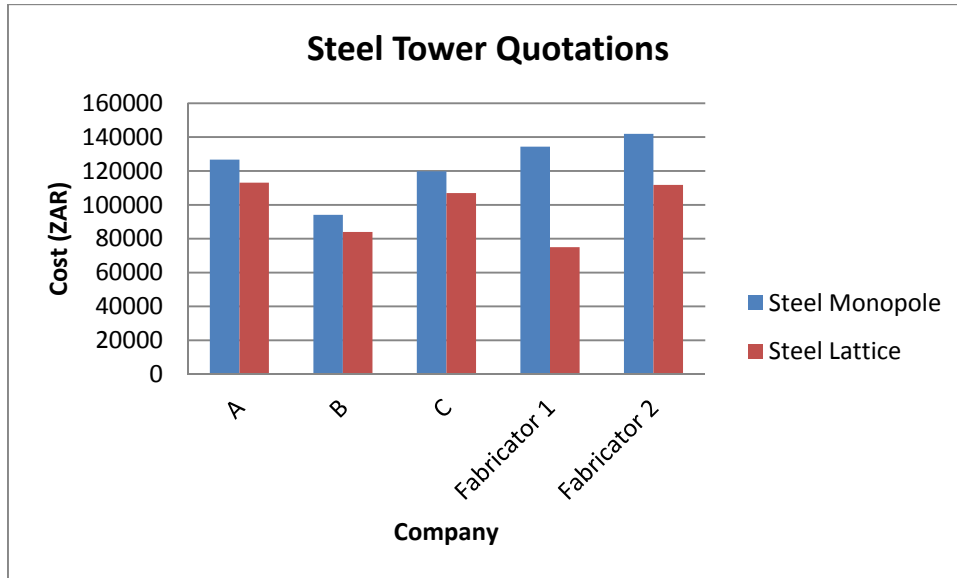


Figure 84: Steel Tower Quotation Comparison

In Figure 85, the differences between the cost of the fabrication of the Steel Lattice tower and the Steel Monopole are shown.

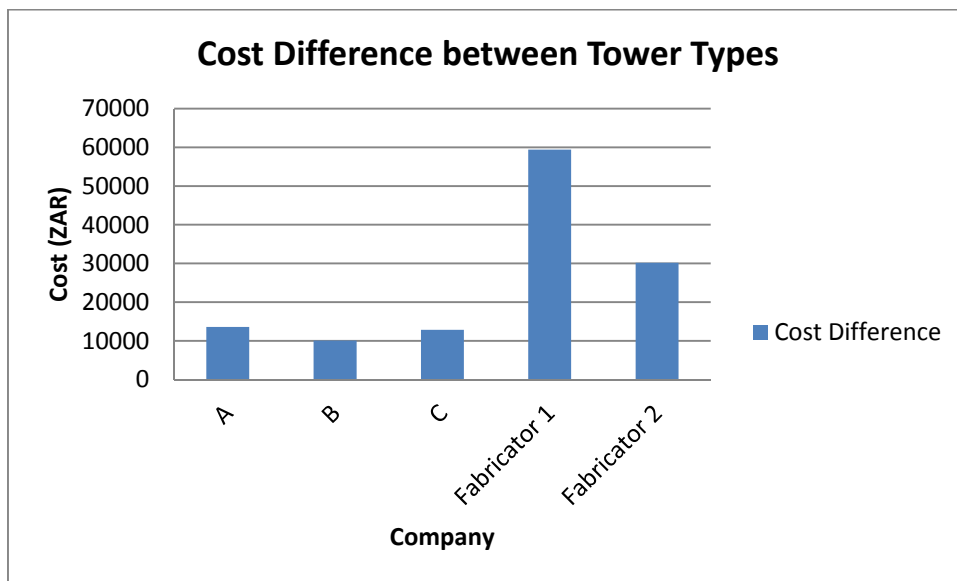


Figure 85: Difference in cost per company and tower design for the cost of the towers

In order to account for the discrepancies in cost from the different companies, the average cost of a steel tower was taken from the Monopole quotations, and an average cost was taken from the Steel Lattice quotations. The average cost for each respectively was the following, R 123 383.35 for Monopoles, and R 98 169.43 for Steel Lattice towers. The average cost difference between the two kinds of towers amounted to R 25 213.92 which was then examined as an overall percentage of the average cost of the Monopole towers and the Steel Lattice towers respectively. As a percentage of cost the average difference would account for 20.45% in price reduction for Monopole towers and a 25.68% increase in Lattice towers respectively for the numbers to even out. These amounts account for a significant percentage of the total cost of each tower, which shall be discussed again later.

FOUNDATION CONSTRUCTION:

As was specified earlier in the chapter, the foundation construction includes the excavation of the ground necessary to construct the foundation, the treatment of the concrete that is exposed to the ground, and the amount of backfill required as well as the volume of concrete necessary for construction.

Figure 86 shows the cost comparison of the foundation construction costs as a separate entity.

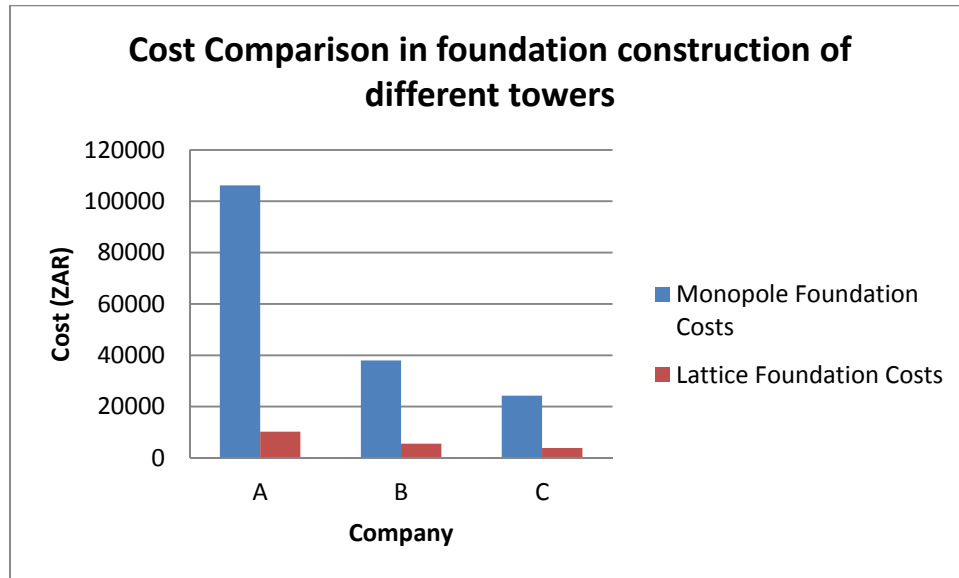


Figure 86: Cost Comparison in foundation construction for different towers and companies

As was the case with the costs of the combined tower and foundation design and the tower fabrication when looked at separately, the Monopole’s foundation construction costs are consistently higher than they are for the Steel Lattice tower’s foundation. Once again it is concluded, in ascending order companies A, B and C are the more cost effective options.

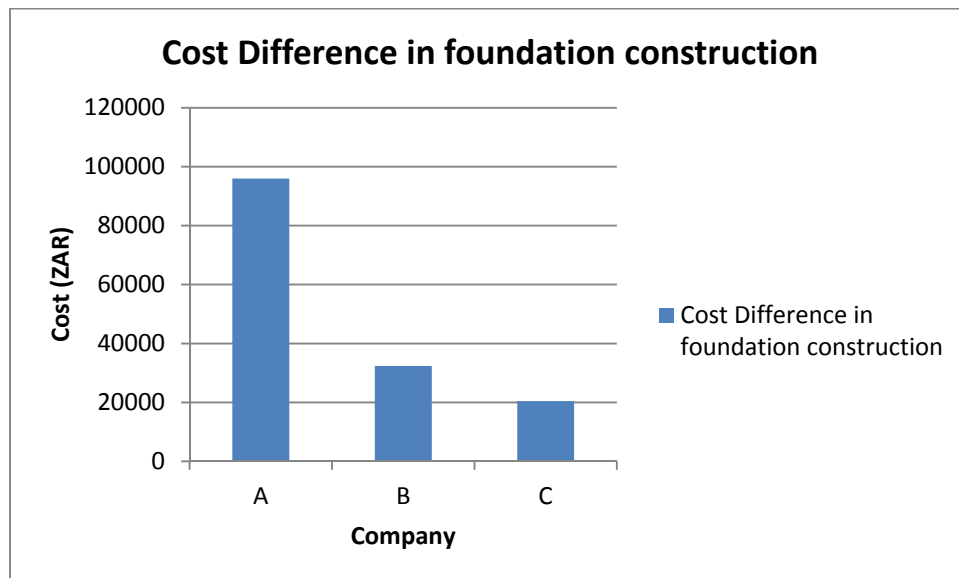


Figure 87: Cost difference in foundation construction for different towers and companies

Figure 88 shows each of the cost differences between the quotation prices for the Steel Lattice tower and the Steel Monopole drawn on the same graph to illustrate which of the entities, foundation costs or steel fabrication costs was a dominating factor in the price discrepancies.



It was determined that in accordance with the particular quotes given from the companies A, B and C that the foundation construction costs were the driving force in price discrepancies between the different companies, in the most dominating instance in Company A, which had the most expensive price per unit for reinforced concrete per cubic metre.

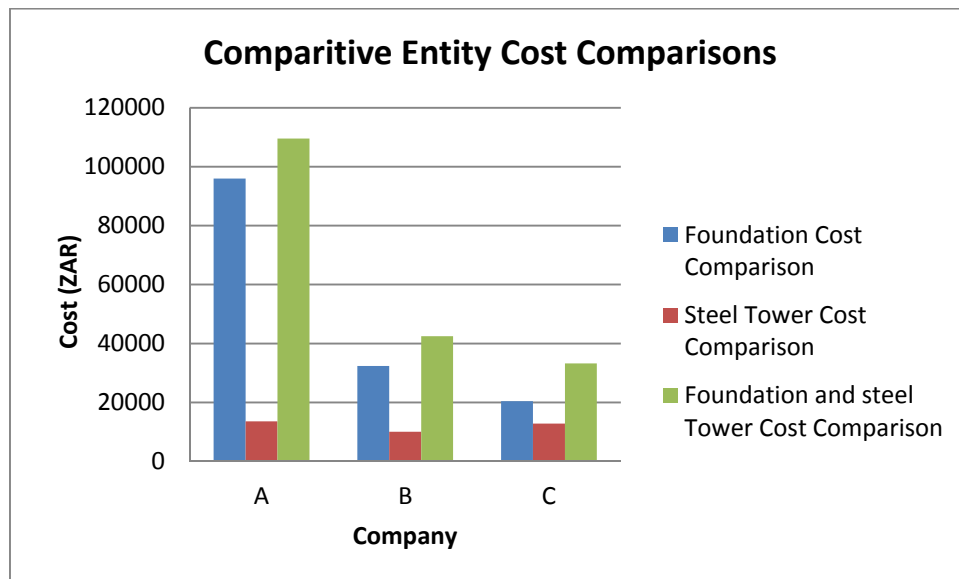


Figure 88: Comparative Entity Cost Differences

### 7.5 CONCLUSION:

The clear conclusion is that regardless of the steel fabricator or Construction Company, the overall costs of constructing the Steel Lattice tower designed for this thesis as compared to the Steel Monopole tower designed for this thesis are lower.

When comparing average prices the Monopole tower and the Steel Lattice tower were compared separately for the Steel Fabrication costs, the foundation construction costs and then the effects of the combined costs as shown in Table 32

Table 32: Summary Table of Cost Comparisons between all entities averaged prices

Summary Table	Monopole	Lattice	Difference
Steel Fabrication Cost (ZAR)	123383.35	98169.43	25213.92
Foundation Construction Cost (ZAR)	56136.31	6537.33	49598.98
Total Construction, Fabrication and Erection Cost (ZAR)	109564.21	42465.32	33255.00

It is likely that wind turbines of the scale designed in this thesis, namely 3kW, would be used in larger numbers, for small wind farms. Bearing this in mind reducing the cost of the tower construction and foundation construction would be ever more appealing the larger the number of turbines. By reducing the tower and foundation construction costs by at least 30%, where the tower proportion of a wind turbine as a whole constitutes as much as up to 30% of the overall costs, the implications are the reduction of the total cost of each wind turbine by as much as 9%, which on a multiple effect scale is most significant.

For the steel monopole towers seen constructed for wind turbines world over, considering the optimised design they have, the fabrication requirements would be far more costly than those of the monopole designed for this thesis out of readily available Circular Hollow Sections. From the estimated price increase in commercial monopole towers seen in industry (as compared to the monopole for this thesis), the inevitable

conclusion can be drawn that Steel Lattice towers are the most cost effective solution to wind turbine supporting towers.

## CHAPTER 8: CONCLUSION AND RECOMMENDATIONS

It was evident from the outset of this research that the topic at hand provided many scattered pockets of insightful information, information which had not been accumulated and arranged in the context that is set out here. Although the research conducted for this thesis is extremely useful in terms of present developments in the wind industry in South Africa, in the sense that it is relatively new and undeveloped, the infancy of the wind energy industry in South Africa was a hindrance because of a lack of information that could contribute to the designs of the wind turbine towers.

European publications proved most useful in terms of the volume of knowledge that they could provide on the wind industry in general as well as the development of energy capturing by means of wind turbines.

It was certainly essential to do complete designs of each tower in order to accurately assess the structural design process and differences between the processes involved with each of the towers. The full extent of the connection and foundations designs was also necessary as it assisted in understanding factors that could possibly influence the design and construction processes of each of the towers.

Having done extensive Finite Element Analyses of the steel lattice and the steel monopole towers, it can be concluded that the steel monopole has more complicating dynamic components to consider in assessing the different effects of vortex shedding. However, the steel lattice tower had to be modelled more extensively for the different possible wind load cases, so overall each of them had certain modelling pros and cons, neither of which stood out from the other as more time consuming to analyse in its finite elements.

It can be concluded from the findings in Chapter 7 that the overall feasibility of a steel lattice tower as a supporting structure for a small scale Wind Turbine is significantly greater than that of a steel monopole tower.

The steel monopole was found to be more costly to fabricate, more costly to construct and had more costly foundations and used more steel than the steel lattice tower.

From the prerequisite of a proposed alternative that provides the same stability, the same height requirements as the existing solution but at a reduced cost, the research conducted in this thesis was certainly successful in producing such an outcome.

In terms of further development in this topic, it would be an interesting extension to create a design optimisation interface between Strand7 and Microsoft Excel which would allow one to have an optimised use of steel. The Strand7 software makes allowance for such interfaces.

It would be recommended that a tapered steel monopole tower also be considered in the cost analyses of further study as well as different cross-sectional designs of the steel lattice tower, and perhaps a hybrid of the steel lattice and steel monopole tower should be investigated to harness the best aspects of each of them in one design.

## LIST OF REFERENCES

### RELEVANT SOUTH AFRICAN DESIGN CODES:

- SANS 10162-1:2005
- SANS 10160-1:2011
- SANS 10160-2: 2011
- SANS 10160-3:2011

### OTHER RESOURCES:

Balas, M.J & Wright, A & Hand, M & Stol, K.2003. Dynamics and Control of Horizontal Axis Wind Turbines, in *Proceedings of the American Control Conference*: Denver, Colorado: 3781-3793.

Gipe, P. 2004. *Wind Power*. White River Junction, Vermont: Chelsea Green Publishing Company.

Graham Kelly, S. 2000. *Fundamentals of Mechanical Vibrations*. Singapore: McGraw-Hill Higher education companies.

Hansen, O. L. M. 2008. *Aerodynamics of Wind Turbines*. United Kingdom: Earthscan.

Harikrishna, P & Shanmugasundaram, J & Gomathinayagam, S & Lakshmanan, N.1999. Analytical and experimental studies on the gust response of a 52m tall steel lattice tower under wind loading. *Computers and Structures* 70 (1999):149-160.

Kato, B., Hirose, R. 1985. Bolted Tension Flanges Joining Circular Hollow Section Members. *Journal of Constructional Steel Research* 5 (2):79-101.

Kiessling, F., Nefzger, P., Nolasco, J.F & Kaintzyk, U. 2003. *Overhead Power Lines, Planning, Design, Construction*. Germany: Springer-Verlag Berlin Heidelberg.

Lee, P & McClure, G. 2006. Elastoplastic large deformation analysis of a lattice steel tower structure and comparison with full-scale tests. *Journal of Constructional Steel Research* 63 (2007):709-717.

Marsh, G. 2005. *Wind turbines, how big can they get?* Refocus, March/April 2005.

Peterson, B. E. 2010 Evaluate the effect of turbine period of vibration requirements on structural design parameters. Applied Physical Sciences corp.

Prokon Software consultants. Prokon Structural Analysis and Design software. © Copyright 1996-2012 Prokon Software Consultants.

Robberts, J. M, Marshall, V.2009. *Analysis and Design of Concrete Structures*. Cement and Concrete Institute.

*Small Wind Turbines*. 2011. [Online]. Available: [www.wind-energy-the-facts.org](http://www.wind-energy-the-facts.org) [2011,February 17].

Sorensen, J.D & Toft, H.S. 2010. *Probabilistic Design of Wind Turbines* [Online]. Available: [www.mdpi.com/journal/energies](http://www.mdpi.com/journal/energies), [2011, March 03].

*South African Steel Construction Handbook*. 2008. South Africa: Paarl Print.

Stottrup-Andersen, U. (1997). Masts and Towers. Tech.Rep., Denmark University IASS Working Group.

Strand7 Software Pty Ltd.

*The energy in the wind*. 2011. [Online]. Available: [www.windpower.org](http://www.windpower.org) [2011,February 16].

The European Wind Energy Association (EWEA): 2009. *Wind Energy-The Facts*. Earthscan: London.

*Turbine Towers*. 2011. [Online].Available: [www.house-energy.com](http://www.house-energy.com) [2011,February 18].

Yeh, T and Wang, L. 2008. A Study on Generator Capacity for Wind Turbines Under Various Tower Heights and Rated Wind Speeds Using Weibull Distribution. *IEEE transactions on Energy Conversion*, 23(2):592-602.

## APPENDIX A: TOWER DESIGN CALCULATIONS

### A1: STEEL MONOPOLE DESIGN

#### A1.1 DESIGN REFERENCE PARAMETERS AND TOWER RESISTANCE CALCULATIONS

TOWER GEOMETRY AND AXIAL COMPRESSION RESISTANCE:

**Slenderness Ratio** **SANS 10162-1:2005 10.4**

**Monopoles: Constant cross-section**

*Inner and outer diameters*

$d_o$  0.508 m

$d_i$  0.4826 m

$t$  0.0127 m

*Length of tower (height)*

$L$  16 m

*Effective length factor*

$K$  2 \*\*cantilever column

*inertia*

$I$  0.0006064 m<sup>4</sup>

*Cross-sectional area*

$A$  0.0197616 m<sup>2</sup>

*Radius of gyration*

$r$  0.1751726 m

*Slenderness ratio*

$KL/r$  182.67702

*Check*

**COMPRESSION SLENDERNESS OK**

**SANS 10162-1:2005 11**

**Width-to-thickness ratios: elements in compression**

**Classification of sections**

**Monopoles: Constant cross-section**

**Table 3: Maximum width-to-thickness ratios:  
elements in axial compression**

circular hollow sections:  $\frac{d}{t} < \frac{23000}{f_y}$

necessary parameters			
$d_o$	508	$t$	12.7
	*mm		*mm
		$f_y$ (MPa)	300
		$E$ (GPa)	200

**CLASS 3 SECTION**

FLEXURAL AND AXIAL COMPRESSION RESISTANCE:

**Table 4: Maximum width-to-thickness ratios: elements in flexural compression**

circular hollow sections:

$$\frac{d}{t} < \frac{13000}{f_y} \text{ class 1 sections} \quad \frac{d}{t} < \frac{18000}{f_y} \text{ class 2 sections} \quad \frac{d}{t} < \frac{66000}{f_y} \text{ class 3 sections}$$

necessary parameters					
$d_o$	508	$t$	12.7	$f_y$ (MPa)	300
	*mm		*mm	E(GPa)	200
$d_o/t$	40				

class 1	43.333333
class 2	60
class 3	220

**CLASS 1 SECTION**

**Axial Compression resistance:**

SANS 10162-1:2005 Section 13.3

Flexural Buckling 13.3.1

**Monopoles: Constant cross-section**

$C_r = \varphi A f_y (1 + \lambda^{2n})^{-\frac{1}{n}}$			
n	1.34	$\phi$	0.9
$\lambda = \frac{KL}{r} \sqrt{\frac{f_y}{\Pi^2 E}}$			

$\lambda$	2.2520586
-----------	-----------

**factored axial compressive resistance**

$C_r$	970903.31	N	970.9033113	kN
-------	-----------	---	-------------	----

**SANS 10162-1:2005 13.5 Bending-Laterally supported members**

\*\*using class classification from flexural compression classification

**Monopoles: Constant cross-section**

Class 1 and 2 sections
$M_r = \phi Z_{pl} f_y = \phi M_p$
Class 3 sections
$M_r = \phi Z_e f_y = \phi M_y$

**Plastic and elastic effective section moduli**

Z <sub>pl</sub>	0.0031163
Z <sub>e</sub>	0.0023874

**factored moment resistance**

M <sub>r</sub>	841393.8	Nm
----------------	----------	----

\*\*takes into account which class section it is

**SHEAR RESISTANCE:**

**SANS 10162-1:2005 13.4.2 Shear resistance of webs of flexural members not having two flanges**

\*\*\*max at ultimate load may not exceed  $0.66\phi f_y$

V <sub>r(MAX)</sub>	178200000	N
---------------------	-----------	---

$V_r = 0.66\phi(0.9A)f_y$

V <sub>r</sub>	3169364.1	N
----------------	-----------	---

check	<b>SHEAR OK</b>
-------	-----------------



## A1.2 WIND CALCULATIONS ON STEEL MONOPOLE TOWER

### SANS 10160-3:2011

#### ULTIMATE LIMIT STATE (ULS)

#### 7.2 Basic Values

location: university of stellenbosch: engineering faculty

#### 7.2.2

**fundamental value of the basic wind speed (from figure 1 in SANS 10160-3)**

$V_{b,0}$	28	m/s	Figure 1 in SANS 10160-3:2011
-----------	----	-----	-------------------------------

**terrain category**

B	Table 2 in SANS 10160-3:2011
---	------------------------------

**return period**

50	years	this return period may be taken as the design
----	-------	---

**design life of components** working life of the structure

20	years
----	-------

**altitude (above mean sea level)**

100	m
-----	---

**hub height (reference height, above ground level)**

16.2	m	(height of tower plus one meter)
------	---	----------------------------------

**tower surface finish**

galvanised steel
------------------

**roughness coefficient**

k	0.2	mm
---	-----	----

#### Calculation procedure in accordance with Table 5 SANS 10160-3:2011

#### ULS

**Fundamental basic wind speed (SANS 10160-3:2011 Figure 1)**

$V_{b,0}$	28	m/s
-----------	----	-----

**probability factor SANS 10160-3:2011 7.2.3**

K	0.2
---	-----

p	0.02
---	------

(annual probability of exceedance for mean return period of 50 years)

n	0.5
---	-----

$C_{prob}$	1
------------	---

**Basic wind speed (SANS 10160-3:2011 Equation 1)**

$V_b$	28	m/s
-------	----	-----

### SANS 10160-3:2011 7.3.1

Variation with height

**terrain roughness factor SANS 10160-3:2011**

z	16.2	m
---	------	---

$z_0$	0
-------	---

$z_g$	300
-------	-----

$z_c$	5
-------	---

$\alpha$	0.095
----------	-------

$c_r(z)$	1.0323091
----------	-----------

$c_0(z)$	1
----------	---

**peak wind speed SANS 10160-3:2011 7.3**

$V_{b,peak}$	39.2	m/s
--------------	------	-----

$V_p(z)$	40.466516	m/s
----------	-----------	-----

**SANS 10160-3:2011 7.4 Peak wind speed pressure**

$\rho$	1.184	(Table 4 SANS 10160-3:2011)
--------	-------	-----------------------------

$q_p(z)$	969.42302	$N/m^2$
----------	-----------	---------

**SERVICEABILITY LIMIT STATE (SLS)**

**7.2 Basic Values**

location: university of stellenbosch: engineering faculty

**7.2.2**

fundamental value of the basic wind speed (from figure1 in SANS 10160-3)

$V_{b,0}$	16	m/s	Figure 1 in SANS 10160-3:2011
-----------	----	-----	-------------------------------

**terrain category**

B	Table 2 in SANS 10160-3:2011
---	------------------------------

**return period**

50	years	this return period may be taken as the design
----	-------	---

**design life of components** working life of the structure

20	years
----	-------

**altitude (above mean sea level)**

100	m
-----	---

**hub height (reference height, above ground level)**

16.2	m	(height of tower plus one meter)
------	---	----------------------------------

**tower surface finish**

galvanised steel
------------------

**roughness coefficient**

k	0.2	mm
---	-----	----

**SLS**

**Fundamental basic wind speed (SANS 10160-3:2011 Figure 1)**

$V_{b,0}$	16	m/s
-----------	----	-----

probability factor SANS 10160-3:2011 7.2.3

K	0.2
---	-----

p	0.02
---	------

(annual probability of exceedance for mean return period of 50 years)

n	0.5
---	-----

$C_{prob}$	1
------------	---

**Basic wind speed (SANS 10160-3:2011 Equation1)**

$V_b$	16	m/s
-------	----	-----

**SANS 10160-3:2011 7.3.1**

Variation with height

**terrain roughness factor SANS 10160-3:2011**

z	16.2	m
---	------	---

$z_0$	0
-------	---

$z_g$	300
-------	-----

$z_c$	5
-------	---

$\alpha$	0.095
----------	-------

$c_r(z)$	1.032309
----------	----------

$C_0(z)$	1
----------	---

**peak wind speed SANS 10160-3:2011 7.3**

$V_{b,peak}$	22.4	m/s
--------------	------	-----

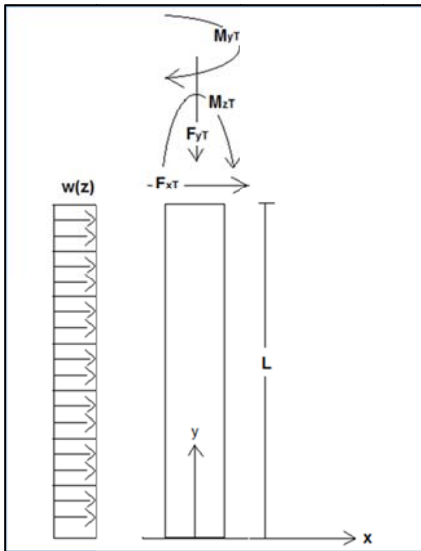
$V_p(z)$	23.12372	m/s
----------	----------	-----

**SANS 10160-3:2011 7.4 Peak wind speed pressure**

$\rho$	1.184	(Table 4 SANS 10160-3:2011)
--------	-------	-----------------------------

$q_p(z)$	316.5463	N/m <sup>2</sup>
----------	----------	------------------

### A1.3 ACTIONS INDUCED ON THE TOWER



<b>Distributed wind load up the height of the tower</b>					
<b>ULS</b> beyond 16m/s wind speed (28m/s)					
w(z)	286.65218	N/m	w(z)	564.2759	N/m <sup>2</sup>
<b>SLS</b> up to 16m/s wind speed					
w(z)	93.600712	N/m	w(z)	184.2534	N/m <sup>2</sup>

**Axial drag force, in x-direction exerted on turbine during operation**

a	0.33	induction factor of the wind turbine
---	------	--------------------------------------

D <sub>blades</sub>	4	m
A	12.56637	m <sup>2</sup>

**Ultimate limit state:**

X <sub>Q,wind</sub>	1.5	SANS 10160-1:2011 table 3
F <sub>xT,ULS</sub>	8080.406	N
F <sub>xT,Unfactored</sub>	5386.937	N

**Serviceability limit state:**

X <sub>Q,wind</sub>	0.6	SANS 10160-1:2011 section 8.3.1.1
F <sub>xT,SLS</sub>	2110.8	N
F <sub>xT,Unfactored</sub>	3518	N

**Vertical self-weight loading, in z-direction**

weights (kgs):

total	120	kg
-------	-----	----

**Ultimate limit state:**

X <sub>G,Dead</sub>	1.2	SANS 10160-1:2011 table 3
F <sub>ZT,ULS</sub>	1412.64	N

**Serviceability limit state:**

X <sub>G,Dead</sub>	1.1	
F <sub>ZT,SLS</sub>	1294.92	N

A1.4 INTERACTION EQUATIONS

$$\frac{C_u}{C_r} + U_{1x} \frac{M_{ux}}{M_{rx}} < 1.0$$

Monopoles: Constant cross-section	
C <sub>u</sub>	1412.64
C <sub>r</sub>	970903.3113 N
M <sub>ux</sub>	282.528
M <sub>rx</sub>	841393.8011 Nm
U <sub>1x</sub>	1

check	O.K
-------	-----

**Shear capacity check at the base of the tower**

$$\frac{V_u}{V_r} < 1.0$$

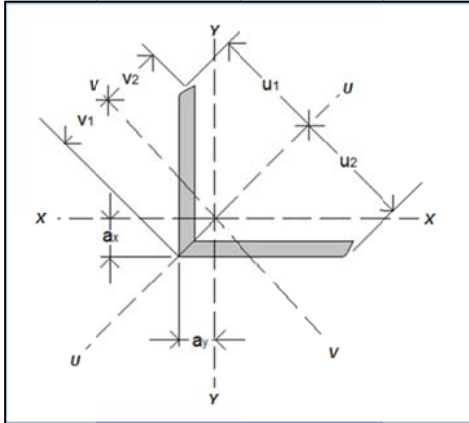
Monopoles: Constant cross-section	
V <sub>u</sub>	17404 N
V <sub>r</sub>	3169364.074 N

check	O.K
-------	-----

## A2: STEEL LATTICE DESIGN

### A2.1 DESIGN REFERENCE PARAMETERS AND TOWER RESISTANCE CALCULATIONS

TOWER GEOMETRY AND AXIAL COMPRESSION RESISTANCE:



#### Member capacity checks:

Attributes of each member

parameter	50x50x5	70x70x6	100x100x8
m(kg/m)	3.77	6.38	12.2
A(mm <sup>2</sup> )	480	813	1550
a <sub>x</sub> (mm)	14	19.3	27.4
a <sub>y</sub> (mm)	14	19.3	27.4
v <sub>1</sub> (mm)	19.9	27.3	38.7
v <sub>2</sub> (mm)	17.6	24.6	35.2
<b>About x-x and y-y</b>			
I(10 <sup>6</sup> mm <sup>4</sup> )	0.11	0.369	1.45
Z <sub>e</sub> (10 <sup>3</sup> mm <sup>3</sup> )	3.05	7.27	19.9
r(mm)	15.1	21.3	30.6
<b>About u-u</b>			
I(10 <sup>6</sup> mm <sup>4</sup> )	0.174	0.585	2.3
Z <sub>e</sub> (10 <sup>3</sup> mm <sup>3</sup> )	4.92	11.8	32.5
r(mm)	19	26.8	38.5
<b>About v-v</b>			
I(10 <sup>6</sup> mm <sup>4</sup> )	0.046	0.153	0.599
Z <sub>e</sub> (10 <sup>3</sup> mm <sup>3</sup> )	2.29	5.6	15.5
r(mm)	9.73	13.7	19.6
J(10 <sup>3</sup> mm <sup>4</sup> )	4.58	11.2	37.6
C <sub>w</sub>	0	0	0
f <sub>y</sub> (Mpa)	355	355	355
f <sub>u</sub> (Mpa)	470	470	470

**Slenderness**

<b>50x50x5</b>	
K	1
L	583.095
KL/r	59.9275

<b>70x70x6</b>	
K	1
L	2605.52
KL/r	190.1839

<b>100x100x8</b>	
K	1
L	3658.04
KL/r	186.6347

Compression Check	<b>OK</b>
Tesion Check	<b>OK</b>

Compression Check	<b>OK</b>
Tesion Check	<b>OK</b>

Compression Check	<b>OK</b>
Tesion Check	<b>OK</b>

**Class Classification**

**Table 3 SANS 10162-1:2005 elements in axial compression**

<b>50x50x3</b>	
<b>Legs of angles</b>	
b	50
t	5
b/t	10
200/f <sub>y</sub> <sup>0.5</sup>	10.6149
class	<b>class 3</b>

<b>70x70x6</b>	
<b>Legs of angles</b>	
b	70
t	6
b/t	11.66666667
200/f <sub>y</sub> <sup>0.5</sup>	10.6149
class	<b>class 4</b>

<b>100x100x8</b>	
<b>Legs of angles</b>	
b	100
t	8
b/t	12.5
200/f <sub>y</sub> <sup>0.5</sup>	10.6149
class	<b>class 4</b>

**Compression Tests**

**Flexural Buckling**

Clause 13.3.3 Class 4 members in compression

<b>50x50x5</b>	
W	10
k	0.43
φ	0.9
C <sub>u</sub>	61865.54 N
f	1.43E+02 MPa
check which f to use	1.43E+02 MPa
E	200000 MPa
W <sub>lim</sub>	1.58E+01

<b>70x70x6</b>	
W	11.6667
k	0.43
φ	0.9
C <sub>u</sub>	61865.54 N
f	8.46E+01 MPa
check which f to use	8.46E+01 MPa
E	200000 MPa
W <sub>lim</sub>	2.06E+01

<b>100x100x8</b>	
W	12.5
k	0.43
φ	0.9
C <sub>u</sub>	61865.54 N
f	4.43E+01 MPa
check which f to use	4.43E+01 MPa
E	200000 MPa
W <sub>lim</sub>	2.84E+01

check	A <sub>ef</sub> =A
-------	--------------------

check	A <sub>ef</sub> =A
-------	--------------------

check	A <sub>ef</sub> =A
-------	--------------------

b <sub>eff</sub>	57.07 mm
------------------	----------

b <sub>eff</sub>	78.42 mm
------------------	----------

b <sub>eff</sub>	89.44 mm
------------------	----------

**effective cross sectional area**

A <sub>eff</sub>	480 mm <sup>2</sup>
------------------	---------------------

**effective cross sectional area**

A <sub>eff</sub>	813 mm <sup>2</sup>
------------------	---------------------

**effective cross sectional area**

A <sub>eff</sub>	1550 mm <sup>2</sup>
------------------	----------------------

**Determining f<sub>e</sub>**

f <sub>ey</sub>	2095.8409
f <sub>ex</sub>	32938.4580

f <sub>ey</sub>	208.8385
f <sub>ex</sub>	10379.0092

f <sub>ey</sub>	218.6524
f <sub>ex</sub>	10576.3877

x <sub>0</sub> <sup>2</sup>	396.01 mm <sup>2</sup>
y <sub>0</sub> <sup>2</sup>	0 mm <sup>2</sup>
r <sub>x</sub> <sup>2</sup>	94.6729 mm <sup>2</sup>
r <sub>y</sub> <sup>2</sup>	361 mm <sup>2</sup>

x <sub>0</sub> <sup>2</sup>	745.29 mm <sup>2</sup>
y <sub>0</sub> <sup>2</sup>	0 mm <sup>2</sup>
r <sub>x</sub> <sup>2</sup>	187.69 mm <sup>2</sup>
r <sub>y</sub> <sup>2</sup>	718.24 mm <sup>2</sup>

x <sub>0</sub> <sup>2</sup>	1497.69 mm <sup>2</sup>
y <sub>0</sub> <sup>2</sup>	0 mm <sup>2</sup>
r <sub>x</sub> <sup>2</sup>	384.16 mm <sup>2</sup>
r <sub>y</sub> <sup>2</sup>	1482.25 mm <sup>2</sup>

r <sub>0</sub> <sup>2</sup>	851.6829 mm <sup>2</sup>
-----------------------------	--------------------------

r <sub>0</sub> <sup>2</sup>	1651.22 mm <sup>2</sup>
-----------------------------	-------------------------

r <sub>0</sub> <sup>2</sup>	3364.1 mm <sup>2</sup>
-----------------------------	------------------------

f <sub>ez</sub>	784.2316
-----------------	----------

f <sub>ez</sub>	584.0104
-----------------	----------

f <sub>ez</sub>	504.7604
-----------------	----------

Ω	0.5350
---	--------

Ω	0.5486
---	--------

Ω	0.5548
---	--------

f <sub>eyz</sub>	648.9137
------------------	----------

f <sub>eyz</sub>	175.0291
------------------	----------

f <sub>eyz</sub>	176.4395
------------------	----------

f <sub>e</sub>	648.9137
----------------	----------

f <sub>e</sub>	175.0291
----------------	----------

f <sub>e</sub>	176.4395
----------------	----------

λ	0.7396
---	--------

λ	1.4242
---	--------

λ	1.4185
---	--------

n	1.34
---	------

n	1.34
---	------

n	1.34
---	------

**Axial Compression SANS 10162-1:2005 13.3**

$C_r$	101739.8005 N
check	Satisfactory Section
SF	0.608076089
check	OK

$C_r$	97492.64562 N
check	Satisfactory Section
SF	0.634566224
check	OK

$C_r$	186686.297 N
check	Satisfactory Section
SF	0.331387686
check	OK

**Tensile Capacity of Members SANS 10162-1:2005**

**clause 13.2 a)**

i)	
$T_r$	153360 N
ii) Block Tear out	
$A_{ne}$	400 mm <sup>2</sup>
$T_r$	143820 N
$T_u$	62000 N
check	Satisfactory Section
$T_u/T_r$	0.404277517
check	OK

**clause 13.2 a)**

i)	
$T_r$	259753.5 N
ii) Block Tear out	
$A_{ne}$	717 mm <sup>2</sup>
$T_r$	257797.35 N
$T_u$	62000 N
check	Satisfactory Section
$T_u/T_r$	0.238687833
check	OK

**clause 13.2 a)**

i)	
$T_r$	495225 N
ii) Block Tear out	
$A_{ne}$	1422 mm <sup>2</sup>
$T_r$	511280.1 N
$T_u$	62000 N
check	Satisfactory Section
$T_u/T_r$	0.125195618
check	OK

**Pinned Connections**

**clause 13.2 b)**

$T_r$	126900 N
check	OK

**clause 13.2 b)**

$T_r$	227468.25 N
check	OK

**clause 13.2 b)**

$T_r$	451129.5 N
check	OK

**Load Bearing Capacity of Members SANS 10162-1:2005**

**clause 13.10 Load Bearing**

$\Phi_{br}$	0.67
t	5
d	16
n	2
a	40
$B_{r,i}$	151152 N
$B_{r,ii}$	125960 N
check	OK

$\Phi_{br}$	0.67
t	6
d	16
n	2
a	40
$B_{r,i}$	181382.4 N
$B_{r,ii}$	151152 N
check	OK

$\Phi_{br}$	0.67
t	8
d	16
n	2
a	40
$B_{r,i}$	241843.2 N
$B_{r,ii}$	201536 N
check	OK

## A2.2 WIND CALCULATIONS ON STEEL LATTICE TOWER

### SANS 10160-3:2011

#### ULTIMATE LIMIT STATE (ULS)

#### 7.2 Basic Values

location: university of stellenbosch: engineering faculty

#### 7.2.2

**fundamental value of the basic wind speed (from figure1 in SANS 10160-3)**

$V_{b,0}$	28	m/s	Figure 1 in SANS 10160-3:2011
-----------	----	-----	-------------------------------

**terrain category**

B	Table 2 in SANS 10160-3:2011
---	------------------------------

**return period**

50	years	this return period may be taken as the design
----	-------	---

**design life of components** working life of the structure

20	years
----	-------

**altitude (above mean sea level)**

100	m
-----	---

**hub height(reference height, above ground level)**

16.2	m	(height of tower plus one meter)
------	---	----------------------------------

**tower surface finish**

galvanised steel
------------------

**roughness coefficient**

k	0.2	mm
---	-----	----

#### Calculation procedure in accordance with Table 5 SANS 10160-3:2011

**Fundamental basic wind speed (SANS 10160-3:2011 Figure 1)**

$V_{b,0}$	28	m/s
-----------	----	-----

**probability factor SANS 10160-3:2011 7.2.3**

K	0.2
---	-----

p	0.02
---	------

(annual probability of exceedance for mean return period of 50 years)

n	0.5
---	-----

$C_{prob}$	1
------------	---

**Basic wind speed (SANS 10160-3:2011 Equation1)**

$V_b$	28	m/s
-------	----	-----

### SANS 10160-3:2011 7.3.1

Variation with height

**terrain roughness factor SANS 10160-3:2011**

z	16.2	m
---	------	---

$z_0$	0
-------	---

$z_g$	300
-------	-----

$z_c$	5
-------	---

$\alpha$	0.095
----------	-------

$c_r(z)$	1.032309
----------	----------

$c_0(z)$	1
----------	---

**peak wind speed SANS 10160-3:2011 7.3**

$V_{b,peak}$	39.2	m/s
--------------	------	-----

$V_p(z)$	40.46652	m/s
----------	----------	-----

**SANS 10160-3:2011 7.4 Peak wind speed pressure**

$\rho$	1.184	(Table 4 SANS 10160-3:2011)
--------	-------	-----------------------------

$q_p(z)$	969.423	$N/m^2$
----------	---------	---------



**SERVICEABILITY LIMIT STATE (SLS)**

**7.2 Basic Values**

location: university of stellenbosch: engineering faculty

**7.2.2**

fundamental value of the basic wind speed (from figure 1 in SANS 10160-3)

$V_{b,0}$	16	m/s	Figure 1 in SANS 10160-3:2011
-----------	----	-----	-------------------------------

**terrain category**

B	Table 2 in SANS 10160-3:2011
---	------------------------------

**return period**

50	years	this return period may be taken as the design
----	-------	---

**design life of components** working life of the structure

20	years
----	-------

**altitude (above mean sea level)**

100	m
-----	---

**hub height (reference height, above ground level)**

16.2	m	(height of tower plus one meter)
------	---	----------------------------------

**tower surface finish**

galvanised steel
------------------

**roughness coefficient**

k	0.2	mm	**see code extracts sheet**
---	-----	----	-----------------------------

**Calculation procedure in accordance with Table 5 SANS 10160-3:2011**

**Fundamental basic wind speed (SANS 10160-3:2011 Figure 1)**

$V_{b,0}$	16	m/s
-----------	----	-----

probability factor SANS 10160-3:2011 7.2.3

K	0.2
---	-----

p	0.02
---	------

(annual probability of exceedance for mean return period of 50 years)

n	0.5
---	-----

$C_{prob}$	1
------------	---

**Basic wind speed (SANS 10160-3:2011 Equation 1)**

$V_b$	16	m/s
-------	----	-----

SANS 10160-3:2011 7.3.1

Variation with height

**terrain roughness factor SANS 10160-3:2011**

z	16.2	m
---	------	---

$z_0$	0
-------	---

$z_g$	300
-------	-----

$z_c$	5
-------	---

$\alpha$	0.095
----------	-------

$c_r(z)$	1.032309
----------	----------

$c_0(z)$	1
----------	---

**peak wind speed SANS 10160-3:2011 7.3**

$V_{b,peak}$	22.4	m/s
--------------	------	-----

$V_p(z)$	23.12372	m/s
----------	----------	-----

**SANS 10160-3:2011 7.4 Peak wind speed pressure**

$\rho$	1.184	(Table 4 SANS 10160-3:2011)
--------	-------	-----------------------------

$q_p(z)$	316.5463	N/m <sup>2</sup>
----------	----------	------------------

**Factored Wind Load:**

**Ultimate Limit State**

w(z)	1454.134526 N/m <sup>2</sup>
------	------------------------------

**Serviceability Limit State**

w(z)	189.9278 N/m <sup>2</sup>
------	---------------------------

**APPLYING THE WIND LOADS:**

**WIND LOAD CASES:**

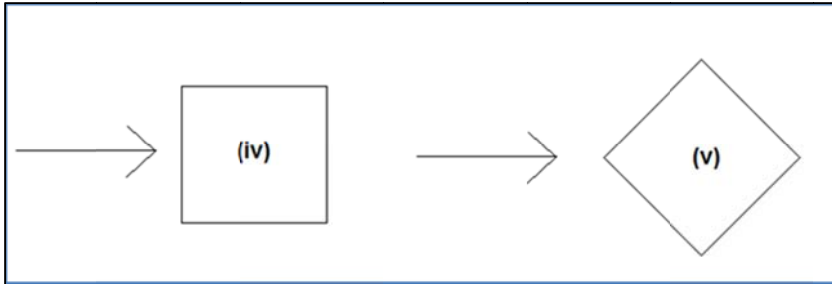


Figure 35 SANS 10160-3: Force coefficients according to the cross sectional shape and wind direction on the cross section

**Square Lattice Cross Section**

**Straight Part**

case:	$\phi$	$C_{f,0}$	$\psi_\lambda$	$C_f$
(iv)	0.573238	1.8	0.925	1.665
(v)	0.553312	2.5	0.93	2.325

**Tapered Part**

case:	$\phi$	$C_{f,0}$	$\psi_\lambda$	$C_f$
(iv)	0.202345	2.36	0.97	2.2892
(v)	0.638628	2.55	0.945	2.40975

**Solidity Ratio**

**Straight Part**

Load case (iv)		Load case (v)	
$\phi$	0.573238	$\phi$	0.553312
Projected Area		Projected Area	
A	0.75 m <sup>2</sup>	A	1.06066 m <sup>2</sup>
Area of Steel		Area of Steel	
A <sub>c</sub>	0.429929 m <sup>2</sup>	A <sub>c</sub>	0.586876 m <sup>2</sup>

**Straight Part**

**Tapered Part**

Load case (iv)		Load case (v)	
A <sub>c</sub>	6.282819 m <sup>2</sup>	A <sub>c</sub>	23.33925 m <sup>2</sup>
A	31.05 m <sup>2</sup>	A	36.5459 m <sup>2</sup>
$\phi$	0.202345	$\phi$	0.638628

**Tapered Part**

### Slenderness Ratio

#### Tapered Part

L	13.5	m
b	2.2997	m
b	0.3	m
L/b	5.870331	m
L/b	45	m

\*average cross section at mid height of tapered part

\*\*smallest possible cross section

In accordance with table 22, SANS 10160-3 No. 1 includes lattice structures

L	13.5	m
$\lambda$	90	
$\lambda_{check}$	70	

for  $L < 15m$ ,  $\lambda = 2L/b$  or 70, whichever is smaller

#### Straight Part

L	2.5	m
b	0.3	m

L/b	8.333333
-----	----------

In accordance with table 22, SANS 10160-3 No. 1 includes lattice structures

L	2.5	m
$\lambda$	16.66667	
$\lambda_{check}$	16.66667	

for  $L < 15m$ ,  $\lambda = 2L/b$  or 70, whichever is smaller

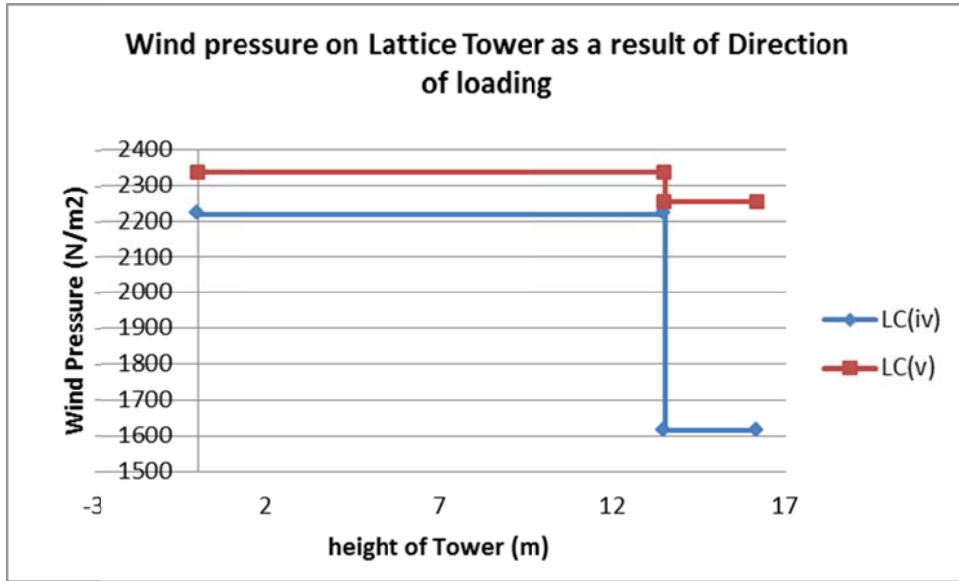
### Wind Load Cases (Factored) ( $N/m^2$ )

LC (iv)		LC (v)	
ULS	SLS	ULS	SLS
<b>Straight Part</b>		<b>Straight Part</b>	
2421.134	316.2297	2421.134	441.5821
<b>Tapered Part</b>		<b>Tapered Part</b>	
3328.805	434.7827	3504.101	457.6785

### Wind Load Cases (Unfactored) ( $N/m^2$ )

LC (iv)		LC (v)		
Straight	Tapered	Straight	Tapered	
1614.089	2219.203	2253.909	2336.067	ULS
527.0496	724.6378	735.9701	762.7974	SLS

height	LC (iv)	LC (v)
0	2219.203	2336.067
13.5	2219.203	2336.067
13.5	1614.089	2253.909
16.2	1614.089	2253.909



### A2.3 ACTIONS INDUCED ON THE TOP OF THE TOWER

#### **Axial drag force, in x-direction exerted on turbine during operation**

a	0.33	induction factor of the wind turbine
---	------	--------------------------------------

$D_{blades}$	4	m
A	12.56637	m <sup>2</sup>

#### **Ultimate limit state:**

$\gamma_{Q,wind}$	1.5	SANS 10160-1:2011 table 3
$F_{xT,ULS}$	8080.406	N

#### **Serviceability limit state:**

$\gamma_{Q,wind}$	0.6	SANS 10160-1:2011 section 8.3.1.1
$F_{xT,SLS}$	2110.8	N

#### **Vertical self-weight loading, in z-direction**

weights (kgs):

total	120	kg
-------	-----	----

#### **Ultimate limit state:**

$\gamma_{G,Dead}$	1.2	SANS 10160-1:2011 table 3
$F_{zT,ULS}$	1412.64	N

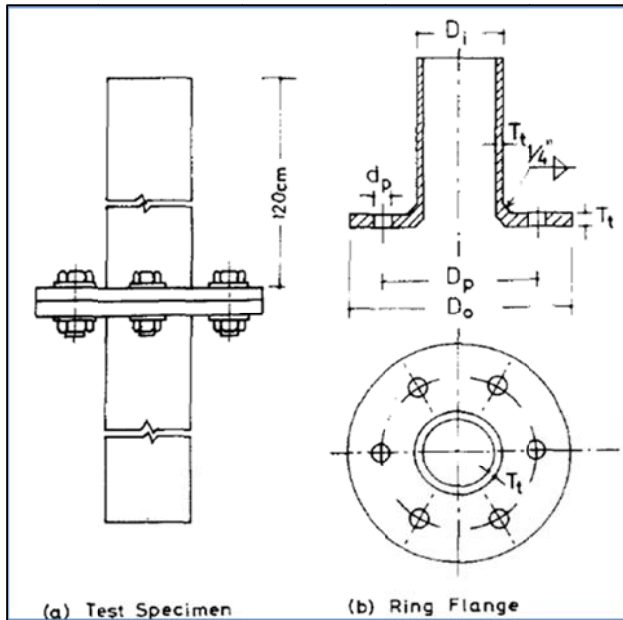
#### **Serviceability limit state:**

$\gamma_{G,Dead}$	1.1	
$F_{zT,SLS}$	1294.92	N

## APPENDIX B: CONNECTIONS

### B.1 STEEL MONOPOLE CONNECTIONS

#### RING FLANGE CONNECTIONS: METHOD 1



#### Parameters

d	20	diameter of the bolt
$D_i$	508	is equal to the outer tube diameter + the width to the centre of the fillets welds.
$D_o$	648	$D_o = D_p + 4d$
$D_p$	568	$D_p = D_i + 3d$
$T_t$	12.7	
$T_f$	25	
n	16	number of bolts

#### perimeter of mid-flange

$\rho_m$	1784.425	mm
----------	----------	----

ratio of tube thickness to flange thickness:

$T_t/T_f$	0.508	**article's lowest 0.21
-----------	-------	-------------------------

#### minimum spacing between bolts along perimeter

$s_{min}$	30	mm
-----------	----	----

#### max No. Bolts in spacing

No. max	59.48082	bolts
---------	----------	-------

#### spacing between bolts along perimeter (actual)

s	111.5265	mm
---	----------	----

**Bolt force at separation:**

The relationship between the force acting on the bolts and the instant of separation

Separation Force

$T_s$	223.3182 kN
-------	-------------

$T_s = \alpha T_o$

Bolt pre-load

$T_o$	178 kN
-------	--------

Table 1 SANS 10094

cross-sectional area of the unthreaded shank of the bolt

$A_b$	314.1593 mm <sup>2</sup>
-------	--------------------------

\*\*area using diameter of bolt before threading

**effective area of the compressed flange plate**

$A_p$	1233.948 mm <sup>2</sup>
-------	--------------------------

\*eqn

$D$	37 mm
-----	-------

diameter of washer face of bolt

\*\*Table 6.4 Red Book

$l_p$	50 mm
-------	-------

grip length = 2T<sub>f</sub>

$d_p$	22 mm
-------	-------

diameter of the bolt hole

\*\*+2mm

$T_y$	254.2857 kN
-------	-------------

yield strength of the bolt

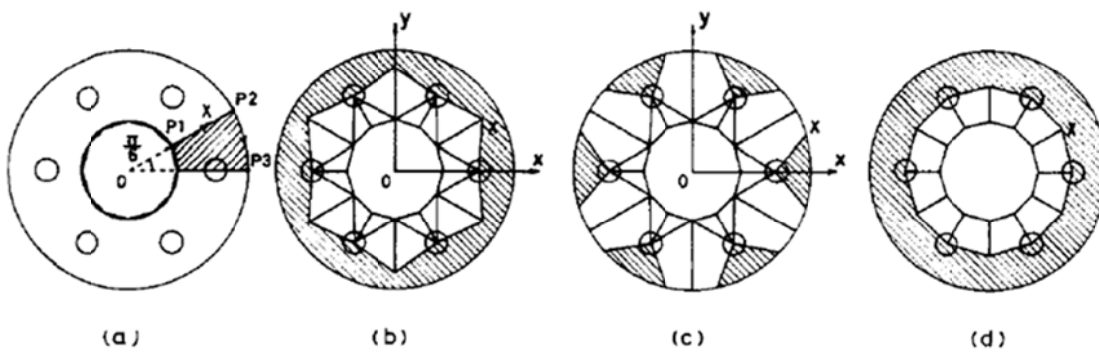
tensile strength of bolt Table 6.1 Red Book

$d$	20 mm
-----	-------

diameter of the unthreaded shank of the bolt

$\alpha$	1.254597
----------	----------

**Bolted tension flanges joining circular hollow section members**



**Yield load of the flange**

$P_p = U m_p$

$P_p$	6.433458 kN
-------	-------------

\*\*check 1/4

$m_p$	53.90625 kNm
-------	--------------

$m_p = (1/4) T_f^2 \sigma_y$

\*\*full plastic moment per unit width of the flange

$U$	0.119345
-----	----------

$U = (48 \tan(\pi/12)) * (D_p / (D_p - D_i))$

$U = (128 \tan(\pi/32)) * (D_p / (D_p - D_i))$

**maximum load of the flange**

$P_u = (\sigma_u / \sigma_y) P_p$

$P_u$	8.764422 kN
-------	-------------

**Flange Strengths**

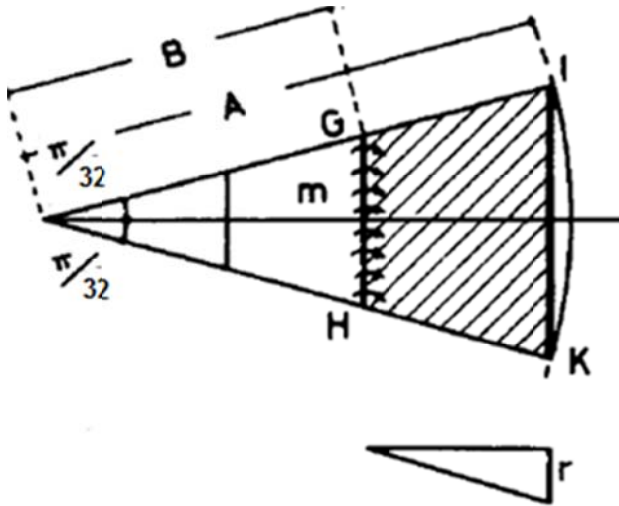
$\sigma_y$	345 MPa
$\sigma_u$	470 MPa

**Maximum bending strength of flange when separation occurs after maximum yielding of the flange**

$U'$	0.2910549
------	-----------

$P'_p$	4.0489417 kN
--------	--------------

$P'_u$	5.5159496 kN
--------	--------------



**Evaluation of prying force**

The prying force acting before separation

Parameters:

B	265.5 mm	$D_p/2 - a/2$
A	324 mm	$D_o/2$
a	37 mm	
m	43.67438 kNm	$(m_p < m < m_u)$

$m_p = (1/4)T_f^2\sigma_y$		$m_u = (1/4)T_f^2\sigma_u$	
$m_p$	13911.26	$m_u$	73437.5 Nm

**Prying force acting before separation**

Reaction force per unit length of line IK:

r	0.088466 kN/m
---	---------------

Total reaction acting throughout the circular flange

R	1844.621 kN
---	-------------

Ratio of Prying Force to external load

$\beta_1$	0.145113
-----------	----------

**Prying force acting after the separation**

Reaction force per unit length of line IK:

$r_s$	0.961693 kN/m
-------	---------------

Total reaction acting throughout the circular flange

$R_s$	1249.435 kN
-------	-------------

Ratio of Prying Force to external Load

$\beta_2$	0.375
-----------	-------

B	284	$D_p/2$
A	324	$D_o/2$
a	37	
m	43.67438	kNm

**Separation load and fracture load of the bolts****Separation load**

$P'$		Tensile force applied to specimen
$\Sigma T_s$	3573.092	
$P_s$	3120.297	Bolt separation load

$$P' = P_s$$

**Fracture load of the bolts****Fracture occurs after yielding of the flange**

$\Sigma T_u$	4068.571	Tensile strength of bolts
${}_b P_m$	2958.961	Maximum tensile strength of a connection

$$P = {}_b P_m$$

**Fracture occurs before yielding of the flange**

$\Sigma T_u$	4068.571	Tensile strength of bolts
${}_b P_m$	4068.571	**since no prying action needs to be taken into account here.

**Maximum Strength of a Connection:****1. Critical loads corresponding to flange failure:**

i) flange yields and reaches its max strength before separation takes place

maximum load of joint:

$P'_u$	5.5159496	kN
--------	-----------	----

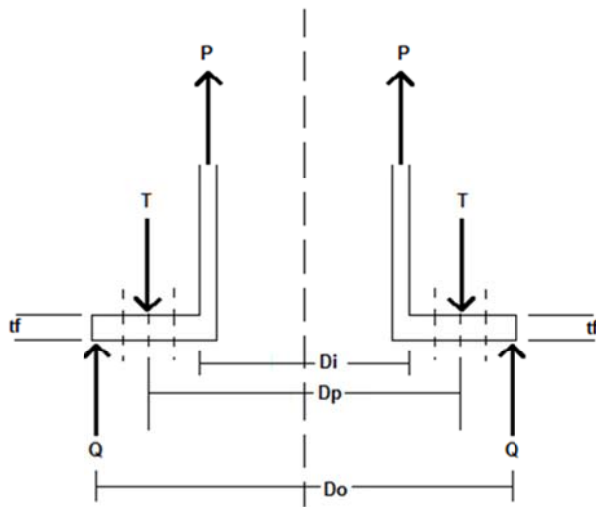
ii) flange yields after separation takes place

maximum load of joint:

$P_u$	8.7644217	kN
-------	-----------	----



METHOD 2: GENERAL THEORY OF RESISTANCE:



From Strand7

P	48.70697	kN
Q	4.870697	kN
T	49.39	kN

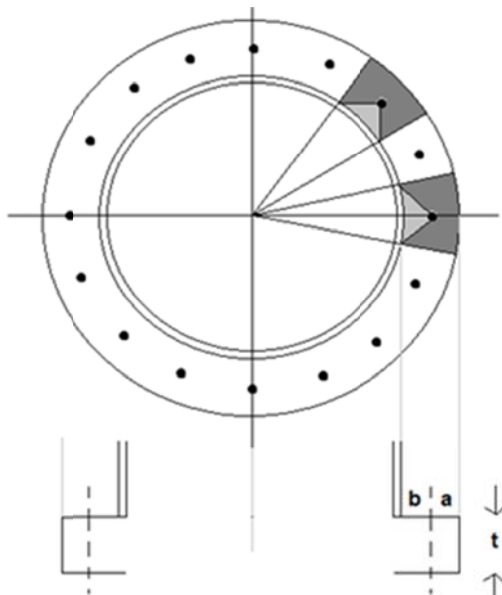
highest singular nodal tension around base circumference  
 limited to  $0.1P$ , to create a thicker more conservative flange thickness  
 Bolt resistance

For a simple stress calculation in the single bolt in the section of tubular tension "P"

A	314.1592654	Area of a bolt in mm <sup>2</sup>
$\sigma = P/A$	155039100.8	Pa
$\sigma$	155.0391008	Mpa

stress per bolt in accordance with highest tensile load on perimeter.  
 would be even less than this for the bolt in the flange, since the force is further away from the centre.

Maximum allowable stresses in each bolt in accordance with clause 13.12.1.3 is 262MPa for a 10.9S rpretensioned bolt.



**Tributary length l**

l	0.099745567	m
$\phi$	0.9	

**flange strength**

$f_y$	3.35E+08	Pa
-------	----------	----

**Maximum design strength of bolt to avoid fatigue**

$f_u$	2.62E+08	Pa	see SANS 10162-1:2005 clause 26
-------	----------	----	---------------------------------

**bolt strength calculated with 262Mpa in accordance with SANS 10162-1:2005 clause 13.12.1.3**

$A_b$	3.14E-04	m <sup>2</sup>	M20
$\phi_b$	0.80		
$T_r$	49385.84	N	

**At Base Connection:**

From Diagram

a	0.05	m
b	0.08	m
t	0.04	m

**Moment resistance of the flanges respectively are:**

**At Base Connection:**

$M_r$	8019.543567	Nm/mm
-------	-------------	-------

**At mid and top connections**

From Diagram

a	0.05	m
b	0.05	m
t	0.02	m

**At mid and top connections**

$M_r$	2004.886	Nm/mm	elastic moments
-------	----------	-------	-----------------

**For Equilibrium: The maximum allowable tensile force would be:**

P	80683.34917	N
---	-------------	---

P	44741.78	N
---	----------	---

**From equilibrium the maximum Prying force would be:**

Q	-31297.51266	N
---	--------------	---

Q	4644.059	N
---	----------	---

check! Q must be smaller than the following:

Q	240586.307	N
---	------------	---

Q	60146.58	N
---	----------	---

## B.2 STEEL LATTICE TOWER CONNECTIONS

### GUSSET PLATE CONNECTIONS

#### Load Bearing Capacity of Gusset Plate SANS 10162-1:2005

##### *clause 13.10 Load Bearing*

$\phi_{br}$	0.67
t	8
d	16
n	2
a	45
$B_{r,i}$	241843.2 N
$B_{r,ii}$	226728 N

check	OK
-------	----

#### Bolt Resistance

Shear Bolt Resistance

SANS 10162-1:2005

Clause 13.12.1.2

##### *Ordinary Grade 8.8 bolt yield strength*

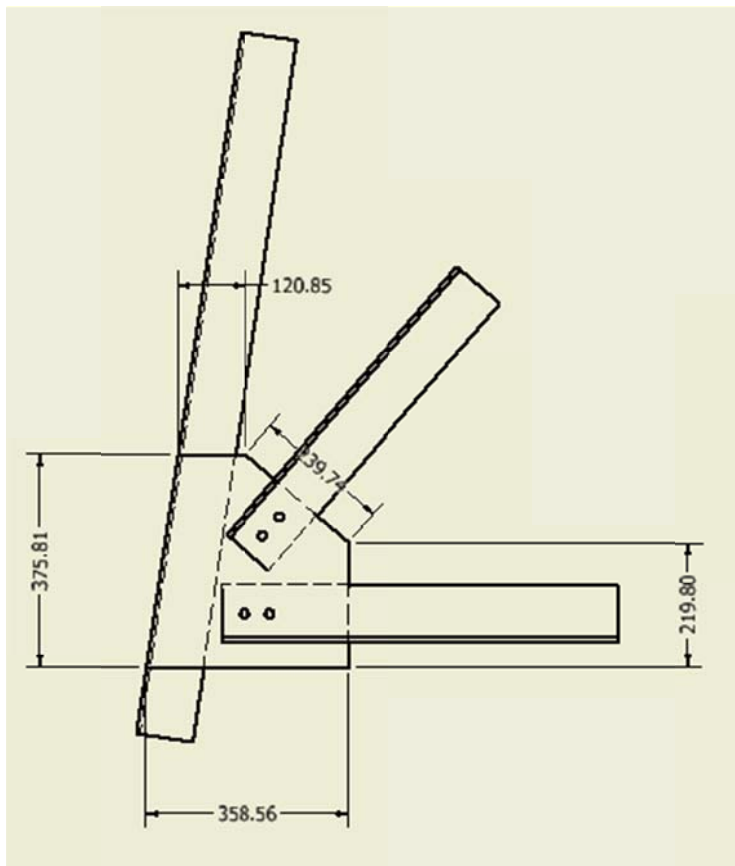
70x70x6			100x100x8		
$g_1$	40	mm	$g_1$	50	mm
$d_{max}$	16	mm	$d_{max}$	24	mm
$\phi_b$	0.8		$\phi_b$	0.8	
$A_b$	201.0619	mm <sup>2</sup>	$A_b$	452.3893	mm <sup>2</sup>
$f_u$	830	Mpa	$f_u$	830	Mpa
n	2				
$V_r$	56072.15	N	$V_r$	126162.3	N
$V_{r,n}$	112144.3				
$V_u$	62016	N	$V_u$	62016	N
$V_u/V_r$	0.553002		$V_u/V_r$	0.491557	
check	OK		check	OK	

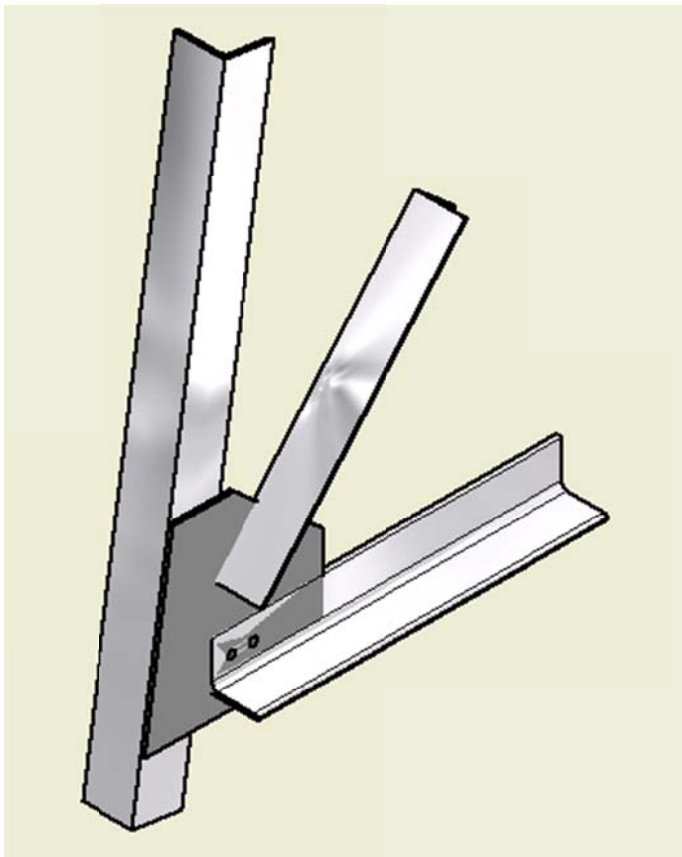
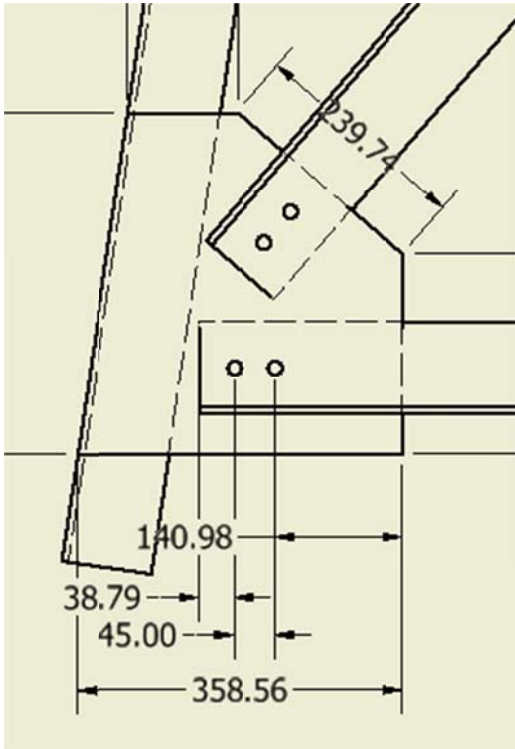
**Taking Fatigue into account with reduced yield stress for Bolts and hence increasing their number**

70x70x6		100x100x8	
$g_1$	40 mm	$g_1$	50 mm
$d_{max}$	20 mm	$d_{max}$	24 mm
$\phi_b$	0.8	$\phi_b$	0.8
$A_b$	314.1593 mm <sup>2</sup>	$A_b$	452.3893 mm <sup>2</sup>
$f_u$	262 Mpa	$f_u$	262 Mpa
$n$	3	$n$	2
$V_r$	27656.07 N	$V_r$	39824.74 N
$V_{r,n}$	82968.21	$V_{r,n}$	79649.48
$V_u$	62016 N	$V_u$	62016 N
$V_u/V_r$	0.747467	$V_u/V_r$	0.778612
check	OK	check	OK

**Spacing and Edge distances for multiple bolts in a row**

$d$	16 mm	Table 6.16 SACSH
$s_{min}$	45 mm	
$d_{edge}$	40 mm	
$d_{end}$	40 mm	



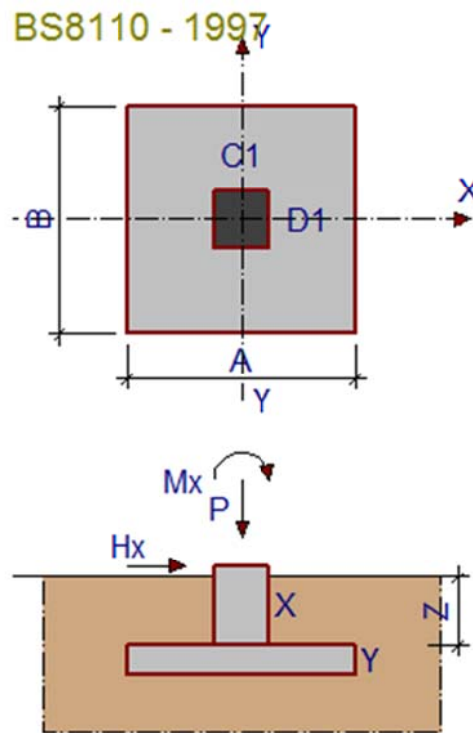


## APPENDIX C: FOUNDATION DESIGN

### C.1 STEEL MONOPOLE TOWER FOUNDATION DESIGN

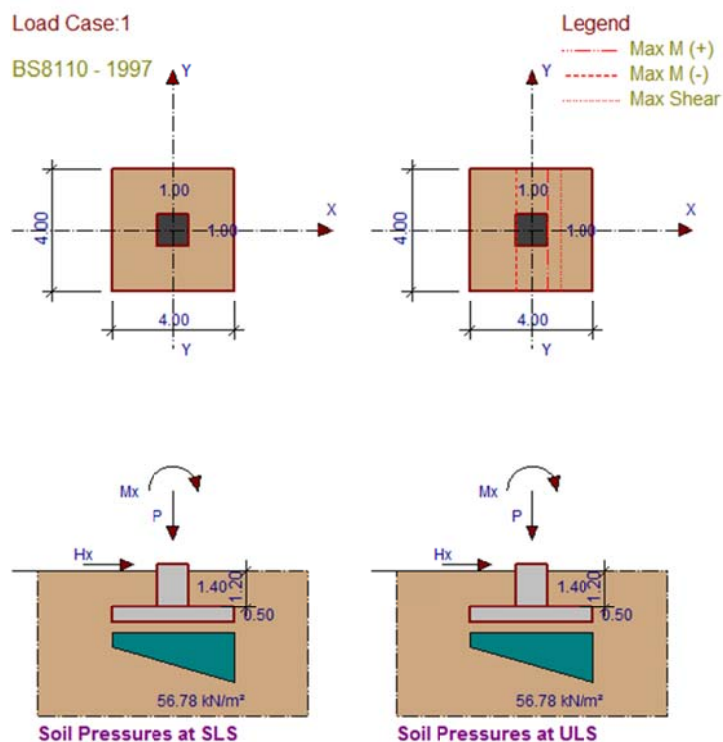
#### INPUT VALUES FOR PROKON FOUNDATION DESIGN

Base length A	(m)	4
Base width B	(m)	4
Column(s)	Col 1	Col 2
C	(m)	1
D	(m)	1
E	(m)	
F	(m)	
Stub column height X	(m)	1.4
Base depth Y	(m)	0.5
Soil cover Z	(m)	1.2
Concrete density	(kN/m <sup>3</sup> )	24.5
Soil density	(kN/m <sup>3</sup> )	18
Soil friction angle (°)		33
Base friction constant		0.33
Rebar depth top X	(mm)	70
Rebar depth top Y	(mm)	80
Rebar depth bottom X	(mm)	70
Rebar depth bottom Y	(mm)	80
ULS ovt. LF: Self weight		1
ULS LF: Self weight		1
Max. SLS bearing pr.	(kN/m <sup>2</sup> )	250
S.F. Overturning (ULS)		1.5
S.F. Slip (ULS)		1.5
f <sub>cu</sub> base	(MPa)	30
f <sub>cu</sub> columns	(MPa)	30
f <sub>y</sub>	(MPa)	450



#### OUTPUT FROM PROKON FOUNDATION DESIGN

Output for Load Case 1		
Soil pressure (ULS)	(kN/m <sup>2</sup> )	56.78
Soil pressure (SLS)	(kN/m <sup>2</sup> )	56.78
SF overturning (SLS)		5.53
SF overturning (ULS)		5.53
Safety Factor slip (ULS)		24.83
Safety Factor uplift (ULS)		>100
Bottom		
Design moment X	(kNm/m)	20.17
Reinforcement X	(mm <sup>2</sup> /m)	126
Design moment Y	(kNm/m)	3.34
Reinforcement Y	(mm <sup>2</sup> /m)	21
Top		
Design moment X	(kNm/m)	-13.50
Reinforcement X	(mm <sup>2</sup> /m)	84
Design moment Y	(kNm/m)	0.00
Reinforcement Y	(mm <sup>2</sup> /m)	0
Linear Shear X	(MPa)	0.043
vc	(MPa)	0.357
Linear Shear Y	(MPa)	0.007
vc	(MPa)	0.357
Linear Shear Other	(MPa)	0.000
Punching Shear	(MPa)	0.038
vc	(MPa)	0.357
Cost		0.00



BENDING SCHEDULE OUTPUT FROM PROKON FOUNDATION DESIGN

Bending Schedule Parameters		Rebar (mm <sup>2</sup> /m)		
Schedule file name	BaseBS	Entered	Required	Nominal
Bars: Bottom X-direction	Y16@300	670	126	650
Bars: Bottom Y-direction	Y16@300	670	21	650
Bars: Top X-direction	Y16@300	670	84	650
Bars: Top Y-direction	Y16@300	670	0	650
Column Parameters		Column 1	Column 2	Cover (mm)
Type:(C)ol,(S)tub,(N)one	S			Bottom 75
Main Bars	4Y32			Sides 50
Middle bars vert faces	4Y25			Top 50
Middle bars hor faces	4Y25			Cols 30
Lap length factor	45			
Link diameter (mm)	12			BS Picture
Link width (mm)	940			<input type="radio"/> A4
Link height (mm)	940			<input checked="" type="radio"/> A5
No. of Links	3			
Column names	col1			

First Bar mark

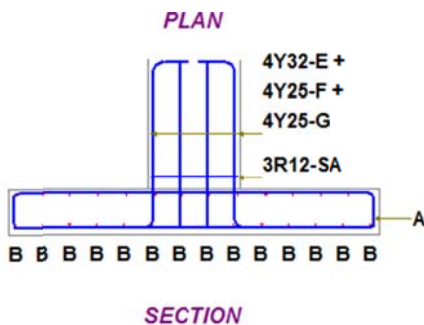
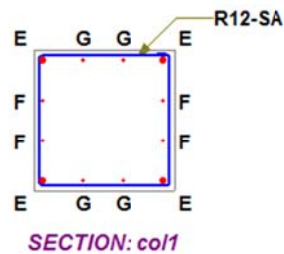
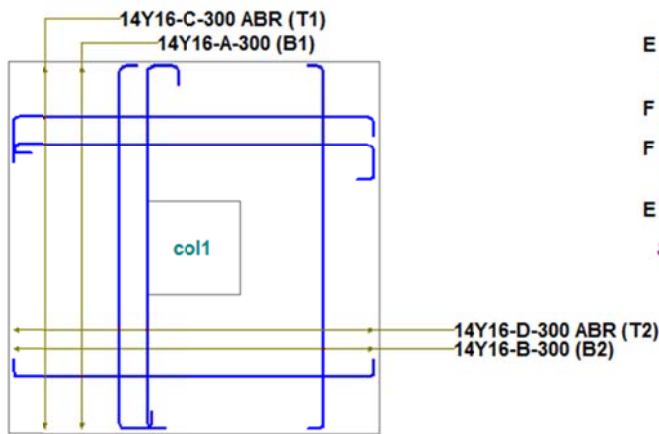
Top bars configuration

- SC 52 ABR
- SC 38 ABR
- SC 55
- SC 35 + stools
- SC 34 ABR + stool
- none

Bottom bars configuration

- SC 35
- SC 34 ABR
- SC 55
- SC 60 X-dir; SC 35 Y-dir.
- SC 60 Y-dir; SC 35 X-dir.

Save bending schedule parameters with input



## HAND CALCULATIONS FOR STEEL MONOPOLE TOWER FOUNDATION DESIGN

ULS:

**Axial load:**

N	34.76136	kN
---	----------	----

**Moment:**

M	241.4008	kNm
---	----------	-----

**Base Shear:**

V	14.96006	kN
---	----------	----

**Eccentricity**

e	6.944516	m
---	----------	---



SLS:

**Axial load:**

N	31.83345	kN
---	----------	----

**Moment:**

M	48.53834	kNm
---	----------	-----

**Base Shear:**

V	3.009367	kN
---	----------	----

e	1.524759	m
---	----------	---



### Variable Parameters

Dimensions of foundation determined through equilibrium of overturn

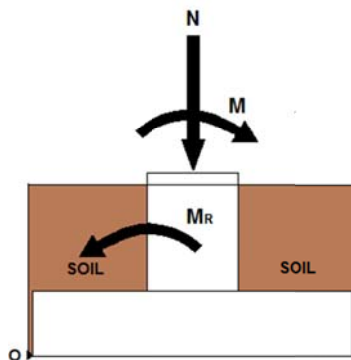
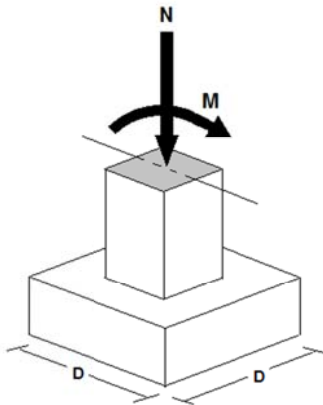
$h_1$	0.5	m
$h_2$	1.2	m
$h_3$	0.2	m

**Upper Block**

D	1	m
---	---	---

**Bottom Block**

B	4	m
---	---	---



### 1. Static equilibrium with a safety factor: ULS

Overturn moment about bottom corner of foundation footing

$M_o$	171.8781	kNm
-------	----------	-----

Resisting Moment about bottom corner of foundation footing

$M_R$	976.6556	kNm
-------	----------	-----

check:	$M_R/M_o >$	1.5
--------	-------------	-----

$M_R/M_o$	5.682258	OK
-----------	----------	----



**2. Maximum bearing pressure:**

**New axial load including own weight of foundation:**

**ULS**

**soil force**

N <sub>1</sub>	508.5504	kN
----------------	----------	----

**concrete force**

N <sub>2</sub>	265.5763	kN
----------------	----------	----

**tower axial force**

N <sub>3</sub>	34.76136	kN
----------------	----------	----

<b>N<sub>TOT</sub></b>	<b>808.8881</b>	<b>kN</b>
------------------------	-----------------	-----------

M	241.4008	kNm
---	----------	-----

e <sub>new</sub>	0.298435	**new eccentricity
------------------	----------	--------------------

check	e < D/6
-------	---------

**SLS**

**soil force**

N <sub>1</sub>	381.4128	kN
----------------	----------	----

**concrete force**

N <sub>2</sub>	243.445	kN
----------------	---------	----

**tower axial force**

N <sub>3</sub>	31.83345	kN
----------------	----------	----

<b>N<sub>TOT</sub></b>	<b>656.6912</b>	<b>kN</b>
------------------------	-----------------	-----------

M	48.53834	kNm
---	----------	-----

e <sub>new</sub>	0.073913	**new eccentricity
------------------	----------	--------------------

**Bearing Capacity of the Ground**

**Bearing capacity of ground:**

p	250	kN/m <sup>2</sup>
---	-----	-------------------

In accordance with 12.3.3 of the Cement and Concrete institute Book

**Maximum bearing pressure:**

Where  $e > D/6$

p <sub>max</sub>	79.22983	kPa
------------------	----------	-----

p <sub>max</sub>	56.82431	kPa
------------------	----------	-----

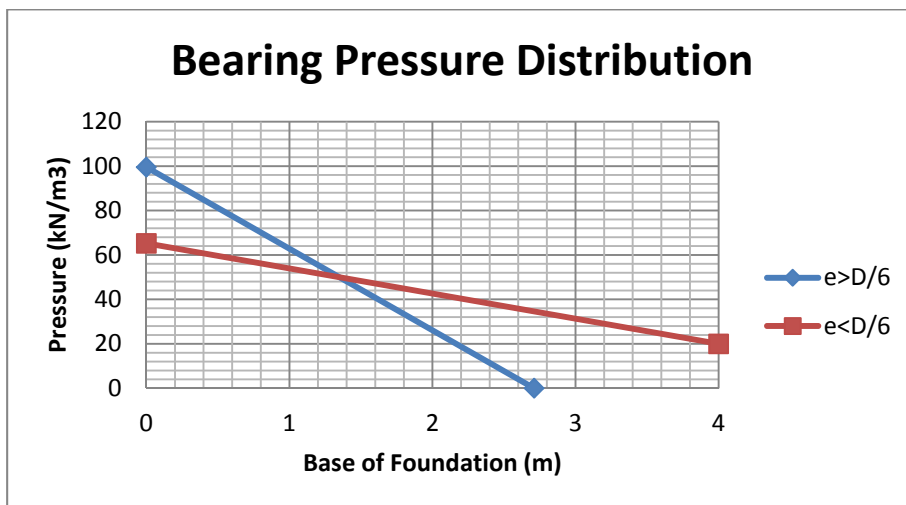
Where  $e < D/6$

p <sub>max</sub>	73.18683	kPa
------------------	----------	-----

p <sub>min</sub>	27.92418	kPa
------------------	----------	-----

check	OK
-------	----

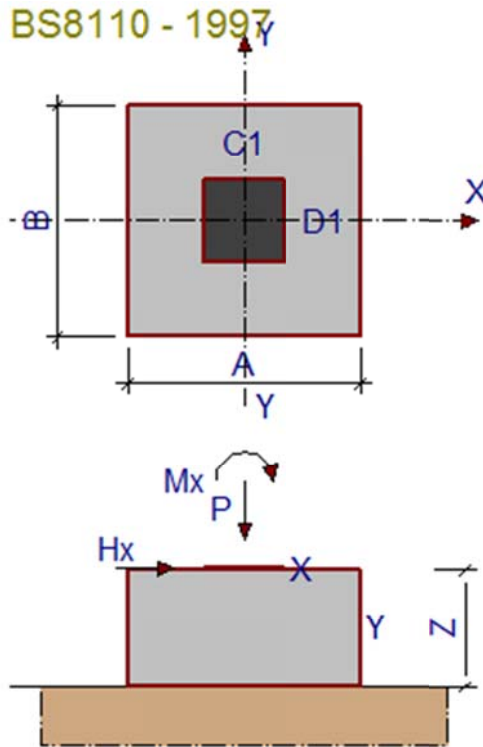
check	OK
-------	----



## C.2 STEEL LATTICE TOWER FOUNDATION DESIGN

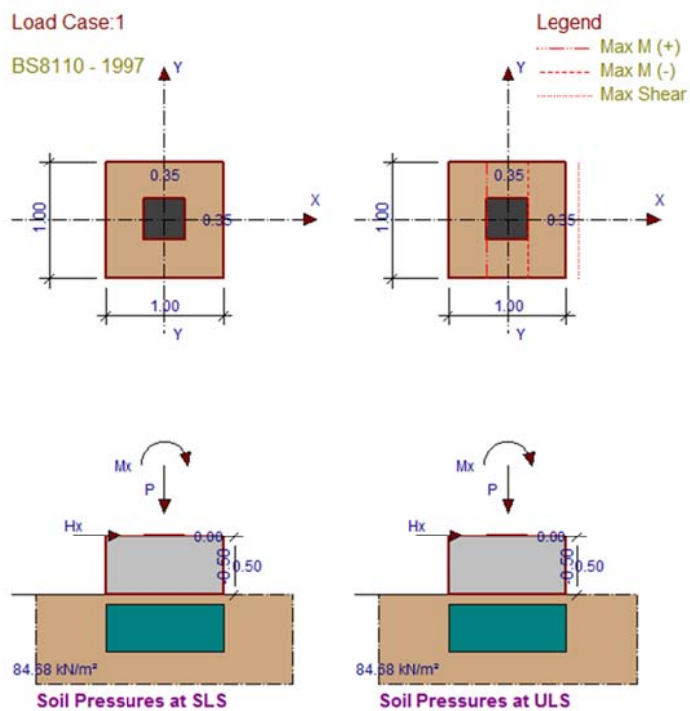
### INPUT VALUES FOR PROKON FOUNDATION DESIGN

Base length A (m)	1	
Base width B (m)	1	
Column(s)	Col 1	Col 2
C (m)	0.35	
D (m)	0.35	
E (m)		
F (m)		
Stub column height X (m)	0.005	
Base depth Y (m)	0.5	
Soil cover Z (m)	-0.5	
Concrete density (kN/m <sup>3</sup> )	24.5	
Soil density (kN/m <sup>3</sup> )	18	
Soil friction angle (°)	33	
Base friction constant	0.33	
Rebar depth top X (mm)	70	
Rebar depth top Y (mm)	80	
Rebar depth bottom X (mm)	70	
Rebar depth bottom Y (mm)	80	
ULS ovt. LF: Self weight	1	
ULS LF: Self weight	1	
Max. SLS bearing pr. (kN/m <sup>2</sup> )	250	
S.F. Overturning (ULS)	1	
S.F. Slip (ULS)	1	
fcu base (MPa)	30	
fcu columns (MPa)	30	
fy (MPa)	450	



### OUTPUT FROM PROKON FOUNDATION DESIGN

Output for Load Case 1	
Soil pressure (ULS) (kN/m <sup>2</sup> )	84.68
Soil pressure (SLS) (kN/m <sup>2</sup> )	84.68
SF overturning (SLS)	>100
SF overturning (ULS)	>100
Safety Factor slip (ULS)	>100
Safety Factor uplift (ULS)	>100
<b>Bottom</b>	
Design moment X (kNm/m)	4.30
Reinforcement X (mm <sup>2</sup> /m)	27
Design moment Y (kNm/m)	4.30
Reinforcement Y (mm <sup>2</sup> /m)	28
<b>Top</b>	
Design moment X (kNm/m)	0.00
Reinforcement X (mm <sup>2</sup> /m)	0
Design moment Y (kNm/m)	0.00
Reinforcement Y (mm <sup>2</sup> /m)	0
Linear Shear X (MPa)	0.000
vc (MPa)	0.357
Linear Shear Y (MPa)	0.000
vc (MPa)	0.357
Linear Shear Other (MPa)	0.000
Punching Shear (MPa)	N.A.
vc (MPa)	N.A.
Cost	0.00



### BENDING SCHEDULE OUTPUT FROM PROKON FOUNDATION DESIGN

Bending Schedule Parameters		Rebar (mm <sup>2</sup> /m)		
Schedule file name	BaseBS	Entered	Required	Nominal
Bars: Bottom X-direction	Y16@300	670	27	650
Bars: Bottom Y-direction	Y16@300	670	28	650
Bars: Top X-direction		0	0	650
Bars: Top Y-direction		0	0	650
Column Parameters		Column 1	Column 2	Cover (mm)
Type:(C)ol,(S)tub,(N)one	S			Bottom 75
Main Bars	4Y16			Sides 50
Middle bars vert faces				Top 50
Middle bars hor faces				Cols 30
Lap length factor	45			
Link diameter (mm)	8			
Link width (mm)	290			
Link height (mm)	290			
No. of Links	3			
Column names	col1			

First Bar mark **A** Generate Schedule

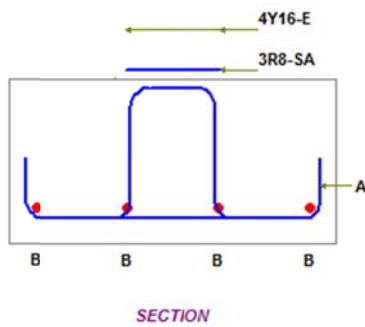
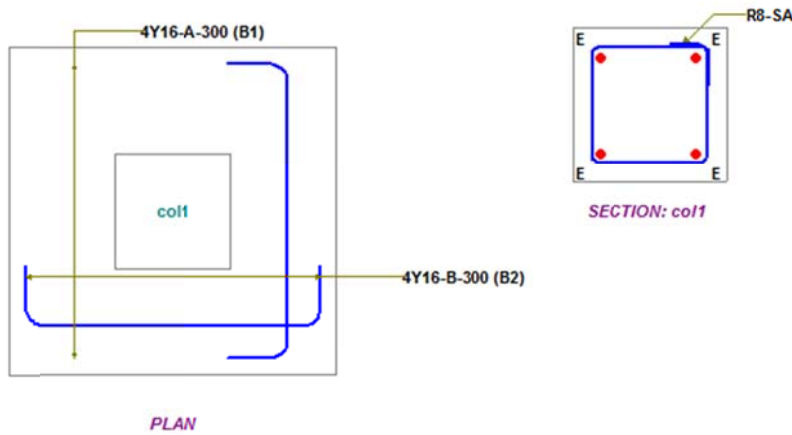
Top bars configuration

- SC 52 ABR
- SC 38 ABR
- SC 55
- SC 35 + stools
- SC 34 ABR + stool
- none

Bottom bars configuration

- SC 35
- SC 34 ABR
- SC 55
- SC 60 X-dir; SC 35 Y-dir.
- SC 60 Y-dir; SC 35 X-dir.

Recalculate BS parameter defaults



## HAND CALCULATIONS DESIGNING THE STEEL BASE PLATES FOR THE STEEL LATTICE TOWER'S FOUNDATION

### Forces at Base of each Leg

#### Worst Case Scenario

$F_{xyz}$	72413 N
$F_z$ (Comp and Tension)	68850 N

In accordance with 4.2.2 Concentrically loaded bases SASCH

#### 1. Determining the size of the base plate

$\phi_c$	0.6
$f_{cu}$	30 MPa
$A_{baseplate}$	0.004023 m <sup>2</sup>
	4022.944 mm <sup>2</sup>

for a square base plate:

b, d	63.42669 mm
check	NOT OK

#### 2. Determining the value of c

$p_{column\ perimeter}$	400 mm
$A_{column}$	1550 mm <sup>2</sup>

for quadratic equation:

a	4
b	400
c	-2472.944

x	5.841169
x	-105.8412

#### Value of c

c	5.841169 mm
---	-------------

#### Thickness of Baseplate

$f_y$	355 MPa
w	18 MPa
t	2.161244 mm
$t_{commercial}$	5 mm
$t_{min, flange\ thickness}$	8 mm

check base plate dimensions

$b_{min, c\ and\ angle\ size}$	107.6823 mm
M24	24 mm
spacing	40 mm
$b_{min}$	315.6823 mm
	350 mm

## APPENDIX D: ATTACHED CD OF DESIGN FILES

Attached CD of Microsoft Excel design calculations as well as the Strand7 designs of each of the Towers designed in this thesis.